PAST GLOBAL CHANGES
MAGAZINE

(PALEO)-EARTHQUAKE AND -TSUNAMI SCIENCE

EDITORS

Katrina Kremer, Michael Strupler, Katleen Wils, Renaldo Gastineau,Tatiana Izquierdo and Iván Hernández-Almeida

PAGES

futurearth
Research. Innovation. Sustainability

News

EGU 2024 Medals and Awards
The PAGES IPO congratulates all recipients of the 2024 EGU Medals and Awards. Special congratulations go to Prof. Michael Sigl, VICS working group steering committee member, and recipient of the Hans Oeschger Medal 2024. This prestigious award is for outstanding achievements in the field of ice research and short-term climatic changes.
Details: egu.eu/awards-medals/hans-oeschger/2024/michael-sigl

Early-Career Award (ECA) 2024
PAGES is pleased to announce the PAGES 2024 ECA recipient is Dr Oana Dumitru. Oana's expertise in geochronology and geochemistry applied in paleoclimatology to improve knowledge of past global sea level within an interdisciplinary framework was recognized. She was also praised for her excellence in science and her leadership role within the PALeo constraints on SEA level rise (PALSEA) working group.
Details: pastglobalchanges.org/science/pages-awardees/early-career-award

Call for applications: PAGES Mobility Fellowships
Applications for African, and Latin American & Caribbean (LAC) Mobility Fellowships are now open and close on 15 Augus. The fellowships aim to provide some financial support for travel and living expenses to early-career researchers studying at an institution in either Africa or LAC, and are interested in gaining experience in another African/LAC country.
Details: pastglobalchanges.org/news/137553

PAGES new promotional video
A new video explaining what the PAGES project is all about, and who the PAGES community is, is available to watch, share and enjoy. The video is also available with Chinese subtitles, and soon with additional languages.
Watch the video: youtu.be/8GQexjfXv-M

SISAL Data Stewardship Scholarship (DSS)
SISAL was awarded a DSS in November 2021 to support the development of a new SISAL WebApp to query the SISAL database. Hatvani IG et al. (2023) published an accompanying description of the app in *Quaternary Research*.
All details: pastglobalchanges.org/news/137399

Paleo Oxygenation (PO2) working group
The new working group, PO2 launched in February 2024, "aims to provide crucial insights into the natural variability of seawater dissolved oxygen concentrations during key time periods in the geological record." They maintain that "it will allow us to constrain the influence of climate, paleoproductivity, and paleocirculation on the marine oxygen cycle and related nutrients (carbon, nitrogen, phosphate, iron). Harnessing paleoceanographic records to answer questions regarding the potential links between warming and marine deoxygenation is a core need."
Find out more and join PO2 activities: pastglobalchanges.org/science/wg/PO2/intro

Working group phase extensions
The following working groups have been successfully granted a new phase: Climate Variability Across Scales (CVAS; Phase 3), Floods WG (Phase 3), Human Traces (Phase 2) and PALeo constraints on SEA level rise (PALSEA-Next; Phase 4). DiverseK has been granted an extension.

Next PAGES Open Science Meeting and Young Scientists Meeting
The 7th Open Science Meeting (OSM) and 5th Young Scientists Meeting (YSM) will be held in Shanghai, China, in 2025. The confirmed dates for the YSM will be 19–20 May with the OSM starting directly afterwards from 21–24 May. The call for sessions is open and close on 15 May 2024. All details: pastglobalchanges.org/news/137491

Apply to be on the Scientific Steering Committee (SSC)
Do you wish to guide PAGES activities and ensure the continuation of a thriving paleoscience network? Then apply to be a part of the PAGES SSC. The next deadline will be in the first quarter of 2025. Details: pastglobalchanges.org/be-involved/ssc/apply

Deadline for funding support and creation of new working groups
The next deadline to propose a new PAGES working group or to apply for financial support for a workshop/meeting is September. Details: pastglobalchanges.org/support

***Past Global Changes Magazine*: Changes to distribution**
Past Global Changes Magazine is a free magazine published twice annually and delivered in hard copy format free of charge to those interested. This can be done by completing the online webform with your postal address details before the deadline.
Details: pastglobalchanges.org/news/137348

Upcoming issue of *Past Global Changes Magazine*
The next PAGES Magazine, guest edited by Shouting Tuo, Ron Hackney, Kenji Matsuzaki, Margarita Caballero, Kaustubh Thirumalai, Lisa Park-Boush, Simona Pierdominici, Katja Heeschen and Antje H. Voelker, will look at achievements and perspectives in scientific ocean and continental drilling. The magazine will be published in the Northern Hemisphere Fall of 2024.

Calendar

6th CRIAS workshop: Climate and Migration: Historical and Present Perspectives
3–4 June 2024 – Brno, Czechia

Climate of the past and societal responses to environmental changes
5–8 June 2024 – Bern, Switzerland

1st PALSEA-Next Meeting: From mud to models
26–28 August 2024 – Santa Barbara, CA, USA

2k Network workshop: Global-scale hydroclimate synthesis of the Common Era
Dates tbc (over 3 days; late August – early September 2024) – London, UK

PAGES Databases: Creation and Analysis
Will directly precede the 2k Network workshop, dates tbc (1-day; late August – early September) – London, UK

22nd Swiss Climate Summer School
1–6 September 2024 – Grindelwald, Switzerland

Q-MARE workshop: Detecting, describing and disentangling pre-industrial climate and human impacts on marine ecosystems
2–6 September 2024 – Crete, Greece

INQUA-PAGES ECR (Early-Career Researcher) workshop (TROPQUA)
4–8 November 2024 – Goa, India

Featured publications

2k Network – Iso2k
Using the PAGES Iso2k database, Konecky B et al. published a paper in *Nature Geoscience* on "Globally coherent water cycle response to temperature change during the past two millennia."
pastglobalchanges.org/publications/137472

CVAS
Laepple T et al. published a paper in *Nature Geoscience* which examines "Regional but not global temperature variability underestimated by climate models at supradecadal timescales."
pastglobalchanges.org/publications/137478

LandCover6k
Li F et al. have published a new paper in *Frontiers in Plant Science* on "Evaluation of relative pollen productivities in temperate China for reliable pollen-based quantitative reconstructions of Holocene plant cover."
pastglobalchanges.org/publications/137508

PALSEA
A new paper by Dumitru OA et al. has been published in *Quaternary Science Reviews* where the authors investigate "Last interglacial global mean sea level from high-precision U-series ages of Bahamian fossil coral reefs."
pastglobalchanges.org/publications/137383

Cover

Image created with a text-to-image model developed by OpenAI using deep learning methodologies (DALL.E 3). The prompt included the words "earthquake", "science" and "tsunami". The AI-generated image was modified by Renaldo Gastineau.

Advances and challenges of (paleo)-earthquake and -tsunami research

Katrina Kremer[1], M. Strupler[1,2], K. Wils[3,4], R. Gastineau[5] and T. Izquierdo[6]

Earthquakes and tsunamis represent natural hazards that can leave various footprints in different geological, archaeological and historical archives. These footprints can be used to infer magnitudes and recurrence rates of past events, which is crucial for better hazard assessments and improved risk mitigation. Depending on the geological setting, different research approaches may be combined to reconstruct past earthquakes and tsunamis.

In this issue, we present a wide range of techniques to study recent (years to decades ago) and (pre)historical earthquakes and tsunamis performed in diverse terrestrial and aquatic settings. The studies presented cover regions that are characterized by high recurrence rates of seismic (and related tsunami) activity, as well as those with large time gaps between events. A broad variety of different methodologies is included, all aiming to better understand location, timing, and recurrence rates of earthquakes and tsunamis. Novel concepts and methodologies, as well as challenges regarding the identification of the seismic and tsunami hazard in the geological record, are presented.

Subaquatic environments (lakes, fjords and oceans) are ideal settings to study recent and past earthquakes because of the high preservation potential compared to terrestrial settings. Such well-preserved archives can be used as "paleoseismometers". For example, lake and fjord sediments from Alaska provide records of recent earthquakes in which the sedimentary signal differs depending on the epicentral distances, type and magnitude of the earthquake (Singleton et al. p. 4). Further calibration 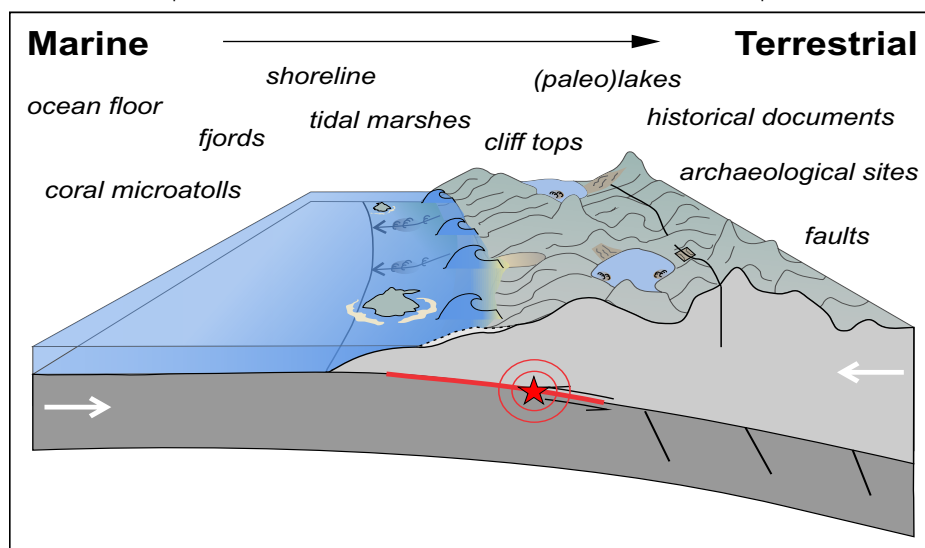of the paleo-seismometer requires verification of the relationship between earthquake parameters and their characteristics in the sediment record. Howarth et al. (p. 6) use the recent 2016 Kaikōura earthquake (New Zealand) to explore the genesis and deposition of deep-sea turbidites over a large area. However, determination of the spatial extent of past seismic events is difficult due to potential chronological uncertainties. The study by Brooks (p. 8) showcases how high-precision varve chronology in lake sediments can be used to define the regional signature of a postglacial earthquake. Lu (p. 10) uses a seismite record of a paleolake as a proxy for regional tectonism in northwestern Tibet.

While previous studies focused on secondary seismic evidence (e.g. mass movements), the following studies focus on primary evidence of earthquakes on terrestrial settings. In Grützner (p. 12), a multi-method approach is used, combining remote sensing, geophysics and paleoseismology to study earthquake activity on a fault in Slovenia. Patria and Daryono's study (p. 14) highlights the high seismic hazard potential on a fault in Indonesia, based on data from trenching. In Lallemand et al. (p. 16), the authors look at geomorphological and archaeological evidence, showing that a potential displacement in walls may indicate evidence for surface rupturing during a recent earthquake. Kleeman (p. 18) uses historical documents and artifacts to determine the exact timing of earthquakes in the last centuries, in order to reconstruct wave propagation in the northwestern USA.

Coastal paleoearthquake records enable the linking of terrestrial and subaquatic evidence of seismicity. The study of Pizer et al. (p. 20) combines on- and offshore paleoseismic evidence for better understanding the size, location and spatial impacts of past large earthquakes at subduction margins. In Philibosian (p. 22) we see how intertidal corals preserve past uplift or subsidence at annual resolution along subduction zones. Another proxy that can archive the seismic deformation along subduction zones are diatoms, as presented in Summers et al. (p. 24) and Dura and DePaolis (p. 26). Hocking et al. (p. 28) show that diatoms not only serve as a proxy for earthquakes, but also for tsunamis. Another approach using geochemical signals in sediment cores from salt marshes to reconstruct abrupt sea-level changes that may be related to earthquakes or tsunamis is conceptually presented by Giang et al. (p. 30).

However, distinguishing between tsunami and other sedimentary processes in coastal areas presents a challenge. For example, Gouramanis et al. (p. 32) could not detect any distinguishable features between recent tsunami and cyclone deposits along the shore of southern India based on a multi-proxy approach, despite including *sed*aDNA analyses. However, the final series of articles propose different approaches to disentangle and detect these deposits. Two studies describe a successful distinction between tsunami and hurricane/storm deposits; Fabbri et al. (p. 34) present a study on historical examples of tsunami and hurricanes from the Caribbean using a sedimentological and geochemical approach, and Prizomwala et al. (p. 36) distinguish between paleotsunamis and cyclone surges along the western shoreline of India with a sedimentological, geochemical and micropaleontological approach. Cuven et al. (p. 38) again show the potential for sedimentological studies revealing the paleotsunami record in Peruvian coastal environments. Izquierdo and Abad (p. 40) close this special issue by presenting evidence for past tsunamis camouflaged in desert environments, as shown in the example of the Atacama Desert.

AFFILIATIONS

[1]Institute of Geological Sciences, University of Bern, Switzerland

[2]Swiss Seismological Service, ETH Zürich, Switzerland

[3]Institute of Geology, University of Innsbruck, Austria

[4]Department of Geology, Ghent University, Belgium

[5]EDYTEM, Université Savoie Mont Blanc, Le Bourget du Lac, France

[6]Department of Biology and Geology, Physics and Inorganic Chemistry, Rey Juan Carlos University, Spain

CONTACT

Katrina Kremer: katrina.kremer@unibe.ch

Figure 1: Cartoon of a subduction zone, indicating the various settings and archives in which earthquake and/or tsunami records can be found. Image credit: Katleen Wils.

Calibrating the subaqueous seismograph: Using recent events to inform our knowledge of the past

Drake M. Singleton[1], D.S. Brothers[2], P.J. Haeussler[3], R.C. Witter[3] and J.C. Hill[2]

Accurate records of past earthquakes improve our understanding of present seismic hazards. We investigate the sedimentary response in Alaskan lakes to recent earthquakes to resolve outstanding uncertainties in the generation of earthquake records from subaqueous environments.

Subduction zone seismicity

Subduction zones host the largest earthquakes in the world, and are formed through the collision of oceanic and continental crust; a process in which the less buoyant oceanic plate dives beneath the continental lithosphere (Fig. 1a). Subduction zones are typically associated with three types of earthquakes. The first type (megathrust) occurs due to movement along the plate interface and has the potential to produce giant earthquakes, such as the 2011 moment magnitude (M_w) 9.1 Tohoku-oki earthquake in Japan. The second type of earthquake (crustal) is caused by tectonic stresses in the upper ~30 km of the crust, and is related to displacement on sub-vertical crustal faults. The 2002 M_w 7.8 Denali Earthquake in Alaska, USA, is an example of a crustal seismic source. The third seismic source is the result of extension related to differential stresses within the oceanic plate as it journeys into the mantle. Earthquakes of this type are

termed intraslab earthquakes because the displacement takes place within the downward oceanic plate (i.e. the slab), and they typically occur at depths greater than 40 km. The angle of subduction and the depth of seismicity are such that intraslab earthquakes can occur directly below coastal population centers (Fig. 1a).

The challenge of developing prehistoric records

Current seismic hazard models for intraslab earthquakes rely on historical rates of intraslab seismicity and empirical earthquake magnitude-recurrence relationships to constrain the hazard from intraslab earthquakes (Frankel et al. 2015). With historic seismological data limited to the past ~120 years, the historical record may not fully capture important patterns in the spatiotemporal distribution of intraslab earthquakes, or resulting ground motions. A longer record of earthquakes, spanning hundreds or thousands of years, could improve hazard

characterization. Unlike megathrust and crustal earthquakes, which produce observable surface faulting and/or significant land-level changes and, therefore, leave a characteristic signal in the geologic record, intraslab earthquakes occur too deep for the associated faulting to reach the surface. However, the shaking produced by intraslab earthquakes is frequently strong enough to produce secondary evidence such as liquefaction, rockfall, and subaqueous sediment gravity flows (Van Daele et al. 2019; West et al. 2020), hinting at the possibility of constructing long records of deep earthquakes from secondary paleoseismic evidence.

Lakes as natural seismographs

Lakes have long been used to investigate natural phenomena that take place across a range of timescales, from glacial-interglacial intervals (e.g. Thomas et al. 2021) to instantaneous events such as earthquakes (e.g. Strasser et al. 2006; Van Daele et al. 2020). If ground motions during an
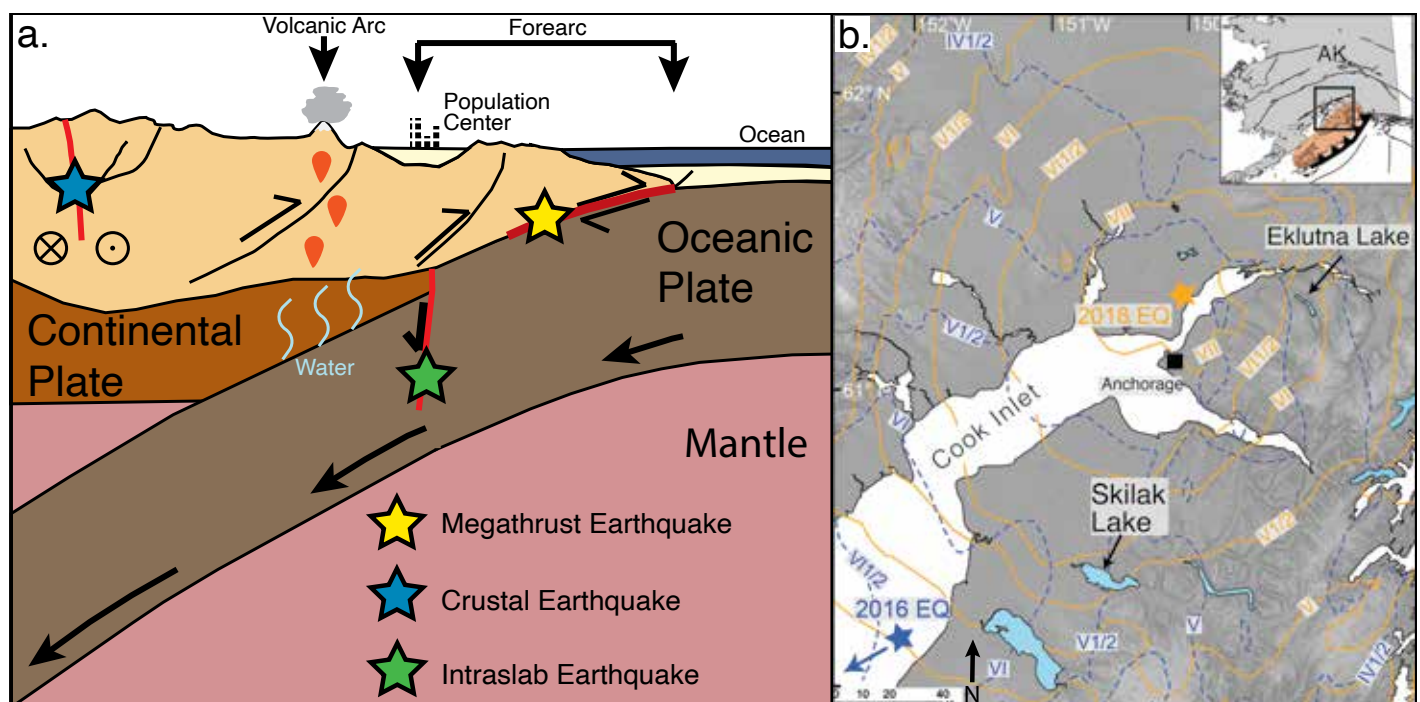
Figure 1: (A) Schematic diagram of a subduction zone. **(B)** ShakeMap Modified Mercalli Intensity (MMI) contours from the 2018 Anchorage earthquake (solid gold lines) and the 2016 Iniskin earthquake (dashed blue lines). Stars are the respective earthquake epicenters. Basins investigated by Singleton et al. (in press) are shown in light blue. Map inset shows study area within the state of Alaska, USA, and the 1964 rupture patch in orange. Figure modified from Singleton et al. (in press). ShakeMap data from USGS (2016, 2018).
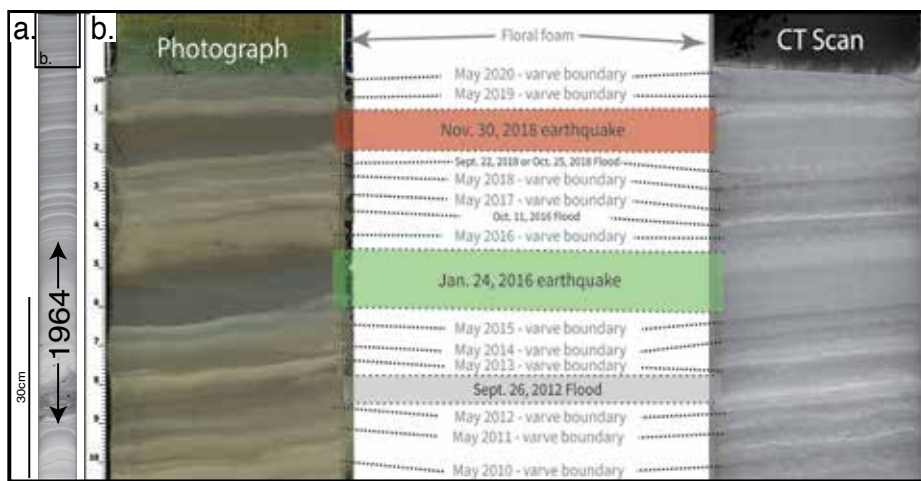
Figure 2: (A) Full CT image of core SK20-02A from Skilak Lake showing the thickness of the 1964 Alaska earthquake deposit. Black box at top corresponds to part b. **(B)** Top 10 cm of core SK20-02A. The two intraslab earthquake deposits are highlighted, as are the varve year boundaries. Figure modified from Singleton et al. (in press).

earthquake are strong enough, sediment that has accumulated on the slopes and in the deltaic environments of a lake can become resuspended in the water column and, under the force of gravity, flow downslope as a subaqueous gravity flow (Molenaar et al. 2021). The sediment gravity flow is then redeposited in the lake basin as a turbidite. Turbidites have previously been used to investigate the paleorecord of very large megathrust earthquakes (e.g. Goldfinger et al. 2012; Moernaut et al. 2014), but recent work has shown that lake basins are also sensitive to shaking produced by intraslab events (Van Daele et al. 2019, 2020; Singleton et al. in press).

However, before a complete and robust paleoseismic record from lake deposits can be developed, the underlying factors governing deposit formation need to be understood to build confidence in the idea that every earthquake that produces shaking above a certain intensity also produces an identifiable deposit. Several factors related to the lake's physiography/sedimentological character, and the character of the seismic waves, can influence the production of earthquake-triggered turbidites. Recent investigations show that both moderately steep slopes, which help facilitate the downslope gravitational movement of resuspended sediment, and coarse-grained rapid-depositional environments (deltas) are conducive to the production of earthquake-triggered turbidites (e.g. Molenaar et al. 2021; Praet et al. 2017).

Less well understood is the range of seismic parameters that influence sediment remobilization, particularly the minimum amount of shaking necessary to trigger remobilization and how variations in shaking intensity affect the resulting deposit. Two recent earthquakes in southcentral Alaska offer an opportunity to further investigate these uncertainties in the generation of earthquake-triggered deposits.

Calibrating the subaqueous seismograph
The epicenters of the 2016 M_w 7.1 Iniskin and 2018 M_w 7.1 Anchorage earthquakes are at opposite ends of Cook Inlet, Alaska

(Fig. 1b) (USGS 2016, 2018). Both earthquakes occurred due to intraslab faulting and were widely felt across the region, with the 2018 event producing strong ground motions and infrastructure damage to the city of Anchorage (West et al. 2020). A few months after the 2018 earthquake, a team of researchers from the University of Ghent and the U.S. Geological Survey (USGS) observed evidence of earthquake-triggered remobilized sediment in the form of a thin (~0.1–2.4 cm) turbidite (Van Daele et al. 2020) at Eklutna Lake. This initial observation motivated an expanded investigation by the USGS into additional lakes across a range of shaking intensity (Fig. 1b), with the objective of identifying the minimum shaking that would produce an identifiable deposit.

Utilizing a dataset consisting of high-resolution sub-bottom profiles and percussion-driven gravity cores, Singleton et al. (in press) investigated six additional subaqueous basins, four lakes and two fjords for evidence of seismically triggered deposits. The steep-sided proglacial lakes receive abundant sediment and contain annual laminations (varves), which allows for yearly resolution of event deposits. The two recent intraslab earthquakes produced a range of deposit characteristics in the 2016 and 2018 varve years (Fig. 2). In those lakes that experienced minimal amounts of shaking near Modified Mercalli Intensity (MMI) values of V (a measure of shaking intensity), remobilized sediment was highly localized to only the most favorable environments (sandy deltaic slopes) (Singleton et al. in press). With increased shaking, thicker (0.5–2.7 cm) and more widespread deposits were observed in the sediment cores, suggesting that an increased amount of material was remobilized in the lake basin. At shaking intensities above MMI V1/2, enough sediment was remobilized that a deposit can be confidently identified across the basin (Singleton et al. in press). Ground motion below MMI ~V appeared insufficient to remobilize enough sediment to be differentiated from background events.

The multi-lake dataset also contains evidence for the widespread impact of the giant 1964 M_w 9.2 Alaska earthquake (Fig. 2a), a megathrust earthquake on the main plate boundary (Fig. 1b) (Singleton et al. in press). Deposits from the 1964 earthquake are generally thicker and observed more widely across the basins than those from the intraslab events, which may reflect the higher intensity and duration of shaking (Praet et al. 2022). The addition of two thin turbidites from intraslab earthquakes contribute additional data points to the hypothesis that a clear division between megathrust and intraslab earthquake deposits can be identified in some lake environments (Praet et al. 2022; Singleton et al. in press; Van Daele et al. 2019). Such a distinction will contribute to expanding the paleoearthquake record through shaking proxies and building an understanding of long-term fault behavior.

In conclusion, a multi-lake survey following two recent intraslab earthquakes constrains the minimum amount of shaking necessary to produce an identifiable earthquake-generated deposit, and confirms that variations in deposit character reflect differences in the causative earthquake.

REFERENCES
Frankel A et al. (2015) Earthq Spectra 31: S131-S148

Goldfinger C et al. (2012) USGS Prof Paper No. 1661-F

Moernaut J et al. (2014) J Geophys Res: Solid Earth 119(3): 1607-1633

Molenaar A et al. (2021) Sedimentology 68(6): 2365-2396

Praet N et al. (2017) Mar Geol 384: 103-119

Praet N et al. (2022) Sedimentology 69(5): 2151-2180

Singleton D et al. (in press) In: Ruppert N et al. (Eds) Tectonics of Alaska and Western Canada. AGU Geophysical Monograph Series

Strasser M et al. (2006) Geology 34(12): 1005-1008

Thomas J et al. (2021) Quat Sci Rev 272: 107215

U.S. Geological Survey (USGS) (2016) Earthquake Hazards Program: M 7.1 – 47 km ESE of Pedro Bay, Alaska accessed 1 March 2022

U.S. Geological Survey (USGS) (2018) Earthquake Hazards Program: M 7.1 - 14km NNW of Anchorage, Alaska, accessed 1 March 2022

Van Daele M et al. (2019) Geology 47(2): 127-130

Van Daele M et al. (2020) Seis Res Let 91(1): 126-141

West M et al. (2020) Seis Res Let 91(1): 66-84

Relationship between fault source, ground motions and marine turbidites emplaced by the 2016 CE Kaikōura earthquake

Jamie D. Howarth[1], A.R. Orpin[2], S.E. Tickle[1], Y. Kenako[3], K.L. Maier[2], L.J. Strachan[4] and S.D. Nodder[2]

Observations of the 2016 CE M_w 7.8 Kaikōura earthquake, and the seafloor deposits it produced, demonstrate a predictable relationship between fault source, ground motions and the deposition of deep-sea turbidites, confirming key assumptions that underpin turbidite paleoseismology.

Resolving persistent debates about turbidite paleoseismology

Subduction zones have produced some of the largest and most damaging historical earthquakes, but our understanding of the dynamics and hazards they pose is critically limited by the paucity of high-resolution paleoseismic records that span millennia (Sieh et al. 2008). To reconstruct among the most comprehensive records of subduction zone earthquakes, turbidite paleoseismology uses earthquake-triggered event beds generated from deep-sea turbidity currents (Goldfinger et al. 2012; Patton et al. 2015). Whilst turbidite paleoseismology studies are growing, debate persists about the key assumptions that underpin the approach and the validity of their earthquake records (Atwater et al. 2014; Goldfinger et al. 2017; Shanmugam 2009; Sumner et al. 2013). Resolving these debates requires accurate measurement of the earthquake source and accompanying strong ground motions (SGM), together with interrogation of earthquake-generated turbidites in discrete sediment dispersal systems along subduction margins.

The 2016 moment magnitude (M_w) 7.8 Kaikōura earthquake provides a compelling case study because it is amongst the best characterized using instrumental data (Clark et al. 2017; Hamling et al. 2017) and models (Ulrich et al. 2019) (Fig. 1). The earthquake ruptured more than 20 onshore and offshore faults along ~180 km of the northeastern South Island of New Zealand (Litchfield et al. 2018). Models of SGM produced by the earthquake are well corroborated by station data and show motion propagated predominantly in a northeasterly direction along the southern Hikurangi Margin (Wallace et al. 2017).

The spatial relationship between SGM and turbidite deposition

Submarine canyons that supply sediment to the Hikurangi Channel are oriented both parallel and perpendicular to the rupture; an ideal context for evaluating the relationship between SGM and turbidite deposition (Fig. 1b). The distribution and stratigraphy of the Kaikōura earthquake event bed (KEB) was determined using an extensive set of multicores that preserve the sediment-water interface. Cores were collected from over 100 sites during multiple field campaigns along the Hikurangi Subduction Margin that occurred from days to five years post-earthquake. The core sites sampled 20 discrete submarine canyons, or slope-basins, along

~700 km of the southern-central Hikurangi Margin and ~1500 km of the Hikurangi Channel. The KEB was identified in 69 cores from 10 consecutive feeder canyons along a >200 km segment of the southern Hikurangi Margin, using a combination of indicators for recent deposition and short-lived radioisotope dating (^{234}Th, ^{210}Pb) (Howarth et al. 2021; Mountjoy et al. 2018). The KEB was emplaced in canyons up to 120 km northeast of the northern rupture tip, and 15 km southeast of the southern extent of the rupture (Hayward et al. 2022; Howarth et al. 2021) (Fig. 1b).

A physics-based ground-motion simulation of the Kaikōura earthquake qualifies the relationship between turbidite deposition and the spatial pattern of shaking. Modeled peak-ground velocities (PGV) were highest along the rupture and northeast of its tip due to the earthquake's nucleation location and rupture direction (Wallace et al. 2017). The pattern of SGM northwards along the rupture, and beyond, directly correlated to the occurrence of the KEB at canyon outlets (Fig. 1b). Comparison of PGV between canyons with the KEB, and those without, indicate that threshold PGVs for emplacing turbidites ranged from 16–25 cm/s, constraining the SGMs required to locally trigger turbidity currents.

These observations reinforce a predictable relationship between fault source, SGM and the deposition of turbidites in discrete canyons along a subduction margin, fundamental to turbidite paleoseismology. However, the Kaikōura earthquake example also demonstrates that asymmetric radiation of ground motions from a specific fault source can complicate the spatial relationships between turbidite emplacement and fault rupture. Careful attribution of fault sources from turbidite paleoseismic reconstructions is needed, informed by physics-based ground-motion simulations to account for nucleation location and directivity effects (Howarth et al. 2021). The nuanced relationship between fault rupture, SGMs and turbidite emplacement realizes the possibility of resolving the dynamics (nucleation location and rupture direction) of paleoearthquakes
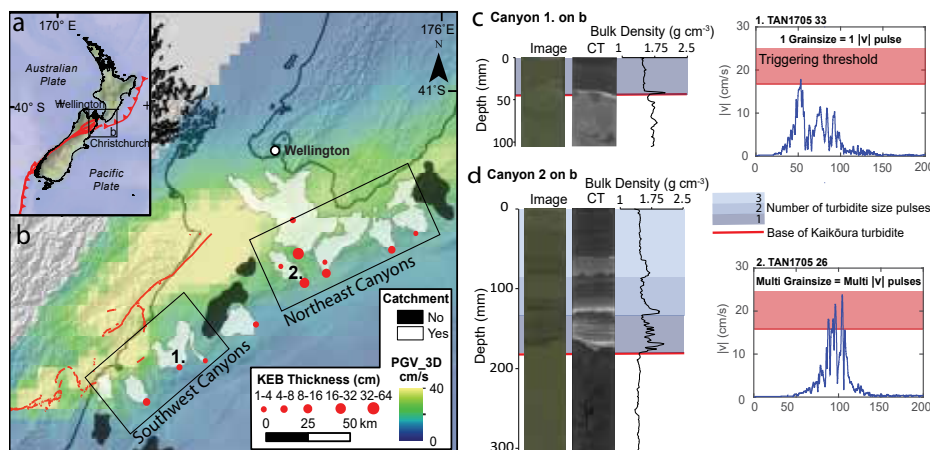
Figure 1: (A) Tectonic setting. **(B)** Kaikōura fault rupture (red lines), ground motions (color ramp) and submarine canyon catchments with the Kaikōura event bed (KEB; irregular white polygons, red circles). **(C-D)** Core image, Computed Tomography (CT) image, density of sediment cores and modeled velocity-time histories for the Kaikōura earthquake at representative canyons. Turbidite structures are sympathetic with contrasts in the SGM between southwestern (C) and northeastern canyons (D). Figure modified from Howarth et al. (2021).

when turbidite paleoseismology is combined with SGM modeling (Howarth et al. 2021).

Establishing turbidite synchronicity
Paleoseismologists often rely on relative dating techniques such as turbidite "fingerprinting" and the "confluence test", to infer along-margin synchronous emplacement of earthquake-generated turbidites, because absolute dating techniques offer only decadal uncertainties. The validity of both approaches remains contentious and might only be resolved through test cases like the Kaikōura earthquake, where the spatial distribution and structure of the KEB can now be defined with unprecedented detail.

Turbidite "fingerprinting" underpins arguments for synchronicity based on the similarities in turbidite structure between different canyon systems (Goldfinger et al. 2012). The KEB is near ubiquitous in the middle and lower reaches of canyons feeding the Hikurangi Channel (Fig. 2a). In these canyon reaches KEB structure is characterized by one or more grain-size pulses (Fig. 1c, d). Core transects across Opouawe Canyon show a consistent number of grain-size pulses in cores located between 10–50 m above the canyon axis. These field insights informed a coring strategy optimized for turbidite paleoseismology.

Regional core analysis shows that in the southwestern canyons the KEB has just a single grain-size pulse, whereas northeastern canyons have multiple pulses (Fig. 1c, d). Grain-size pulses in the KEB broadly correlate to the number of high amplitude peaks above the triggering threshold (16–25 cm/s) in SGM histories felt in these canyons (Fig. 1c, d). This potential link between ground motion and turbidite structure provides a mechanism to explain why turbidites in discrete canyons, separated by hundreds of kilometers, often have the same number of grain-size pulses (Goldfinger et al. 2012; Howarth et al. 2021), supporting application of turbidite "fingerprinting" as a paleoseismological tool. Regional variability in KEB structure, however, also highlights the challenge of a fingerprinting approach based on turbidite structure alone. If the suite of KEB deposits occurred in the geologic record, a dual fingerprint of single- and multi-pulse turbidites would likely be misinterpreted as two separate earthquakes.

In silt-rich turbidity current systems, such as the Hikurangi Subduction Margin, turbidite fingerprints may be further compounded by the low-preservation potential of silt-rich turbidites. Repeat coring at specific sites, over a five-year period post-earthquake, demonstrates substantial bioturbation is overprinting primary sedimentary structures of the KEB where it is thin (<10 cm) and dominated by silt-rich facies (Fig. 2c). Ongoing work quantifying variability in the volume and rate of bioturbation, together with its sedimentary and biological controls, will evaluate the KEB preservation potential and possible
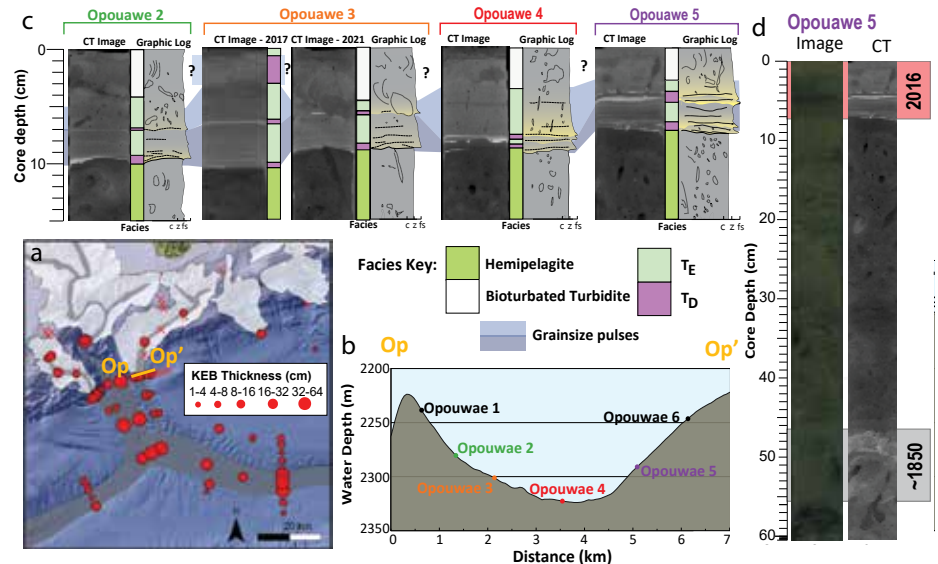
Figure 2: (A) Dense sampling of the Kaikōura event bed (KEB) through a major confluence traversed by the Kaikōura earthquake-triggered turbidity current. **(B)** Core transect across the mid-reaches of the Opouawe Canyon (Op-Op' in yellow) showing correlated KEB structures (grain-size pulses) between turbidites and the influence of bioturbation on preservation **(C). (D)** Representative multicore showing KEB and the underlying penultimate event bed.

implications for the geological record. Hence, we recommend future attempts at turbidite fingerprinting utilize a multi-proxy approach that incorporates both the physical and geochemical characteristics of event beds.

The confluence test assumes that synchronously triggered flows in separate canyons produce a single turbidite above and below the confluences of submarine canyons/channels. Asynchronous flows are additive, producing one deposit in each channel above the confluence, and more than one below (Goldfinger et al. 2012). In practice, the confluence test is achieved by quantifying the number of turbidites between two temporal datums, above and below the confluence. The 2016 Kaikōura earthquake emplaced a single turbidite above and below major canyon/channel confluences (Howarth et al. 2021). Preliminary radiometric ages of the penultimate turbidite across multiple canyons suggests preservation of historical earthquakes (e.g. 1855 CE M_w 8.2 Wairarapa, 1848 CE M_w 7.5 Marlborough) (Fig. 2d), ideal for a critical assessment of the confluence test in the southern Hikurangi Margin.

Conclusions
The predictable relationship between well-constrained observations of the 2016 Kaikōura earthquake fault source, SGMs and turbidite emplacement in discrete distributary systems along the southern Hikurangi Margin validates key assumptions in turbidite paleoseismology. More observational studies of turbidite deposition following well-instrumented earthquakes are required to refine our understanding of how turbidites record earthquake SGMs. However, turbidite paleoseismology's future is bright. Our improved ability to elucidate the dynamics of paleoearthquakes by qualifying spatial variations in ground motions may inform attributes, such as nucleation location and rupture direction,

that were previously beyond the reach of paleoseismic investigation.

AFFILIATIONS
[1]School of Geography, Environment and Earth Sciences, Victoria University of Wellington, New Zealand
[2]National Institute of Water and Atmospheric Research (NIWA), New Zealand
[3]Graduate School of Science, Kyoto University, Japan
[4]School of Environment, University of Auckland, New Zealand

CONTACT
Jamie D. Howarth: jamie.howarth@vuw.ac.nz

REFERENCES
Atwater BF et al. (2014) Geology 42: 827-830

Clark K et al. (2017) Earth Planet Sci Lett 474: 334-344

Goldfinger C et al. (2012) US Geol Surv Prof Pap 1661–F: 170 pp

Goldfinger C et al. (2017) Mar Geol 384: 4-46

Hamling IJ et al. (2017) Science 356: eaam7194

Hayward BW et al. (2022) New Zealand J Geol Geophys: 1-14

Howarth JD et al. (2021) Nat Geo 14: 161-167

Litchfield NJ et al. (2018) Bull Seismol Soc Am 108: 1496-1520

Mountjoy JJ et al. (2018) Sci Adv 4: eaar3748

Patton JR et al. (2015) Geosphere 11: 2067-2129

Shanmugam G (2009) Bull Seismol Soc Am 99: 2594-2598

Sieh K et al. (2008) Science 322: 1674-1678

Sumner EJ et al. (2013) Geology 41: 763-766

Ulrich T et al. (2019) Nat Comms 10: 1213

Wallace LM et al. (2017) Nat Geo 10: 765-770

A major paleoearthquake in central Canada interpreted from early postglacial subaqueous mass transport deposits

Gregory R. Brooks

Stratigraphic and chronologic evidence reveal that widespread mass transport deposits (MTDs) accumulated synchronously within glacial Lake Barlow-Ojibway, central Canada. This MTD signature is best explained by a strong paleoearthquake of M_w ~7.3.

Regional context

Glacial Lake Barlow-Ojibway formed against the Laurentide Ice Sheet as it retreated northwards through western Quebec-northeastern Ontario, central Canada (Veillette 1994; Vincent et al. 1979). The lake persisted between about 11.0–8.2 kyr cal BP (Brouard et al. 2021; Dyke 2004), then drained catastrophically northwards into the Hudson Bay basin. Extensive glaciolacustrine sediments containing interbedded subaqueous landslide deposits (or mass transport deposits [MTDs]) accumulated within the lake and now underlie large areas of the former basin, including the beds of modern lakes. A paleoseismic investigation into the spatial distribution and age of such buried MTDs can recognize a regional signature of similarly aged MTDs that may be evidence of a major paleoearthquake, as summarized in this article.

Recognizing a regional MTD signature

To recognize the presence of a possible regional MTD signature in the Barlow-Ojibway basin, sets of "event horizon" maps were compiled using data from sub-bottom geophysical surveys at Dasserat, Duparquet, and Dufresnoy lakes (Fig. 1b). An individual event horizon map depicts the MTD(s) that occur at a specific stratigraphic level within a study area (e.g. Fig. 2a). Each map may contain a single, or multiple, MTD(s), depending on the deposits present at that stratigraphic level. Where two or more MTDs are depicted on a given map, the deposits are the same age. In total, 26 event horizon maps were compiled for the Dasserat (five), Duparquet (13), and Dufresnoy (eight) study areas, which are located 24 to 38 km apart (Fig. 1b; Brooks 2016; 2018).

To establish chronology for the event horizon maps, core samples were collected targeting sequences of glaciolacustrine sediments overlying the MTDs depicted on the individual maps (see Brooks 2016, 2018). The recovered glaciolacustrine sediments were composed of clastic rhythmic couplets, interpreted to be annual varves, which are widespread throughout the Barlow-Ojibway basin (Antevs 1925). A composite varve series was compiled for each study area by correlating overlapping varve thickness patterns between the core sampling sites. Each composite series was then correlated to a published regional series of varve thickness data compiled for the Barlow-Ojibway basin (see Breckenridge et al. 2012). Known as the Timiskaming varve series, the regional series consists of about 2100 varves that are numbered individually from varve (v) v1 (oldest) to ~v2100 (youngest). Applying the regional series numbering to the three study areas, varves provided common numbering for stratigraphically equivalent (or nearly equivalent) couplets, as exemplified in figure 2d. Since each varve is an annual deposit, the Timiskaming series also represents a high-resolution, relative chronology consisting of varve years that are numbered identically to the varve deposits, e.g. v1528 is the couplet deposited in varve year (vyr) 1528. The varve year numbering does not correspond to BP years, but the ~2100 vyr range falls within the 11.0–8.2 kyr cal BP duration of the glacial lake.

The varve age of the MTD(s) on each event horizon map is interpreted to be the varve year immediately prior to the number of the first complete couplet in the varve sequence overlying the MTD (see Fig. 2d). This first overlying varve represents fully restored varve sedimentation during the year following the MTD, which would have interrupted varve formation. Remarkably, the varve chronology revealed that the event horizon map containing the greatest number of, and most widely distributed, MTDs within each study area have identical ages of vyr 1483 (equivalent to about 9.1 kyr cal BP; Fig. 2a-c; Brooks 2018). The high precision of the interpreted vyr 1483 ages is apparent in figure 2d from the consistency of the varve numbering and thickness patterns within the v1484–v1528 sequence between the study areas. Key to this precision is the identification of v1528, a distinctive, easily recognized, marker varve in the Barlow-Ojibway basin (see Breckenridge et al. 2012). The MTDs on the three vyr 1483 event horizon maps are clearly part of a widespread MTD signature.

Investigation at Chassignolle and Malartic lakes extended the vyr 1483 signature further to the east (Fig. 1b). Here, coring targeted MTDs overlain by varves with reflection patterns in sub-bottom geophysical profiles that were similar to the reflection patterns overlying the vyr 1483 MTDs in the Dasserat, Duparquet, and Dufresnoy study areas. The interpreted varve ages for the respective MTDs in sediment cores from
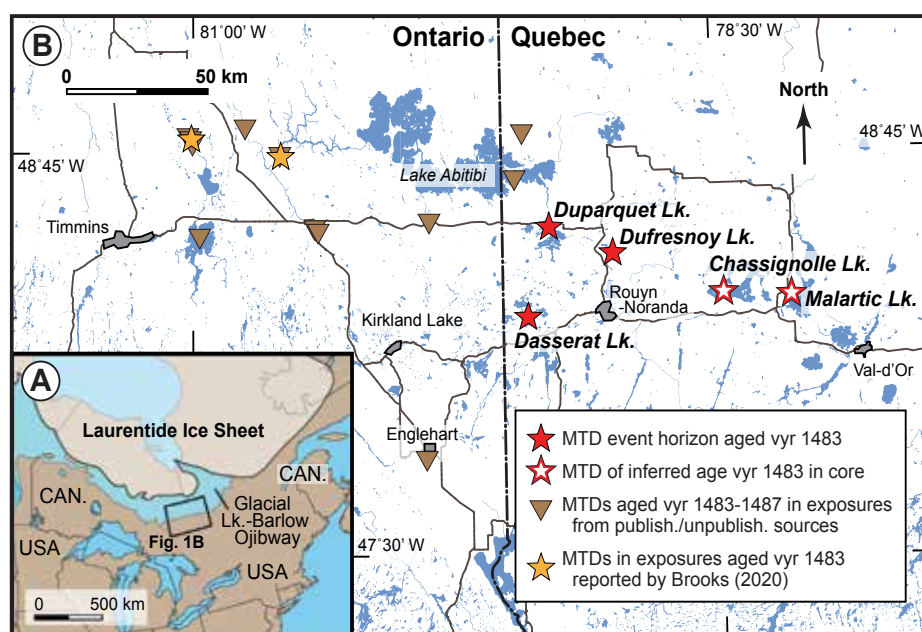
Figure 1: (A) Map showing the study area and regional environmental setting at 8.98 kyr cal BP (modified from Dyke 2004). **(B)** Map showing the distribution of sites comprising the vyr 1483 MTD signature in western Quebec-northeastern Ontario. Modified from Brooks (2020).
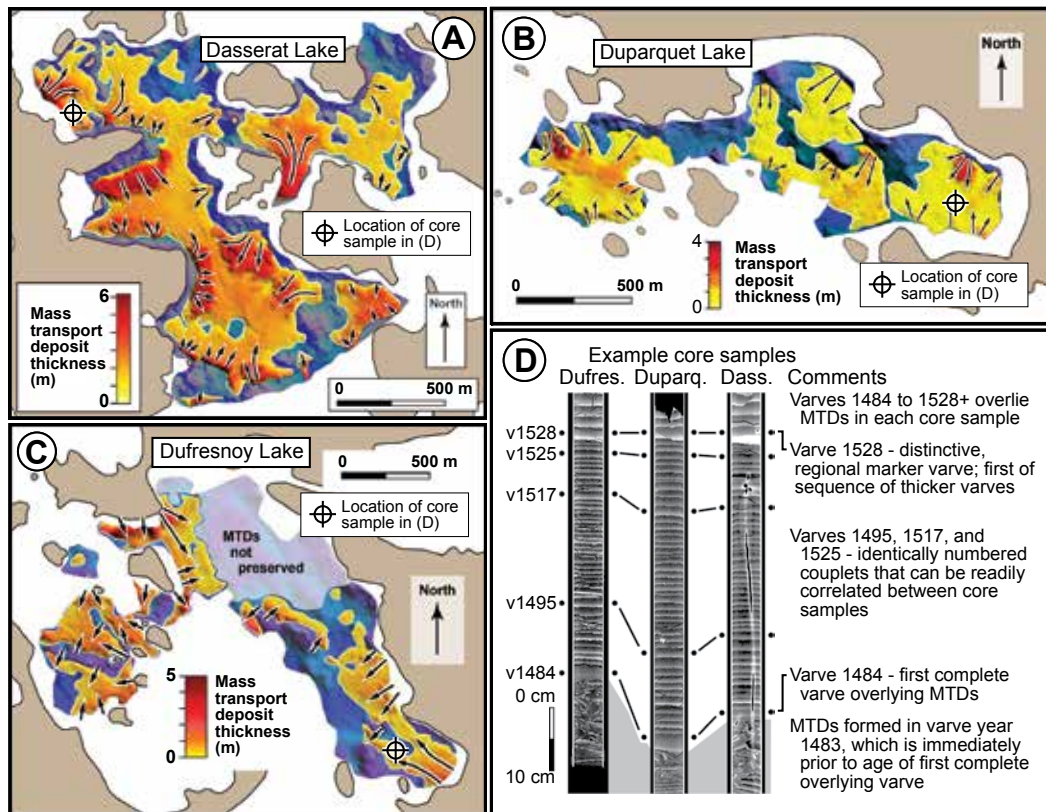
Figure 2: Event horizon maps showing the vyr 1483 MTDs at the Dasserat **(A)**, Duparquet **(B)**, and Dufresnoy **(C)** study areas. **(D)** CT-scan radiograph images of core samples showing the varve sequences overlying the vyr 1483 MTDs at each study area. Modified from Brooks (2020).

Chassignolle and Malartic lakes, however, are vyr 1485 rather than vyr 1483. Brooks (2020) attributed this slight age difference to varve counting that did not recognize two thin rhythmic couplets between the MTDs and v1528 in these sediment cores. He thus inferred that the vyr 1483 MTD signature is present in Chassignolle and Malartic lakes.

The signature was extended further to the west and southwest of Dasserat, Duparquet, and Dufresnoy lakes using published and unpublished records of varve sequences that overlie MTDs in subaerial outcrops of glaciolacustrine deposits (Fig. 1b). The varve numbering in these sequences revealed three sites with MTDs aged vyr 1483 and nine sites with MTDs aged between vyr 1484–1487 (Brooks 2020). To assess whether the latter differences were significant or not, outcrops were examined at two locations near sites where the published/unpublished logs suggest slightly younger MTD ages (Fig. 1b). At both exposures, careful varve counting relative to v1528, the regional marker varve, confirmed the vyr 1483 ages for the MTDs (Brooks 2020). This indicates that the slightly younger ages probably reflect differences in varve counting over what are deemed to be vyr 1483 MTDs. Overall, collectively, there is strong stratigraphic and chronologic evidence for a regional MTD signature that extends across at least 220 km of the glacial Lake Barlow-Ojibway basin (Fig. 1b) and which formed in vyr 1483 (about 9.1 kyr cal BP).

Origin of the MTD signature
Shaking from a significant paleoearthquake can readily explain the triggering of the vyr 1483 regional MTD signature, but plausible aseismic mechanisms also need

to be considered. Brooks (2016, 2018, 2020) assessed aseismic mechanisms relative to a deep water, distal glaciolacustrine depositional environment consistent with the regional setting at that time (Fig. 1a). Candidate aseismic mechanisms were: i) overloading-oversteepening of slopes from high glaciolacustrine sedimentation rates, ii) grounding of icebergs, iii) wave actions during major storms on the lake, and iv) rapid, major drawdown of lake level. The first three mechanisms could certainly trigger failures, but none seems likely to generate them over the scale of the regional MTD signature within a single varve year (see Brooks 2016, 2020). A rapid, major drawdown event resulting in the extensive exposure of lake-bottom sediments, however, is a viable mechanism. This would generate high pore-water pressures within the poorly draining silt and clay glaciolacustrine sediments, undoubtedly triggering widespread failures across the glacial lake basin (Brooks 2020).

Godbout et al. (2020) identified two drawdowns of glacial Lake Barlow-Ojibway that represent late stage (between vyr 1877–2065) and final (vyr ~2129) drainage events of the lake. Both are interpreted from anomalous sediment textures and structures within, or immediately overlying, the varve sequence. In contrast, Brooks (2020) reported there is nothing remarkable about the thickness and texture of v1483 relative to the immediately under- and overlying varves that might indicate a drainage event. This lack of evidence thus excludes the draw-down mechanism as an explanation for the regional MTD signature.

By a process of elimination, the regional MTD signature in vyr 1483, or about 9.1 kyr cal BP, was hypothesized to be best explained by a strong paleoearthquake. Brooks (2020) estimated a minimum magnitude of M_w ~7.3 for this paleoearthquake, using a relationship between the area affected by earthquake-triggered landsliding and moment magnitude from Keefer (2002). Fundamental to establishing this paleoearthquake hypothesis is the high-precision varve chronology used to define the regional MTD signature, and which indicates that the signature formed within a single varve year.

REFERENCES
Antevs E (1925) Geol Surv Can Memoir 146, 142 pp

Breckenridge A et al. (2012) Quat Int 260: 43-54

Brooks GR (2016) Quat Res 86: 184-199

Brooks GR (2018) Sedimentology 65: 2439-2467

Brooks GR (2020) Quat Sci Rev 234: 106250

Brouard E et al. (2021) Quat Sci Rev 274: 107269

Dyke AS (2004) In: Ehlers J et al. (Eds) Developments in Quaternary Science 2: 373-424

Godbout PM et al. (2020) Quat Sci Rev 238: 106327

Keefer DK (2002) Sur Geophys 23: 473-510

Veillette JJ (1994) Quat Sci Rev 13: 945-971

Vincent JS et al. (1979) Geol Surv Can Bull 316, 18 pp

Seismites as new indicators of regional tectonism

Yin Lu

By linking paleoearthquakes and fault-zone rupture behavior with regional deformation, long-term seismite records can provide a fresh perspective for understanding regional tectonism.

Problematic sedimentary indicators of tectonism

Sharp increases in sediment accumulation rates and grain sizes around most steep mountain ranges, such as the Rocky Mountains, have been interpreted to result from intensive tectonic activity (Blackstone 1975). Using similar arguments, previous studies have inferred intensive tectonic activity in NE Tibet during the time interval ~4.5–1.7 Ma (Li et al. 1979; Zheng et al. 2000). However, these interpretations have been challenged by others who argue that the sedimentary evidence used to infer tectonism could be climatically induced (Molnar and England 1990; Peizhen et al. 2001).

Since erosion may be enhanced either by intense tectonic activity or by high-amplitude climate change, some form of independent evidence or sedimentary criteria is required to distinguish between the two alternatives. Seismite –sedimentary units preserved in subaqueous stratigraphic sequences that are caused by earthquake shaking (Seilacher 1969)– are potential indicators of regional tectonic activity. Here, a case study from the Qaidam Basin (NE Tibet) is used as an example to show the potential of this option (Lu et al. 2021).

Drilling for seismites in NE Tibet

The Qaidam Basin is the largest topographic depression in Tibet. It was formed by the ongoing India-Asia collision and bounded by the Altyn Tagh Fault on the west and the Kunlun Fault on the south (Tapponnier et al. 2001) (Fig. 1b). The late Cenozoic northeastward growth of Tibet, and the propagation of deformation along the Kunlun Fault, formed a series of NW-trending folds in the basin. One such fold is the Jianshan Anticline, which is linked to a shallow thrust that developed beneath the paleo-Qaidam lake floor since the Oligocene (Lu et al. 2021) (Fig. 1b). The crest of the anticline has been in a shallow lake environment since ~3.6 Ma, and finally dried up at ~1.6 Ma (Lu et al. 2015). Late Cenozoic regional deformation may have been recorded by the continuous lacustrine sedimentary sequence accumulated above the anticline.

A 723 m deep Core SG-1b (SG: Sino-German) was drilled on the crest of the Jianshan Anticline in 2011 (Fig. 1c). The core section consists of laminations, layered mud, massive mud, marl, ooids, and mud containing evaporites (Lu et al. 2020a). Four types of seismites have been identified in Core SG-1b. A 2 Myr long seismite record was recovered based on the upper 260 m (3.6–1.6 Ma) of the drill core (Lu et al. 2021).

Types of seismites

Type I: in situ soft-sediment deformations. These are observed within laminated (mm scale) and layered (cm scale) sediments, featured by layer-parallel displacements (Fig. 2a–b). They are formed in situ since no erosional base is observed. Gravitational instability (mechanism for overloading; Owen et al. 2011) and Kelvin-Helmholtz instability (mechanism for layer-parallel displacement; Lu et al. 2020b) are the most common driving mechanisms for soft-sediment deformations.

The layered and laminated sediments are not susceptible to gravitational instability (requires inverted density) due to their stable density structures. No soft-sediment deformations are observed beneath dense sand layers. Further, these deformations show no association with ooid layers (indicating strong marine waves) and tempestites (indicating storms), and are thus not triggered by strong waves or storms.

Similar to in situ soft-sediment deformations observed in tectonically active regions, such as the Dead Sea (Lu et al. 2020b) and California (Sims 1973), the deformations observed in the Qaidam drill core are interpreted as seismites. Earthquake-triggered Kelvin-Helmholtz instability is the most plausible mechanism for these deformations (Lu et al. 2021).

Type II: Micro-faults. These are characterized by millimeter- to-centimeter-scale displacements (Fig. 2c) and developed within layered and laminated sediments which have stable density structures. Also, no micro-faults are observed beneath sand layers. Thus, these micro-faults are unlikely to be induced by gravitational loading. In addition, the micro-faults are not confined to the edge of the drill core, and thus, are unlikely to be triggered by drilling disturbance.

Micro-faults are usually the result of brittle deformation induced by high strain rates,
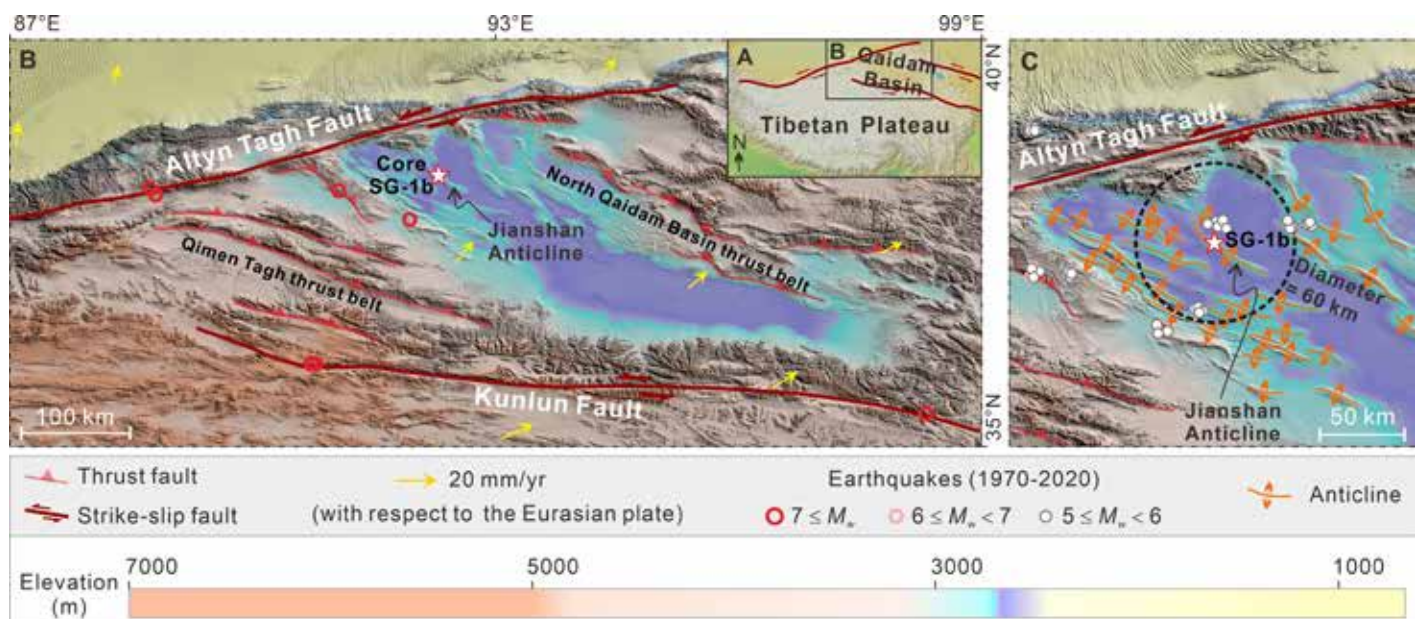
Figure 1: Geological setting of the study area (modified from Lu et al. 2021). **(A-B)** Location of Qaidam Basin and major faults. **(C)** Folds-thrusts system, drill site, and seismicity within the basin. Figure reused under the CC-BY-4.0 license.
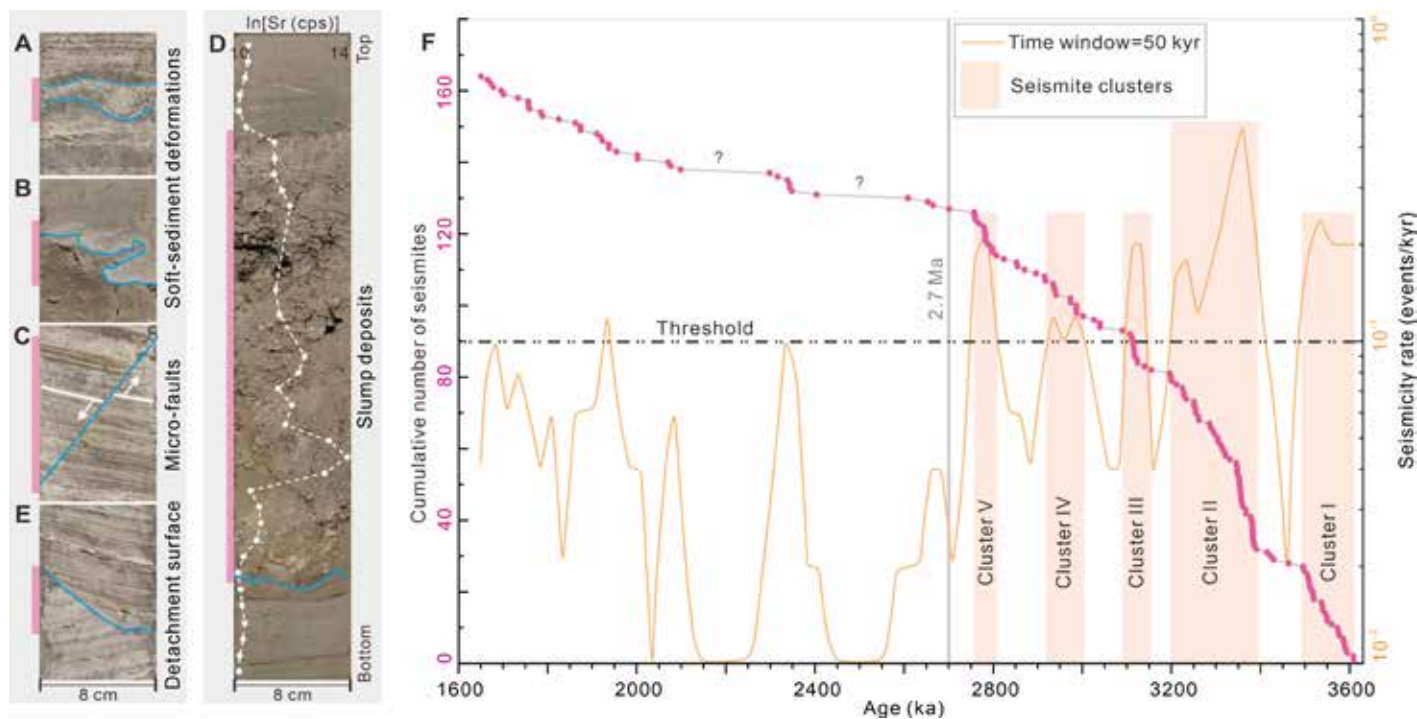
Figure 2: A 2 Myr long seismite record (modified from Lu et al. 2021). **(A-E)** Four types of seismites; **(A-B)** Soft-sediment deformations; **(C)** Micro-fault; **(D)** Slump deposits; **(E)** Detachment surface. Sr counts in **(D)** were measured using an XRF-core scanner, showing the variation in evaporite elements; cps: count per second. **(F)** A 2 Myr seismite record and distribution of five seismite clusters during the time interval 3.6–1.6 Ma. Figure reused under the CC-BY-4.0 license.

and are commonly triggered by seismic shaking (Seilacher 1969). Thus, these Qaidam micro-faults are interpreted as seismites.

Type III: Slump deposits. These are characterized by deformed laminations or mud layers with a high content of evaporite (as indicated by Sr content shown as a dashed white line in Fig. 2d). They are mainly sourced from the crest of the Jianshan Anticline. The crest of the anticline has very gentle slope gradients (<1°) and lacks coarse particles, thus making gravitational sliding or sediment overloading unlikely. Under such conditions, seismic shaking is the most plausible trigger for these slump deposits.

Type IV: Detachment surfaces. These are characterized by having had sharp contact with underlying sediment layers (Fig. 2e). These structures are interpreted as head scarps of earthquake-triggered slumps.

A 2 Myr long seismite record and implications

In total, 34 soft-sediment deformations, 79 layers with micro-faults, 41 slump horizons, and 10 detachments have been identified in Core SG-1b during the time interval 3.6–1.6 Ma. Since sedimentation rate between 2.7–2.1 Ma and coring rate during the 2.1–1.6 Ma period are relatively low, fewer earthquakes have been recorded in Core SG-1b. Thus, the seismite record of 2.7–1.6 Ma was not considered for further analysis. Moreover, the maximum seismicity rate during the 2.7–1.6 Ma period (~10^{-1} events/kyr) is used as a threshold for identifying earthquake clusters from the rest of the record (Fig. 2f). The seismite record during the time interval 3.6–2.7 Ma comprises five paleoearthquake clusters, with a mean recurrence rate of 6.8 kyr. In contrast, the mean recurrence rate within the clusters ranges between 4 and 6 kyrs.

Usually, earthquake moment magnitude (M_w) >5 (or shaking intensity >IV) is required to form a seismite (Lu et al. 2021). Two potential source regions of these recorded paleoearthquakes are discussed in the literature (Lu et al. 2021): one proximal source area within 60 km (5< M_w <6.6) and one distal source with distances >70 km (6.6< M_w <8). Applying these findings to the study site, the potential source could be either the proximal Jianshan Anticline and its surrounding folds-thrusts system, or more distal Kulun, and Altyn Tagh strike-slip faults. Large earthquakes occurred on the distal Kulun and Altyn Tagh strike-slip faults show a much shorter recurrence (~1 kyr; Van Der Woerd et al. 2002; Yuan et al. 2018) compared to those in Core SG-1b (6.8 kyr). Thus, the former is more likely the major source for the recorded paleoearthquakes at the SG-1b drill site. Therefore, the clustered seismite record during the 3.6–2.7 Ma period points to a clustered rupture behavior of the folds-thrusts system within the basin during that time interval, and thus indicates episodic deformation in the region. Such clustered rupture behavior further implies that the regional deformation is focused more in the folds-thrusts system within the basin during the earthquake clusters, while more deformation is concentrated along the strike-slip faults that bound the basin during the intervening quiescent periods (Lu et al. 2021).

Outlook

By applying the subaqueous paleoseismology method, we are able to discriminate tectonic-induced sedimentation from climate-forced deposits in a sedimentary sequence. This study case from NE Tibet highlights the great potential of using seismites to understand the history of regional seismo-tectonic deformation. The innovative method may also be suitable for similar tectonically

active regions elsewhere in the world. Such research provides a fresh perspective for understanding regional tectonism by linking paleoseismic events and fault zone rupture behavior, with regional deformation, which can expand the ability of paleoseismology to understand regional deformation.

AFFILIATION

State Key Laboratory of Marine Geology, Tongji University, Shanghai, China

CONTACT

Yin Lu: yinlu@tongji.edu.cn

REFERENCES

Blackstone Jr D (1975) Geological Society of America Memoirs 144: 249-279

Li JJ et al. (1979) Science China (in Chinese) 9: 608-616

Lu Y et al. (2015) Sediment Geol 319: 40-51

Lu Y et al. (2020a) Paleoceanogr Paleoclim 35: PALO20864

Lu Y et al. (2020b) Sci Adv 6: eaba4170

Lu Y et al. (2021) Geophys Res Lett 48: e2020GL090530

Molnar P, England P (1990) Nature 346: 29-34

Owen G et al. (2011) Sediment Geol 235: 133-140

Peizhen Z et al. (2001) Nature 410: 891-897

Seilacher A (1969) Sedimentology 13: 155-159

Sims JD (1973) Science 182: 161-163

Tapponnier P et al. (2001) Science 294: 1671-1677

Van Der Woerd J et al. (2002) Geophys J Int 148: 356-388

Yuan Z et al. (2018) Earth Planet Sci Lett 497: 193-203

Zheng H et al. (2000) Geology 28: 715-718

Combining remote sensing, geophysics and paleoseismology to study earthquakes on the Idrija Fault in Slovenia

Christoph Grützner

Slow faults only rarely produce large earthquakes, we often know little about their past activity, and they are difficult to study. Here, I show how using a combination of different tools helps to reveal past fault-surface ruptures in Slovenia.

Slow-moving faults are difficult beasts
Faults with high slip rates of several millimeters, or even centimeters, per year can host large earthquakes with typical recurrence intervals of a few hundred years. Good examples are the Alpine Fault in New Zealand, the North Anatolian Fault in Türkiye, or the San Andreas Fault System in California (e.g. Onderdonk et al. 2018). Living in such regions comes with the obvious problem of frequent strong quakes. However, perhaps surprisingly, there is also good news: people know about the seismic hazard because the last strong event was not long ago, and they are usually prepared. Chile, for example, was struck by a subduction earthquake moment magnitude (M_w) 8.8 in 2010, yet less than 600 people lost their lives—remarkable for the sixth strongest earthquake ever measured. The same is true for Japan. Slow-moving faults, on the other hand, cause infrequent strong quakes (Liu and Stein 2016). We saw this in Morocco on 8 September 2023, when an earthquake of M_w 6.8 occurred in a region of low instrumental and historical seismicity, and tragically caused thousands of deaths. In fact, more people have been killed by earthquakes in continental interiors than by those that occurred on plate boundaries (England and Jackson 2011).

Apart from the issues with estimating the seismic hazard of areas that are slowly deforming, slow faults come with another problem: their movement often leaves only subtle traces in the landscape because it is outpaced by other processes such as erosion, sedimentation and modification by humans. Studying their tectonic activity, slip rate etc. can, therefore, be very difficult (Diercks et al. 2023; Grützner et al. 2017).

The Idrija Fault in Slovenia
In the framework of the German Priority Program "SPP2017 – Mountain Building Processes in 4D" we looked into the tectonic activity of the Alps-Dinarides junction (Fig. 1). Here, the northward motion of the Adriatic Plate of about 2–3 mm/yr, with respect to stable Europe, is accommodated by a strike-slip fault system in Western Slovenia. The system is made up of at least four major faults and several smaller ones. They strike NW–SE and are parallel to each other (Fig. 1). Seismicity is low to moderate and only one of these faults had strong instrumental earthquakes

of magnitudes M_w 5.7 and M_w 5.2 in 1998 CE and 2004 CE, respectively. Swarm activity, however, has been proven for the largest faults (Vičič et al. 2019).

A destructive earthquake in 1511 CE devastated the city of Idrija, back then an important mercury mining town. Still, there is debate as to whether this quake occurred on the Idrija Fault, the longest fault of the system (~100 km), or on another fault in Italy (Falcucci et al. 2018; Fitzko et al. 2005). The quake's magnitude was perhaps close to M_W 7. Because of the slow motion of Adria, individual faults in our study area have low slip rates, probably not exceeding 1 mm/yr (Atanackov et al. 2021; Grützner et al. 2021; Moulin et al. 2016). This, in return, means that it may take thousands of years before enough strain is accummulated to be released in a major earthquake in which the fault slips by a meter or more, and which breaks the surface. One therefore has to go beyond the instrumental and historical record to investigate the Idrija Fault's earthquake history.

While a few studies could prove fault activity during the Late Quaternary and estimated the slip rate, only one attempt has

been made to date the last major earthquake on the fault by paleoseismological trenching—that is, excavating the fault zone and dating offset or deformed geological layers (Bavec et al. 2013). The results of this study imply that the Idrija Fault ruptured in 1511 CE. But how often do these large earthquakes happen? In order to find out, we decided to open another paleoseismological trench across the fault, but choosing the right place is not an easy task.

Combining different methods helps to reveal past earthquakes
A suitable trench site needs to fulfill a couple of prerequisites. First, there needs to be young geological units that have recorded fault motion. We therefore had to find a site with Late Quaternary sediments and constant sediment input. The idea is that dating the youngest deformed units and the oldest non-deformed units enables bracketing the date of the earthquake. Second, we need to find sediments that can actually be dated by radiocarbon, luminescence, or other methods. Third, the trench needs to hit the actual fault zone. Fourth, the logistics must work: Can I reach the site with an excavator? Is the site within a National Park? Does
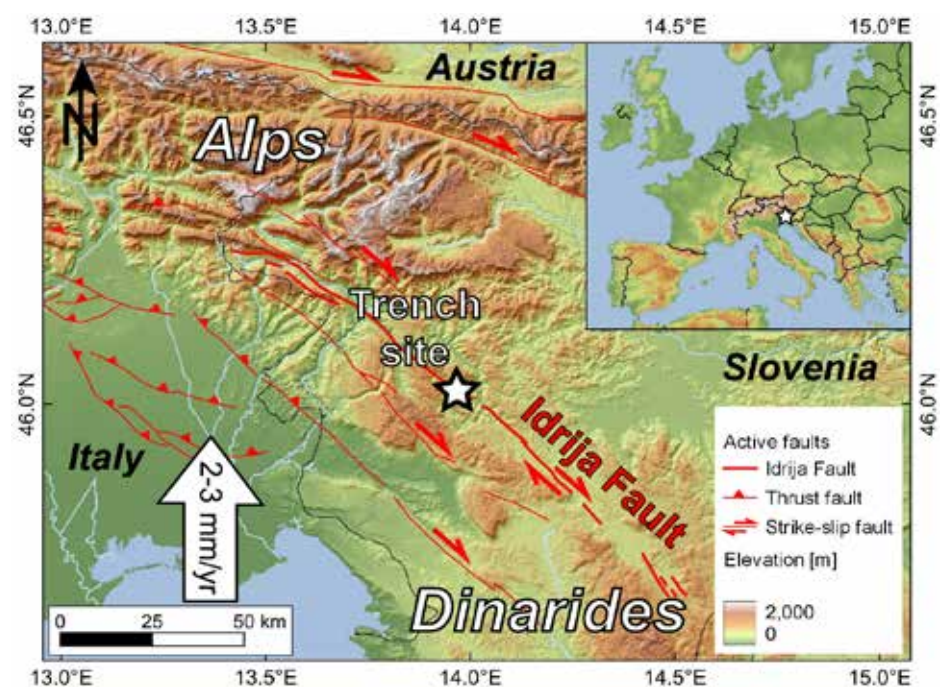
Figure 1: Map of the study area in Slovenia. Faults (simplified) in red, the Idrija Fault in bold. Adria moves north with respect to Eurasia with 2–3 mm/yr.

the landowner agree? Will I need to pump groundwater?

After mapping the fault trace using a 1 m digital elevation model created from airborne laserscanning data (ARSO 2015), we ran an extensive geophysics campaign and collected kilometers of georadar and geoelectrics profiles across the fault.

One site fulfilled all requirements—a small basin on the fault trace with a strong contrast of resistivities in the subsurface (Fig. 2a). This contrast indicates that two different types of rocks are juxtaposed, in this case probably bedrock and basin fill, which hints at a tectonic origin of the basin. We opened a 20 m long trench exposing coarse fluvial deposits and channels filled with fine-grained sediment (Fig. 2b). The exposure was cleaned, gridded and photographed in detail. We identified different sediment units based on color, grain size and lithology, and we sketched the entire trench at a scale of 1:10. We found hints for faulting in a zone right on top of the resistivity contrast (Fig. 2c–d). Several fine-grained layers (U4, U6, U8; Fig. 2b) terminate abruptly, indicating they were cut by fault motion. We found a dark gray, funnel-shaped unit (U9) that we interpreted as a fissure filled with material rich in organics (Fig. 2d). Such fissures are commonly observed in strike-slip earthquakes (e.g. Quigley et al. 2010).

On the opposite trench wall, and again right on the projected fault trace, we encountered pebbles that were vertically aligned. Their long axis is vertical instead of (sub-)horizontal, as in undistorted sediments. Such an arrangement is known to be associated with shear motion and has been observed in other strike-slip fault zones (e.g. Zabcı et al. 2017). Finally, a large fractured clast testifies to abrupt fault motion or intense shaking. Since this is the only fractured clast out of hundreds in the trench, localized fault slip is a much more likely explanation. Nowhere else in the trench, other than this narrow zone, did we observe vertically aligned pebbles, abruptly terminating layers, broken clasts, or filled fissures. We sampled pieces of charcoal and bulk organic material for radiocarbon dating. All the units affected by faulting are ca. 2000–2600 years old (U3, U4, U6, U8). The fill of the fissure is not younger than 2300 years and overlain by younger, unfaulted sediments. This means that the last fault motion here happened between 2.3–2.6 kyr cal BP, because the sediments affected by faulting are ca. 2600 years old, and the filling of the fissure must have happened after it opened during the earthquake.

Lessons learned
Our trench shows that the last surface-rupturing earthquake on this fault strand pre-dates the 1511 CE event. This does not mean that the 1511 CE earthquake did not happen on this fault, but we see no evidence for it. Another strand could have moved, or the movement at our trench site
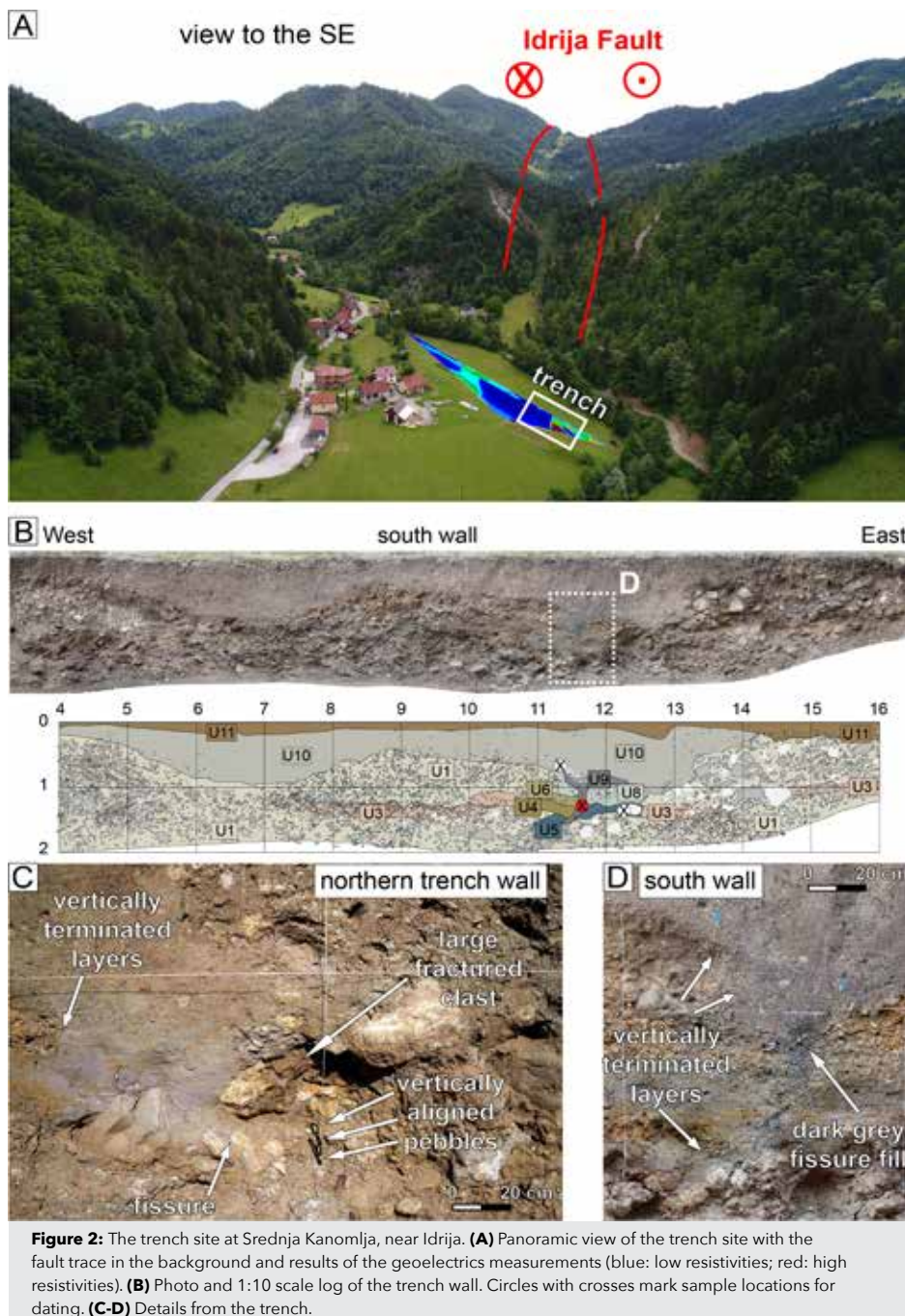
Figure 2: The trench site at Srednja Kanomlja, near Idrija. **(A)** Panoramic view of the trench site with the fault trace in the background and results of the geoelectrics measurements (blue: low resistivities; red: high resistivities). **(B)** Photo and 1:10 scale log of the trench wall. Circles with crosses mark sample locations for dating. **(C-D)** Details from the trench.

could have been too small to be detectable. It is not rare for slip to vary significantly along the strike of a fault. Our example illustrates that a combination of different-techniques can help to look into a slow fault's earthquake history. High-resolution elevation data helped us map the fault, geophysics allowed narrowing down the best trench site, and paleoseismic trenching combined with radiocarbon dating revealed the age of the last surface-rupturing earthquake (Grützner et al. 2021).

AFFILIATION
Institute for Geosciences, Friedrich-Schiller University Jena, Germany

CONTACT
Christoph Grützner: christoph.gruetzner@uni-jena.de

REFERENCES

ARSO (2015) Slovenian Environment Agency lidar data

Atanackov J et al. (2021) Front Earth Sci 9: 604388

Bavec M et al. (2013) Evidence of Idrija fault seismogenic activity during the Late Holocene including the 1511 Mm 6.8 earthquake. 4th International INQUA Meeting on Paleoseismology, Aachen, Germany

Diercks ML et al. (2023) Geomorphology 440: 108894

England P, Jackson JA (2011) Nat Geosci 4: 348-349

Falcucci E et al. (2018) Solid Earth 9: 911-922

Fitzko F et al. (2005) Tectonophysics 404: 77-90

Grützner C et al. (2017) Earth Plan Sci Lett 459: 93-104

Grützner C et al. (2021) Solid Earth 12: 2211-2234

Liu M, Stein S (2016) Earth-Sci Rev 162: 364-386

Moulin A et al. (2016) Tectonics 35: 10: 2258-2292

Onderdonk A et al. (2018) Geosphere 14: 2447-2468

Quigley M et al. (2010) Bull New Zealand Soc for Earthquake Eng 43: 236-242

Vičič B et al. (2019) Geophys J Int 217: 1755-1766

Zabcı C et al. (2017) J Seismology 21: 1407-1425

Paleoseismic studies reveal the high seismic hazard potential of the Matano Fault, Sulawesi, Indonesia

Adi Patria and Mudrik R. Daryono

The Matano Fault in Sulawesi, Indonesia, has remained unruptured for the last two centuries. However, paleoseismic investigations reveal a seismic hazard potential as large as that of the M_w 7.5 Palu earthquake in 2018 CE.

Background

Sulawesi, Indonesia, is an actively deforming region with intense seismicity due to the rapid convergence between the Eurasian, Pacific, and Australian plates (Fig. 1; Bock et al. 2003). The most recent surface-faulting event was the 2018 CE M_w 7.5 Palu earthquake that ruptured a ~170 km long portion of the Palu-Koro Fault in central Sulawesi, and caused massive destruction in Palu City and surrounding areas (Natawidjaja et al. 2021). A question has been raised about the seismic hazard of Sulawesi. Where are the next large earthquakes (M_w ≥7) likely to occur?

The Matano Fault is the southeastern extension of the Palu-Koro Fault. This fault has the considerable capability of producing large earthquakes (Center of National Earthquake Study (PuSGeN) 2017; Watkinson and Hall 2017). The fact that no historical report about large earthquakes on the fault is available indicates that the fault has remained unruptured for at least two centuries, and has been storing enough slip (energy) to be released for the next surface-rupturing earthquakes. To date, the largest modern seismicity on the Matano Fault was the 2011 CE M_w 6.1 earthquake near Lake Matano.

The left-lateral motion in eastern Indonesia, due to the fast westward motion of the Pacific plate relative to the Australian plate, is accommodated by the Palu-Koro and Matano faults in Sulawesi (Fig. 1). The Palu-Koro Fault slips at ~ 40 mm/yr (Socquet et al. 2006) while the Matano Fault moves at ~20 mm/yr (Khairi et al. 2020; Walpersdorf et al. 1998). These motion rates are comparable to the San Andreas Fault's motion in the US, at ~30 mm/yr (Sieh and Jahns 1984). However, limited fundamental geological information on the Matano Fault, such as history of large seismic events, the potential maximum magnitude and the extent of surface-rupturing earthquakes, has been a significant barrier to evaluating the seismic hazard posed by the fault.

Recent paleoseismic investigations that examine the relationship between stratigraphy and fault structures at the shallow subsurface have revealed the seismic behaviors of the Matano Fault, which is helpful to better mitigate seismic hazards for the areas near the fault (i.e. Daryono et al. 2021; Patria et al. 2023).

Seismic behaviors of the Matano Fault

The Matano Fault traverses central Sulawesi for ~190 km in a NW-SE direction and consists of six geometric segments separated by structural discontinuities (Fig. 1). The first evidence of surface-rupturing earthquakes in the past on the Matano Fault was revealed by Daryono et al. (2021), who found evidence of two seismic events dated to ~4200–3000 BCE on the fault segment east of Lake Matano (Loc. 1 in Fig. 1). Geomorphic reconstruction by Daryono et al. (2021) also indicated a total left-lateral offset of ~400 m due to the fault motion. The Matano Fault has repeatedly moved and produced M_w 7-class earthquakes, rupturing multi-fault segments, similar to the 2018 M_w 7.5 Palu earthquake (Daryono et al. 2021).

A recent study by Patria et al. (2023) investigated the easternmost portion where the
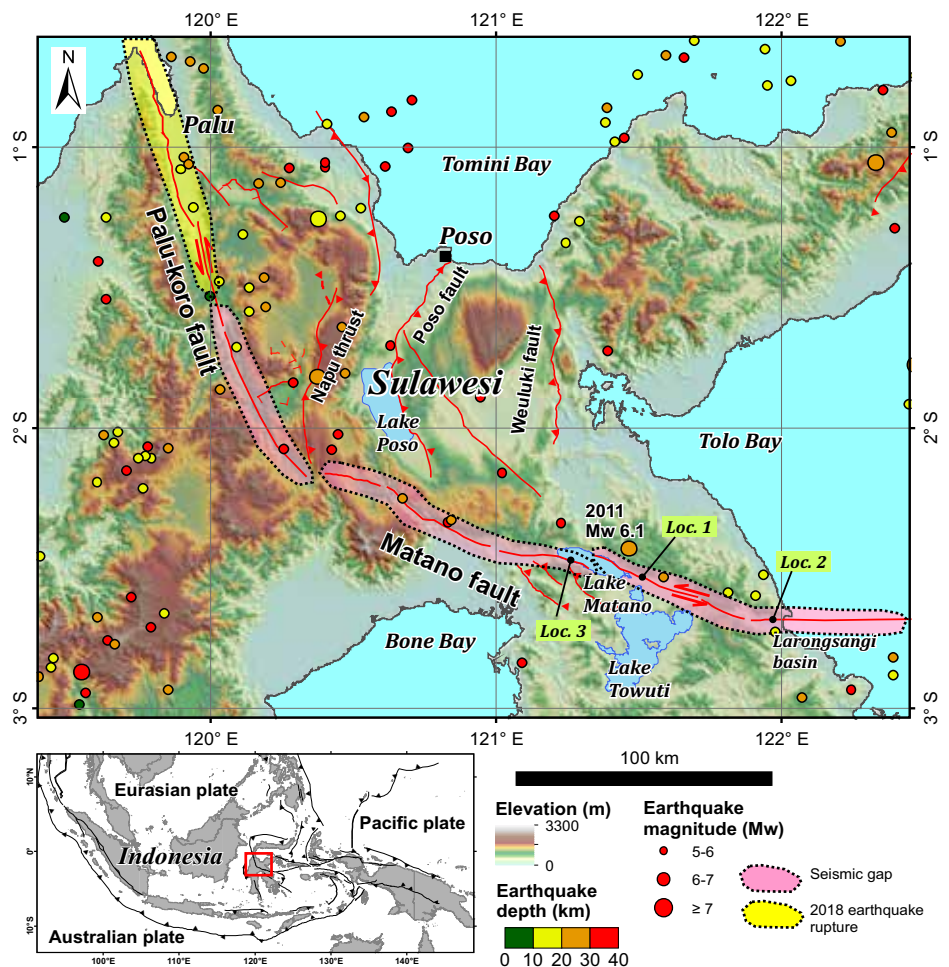
Figure 1: Active fault map of central Sulawesi with modern seismicity (modified from Center of National Earthquake Study (PuSGeN, 2017). Locs. 1, 2, and 3 indicate the locations of fault ruptures observed by Daryono et al. (2021), the paleoseimic trench by Patria et al. (2023), and submerged iron production settlement at Lake Matano (Adhityatama et al. 2022), respectively. Note that the 2018 M_w 7.5 earthquake's rupture still extends further north, beyond the map.

a)

b)
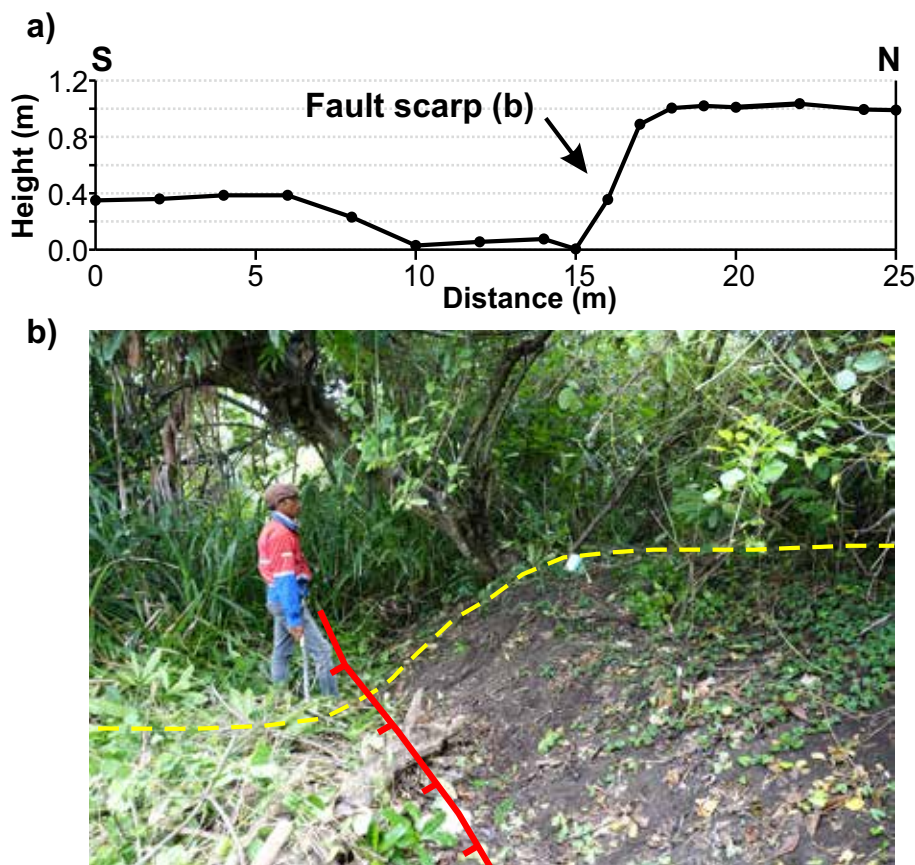
Figure 2: (A) Topographic profile and **(B)** photograph of the smallest fault scarp cutting the youngest beach ridge on the eastern Matano Fault. This geomorphic feature was interpreted as a result of a single surface-rupturing earthquake.

fault runs within a quaternary basin, called the Larongsangi basin (Loc. 2 in Fig. 1). Based on tectonic geomorphic interpretation using a high-resolution digital elevation model (DEM) generated from the LiDaR (Light Detection and Ranging) data, they mapped geomorphic features and surface traces of the Matano Fault. Along the fault, the smallest left-lateral offset was on the beach ridge, ~7 m, accompanied by a 1 m high fault scarp (Fig. 2). These features were interpreted as a result of a single earthquake because they were found on the youngest geomorphic surface.

Based on the scaling relations by Wells and Coppersmith (1994), the 7 m offset was likely caused by a M_w 7.4 earthquake rupturing a 110 km long fault. A paleoseismic trenching on a 2 m high fault scarp revealed the history of surface-rupturing earthquakes (Loc. 2 in Fig. 1). Using the trench observation and radiocarbon dating, the most recent surface-rupturing earthquake was dated between 1432–1819 CE. The penultimate and antepenultimate surface-rupturing earthquakes were constrained between 1411–1451 CE and 981–1355 CE, respectively. There were two other older earthquakes which occurred prior to 1000 CE. Therefore, based on the timing of these earthquakes, the reccurence interval was estimated at 335 ± 135 years.

Seismic hazard evaluation

Lake Matano in the center of the Matano fault occupies a 6 km wide stepover between two fault segments (Fig. 1). According to Wesnousky (2006), stepovers wider than 4 km behave as earthquake-rupture terminations for large earthquakes. Patria et al. (2023) postulated that the surface-rupturing earthquake observed in the paleoseismic trench (Loc. 2 in Fig. 1) spanned ~110 km from Lake Matano to the offshore east of the Larongsangi basin (Fig. 1). The absence of a surface-faulting event on the Matano Fault in the last two centuries suggests that the fault may have formed two seismic gaps, separated by Lake Matano, which are potential locations for the next surface-rupturing earthquakes.

Large seismic events on the Matano Fault could be devastating. Within Lake Matano, an iron production village dating back to the eighth century had submerged at a depth of 3–15 m (Loc. 3 in Fig. 1) (Adhityatama et al. 2022). This iron production site's subsidence could have been caused by catastrophic events, possibly repeated large earthquakes on the Matano Fault. For the eastern portion of the Matano Fault, the elapsed time since the most recent surface-faulting event is more than 200 years, exceeding the minimum calculated recurrence interval. Thus, the next surface-rupturing earthquake is plausibly due for the eastern portion. In addition to the shaking and ground deformation, large earthquakes on the Matano Fault, particularly the eastern portion, could cause a submarine-landslide tsunami.

Structural interpretion by Titu-Eki and Hall (2020), based on high-resolution multibeam bathymetry, indicated the existence of large submarine landslides at continental slope near the fault. Such landslides could have been triggered by strong shaking, and may have generated tsunamis.

Summary

Paleoseismic studies on the Matano Fault have revealed the history of large seismic events on the fault and the magnitude and extent of surface-rupturing earthquakes, which are helpful for seismic-hazard assessment. The Matano Fault forms two seismic gaps that could produce the next large earthquakes. Studies on the Matano Fault demonstrated the benefits of paleoseismic investigation to understand the seismic hazard posed by the fault.

In Indonesia, many active faults have been identified, but geological information on these faults is still lacking. Therefore, more paleoseismic studies are required to understand the seismic behaviors and evaluate the seismic hazard of these active faults. Subaqueous paleoseismic investigations on Lake Matano may also be useful in providing a longer and more complete record of earthquakes than the conventional paleoseismic method, as demonstrated by Tournier et al. (2023) in Lake Towuti, southeast of Lake Matano.

REFERENCES

Adhityatama S et al. (2022) Archaeol Res Asia 29: 100335

Bock Y et al. (2003) J Geophys Res 108: 2367

Center of National Earthquake Study (PuSGeN) (2017). Earthquake sources and hazards map of Indonesia 2017 (Peta Sumber dan Bahaya Gempa Indonesia Tahun 2017). Pusat Penelitian dan Pengembangan Perumahan dan Permukiman, Bandung, 376 pp (in Indonesian)

Daryono MR et al. (2021) IOP Conf Ser Earth Environ Sci 873: 12053

Khairi A et al. (2020) J Geod Undip 9: 32-42 (in Indonesian with English abstract)

Natawidjaja DH et al. (2021) Geophys J Int 224: 985-1002

Patria A et al. (2023) Tectonophysics 852: 229762

Sieh KE, Jahns RH (1984) GSA Bull 95: 883-896

Socquet A et al. (2006) J Geophys Res 111: B08409

Titu-Eki A, Hall R (2020) Indones J Geosci 7: 291-303

Tournier N et al. (2023) Quat Sci Rev 305: 108015

Walpersdorf A et al. (1998) Geophys J Int 135: 351-361

Watkinson IA, Hall R (2017) Geol Soc Spec Publ 441: 71-120

Wells DL, Coppersmith KJ (1994) Bull Seismol Soc Am 84: 974–1002

Wesnousky SG (2006) Nature 444: 358-360

Combining geological and archaeological evidence to infer the recent tectonics of the Montagne du Vuache Fault, Jura Mountains, France

Théo Lallemand[1], A. Quiquerez[2], L. Audin[1], S. Baize[3], R. Grebot[2] and M. Mathey[3]

A multidisciplinary study combining structural geology, geomorphology and archaeoseismology on a Gallo-Roman site in the Jura Mountains shows potential evidence of recent tectonic deformation along the northern Montagne du Vuache Fault. These new findings question the role of past earthquakes in the site abandonment.

Seismotectonic background of the Montagne du Vuache Fault (MVF)

The MVF is a major fault system extending over ~80 km from the edge of the Alpine range to the Jura Mountains (calcareous rocks), through the southernmost Swiss Molasse basin (sandstones and siltstones, Baize et al. 2011; Fig. 1). The recent tectonics of the MVF have been studied in its southeastern part, following the damaging Epagny earthquake near Annecy (13 July 1996; moment magnitude [Mw] 4.8; Thouvenot et al. 1998; Courboulex et al. 1999; Fig. 1a).

While Quaternary left-lateral faulting has been confirmed there (e.g. displacement of small valleys, syn-depositional deformation, Baize et al. 2011; De La Taille 2015), these studies have not yet demonstrated the occurrence of surface-rupturing events during the last thousands of years. Tracking those surface-rupture events is crucial to defining the seismic hazard related to the fault. This can be achieved by dating deformed features, either on natural or anthropogenic objects.

As the fault extends northwestward into the Jura Mountains, it splits into multiple segments. In this area, the youngest evidence of fault activity at the surface relies on syntectonic mineralized calcites, the dating of which indicates a main phase of activity at around 10 Ma followed by a reactivation phase at ~5 Ma (Smeraglia et al. 2021).

What's new along the northern section of the MVF? A morphotectonic and structural perspective

We analyzed the geomorphological imprint of the fault, based on a regional 5 m spatial resolution Digital Elevation Model (DEM), as well as a 25 cm spatial resolution DEM around the Villards d'Héria area (black square in Fig. 1a), to identify geomorphic markers (lineaments, surface fractures, watercourses, limestone beds, ridge lines, valley bottoms, and geological units), revealing horizontal displacements.

Along the MVF trace running from Annecy to the Jura Mountains, we detected 342 lineaments (Fig. 1a). About 45% of them were identified as fault segments, showing signs of kinematics, with 75% of them exhibiting left-lateral motion (red segments, Fig. 1a), predominantly in the NW-SE direction. Segments with other orientations and kinematics may be old inherited faults, or secondary faults conjugated to the main faults (black segments, Fig. 1a).

As suggested by the potentially active fault map of France (Jomard et al. 2017), the MVF signature in morphology splits as it reaches the Jura mountain range, with one section crossing the area of interest around Villards d'Héria, suggesting that the distribution of the deformation is controlled by surface lithology. Where "hard" rocks (limestones) are close to the surface, the subparallel segments are numerous (Jura domain, NW part of the fault). Conversely, fault segmentation is limited, and the geometry appears rather continuous where "soft" rocks (molasse) are dominant (Savoy area, southeastern part of the fault). A splay fault structure can thus be observed in our study area, which is located at the northwestern end of the MVF (Fig. 1a). Numerous fault segments can be observed in the morphology there (Fig. 1a). Field investigations confirmed numerous NW-SE fault planes with left-lateral, strike-slip kinematics, evidenced by calcite steps (Fig. 1b). When associated with their conjugate faults (right-lateral, NE-SW), the paleostresses accommodated by these faults can be well constrained.

A preliminary slip rate was estimated from limestone bed offsets (Fig. 1c), based on the analysis of the lineaments detected on the DEM. The displacement classification shows that the most represented classes occur between 200 m and 1000 m of cumulative horizontal displacement. Smeraglia et al. (2021) proposed that the first phase of deformation occurred at 10 Ma (onset of Jura NW-SE shortening), and that a second phase occurred at around 5 Ma, with corresponding slip rates between 0.02-0.1 mm/yr and 0.04–0.2 mm/yr, respectively. These values fall in the lower range of the slip rates proposed by Baize et al. (2011) based on regional correlations.

The Gallo-Roman site and the potential for archaeo-earthquakes

The sanctuary area of Villards d'Héria provides the ideal archaeological context for studying the cause-and-effect relationship between a faulted bedrock and deformation of archaeological remains. The sanctuaries are spread over two sites (Fig. 1c). The upper site, near Lake d'Antre (802 m asl) is bounded by the Antre Fault. The lower site, "Pont-des-Arches", in the Héria Valley (712 m asl) consists of a worship area and bathing facilities. The two sites are connected by karstic conduits (Nouvel et al. 2018), whose flow is driven by a dense fracture network. Excavations have provided evidence of continuous occupation
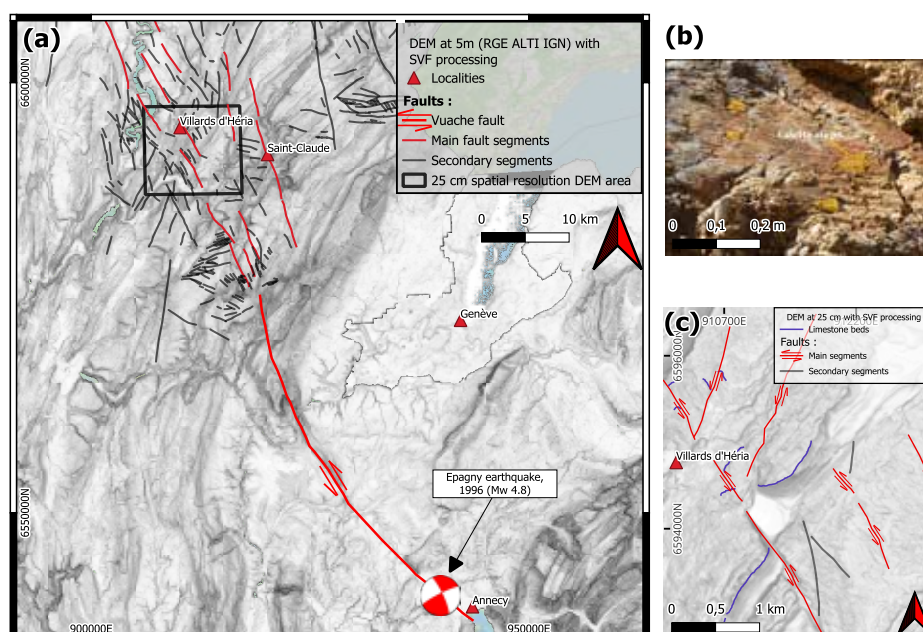
Figure 1: (A) Geomorphological imprint of the fault based on a 5 m spatial resolution DEM, and on a 25 cm spatial resolution DEM in the boxed area. **(B)** Calcite steps observed on a fault plane, here with left-lateral strike-slip kinematics. **(C)** Example of left-lateral offset across limestones along one of the main fault segments. Projected coordinate system: EPSG 2154, RGF93 / LAMBERT 93.
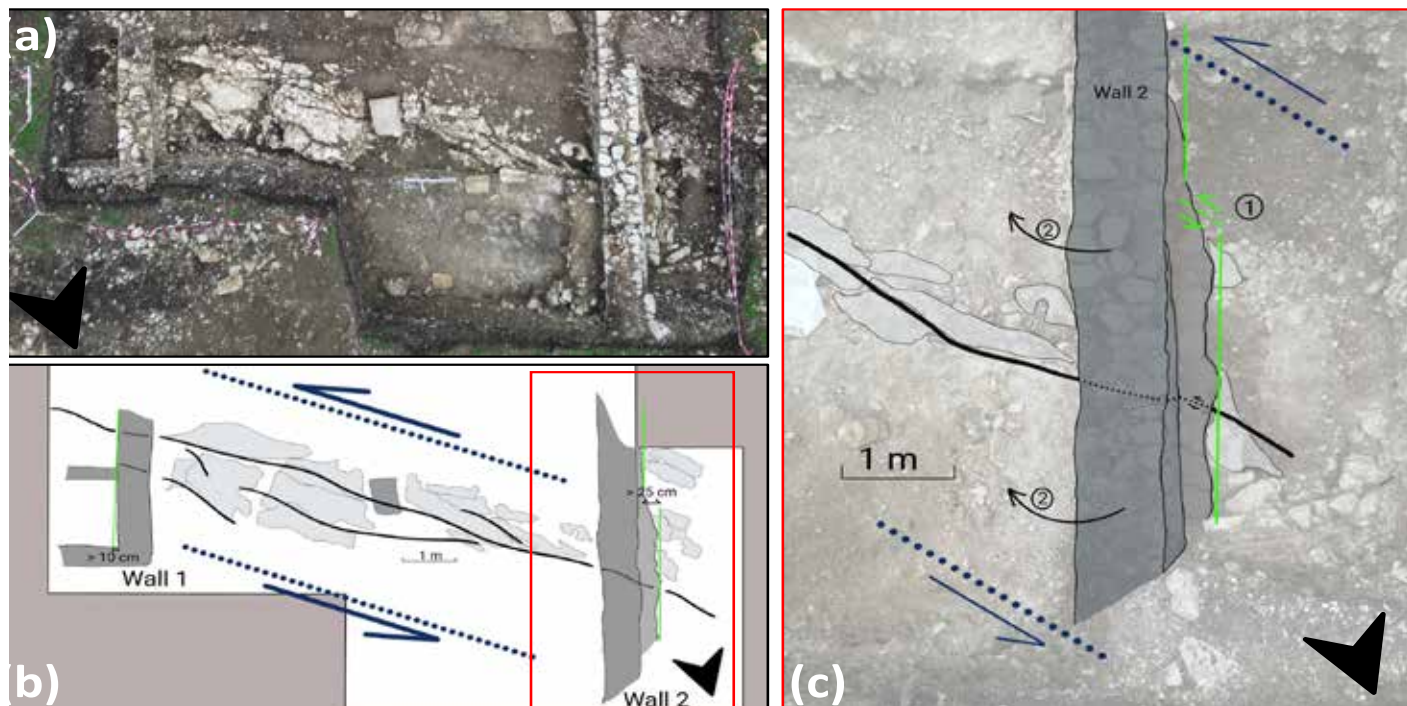
Figure 2: Area of archaeoseismological investigations. **(A)** Zenithal view of deformed walls, and **(B)** structural diagram of the faulted zone, and impacted infrastructures. **(C)** Focus (red box on (B)) on Wall 2 displaying two phases of damage: a sinistral offset at the base (phase 1), and a tilting of the structure in the upper part (phase 2).

from the first century BCE until the last decades of the third century.

In 2021, while conducting excavations at the lower site, unexpected signs of damage and disorders were identified on the archaeological remains, specifically on walls (Wall 1 and Wall 2, Fig. 2). Further exploratory field surveys in 2023 revealed that the archaeological deformation features were collocated with left-lateral kinematics in the bedrock. The facing of the two walls displays obvious misalignments, visible in both plan and zenithal views (Fig. 2b). At this point, Wall 1 exhibits a minimum left-lateral offset of 10 cm, taking the wall orientation without deformation as reference. Deformation features on Wall 2 potentially imply two phases of deformation. The base of the wall is left-laterally shifted with an offset of 25 cm (phase 1), assuming an initial straight shape when it was built (indicated by the green line, Fig. 2c). Some of the blocks are broken, and a mortar was used to reinforce this part of the wall, which could have been used then as a foundation of the upper wall. Later, this latter wall was tilted (phase 2), dipping 70° to the east (Fig. 2c). All the Roman remains are sealed by a backfill layer, from the early third century. The disorders observed on the walls, and the geological deformation features observed in the bedrock, are consistent with each other and with regional observations. The sinistral displacements observed on the walls could be the result of one or more ruptures during an earthquake(s) on a segment of MVF faults that needs to be further investigated.

Quantifying deformation through 3D reconstruction of the archaeological remains

At locations where the remains are well preserved, we plan to quantify deformations at a subcentimeter and millimeter scale on geological and archaeological markers

through a detailed analysis of ortho-images and a high-resolution Digital Surface Model. This approach will facilitate the systematic examination of disorders, linear and/or angular deformations, and their comparison, by juxtaposing surveys a few meters apart. We also need to check the kinematic consistency of different archaeological markers at the archaeological site scale, to confirm the surface-rupture hypothesis.

Paleoseismological investigation

To better assess the tectonic history of the MVF, we intend to conduct a statistical analysis of striation orientations, coupled to dating of kinematic markers (U-Pb or U-Th, depending on their age). In addition, to enrich the timing of surface-rupturing events, we will perform a twofold paleoseismological investigation. We will focus on: 1) examining the stratigraphic records in the lacustrine sediments of Lake d'Antre, which is bounded by a MVF segment to the south (Fig. 1c); and 2) trenching across fault scarps to unearth rupture traces in the Holocene sediments and soils. These two datasets will, we hope, enable us to complete the chronology by going back in time, covering (partly) the Holocene. A set of sediment cores was already retrieved from the lake in June 2023, and their analysis is currently in progress. Concurrently, we will conduct Electric Resistivity Tomography profiles and explore prospective pits to locate suitable locations for paleoseismological trenches. We are also experimenting with subaqueous imaging techniques to investigate whether any tectonic deformation extends to the lake bottom.

The preliminary results reported here suggest the occurrence of tectonic events during Antiquity along the northern segments of the MVF. Surface-rupture faulting could have damaged and offset Gallo-roman remains, and strong local shaking during those events

could have coevally damaged the constructions. If confirmed, the 20–30 cm wall offset could fit with the deformation characteristic of a shallow to very shallow moderate-magnitude earthquake, capable of causing strong shaking in the vicinity of the fault. From an archaeological point of view, this new hypothesis raises the question of the role of earthquakes on the site abandonment, whether due to the direct effects of earthquakes or their potential impact on hydrological flows in this karstic environment.

AFFILIATIONS
[1]Université Grenoble Alpes, IRD, ISTerre, Grenoble, France
[2]ARTEHIS, Bourgogne University, France
[3]Institute for Radioprotection and Nuclear Safety, Fontenay aux Roses, France

CONTACT
Théo Lallemand: theo.lallemand@univ-grenoble-alpes.fr

REFERENCES
Baize S et al. (2011) Bull Soc Géol Fr 182: 347-365

Courboulex F et al. (1999) Geophys J Int 139: 152-160

De La Taille C (2015) PhD thesis, Université Grenoble Alpes, 259 pp

Jomard H et al. (2017) Nat Hazards Eath Syst Sci 17: 1573-1584

Nouvel P et al. (2018) Rec Archeol 32: 103-114

Smeraglia L et al. (2021) Journal of Structural Geology 149: 104381

Thouvenot F et al. (1998) Geophys J Int 135: 876-892

Seismic seconds: The challenges of precisely dating and timing earthquakes in New England in the past four centuries

Katrin Kleemann

New England has the longest continuous earthquake record in the United States. Earthquake catalogs document the exact time that an earthquake struck. When consulting historical sources, however, it becomes clear that there is much more ambiguity concerning these documented times.

Earthquakes in New England

Earthquakes that took place during historical times are often recorded in historical documents. Where earthquakes are infrequent, they are perceived as something extraordinary and are remarked upon as such in diaries, letters, newspapers, and sermons. A list of regions in the United States that evoke associations with earthquakes include California, Alaska and Washington. New England does not necessarily spring to mind. However, despite being located on a tectonic plate, some distance away from the active continental margins, earthquakes do occur there. These seismic events are called intraplate earthquakes.

The seismic activity in this region is caused by the repercussions of the ancient collision between the African continent and the North American continent, which formed the supercontinent Pangea 450 to 250 million years ago, and the subsequent breakup of Pangea, which formed the Atlantic Ocean. Today's fault lines are echoes of these events in deep geological time (Kafka 2004). Some of these fault lines are occasionally reactivated by stress caused by the movement of the North American plate, moving away from the mid-Atlantic ridge, and by postglacial rebound, which is an uplift of a tectonic plate formerly weighed down by thick sheets of ice during an ice age; in this case, the ice sheets that started to melt around 10,000 years ago (Natural Resources Canada).

In North America, earthquakes to the east of the Rocky Mountains are felt in a much larger geographic area than those to the west. Indigenous peoples residing in North America experienced earthquakes here for a long time and passed on knowledge about them through oral history. Settlers arriving from Europe in the 17th century started recording them in written form after their arrival. In annotated almanacks, for instance, we can see that locals recorded when they felt the "small shock of an earthquake" (Fig. 1). The Massachusetts-based physician, Cotton Tufts, wrote that particular entry about an earthquake on 29 November 1783 CE that originated in northern New Jersey and was felt across New England (Kleemann 2018). Early American residents of the northeastern parts of the country, unlike modern residents,

did not regard earthquakes as "such an anomaly" (Robles 2017).

Notable earthquakes felt in New England (Fig. 2) originated in New Hampshire in 1638 CE; in Newburyport, Massachusetts, in 1727 CE; off the coast of Cape Ann near Boston in 1755 CE; in Moodus, Connecticut, in 1791 CE; in New York City in 1884 CE, in New Hampshire in 1940 CE; and in Virginia in 2011 CE.

Earthquakes put early American timekeeping practices to the test

The above-mentioned earthquakes are listed in earthquake catalogs. In addition to the approximate magnitude and intensity, these listings also include information on the date and time of the earthquake. Today, this is common practice and relatively easy to reconstruct, as a network of hundreds of seismographs around the world are recording earthquakes near and far. Seismographs were only invented in the late 19th century (Coen 2012). Seismographic records for New England date back to 1900 CE (Ebel et al.

2020). Older earthquake catalogs, however, also list precise times for those earthquakes that took place before the invention of the seismograph.

One problem that can arise, when considering the timing of historical earthquakes in this period, is the apparent discrepancy between the dates documented across certain borders. This occurs because some regions at the time still used the Julian calendar, whereas other regions had already adopted the Gregorian calender, which was first introduced in 1582 CE as a modification of the Julian calendar. In historical earthquake catalogs, this has sometimes led to confusion and incorrect listings. For instance, the geologist William T. Brigham listed 26 January 1662 CE and 5 February 1663 CE as separate earthquakes in his Historical Notes on the Earthquakes of New England; however, they are one and the same event. This earthquake was felt widely and originated in La Malbaie, New France, today's Canada; a Catholic area that used the Gregorian calendar while the American colonies were still using the Julian
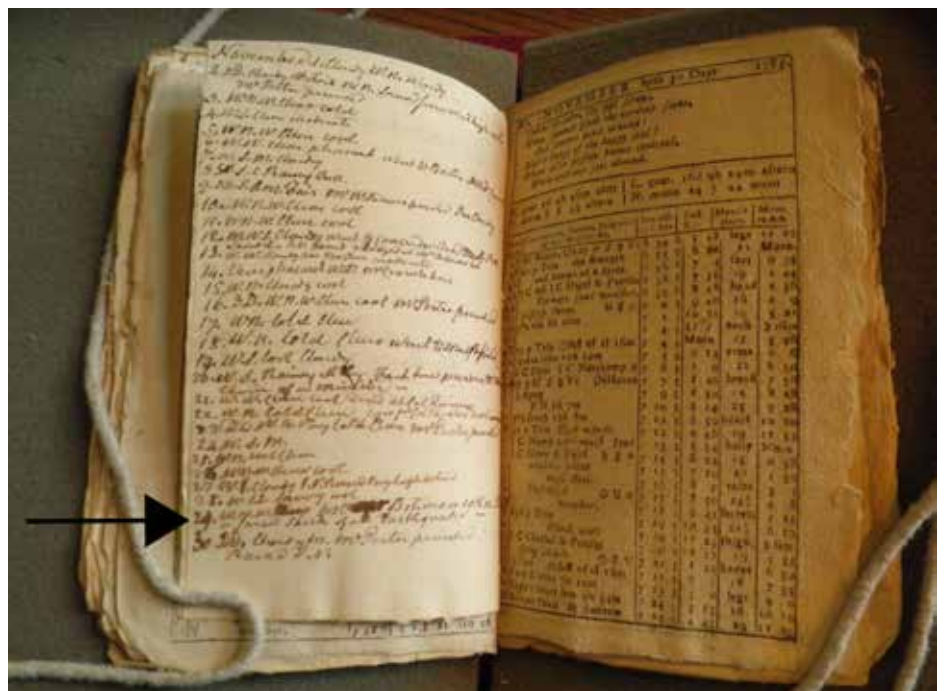
Figure 1: A page of Cotton Tufts' annotated almanack showing his entry for an earthquake on 29 November 1783 CE (see black arrow). Photography by the author. Credit: Cotton Tufts' diary, 29 November 1783 CE, Collection of the Massachusetts Historical Society.

calendar (Brigham 1871; Ebel 1996). In New France, the new year began on 1 January, whereas it only began on 25 March in New England. January was considered part of 1662 CE in New England and 1663 CE in New France; this observation explains the huge discrepancy in recorded dates and the subsequent mix-up by Brigham (1871).

The most specific time listed for an early modern earthquake in the United States Earthquake Intensity Database (United States Geological Survey 1986) catalog is for the 1755 CE Cape Ann earthquake. The time given for the event is 4:11:35 a.m. How was such a precise time recorded? In 1620 CE, the Mayflower ferried pilgrims across the Atlantic without a single timepiece on board (Hering 2009). At first, little metal was available in the New World, which made it challenging to produce clocks locally. Therefore, settlers began bringing timepieces with them from Europe, starting in 1650. Towers of churches, town hall, and other public buildings also began to install clocks around the same time (Distin and Bishop 1976). By 1700 CE, every colony had clockmakers (O'Malley 1990). The clocks available in the 17th and 18th centuries needed to be wound up regularly to run. Over time, as would be expected, the clocks in the New World improved (Distin and Bishop 1976).

Clocks were relatively expensive, only becoming more affordable and accessible toward the end of the 18th century with the beginning of mass production. Before this, it was mostly merchants, professionals, and shopkeepers who owned clocks and watches. Townspeople were more likely to have access to timepieces than those in the country (O'Malley 1990).

Coming back to the question of precise timing of the 1755 CE earthquake, John Winthrop, a professor at Harvard College, had found that one of his clocks had stopped precisely at 4:11:35 a.m (Winthrop 1755). For the purpose of another experiment, he had previously placed an item inside his clock's case, which had dislodged during the earthquake and fell against the pendulum inside the case, thereby stopping the clock. When consulting the sources, however, it becomes apparent that many other times when the 1755 CE Cape Ann earthquake allegedly struck are available, ranging from 3 to 5 a.m. While Winthrop, as a professor and person of science, likely took good care of his clocks, it should still be considered as one reading among many. It remains impossible to know precisely when the earthquake occurred.

Earthquakes and timekeeping from the 19th century onward
Before the widespread use of railroads made the standardization of time zones necessary, the local time of a given town was set when the sun crossed the meridian. Every town had its own time zone, slightly different from those towns to the east and west (Bartky 2000). While travel during this time was slow, measured in days rather than hours and minutes, the almost instantaneous spread
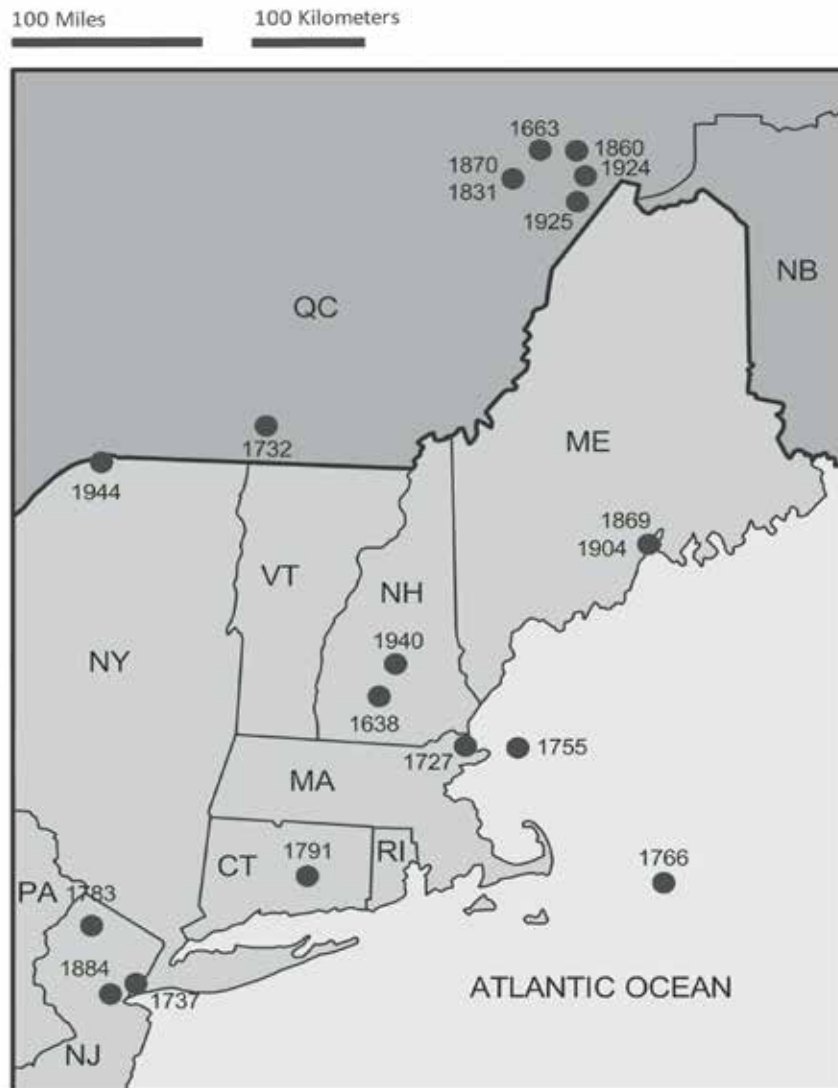
Figure 2: A map showing the assumed epicenters of selected earthquakes that affected New England over the past four centuries. The abbreviations on the map refer to the American states and Canadian provinces (NJ refers to New Jersey, QC to Quebec, etc.). Artwork credit: Jack Walsh, used with permission.

of an earthquake's waves put timekeeping practices to the test. In 1883 CE, delegates from the US railroads adopted the Standard Time System, which was officially recognized by the passing of the Standard Time Act by the US Congress in 1918 CE (Olmanson 2011). Today, towns no longer observe their own time zones based on solar time. Not only does this make communication and transportation more practical, but it also makes recording earthquakes around the globe easier.

CONTACT
Katrin Kleemann: k.kleemann@dsm.museum

REFERENCES
Bartky IR (2000) Selling the True Time: Nineteenth-Century Timekeeping in America. Stanford Univ. Press, 310 pp

Brigham WT (1871) Historical Notes on the Earthquakes of New England: 1638-1869. (From the Memoirs of the Boston Society of Natural History, Vol. II. January 1871), 28 pp

Coen DR (2012) The Earthquake Observers: Disaster Science from Lisbon to Richter. The University of Chicago Press, 348 pp

Distin WH, Bishop R (1976) The American Clock: A Comprehensive Pictorial Survey, 1723-1900, with a Listing of 6153 Clockmakers, 1st ed. Dutton, 359 pp

Ebel JE (1996) Seismol Res Lett 67: 51-68

Ebel JE et al. (2020) Seismol Res Lett 91: 660-676

Hering DW (2009) Accessed 5 Dec 2023, collectorsweekly.com

Kafka AL (2004) accessed 5 Dec 2023, aki.bc.edu

Kleemann K (2018) accessed 5 Dec 2023, envhistnow.com

Natural Resources Canada (website), accessed 5 Dec 2023

Olmanson ED (2011) Promotion and Transformation of Landscapes along the CB&Q Railroad. Rachel Carson Center for Environment and Society

O'Malley M (1990) Keeping Watch: A History of American Time. Viking, 384 pp

Robles WB (2017) The New England Quarterly 90: 7-35

United States Geological Survey (website), accessed 5 Dec 2023, ncei.noaa.gov

Winthrop J (1755) A Lecture on Earthquakes: Read in the Chapel of Harvard-College in Cambridge, N.E. 26 November 1755. On Occasion of the Great Earthquake which Shook New-England the Week Before. Edes & Gill, 38 pp

Combining onshore–offshore paleoseismic records to test for synchronicity of coastal deformation

Charlotte Pizer[1,2], J.D. Howarth[2] and K.J. Clark[3]

Linking onshore evidence of coseismic vertical deformation with offshore evidence of shaking is a powerful technique for better understanding the size, location and spatial impacts of past large earthquakes at subduction margins.

Coastal paleoearthquake records at subduction margins

Geologic evidence of coastal uplift and subsidence is commonly used to investigate the size, location and recurrence of past earthquakes along subduction margins (e.g. Clark et al. 2019). Large ruptures of the subduction interface are inferred by correlating coseismic deformation over large distances (>100 km). However, such spatial correlations are often based on temporal overlap between earthquake ages with uncertainties of >100 years, meaning that coseismic deformation may not have been synchronous (McNeill et al. 1999). That is, the same patterns of coastal uplift and subsidence could have been generated sequentially over decades by multiple smaller earthquakes.

Accurate correlation of coastal paleoearthquake evidence is further complicated by changes in preservation potential between sites and through time according to sea level and local erosion. Challenges imposed by incompleteness and large age uncertainties are compounded at complex subduction margins, such as the Hikurangi margin in New Zealand, where both upper plate faults and the subduction interface contribute to coseismic coastal deformation (Clark et al. 2019; Delano et al. 2023; Pizer et al. 2023a). Ultimately, incorrect paleoearthquake correlations can have implications for hazard preparedness because the spatial extent and age of past ruptures is used to inform the expected size and timing of future earthquakes (e.g. Nelson et al. 2021). Precise dating and careful interpretation of similarly

timed paleoearthquake evidence is therefore essential for inferring synchronicity and potential source faults.

Developing turbidite paleoseismology

Submarine turbidites provide a proxy for past earthquakes recorded in the offshore portion of subduction margins where sediment archives are often longer and more complete than at the coast (Goldfinger 2011). Offshore, large gravity flows called "turbidity currents" transport remobilized sediment to the deep ocean where "turbidites" are deposited and preserved. Turbidity currents can be triggered by a number of processes, including gas-hydrate destabilization, storms and shaking during large earthquakes (Howarth et al. 2021).

The most robust way to rule out non-seismic triggers is to demonstrate that turbidity currents were initiated simultaneously over large areas (>100 km), since regionally synchronous triggering is unlikely to occur by coincidence (Goldfinger 2011). Usually, this is achieved by correlating event beds between cores from widely spaced, disconnected submarine distributary systems based on overlapping age ranges. Therefore, precise dating of turbidites is imperative to minimize age uncertainties and ensure that core-to-core correlations are unique (Hill et al. 2022).

## Using turbidites to test for synchronicity of spatially-distributed coastal deformation

An independent test for an earthquake-related trigger for episodes of regional

turbidite emplacement can be conducted by comparing turbidite ages against the coastal paleoearthquake record (Ikehara et al. 2016; Usami et al. 2018). Good agreement between the timing of events in both records indicates that turbidity currents were probably initiated by ground shaking during the same earthquakes that produced coseismic coastal deformation. Integrating the spatial information from both proxies can therefore help to reconstruct the extent of past earthquakes. In particular, the combined approach provides an opportunity to test the synchronicity of correlated coastal deformation by examining the number of turbidites deposited in each distributary system within the timeframe of onshore earthquake-age uncertainty (Fig. 1). For example, if a single large earthquake caused widespread synchronous deformation at the coast, we would expect to observe a single turbidite event bed in multiple submarine distributary systems (Fig. 1a). However, if multiple smaller earthquakes caused local deformation at different coastal sites within a few decades, we would expect to observe multiple turbidites offshore (Fig. 1b).

We tested the hypothesis in figure 1 with an example from the central Hikurangi subduction margin, New Zealand (Fig. 2), where two coastal sites ca. 100 km apart record similarly timed coseismic deformation. In southern Hawke's Bay, coastal sediments from Pākuratahi display an abrupt change from estuarine silt to forest peat (Fig. 2d), indicating rapid sea-level fall, interpreted as coseismic uplift at 3630–3564 cal yr BP (Pizer et al. 2023a; Fig. 2c). In northern Hawke's Bay, coseismic uplift of a marine terrace at Māhia Peninsula is dated to 3636–3468 cal yr BP (Berryman et al. 2018; Fig. 2c). The earthquake ages are uniquely well-constrained due to stratigraphic evidence of the precisely dated Waimihia tephra isochron, deposited decades after the earthquake (Pizer et al. 2023b). Independent of the overlapping ages, the simplest explanation for coseismic uplift at both sites is earthquakes on nearby upper plate faults. Pākuratahi was recently uplifted by ca. 2 m in the 1931 CE moment magnitude (M_w) 7.4 Napier earthquake (Hull 1990), so similar earthquakes on the Awanui fault could generate comparable vertical deformation. No historical earthquakes have occurred on the Lachlan fault, but coseismic uplift of the

A: Single large earthquake

B: Multiple local earthquakes
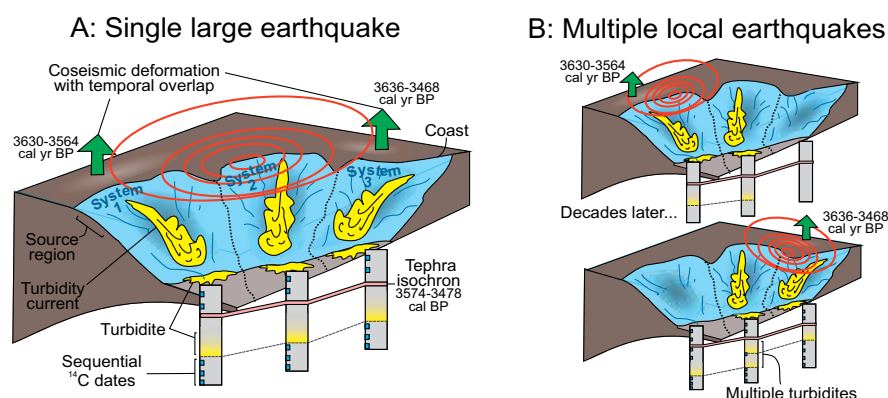
Figure 1: Schematic demonstrating the expected patters of turbidite deposition if coastal coseismic deformation (uplift) was caused **(A)** synchronously at both sites in a single large earthquake, or **(B)** sequentially in multiple smaller earthquakes. Chronology corresponds to the example in figure 2.
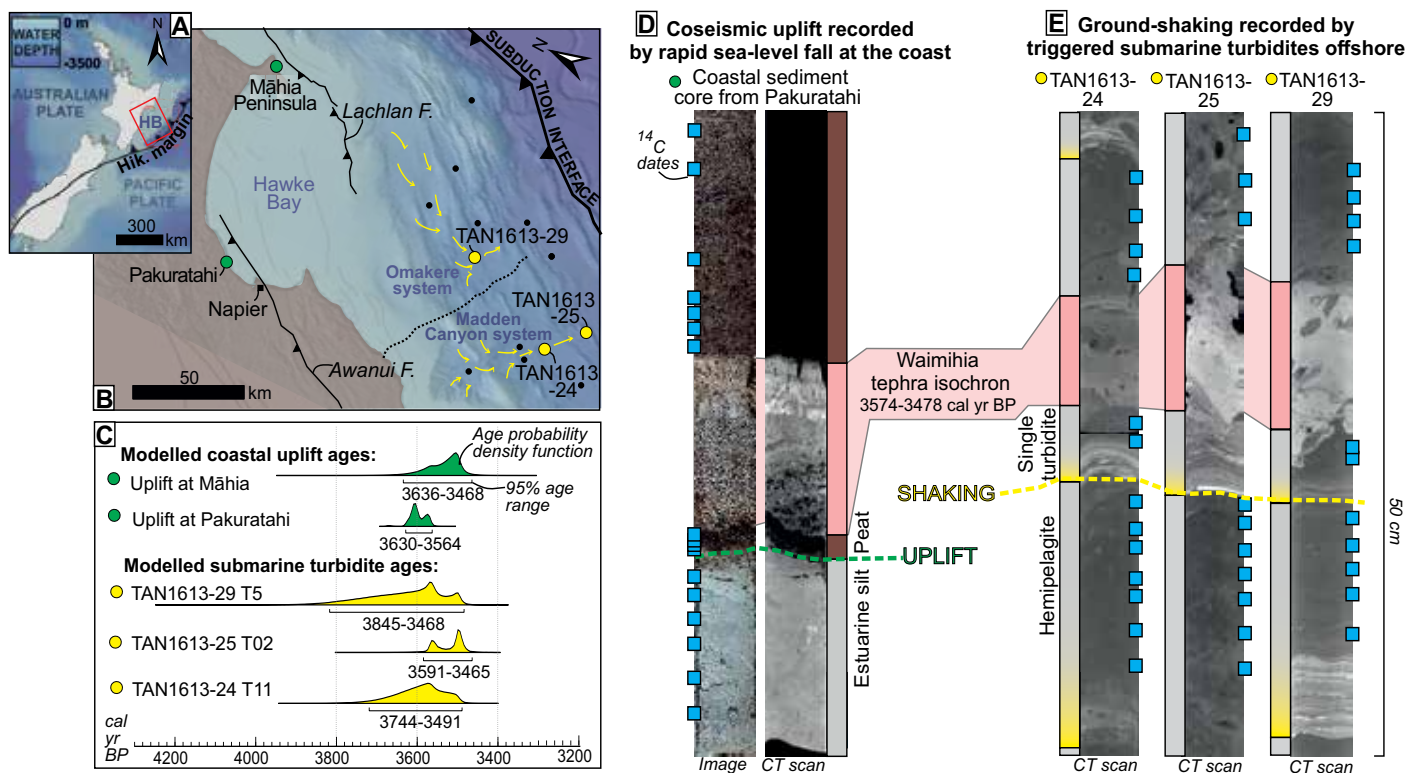
Figure 2: (A) Location of the Hikurangi (Hik.) margin off the east coast of the North Island, New Zealand, and **(B)** central section spanning Hawke's Bay (HB) with faults and paleoseismic sites. Green dots are coastal sites Māhia Peninsula (Berryman et al. 2018) and Pakuratahi (Pizer et al. 2023a). Black dots are submarine turbidite cores. Yellow dots are cores from Madden Canyon and Omakere distributary systems (Barnes et al. 2017), dated in Pizer et al. (2023b). Yellow arrows represent the flow direction of turbidity current pathways. The dotted line represents the boundary between catchments. **(C)** Modeled age probability density functions (PDFs) for correlated turbidites offshore and coseismic uplift onshore. **(D)** Evidence for coseismic uplift at Pakuratahi and **(E)** turbidites in the Omakere and Madden Canyon (as X-ray computed tomography (CT) scans).

Māhia Peninsula has been demonstrated in elastic dislocation models (and repeatedly in the paleorecord; Berryman et al. 2018).

Offshore, sediment cores containing Holocene sequences of submarine turbidites and hemipelagic background sediment were collected from discrete distributary systems along the central Hikurangi margin (Barnes et al. 2017; Fig. 2b). Correlation between the cores is facilitated by the same macroscopic Waimihia tephra isochron identified onshore (Pizer et al. 2023b). In all cores there is a single turbidite directly beneath the tephra layer (e.g. Fig. 2e). Three cores from the Madden Canyon and Omakere distributary systems were selected for high-resolution, sequential radiocarbon dating and age-depth modeling which produced turbidite ages closely matching the coseismic uplift at Pākuratahi and Māhia Peninsula (Fig. 2c).

Together, the upper-slope source areas for turbidity currents in the Madden Canyon and Omakere distributary systems span northern and southern Hawke's Bay (Fig. 2). As a result, we would expect to see multiple turbidites if separate earthquakes were responsible for generating the similarly timed deformation at Pākuratahi and Māhia Peninsula. Since we only observe a single turbidite offshore, we suggest that the coastal deformation at both sites was caused by a single earthquake. The extent of synchronous deformation (and shaking) across >100 km indicates a large magnitude earthquake which probably involved many upper plate faults rupturing together. This style of multi-fault rupture has

not previously been considered in Hawke's Bay due to the large stepovers between faults (Fig. 2b). However, as seen for the 2016 M_w 7.8 Kaikōura earthquake on the southern Hikurangi margin (Wang et al. 2018), slip on the subduction interface can help to propagate rupture across seemingly disconnected upper plate faults. The new insights from our integrated onshore–offshore paleoearthquake evidence highlight a need to incorporate complex rupture scenarios within seismic-hazard models and planning for future earthquakes on the central Hikurangi margin.

Summary
Correlating paleoseismic evidence across multiple sites is fundamental for deciphering the spatial extent and source faults for past earthquakes so that future hazard can be accurately assessed. Earthquake age-uncertainties within coastal deformation records are often too large to make unique correlations to confirm synchronous coseismic deformation. Offshore, the same events can be recorded by seismically-triggered submarine turbidites which, if carefully dated and correlated between multiple discrete distributary systems, can aid interpretation of coastal paleoearthquake evidence. For periods where regional turbidite-triggering coincides with coseismic deformation, the number of turbidites can indicate whether correlated coastal evidence represents multiple smaller earthquakes, or one larger one. Using an example from the central Hikurangi margin, we demonstrate the novel perspective provided by integrating onshore and offshore proxies, which has helped to link

evidence of coastal uplift at sites separated by >100 km, to a single earthquake. Where possible, the same approach should be developed at other subduction margins to more robustly estimate the size, recurrence and source of past earthquakes.

AFFILIATIONS
[1]Department of Geology, University of Innsbruck, Austria
[2]School of Geography, Environment and Earth Sciences, Victoria University of Wellington, New Zealand
[3]GNS Science, Lower Hutt, New Zealand

CONTACT
Charlotte Pizer: charlotte.pizer@uibk.ac.at

REFERENCES

Barnes PM et al. (2017) National Institute of Water and Atmospheric Science, 385 pp

Berryman K et al. (2018) Geomorphology 307: 77-92

Clark KJ et al. (2019) Mar Geo 412: 139-172

Delano JE et al. (2023) Geochem Geophys Geosyst 24: e2023GC011060

Goldfinger C (2011) Annu Rev Mar Sci 3: 35-66

Hill JC et al. (2022) Earth Planet Sci Lett 597: 117797

Howarth JD et al. (2021) Nat Geo 14: 161-167

Hull AG (1990) New Zealand J Geol. Geophys 33: 309-320

Ikehara K et al. (2016) Earth Planet Sci Lett 445: 48-56

McNeill LC et al. (1999) Geol Soc Spec Publ 146: 321-342

Nelson AR et al. (2021) Quat Sci Rev 261: 106922

Pizer C et al. (2023a) GSA Bulletin

Pizer C et al. (2023b) Quat Sci Rev 307: 108069

Usami K et al. (2018) Geos Lett 5: 11

Wang T et al. (2018) Earth Planet Sci Lett 482: 44-51

Investigating past earthquakes with coral microatolls

Belle Philibosian

Intertidal corals (microatolls) preserve evidence of past uplift or subsidence with annual precision. Microatoll records are particularly useful along subduction zones, and can reveal past earthquake ruptures at a level of detail that is ordinarily limited to the instrumental era.

The need for high-precision, widely distributed paleoseismic data

Decades of research have led to the realization that earthquake recurrence is complex, but nevertheless often follows a recognizable pattern (Philibosian and Meltzner 2020). Common patterns include rupture cascades (series of earthquakes on neighboring fault sections) and superimposed cycles (two or more neighboring fault sections with different recurrence intervals). To determine the types of recurrence patterns exhibited by a particular fault, it is necessary to establish details of past ruptures –timing, rupture extent, amount of fault slip –over several earthquake cycles. The required level of detail can be achieved only by using techniques with high temporal and spatial precision, as well as a wide distribution of study sites. The coral-microatoll technique, while limited in its applicability by the occurrence of reef-building corals above faults producing vertical movement, is perhaps the most precise among geologic-paleoseismic techniques.
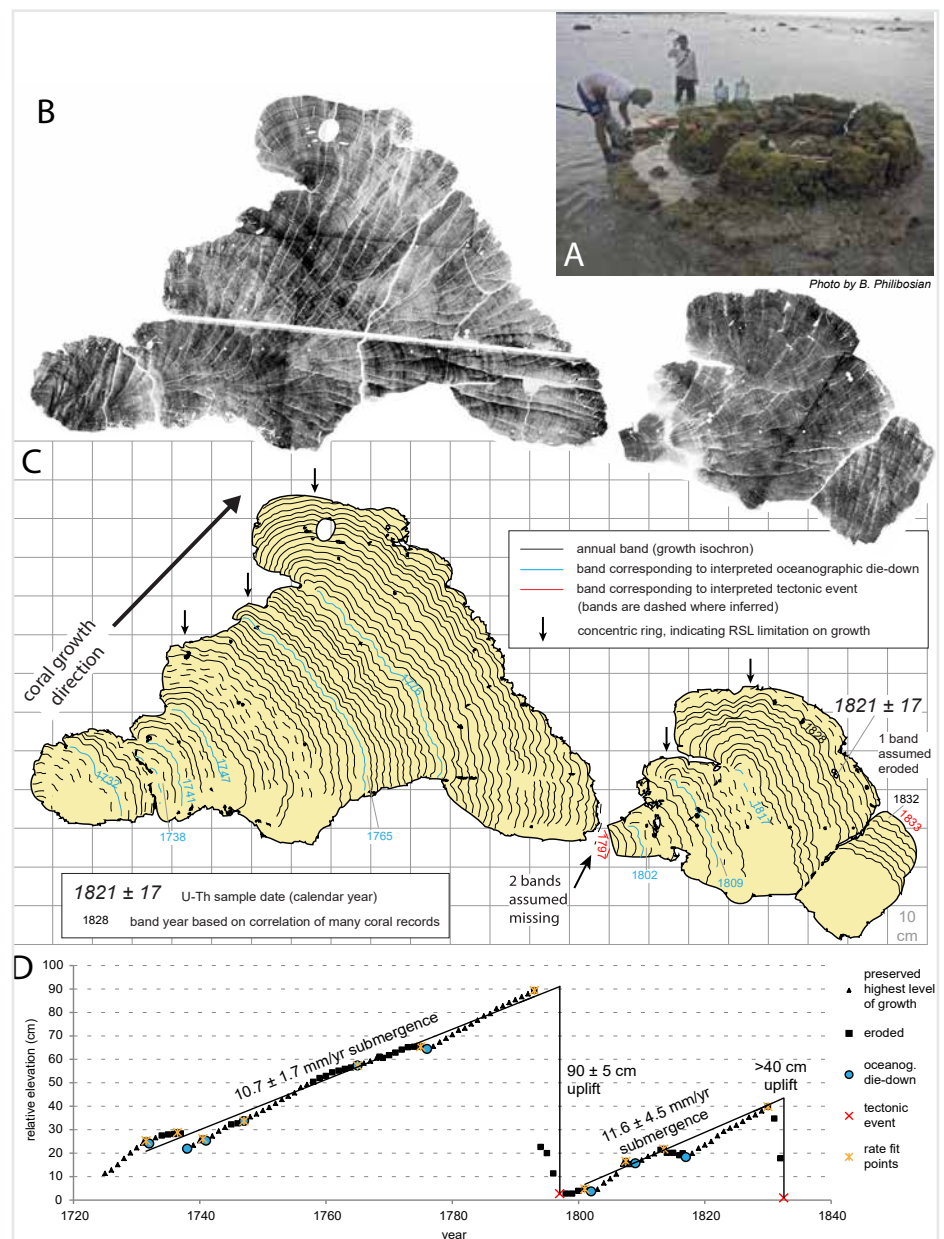
The microatoll technique

The upward growth of corals in the intertidal zone is limited by relative sea level (RSL), as corals cannot survive for long out of the water. Reef-building coral species that grow radially outward generally form roughly hemispherical colonies underwater, but in the intertidal zone typically produce a colony with a flat, dead top, surrounded by a ring of living tissue that extends below the water.

The term "microatoll" was coined for these specimens based on their resemblance to ring-shaped coral reef atoll islands. As a microatoll grows outward, the height of the living outer ring responds to changes in RSL. Thus, the upper surfaces of microatolls record RSL over the lifetime of the colony, which in some species can reach hundreds of years. Furthermore, microatolls can be preserved in or near the intertidal zone for hundreds, or even thousands, of years after they die. Most coral species produce annual density bands analogous to tree rings. This combination of characteristics allows records of RSL to be reconstructed with annual precision over centuries, or millennia. Absolute ages of corals that died in the past are still limited by the precision of radiometric dating, but uranium-thorium disequilibrium dating can be used on corals, potentially yielding ages with uncertainties of less than a decade. Furthermore, the relative

timing of events (annual precision) within a given coral record is not affected by absolute dating uncertainties.

Coral microatolls are sampled by cutting a radial slice, obtaining an X-ray image of

the slice to reveal the annual bands, and measuring the growth height of each band (Fig. 1). Large, sudden height changes can be interpreted as earthquakes, whereas gradual trends in growth height over time record interseismic behavior. However,

Figure 1: Example microatoll interpretation (modified from Philibosian et al. 2014; Philibosian 2024). **(A)** A microatoll from which a radial slice is being cut with a hydraulic chainsaw. **(B)** X-ray image of the collected slice showing annual banding. **(C)** Interpreted microatoll cross-section. **(D)** Plot of annual coral growth height with measured uplifts and submergence rates estimated by linear fits to points preceding die-downs. This microatoll recorded two earthquakes 36 years apart; others have similarly recorded doublets separated by as little as four years (e.g. Philibosian et al. 2017).

there are several interpretive steps between coral growth height and tectonic uplift or subsidence. The relationship between coral upward growth and RSL change is asymmetric, as a drop in sea level will cause the upper part of the coral to die within days, but a rise in sea level will usually leave an intertidal coral within its depth range, simply providing space for the coral to grow. This response takes years to be recorded (Fig. 2). In combination with the noise generated by interannual oceanographic fluctuations in sea level (such as those associated with the El Niño – Southern Oscillation), this means that gradual changes in RSL derived from microatoll records are often inaccurate unless averaged over a decade or more (as in Fig. 1d).

Finally, to isolate tectonic uplift or subsidence, all other signals (most significantly eustatic sea-level change) must be removed from the RSL record (see Philibosian 2024). For sudden uplift or subsidence events (as often occur during earthquakes), the nontectonic contributions are generally negligible, but their impact can be more significant on estimates of gradual interseismic motion. Fortunately, most of the other potential signals affect large regions equally, such that any differences in RSL trend between nearby sites (up to a few hundred kilometers apart) can confidently be attributed to active tectonics.

In regions where coral microatolls are plentiful, numerous study sites can be fairly easily established over a broad area (Philibosian 2024). Whereas the specialized equipment and logistics for sampling microatolls are expensive, there are significant economies of scale that many other paleoseismic techniques (such as trenching) do not have.

Past and current applications
The coral-microatoll technique has long been used in paleoclimate studies (beginning with Scoffin and Stoddart 1978), and has since been applied and further tailored to earthquake research beginning with Taylor et al. (1987), but primarily in the 21st century. Thus far, the most extensive and successful use in an active tectonic context has been to establish the history of uplift and subsidence during and between earthquakes along the Sumatran Sunda Megathrust. The majority of the now-known best practices were established over the course of the Sumatran tectonic studies (see Meltzner and Woodroffe (2015) and Philibosian (2024) for details). These microatoll studies enabled multiple cycles of paleoearthquakes to be examined in unprecedented detail, including disambiguating individual events that occurred only a few years apart, and estimating rupture extent and slip magnitude for each event.

The Sumatran microatoll records have illuminated many hitherto underappreciated aspects of fault behavior, such as persistent rupture segmentation (e.g. Meltzner et al. 2012), complex earthquake recurrence cycles (Philibosian et al. 2012; Philibosian et al. 2017; Sieh et al. 2008), years-long
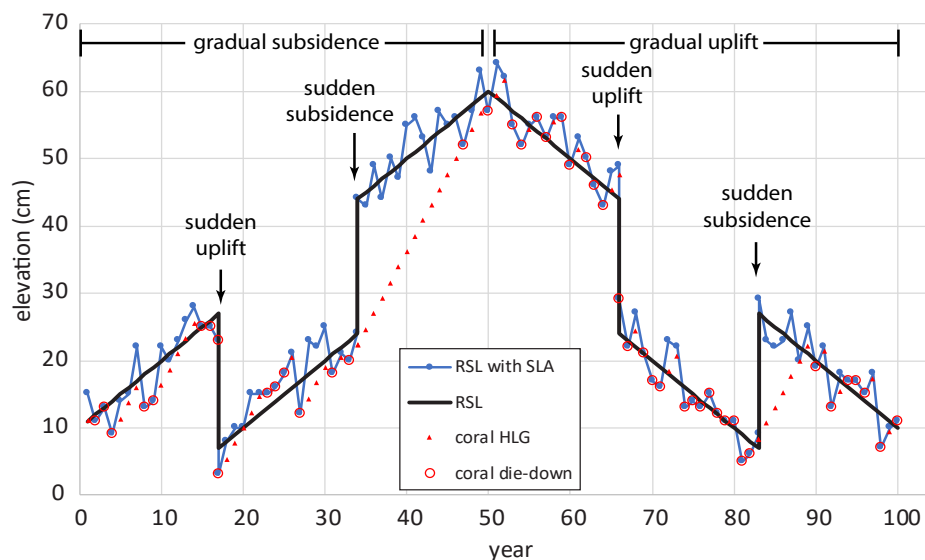
Figure 2: Synthetic illustrative RSL history and resultant microatoll growth record (modified from Philibosian 2024). Black line shows RSL history with steady 1 cm/yr submergence over the first 50 years and equivalent emergence over the second 50 years, with sudden 20-cm emergence and submergence events during each period. Blue line with markers shows the same RSL curve with random ±5 cm interannual sea-level anomaly (SLA) fluctuation added. Red markers show response of a coral with 2.3 cm/yr upward growth rate; triangles indicate years in which height is limited by growth rate (highest level of growth, HLG) and circles show years when it is limited by sea level (die-downs).

slow-slip events (Tsang et al. 2015b), and variable strain accumulation over time (e.g. Meltzner et al. 2015; Philibosian et al. 2014; Tsang et al. 2015a).

The microatoll technique is gradually spreading to other tropical active-tectonic study areas, having been applied with varying degrees of success to subduction paleoseismology and paleogeodesy along the northernmost Sunda (Arakan) margin, the Solomon Islands, the Lesser Antilles, and the Ryukyu Arc, with nascent application in the Philippines. Microatolls have also served as vital recorders of uplift and subsidence during recent subduction earthquakes in Vanuatu and the Solomon Islands, as well as those along the Sumatran Sunda Megathrust. They have additionally been applied in an oblique strike-slip environment to measure vertical motion during the 2010 Haiti earthquake. Philibosian (in press) includes a complete current list of publications that have used coral microatolls in active tectonic studies.

Successful coral-microatoll studies ultimately provide maps of tectonic vertical motion with annual precision. This precision allows individual earthquakes that occurred only a few years apart to be distinguished in the geologic record, and demonstrates that no earthquakes producing significant uplift or subsidence occurred during parts of the record that lack sudden RSL changes. For each individual earthquake rupture, the distribution of uplift and subsidence can be modeled to obtain the rupture extent and fault-slip distribution, using the same procedures as would be done for any other type of surface-deformation measurement. Similarly, gradual interseismic vertical motion can be modeled to estimate the distribution of fault coupling and concomitant strain accumulation.

Obtaining such precise characteristics of individual paleoearthquakes is vital for assessing fault behavior, including the persistence of rupture segmentation, recurrence patterns, and similarity of successive events; key issues in both fault mechanics and hazard assessment. The coral-microatoll technique may be a useful component for any study involving active tectonic uplift or subsidence along coastlines where corals grow.

REFERENCES
Meltzner AJ, Woodroffe CD (2015) In: Shennan I, Long AJ, Horton BP (Eds) Handbook of Sea-Level Research. Wiley

Meltzner AJ et al. (2012) J Geophys Res 117: Article B04405

Meltzner AJ et al. (2015) Quat Sci Rev 122: 258-281

Philibosian B (in press) In: Elliott AJ, Grützner C (Eds) Understanding Past Earthquakes. Springer-Nature

Philibosian B, Meltzner AJ (2020) Quaternary Science Reviews 241: 106390

Philibosian B et al. (2012) J Geophys Res 117: B05401

Philibosian B et al. (2014) J Geophys Res 119: 7258-7287

Philibosian B et al. (2017) J Geophys Res Solid Earth 122: 642-676

Scoffin TP, Stoddart DR (1978) Philos Trans R Soc London Ser B 284: 99-122

Sieh K et al. (2008) Science 322: 1674-1678

Taylor FW et al. (1987) J Geophys Res 92: 4905-4933

Tsang LLH et al. (2015a) Geophys Res Lett 42: 10585-10594

Tsang LLH et al. (2015b) Geophys Res Lett 42: 6630-6638

The importance of diatoms for understanding subduction-zone earthquakes in Alaska

Grace F. Summers, S.E. Engelhart and S.A. Woodroffe

Past earthquakes have left geological imprints, and microfossil approaches using coastal sediments offer ways to constrain rupture characteristics over centennial to millennial timescales. New approaches may provide a means to reconstruct smaller earthquakes and improve our understanding of seismic hazards.

Great subduction-zone earthquakes (moment magnitude [M_w] >8) pose a significant threat to human populations, the environment and infrastructure, yet the spatial and temporal patterns of these hazards before the 20th century are often poorly constrained. Limited instrumental data (~100 years) offer only partial information on the potential magnitude, recurrence intervals and spatial variability of rupture area for past earthquakes due to infrequent occurrence (typically multi-centennial recurrence intervals) of great earthquakes. Impacts from the 2004 Sumatra and 2011 Japan earthquakes demonstrate the dangers of heavy reliance on temporally limited records (Dura et al. 2016). Great earthquakes can also trigger tsunamis that impact coastlines far from the rupture area and necessitate a better understanding of the hazard.

Paleoseismology, in general, can extend and constrain earthquake records beyond instrumental and historical data. Coastal sediments from low-energy environments contain valuable archives of past relative sea-level (RSL) changes and have been utilized globally (Dura et al. 2016). Sharp lithological contacts of alternating organic (peat) and minerogenic (silt) sediments often indicate abrupt vertical land-level changes associated with an earthquake. In Alaska, diatoms are the most common microfossil used to reconstruct RSL changes associated with great earthquakes due to their preservation potential, high abundance and ecological niches with respect to elevation within the tidal frame.

Use of diatoms in Alaskan paleoseismology

Alaska has played a pioneering role in our understanding of plate tectonics with the demonstration via multiple lines of evidence that the M_w 9.2 1964 CE earthquake was caused by a megathrust (e.g. Plafker 1965). Observations of land-level changes during this earthquake provided a framework for subduction-zone paleoseismology both in Alaska and globally. Initial studies focused on radiocarbon dating to understand the chronology of past events and used plants and lithology to estimate the magnitude of deformation (e.g. Combellick 1991). However, such approaches have limited vertical resolution with errors typically >0.5 m and, therefore, limit the ability to differentiate between different magnitudes of events. One approach to increasing the precision

is to utilize microfossils such as diatoms (e.g. Hemphill-Haley 1995).

Diatoms are a group of photosynthetic, single-celled algae that are highly resistant to degradation due to their siliceous valves, allowing them to be incorporated into coastal sedimentary sequences, and preserved. Individual diatom taxa possess optima and tolerances to various environmental factors such as temperature, salinity and pH, making them highly sensitive to environmental change. The use of diatoms within Alaskan paleoseismology began through research conducted by Shennan et al. (1999) who examined the utility of diatoms to reconstruct the magnitude of land-level change at Girdwood. Since then, diatoms have been the most commonly utilized microfossil in Alaskan paleoseismology. Diatoms can be used in paleotsunami identification, with common characteristics of tsunami deposits including mixtures of fresh, brackish and marine diatoms (e.g. Fig. 1c), as well as broken and abraded valves (e.g. Dura et al. 2016; Hemphill-Haley 1995).

Paleoseismic evidence from coastal sediments currently provides a good

understanding of great earthquakes in south-central Alaska, with records of approximately seven great earthquakes in the past 4000 years and 10 in the last 6000 years (Shennan et al. 2014). However, absolute correlations between sites are limited by uncertainties in radiocarbon chronologies (Barclay et al. 2024). Detailed diatom studies in this region from Cook Inlet, Cape Suckling and Cape Yakataga reveal two additional great earthquakes, in addition to the 1964 CE event, radiocarbon-dated to ~900 and ~1500 cal yr BP (Shennan et al. 2009, 2014). At the stratigraphic contact (peat-silt), diatoms display an increased abundance of marine taxa, indicating coseismic subsidence (Fig. 1b-c).

At the southwestern termination of the 1964 CE rupture, diatom analysis has also documented evidence of both uplift and subsidence at Sitkinak Island with five instances of vertical land-level motion over ~1200 years (Briggs et al. 2014). For example, coseismic subsidence is recorded in 1964 CE where diatom taxa show a shift from a freshwater and brackish assemblage to a brackish and marine assemblage. This is interpreted as indicative of the arrest of
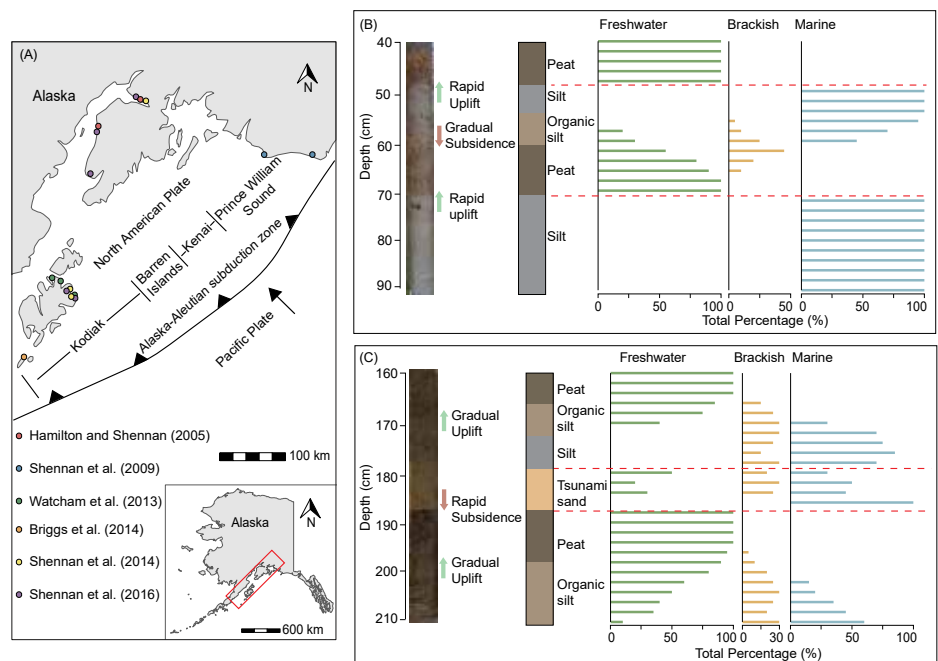
Figure 1: (A) Location of Alaskan diatom research discussed within this article. For detailed information on diatom analysis for each site see the reference list. **(B)** Schematic showing simplified stratigraphy and theoretical diatom assemblages representing coseismic uplift and gradual interseismic subsidence. Photo credit: Dr. Rich Briggs. **(C)** Schematic showing simplified stratigraphy and theoretical diatom assemblages representing coseismic subsidence, a tsunami deposit and gradual interseismic uplift.

rupture at, or near, the island. In contrast, coseismic uplift, potentially related to a historically documented earthquake in 1788 CE, is identifiable by a change from a marine-dominated to freshwater-dominated assemblage. This variability in uplift and subsidence is also found for three older earthquakes. This finding of mixed uplift and subsidence suggests that rupture boundaries in the Alaskan–Aleutian subduction zone are not persistent. Similar conclusions regarding rupture variability were reached by Shennan et al. (2014) who, utilizing diatoms, inferred the possibility of both multi-section (rupture spanning the Kodiak section) and at least one other section (e.g. at 1964 CE) and single section (Individual section rupture where only the Kodiak section ruptured e.g. at 1440–1620 CE) ruptures. These results suggest shorter recurrence intervals within the Kodiak section, impacting hazard analysis.

Application of transfer functions
In paleoseismology, transfer functions quantify the relationship between modern diatom taxa and elevation. They can produce precise estimates of RSL change and have been tested against known amounts of subsidence, and shown to produce accurate results (e.g. Hamilton and Shennan 2005). The known contemporary relationship between modern diatom taxa and elevation (modern training set) can be applied to fossil assemblages within coastal stratigraphic sequences, to calculate the RSL changes throughout an earthquake cycle (Dura et al. 2016). However, diatom assemblages are very diverse and can result in challenges where the fossil diatom assemblage is not well represented in the modern training set; a no-modern analog situation (Watcham et al. 2013). When this occurs, quantitative reconstructions may not be reliable. Regional modern diatom datasets are more appropriate given the high diversity of diatom assemblages. They encompass modern taxa from a wide range of intertidal environments providing analogs for fossil diatom assemblages (Watcham et al. 2013). Further, Watcham et al. (2013) demonstrated that regional modern training sets with good modern analogs most closely matched observed subsidence when available.

Future directions
The methods used to study and identify great earthquakes within paleorecords are well-established. However, there remains a significant gap in our knowledge of the detection limit for smaller earthquakes. In November 2018 a M_w 7.1 earthquake occurred near Anchorage and produced land-level changes ranging from +2 to -5 cm (West et al. 2020), lying below our current estimates for detection within coastal sediments (0.1–0.2 m; Shennan et al. 2016). This earthquake had significant impacts on society, emphasizing the importance of a better understanding of the recurrence intervals of smaller earthquakes. Therefore, improving our understanding about the range of earthquake sizes which can be identified in coastal sediments is an important research objective.
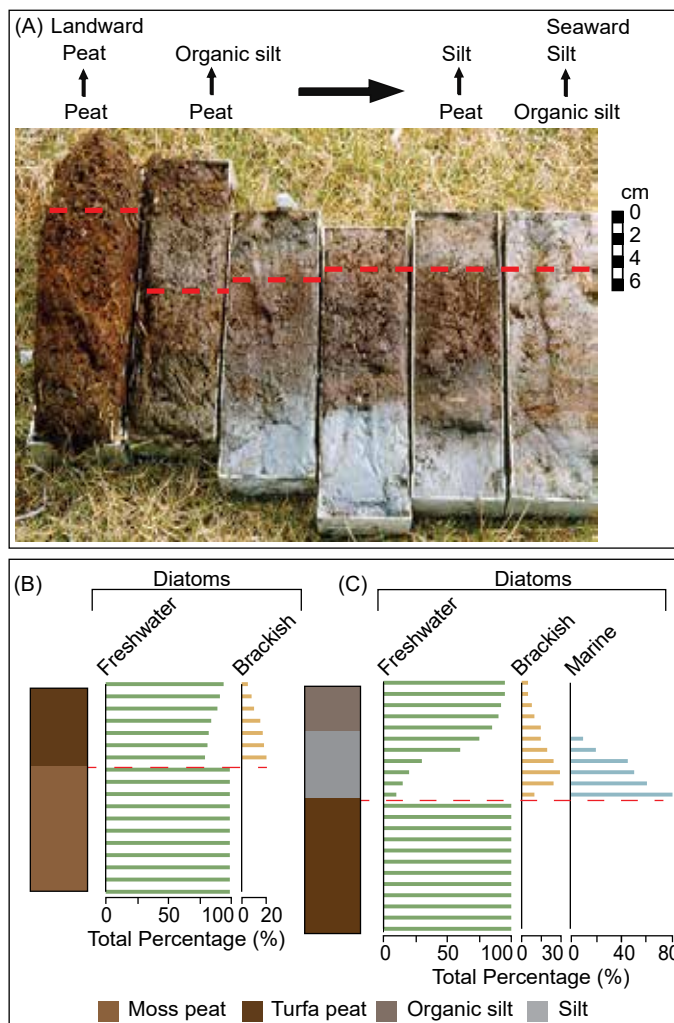
Figure 2: (A) Sediment cores from near the city of Kenai demonstrating how the peat-silt subsidence contact from the great M_w 9.2 1964 CE earthquake (red dashed line) can be traced landward (from right to left) until the subsidence is expressed as a peat-to-peat contact. Photo credit: Prof. Ian Shennan. **(B)** Theoretical diatom assemblage for a peat-peat couplet. **(C)** Theoretical diatom assemblage for a peat-silt couplet.

Detection limits of coastal sediments are dependent on the tidal range, stratigraphy and choice of transfer function. Current criteria used to identify land-level change in coastal sediments rely heavily on clear and abrupt changes in sediment stratigraphy (peat-silt or silt-peat couplets) indicative of larger changes in RSL. However, the long interval between the penultimate earthquake, (1169–1189 CE; Barclay et al. 2024) and the great 1964 CE earthquake may require either significant strain to be carried to a future great earthquake, or to have been released by aseismic creep (steady fault movement generally without an associated earthquake), or smaller earthquakes in the intervening time period (Barclay et al. 2024). Diatom assemblages at Kenai and Shuyak Island identify coseismic subsidence associated with the 1964 CE earthquake within peat-peat couplets that are associated with the most precise transfer function estimates (Fig. 2a-c; Hamilton and Shennan 2005; Shennan et al. 2018; Watcham et al. 2013). Identifying peat-peat couplets associated with land-level change opens the possibility for detecting smaller earthquakes in coastal sediment sequences and is a topic of current and future research. New data generated from peat-peat couplets could also be correlated to recent lake paleoseismology research in south-central Alaska (e.g. Praet et al. 2017). The combination of these two techniques would allow for an integrated investigation into paleoseismic events.

AFFILIATION
Department of Geography, University of Durham, UK

CONTACT
Grace F. Summers: grace.f.summers@durham.ac.uk

REFERENCES
Barclay DJ et al. (2024) Quat Sci Adv 13: 100142

Briggs RW et al. (2014) Geophys Res Lett 41: 2289-2296

Combellick RA (1991) DGGS Report of Investigations 112: 1-52

Dura T et al. (2016) Earth-Sci Rev 152: 181-197

Hamilton S, Shennan I (2005) Quat Sci Rev 24: 1479-1498

Hemphill-Haley E (1995) GSA Bulletin 107: 367-378

Plafker G (1965) Science 148: 1675-1687

Praet N et al. (2017) Mar Geol 384: 103-119

Shennan I et al. (1999) Quat Int 60: 55-73

Shennan I et al. (2009) Quat Sci Rev 28: 7-13

Shennan I et al. (2014) Geology 42: 687-690

Shennan I et al. (2016) Quat Sci Rev 150: 1-30

Shennan I et al. (2018) Quat Sci Rev 201: 380-395

Watcham EP et al. (2013) Quat Sci Rev 28: 165-179

West ME et al. (2020) Seis Res Lett 91: 66-84

Diatoms as indicators of coseismic, postseismic and interseismic deformation along subduction zones over centennial and millennial timescales

Tina Dura and Jessica DePaolis

Diatoms are invaluable to subduction-zone paleoseismic studies due to their ability to provide a continuous record of coseismic, postseismic and interseismic deformation, helping to better define the spatial variability of seismicity over centennial to millennial timescales.

Recent GPS instrumentation and Interferometric Synthetic Aperture Radar (InSAR) observations, coupled with increasingly sophisticated modeling, have identified complex patterns of subduction-zone deformation during earthquakes (coseismic), immediately after earthquakes (postseismic), and in between earthquakes (interseismic) (e.g. Klein et al. 2017). However, GPS and InSAR datasets span only decades, which is a fraction of the hundreds to thousands of years great earthquake cycle. Thus, the degree to which they reflect long-term rates of deformation is widely debated (Sieh et al. 2008). Are modern measurements and observations of subduction-zone earthquakes and tsunamis consistent with past events and, thus, reliable indicators of the future behavior of the subduction zone? Coastal paleoseismic studies that reconstruct rupture histories over multiple earthquake cycles suggest that the answer to this question is no, and that relying on short instrumental and historical earthquake and tsunami observations can lead to devastating societal impacts (Philibosian and Meltzner 2020; Witter et al. 2016).

Coastal paleoseismic studies, which use the methods of coastal stratigraphy, sedimentology, micropaleontology, and geophysical and sediment transport modeling to reconstruct vertical tectonic deformation along subduction zones coasts, have proven to be a powerful tool for examining the earthquake deformation cycle over centennial to millennial timescales. Past earthquakes are expressed in tidal wetland stratigraphy as sharp stratigraphic contacts between organic-rich peat below the contact, and tidal mud above (coseismic subsidence), or between tidal mud below the contact and organic-rich peat above (coseismic uplift) (Atwater 1987; Dura et al. 2017). The stratigraphic transitions captured in between earthquakes reflect the postseismic and interseismic period of the earthquake deformation cycle. Microfossils, such as diatoms, preserved in tidal wetland stratigraphy can provide quantitative estimates of the vertical surface deformation associated with the subduction-zone earthquake cycle (Shennan and Hamilton 2006). Diatom assemblages (groups of diatom species) are particularly useful in paleoseismic studies because their sensitivity to differences in tidal inundation, substrate and salinity can be precisely related to elevation within the tidal frame (Dura et al. 2016). Quantitative models, termed transfer functions, can be constructed from the relative abundance of

diatom assemblages at modern tidal-marsh elevations, which can then be applied to diatom assemblages found in cores and/or outcrops, to reconstruct the elevation of a sample when it was deposited. Transfer function analysis can provide a continuous record of coseismic, postseismic and interseismic deformation along subductions zones (e.g. Hawkes et al. 2011; Sawai et al. 2004a).

Here, we provide three examples of the application of diatoms to paleoseismic studies, and the valuable information they provide about the spatial variability of subduction-zone ruptures over centennial to millennial timescales.

Mixed coseismic subsidence and uplift detected with diatoms

Diatom-based paleoseismic work at the Chilean and Alaska–Aleutian subduction zones helped address questions regarding the sources and segmentation of past

earthquakes. Stratigraphic, sedimentological and diatom analyses revealed a >1000-year-long mixed record of coseismic subsidence and uplift at a series of coastal sites spanning proposed segment boundaries in south-central Chile (Fig. 1; Dura et al. 2017) and the eastern Aleutian Islands (Briggs et al. 2014), illustrating the variability of coseismic slip on the subduction zone over millennial timescales. At the Tirúa and Quidico coastal sites in south-central Chile, Dura et al. (2017) interpreted the mixed uplift and subsidence record to reflect variability in the rupture depth offshore of the study sites, and concluded that a proposed segment boundary in the region has persisted as a long-term impediment to slip through at least seven of the last subduction-zone earthquakes. At Sitkinak Island in Alaska, Briggs et al. (2014) interpreted the mixed uplift and subsidence record to reflect the location of the study site relative to the edge of past ruptures, concluding that when ruptures stop at Sitkinak, the
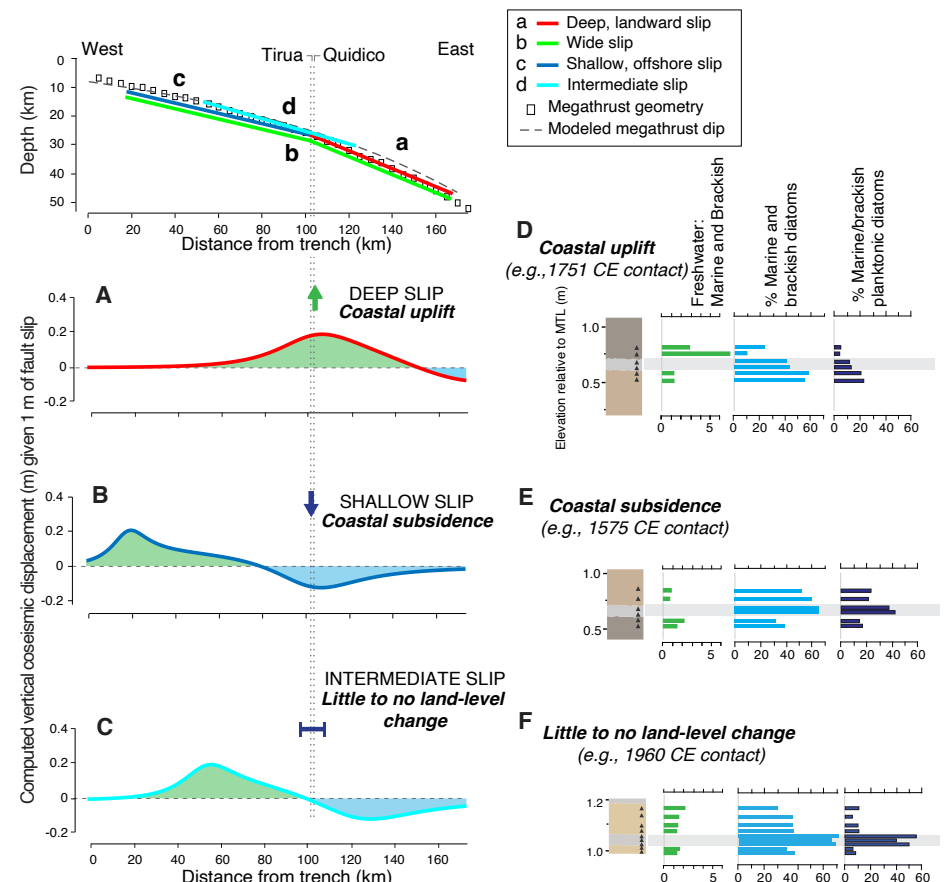
Figure 1: A simple model of constant coseismic slip and corresponding vertical deformation on a subduction zone in which slip is confined to a **(A)** deep; **(B)** shallow; or **(C)** intermediate zone. **(D)** An example of the diatom response to coastal uplift; **(E)** coastal subsidence; and **(F)** little to no coastal deformation. Figure and caption are modified from Dura et al. (2017).
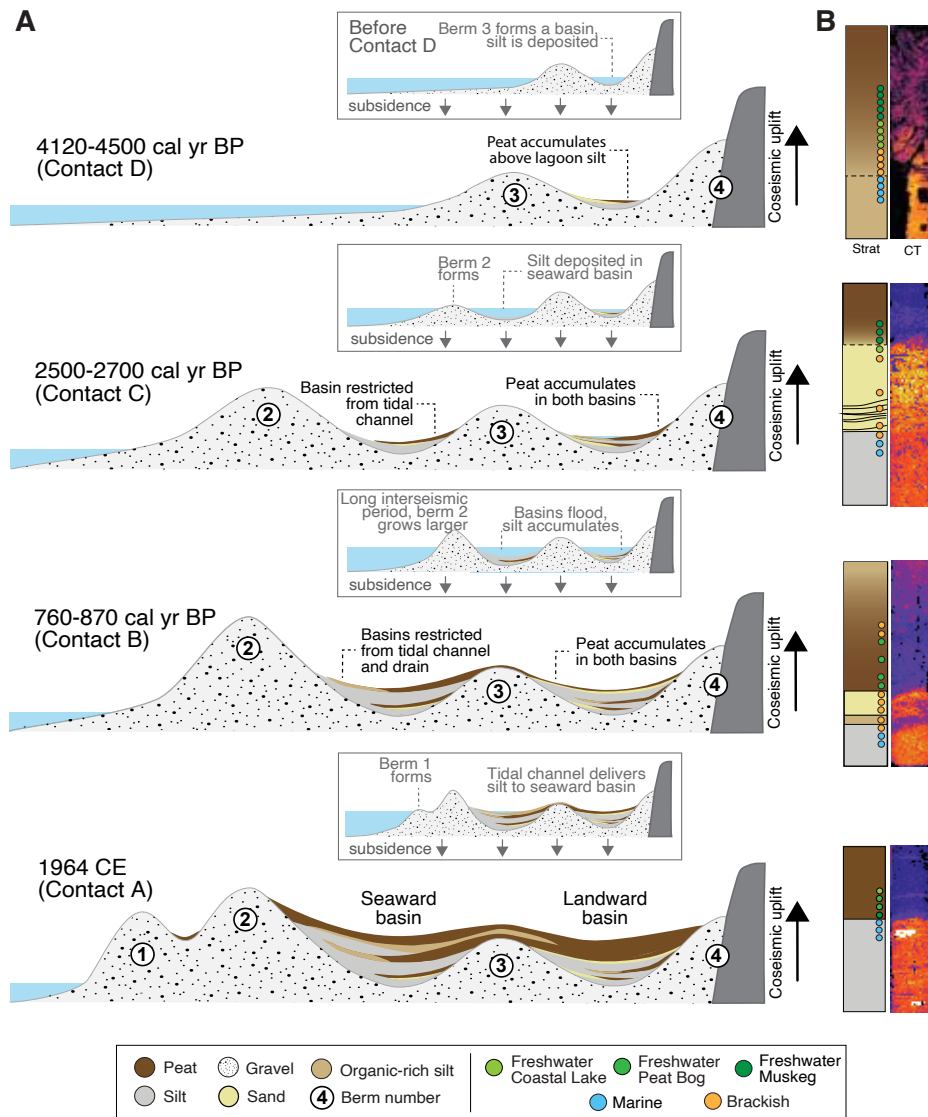
island subsides due to subsidence wrapping around the edges of surface uplift, while ruptures that propagate through the island cause uplift. Because the region east of Sitkinak Island was a proposed segment boundary, the results of Briggs et al. (2014) revealed the potential for multi-segment ruptures in this region, which will be included in future USGS hazards maps.

Diatoms as indicators of coseismic uplift
During the 1964 CE M_w 9.2 Great Alaska Earthquake, the Patton Bay Splay Fault System, a steeply dipping fault system connected to the subduction zone at depth, was activated, contributing to the formation of local tsunamis, and causing significant (4–1 m) uplift of Montague Island in Prince William Sound (PWS; Plafker 1967). Aerial imagery from before and after the 1964 earthquake shows the gradual draining of coastal lagoons along its northwestern coast. DePaolis et al. (2024) investigated the coastal stratigraphy and diatom signature of the 1964 CE earthquake at Hidden Lagoons, Montague Island, and found a distinct silt-peat contact representing the draining of the coastal lagoon system. Diatom analysis showed the pre-earthquake lagoon system was a marine environment with direct tidal communication with the sea, while the post-earthquake diatoms indicated a gradual transition to a brackish, then freshwater lake, then freshwater bog environment, reflecting the gradual freshening and draining of the lagoon (Fig. 2). The ecological changes documented across the 1964 CE contact indicate >3 m of coseismic uplift, exceeding the amount of uplift expected from a subduction-zone-only rupture, and supporting the concurrent rupture of the splay fault system. Further investigation of the subsurface stratigraphy revealed an additional three sharp silt-peat contacts with diatoms displaying similar marine to freshwater ecological shifts across them. The older contacts overlap the timing of three of the seven independently constrained (Shennan and Hamilton 2006) prehistoric subduction zone earthquakes in PWS in 760–870, 2500–2700, and 4120–4500 yr BP. This suggests that the splay fault system may rupture jointly with the subduction zone every other, or every couple of, subduction-zone earthquakes, with a mean recurrence interval of ~1030 years. DePaolis et al. (2024) conclude that future hazard assessments should consider the potential risks of tsunamis associated with combined ruptures of subduction-zone splay fault systems, similar to those observed in historical and prehistoric events.

Post seismic land-level change detected with diatoms
Diatoms have been used to quantify episodic postseismic uplift over the last 3000 years along the Kuril subduction zone in Japan, helping reconcile differences between long-term geologic uplift and shorter-term measurements of interseismic coastal subsidence. Despite no modern earthquake producing more than a few centimeters of uplift along coasts bordering the Kuril Trench, Sawai et al. (2004b) found stratigraphic and

diatom evidence of episodic seismically triggered uplift of >1 m that repeatedly changed tidal flats into lowland forests on the island of Hokkaido, Japan, bordering the Kuril Trench. Sawai et al. (2004a, b) developed and applied a diatom-based transfer function to quantify the deformation following one of the events, a significant 17th-century earthquake and resulting tsunami, and found that fossilized diatom assemblages revealed a gradual, rather than sudden, transition from tidal flats into freshwater upland environments in the decades following the earthquake. Due to the gradual nature of the environmental transition, Sawai et al. (2004b) interpreted the 1.5 m of uplift to represent postseismic uplift of the coast. The results suggest that the earthquake ruptured the shallower parts of the subduction zone, triggering a tsunami, but did not produce coseismic uplift along the coast. Instead, Sawai et al. (2004b) attribute the uplift to postseismic slip deep on the plate boundary beneath the island on Hokkaido. Although it is unclear if the episodic uplift events documented by Sawai et al. (2004b) completely account for the long-term net uplift of marine terraces observed in Hokkaido,

postseismic and possibly coseismic uplift from large and small earthquakes in the region certainly contribute to the long-term deformation of the coast.

AFFILIATION
Department of Geosciences, Virginia Tech, Blacksburg, USA

CONTACT
Tina Dura: tinadura@vt.edu

REFERENCES
Atwater BF (1987) Science 236 (4804): 942-944

Briggs R et al. (2014) Geophys Res Lett 41(7): 2289-2296

DePaolis J et al. (2024) PhD Thesis, Virginia Tech, 137

Dura T et al. (2016) Earth-Sci Rev 152: 181-197

Dura T et al. (2017) Quat Sci Rev 175: 112-137

Hawkes A et al. (2011) Quat Sci Rev 30(3-4): 364-376

Klein E et al. (2017) Earth Planet Sci Lett 469: 123-134

Philibosian B, Meltzner AJ (2020) Quat Sci Rev 241: 106390

Plafker G et al. (1967) US Geol Surv Prof Pap: 1-42

Sawai Y et al. (2004a) Quat Sci Rev 23(23-24): 2467-2483

Sawai Y et al. (2004b) Science 306(5703): 1918-1920

Shennan I, Hamilton S (2006) Quat Sci Rev 25(1-2): 1-8

Sieh K et al. (2008) Science 322(5908): 1674-1678

Witter RC et al. (2016) Geophys Res Lett 43(1): 76-84

Figure 2: (A) Inferred geomorphological change of the seaward and landward basins during and between major earthquakes (Contacts A-D) recorded at Hidden Lagoons, Montague Island, Alaska. **(B)** Representative stratigraphy and the corresponding Computed Tomography (CT) scan of each major contact are on the far right. Colored circles represent the transitions in diatom ecology at each sample location within the core. Figure and caption are modified from DePaolis et al. (2024).

Diatoms in earthquake and tsunami reconstruction along the Chilean subduction zone: Valuable proxies of a paleoseismologist's toolkit

Emma P. Hocking[1], E. Garrett[2] and T. Dura[3]

Diatoms form a powerful proxy for reconstructing subduction-zone earthquake and tsunami histories. Using examples from Chile, we explore what diatoms have been able to tell us to ultimately help improve seismic hazard assessment, and highlight challenges and opportunities.

Globally, great subduction-zone earthquakes (moment magnitude [M_w] >8), and the tsunamis they generate, produce cascading hazards along coastlines. As the largest events can be so devastating, yet so infrequent, geologic records of earthquakes and tsunamis spanning centuries to millennia are required to understand subduction-zone behavior, and account for variability in earthquake size, rupture style and tsunami generation. Coastal sediments are excellent recorders of past earthquakes and tsunamis, and microfossils, such as diatoms (siliceous single-celled algae) found within them, have become one of the most commonly used proxies for reconstructing subduction-zone earthquake and tsunami histories (Dura et al. 2016).

Since the seminal work in the Pacific Northwest (e.g. Atwater 1987; Darienzo and Peterson 1990), the last 40 years have seen major advances in diatom-based reconstructions of earthquakes and tsunamis (Dura et al. 2016). Due to the close control of salinity on diatom distribution in intertidal environments, diatoms can be used to quantify vertical land-level change associated with great earthquakes, not only coseismically during earthquakes, but also potential pre- and post-earthquake deformation. Due to their resistance to degradation, diatoms have also been widely used to determine the provenance of tsunami sediments and changing flow conditions during tsunamis. Here we review three case studies from the Chilean coast that demonstrate how diatoms are being used to reconstruct earthquake and tsunami history on a highly active subduction zone, and highlight important lessons from our research.

Extending historical records
At Chucalén, south-central Chile, in the centre of the area which ruptured in the world's largest instrumentally recorded earthquake, a M_w 9.5 event in 1960 CE, diatoms formed a powerful proxy for reconstructing coseismic land-level change that occurred in that event, and three earlier earthquakes during the last millennium (Fig. 1; Garrett et al. 2015). Diatom-based estimates of coseismic land-level change varied for the four earthquakes,

ranging from meter-scale subsidence to slight uplift, suggesting variability in slip distribution. The length of the paleoseismic record at Chucalén is twice as long as the historical record, yet historically documented events in 1737 and 1837 CE are absent, critically suggesting variability in magnitudes and longer recurrence intervals between the largest events.

The importance of utilizing multi-proxy geological and historical evidence in tandem
Historical records most commonly used in assessing seismic hazards are often too short to account for variability in earthquake size, rupture style and tsunami generation. Moreover, even where long written chronicles exist, failures in reporting, loss of documents in times of political instability or low-quality records may result in temporal gaps. Albeit with other limitations, geologic records are free from these problems. An example from Chaihuín, south-central Chile, close to the region of maximum slip in 1960 CE, demonstrates that it is imperative to supplement historical data with geologic records (Hocking et al. 2021).

Previously, the lack of reports of tsunami inundation from the 1737 CE south-central Chile earthquake had been attributed to either civil unrest (which restricted Spanish settlers from occupying all, bar two, coastal towns) or a small tsunami due to deep-fault slip below land. However, using sedimentological and diatom analyses of tidal marsh sediments, we found evidence for a previously unreported, locally sourced tsunami consistent in age with this event. Diatoms confirmed coseismic subsidence of up to 0.9 m and abrupt marine inundation (Fig. 2). Coupled dislocation-tsunami models placed the causative fault slip mostly offshore, rather than below land, and our findings reduced the average recurrence interval of tsunami inundation derived from historical records alone.

The importance of millennial-scale geologic records in characterizing earthquake and tsunami hazards
In central Chile, historical accounts, and later instrumental measurements of a series of ~M_w 8.0–8.5 earthquakes and low (<4 m) tsunamis affecting the region in 1575, 1580, 1647, 1730, 1822, 1906 and 1985 CE, suggest
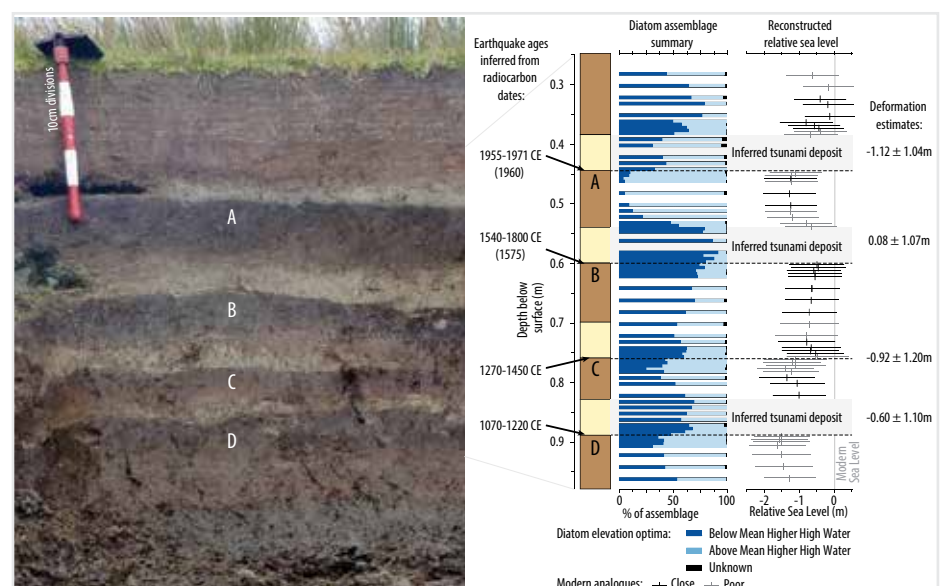
Figure 1: A 1000-year record of great earthquakes at Chucalén, south-central Chile, shown by the laterally extensive buried soils (A–D) and diatoms. Figure modified from Garrett et al. (2015).
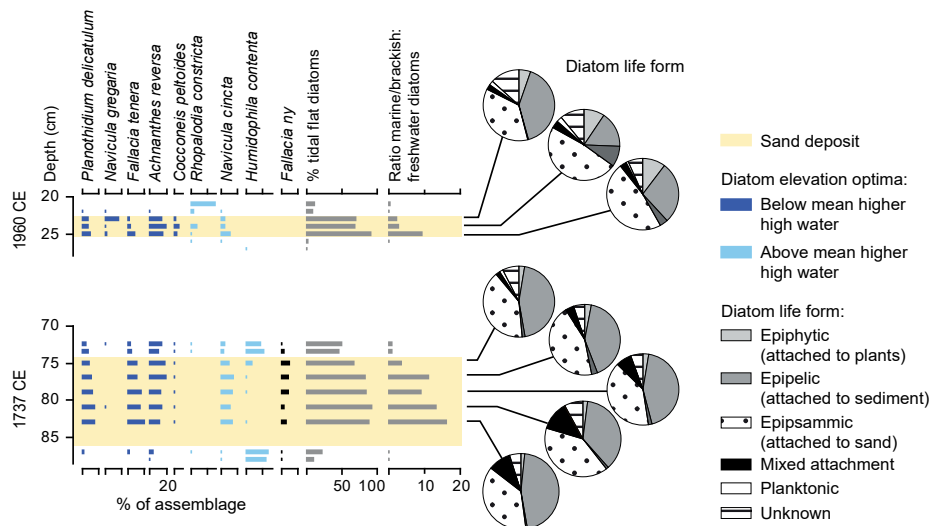
Figure 2: Sand deposits at Chaihuín, south-central Chile, dominated by marine and brackish diatoms characteristic of low elevations, provide evidence for marine-sourced sand and rule out fluvial deposition. In combination with sedimentological evidence and coincident subsidence discounting storm-surge origin, sand layers are interpreted as tsunami deposits.

a consistent recurrence interval of ~80 years for large earthquakes in the region. However, more recently uncovered historical clues from the 1730 CE event suggest this earthquake was larger (>M_w 9) than other earthquakes in the historical series, and produced a high tsunami that affected both the Chilean and Japanese coasts (Carvajal et al. 2017).

To dig deeper into the history of past >M_w 9 earthquakes along the densely populated central Chilean coast, Dura et al. (2015) conducted a stratigraphic, sedimentological and diatom investigation at Quintero. The study found evidence of six instances of high tsunami inundation and coastal uplift between 6200 and 3600 cal yrs BP, similar to that documented in 1730 CE. Diatom data were critical to supporting a marine source of the anomalous sand beds found in the stratigraphy, and for estimating uplift of ~0.5 m in each earthquake. The new tsunami and land-level change evidence shows a recurrence interval of ~500 years for outsized earthquakes and tsunamis in central Chile, and demonstrates that basing hazard assessments on only the most recent, but smaller, earthquakes and tsunamis overlooks the higher hazard posed by less frequent, but larger, events.

Challenges, opportunities and outlook
The examples demonstrate the value of utilizing diatoms in paleoseismology. However, as with any proxy, there remain challenges associated with their application. First, the above examples adopt transfer functions to quantify land-level change and, whilst such approaches enable more precise estimations of land-level change than earlier qualitative assessments, transfer functions have inherent assumptions and limitations. Diatom taxa in fossil sediments that are not present in our modern datasets (non-analogue situations) limit our ability to reconstruct past environmental change and accurately quantify land-level change.

Modern diatom dataset development is particularly challenging in places that have

recently undergone coseismic subsidence, as the present-day tidal marsh may not provide a good modern analogue for the entire fossil sequence. Every effort must be made to improve modern diatom datasets by increasing numbers of samples across a range of coastal environments (capturing the full gradients of elevation, vegetation, substrates) to help mitigate against non-analogue situations (Hocking et al. 2017). Even then, reconstructions can be complicated by reworked microfossils, with certain taxa being prone to transport across the intertidal zone, and thus not being representative of their depositional environment (Hemphill-Haley 1995). In such instances, it may be necessary to exclude specific taxa when performing reconstructions. We emphasize that improved understanding of relationships between diatoms, salinity and substrates in the modern environment, as well as variations in the preservation and transport of specific taxa, will ensure more reliable identification of earthquakes and tsunamis in the geological record, and quantification of land-level change.

There is also the assumption when quantifying land-level change using a transfer function that sedimentary hiatuses do not occur post-earthquake. If sediment accumulation does not recommence before significant postseismic deformation occurs, the magnitude of coseismic deformation may be underestimated in transfer function reconstructions. Such delay in postseismic sediment accumulation was observed at two sites following the 2010 CE earthquake (Garrett et al. 2013), and the duration of such hiatuses are difficult to identify in fossil records.

Finally, as well as potentially underestimating the magnitude of deformation, geologic records may also underestimate the occurrence of M_w 7–8 earthquakes. Diatom analyses of tidal-marsh sediments within the rupture area of the 2016 CE M_w 7.6 Chiloé earthquake, south-central Chile, showed records of low-level (<0.1 m) land-level change were created for a limited period of

time in limited parts of the tidal wetland, following the earthquake, with statistically significant changes observed between diatom assemblages pre- and immediately post-earthquake (Brader et al. 2021). However, the signal was temporary, and after nine months such assemblage changes were not preserved due to sedimentation processes (Brader et al. 2021). This highlights the limits of detection of this microfossil-based technique, and the potential underestimation of major, but not great, earthquakes in coastal paleoseismological records. This has important implications for estimating recurrence intervals in seismic hazard assessment, and further highlights the need to utilize multiple lines of evidence.

Diatoms are extremely useful for quantifying land-level change associated with subduction-zone earthquakes, and for determining tsunami provenance, ultimately helping to better understand recurrence intervals and variability in ruptures. However, their application must be seen as a key component of the paleoseismology toolkit; other proxies, as well as other approaches to reconstructing past earthquakes and tsunamis, such as the use of documentary evidence and modeling, are equally important. The power comes from combining approaches, and through such multidisciplinary research we can continue the remarkable advances in seismic-hazard assessment which have occurred over the last decade.

AFFILIATIONS
[1]Department of Geography and Environmental Sciences, Northumbria University, Newcastle-upon-Tyne, UK
[2]Department of Environment and Geography, University of York, UK
[3]Department of Geosciences, Virginia Tech, Blacksburg, USA

CONTACT
Emma P. Hocking: emma.hocking@northumbria.ac.uk

REFERENCES
Atwater BF (1987) Science 236 (4804): 942-944

Brader M et al. (2021) J Quat Sci 36: 991-1002

Carvajal M et al. (2017) J Geophys Res: Sol Earth 122: 3648-3660

Darienzo ME, Peterson CD (1990) Tectonics 9: 1-22

Dura T et al. (2015) Quat Sci Rev 113: 93-111

Dura T et al. (2016) Earth-Sci Rev 152: 181-197

Garrett E et al. (2013) Quat Sci Rev 75: 11-21

Garrett E et al. (2015) Quat Sci Rev 113: 112-122

Hemphill-Haley E (1995) Geol Soc Am Bull 107: 367-378

Hocking EP et al. (2017) J Quat Sci 32: 396-415

Hocking EP et al. (2021) Commun Earth Environ 2: 245

Reconstructing coastal evidence for earthquakes and tsunamis using elemental (XRF) geochemistry

Anthony Giang[1], I. Hong[2] and J.E. Pilarczyk[1]

X-ray fluorescence (XRF) analysis is a geochemical technique that reveals subtle environmental changes over sub-annual to millennial timescales. Elemental geochemistry of salt-marsh sediments responds to tidal frequency similar to microfossil distributions, which are used to reconstruct sea- and land-level change.

Subduction zones are known to generate some of the largest magnitude earthquakes and their subsequent tsunamis are capable of inundating local and distant coastlines. The recurrence interval of large earthquakes rupturing along a subduction interface are generally on the order of hundreds to thousands of years, making risk assessment challenging because the observational records do not fully capture these larger timescales (e.g. Sawai et al. 2012). Therefore, we must rely on the geologic record to extend our understanding of earthquake-rupture mechanisms, magnitudes, and frequencies (e.g. Atwater et al. 2003; Nelson et al. 2021).

Salt-marsh archives
In salt marshes, tides result in distinct environmental zones that are controlled by the frequency and duration of tidal inundation. Tidal inundation in salt marshes is controlled by the elevation gradient relative to sea level; where lower elevations are inundated more frequently and for longer durations than sections of the marsh situated at higher elevations. The predictable response of salt-marsh sediments to tidal inundation forms the basis for applying proxies (i.e. microfossils, XRF-elemental geochemistry) to reconstruct sea-level change, and in doing so, identifying paleoearthquakes and tsunamis in the geologic record (Atwater and Hemphill-Haley 1997).

In salt marshes, megathrust earthquakes may result in coseismic subsidence (instantaneous land-level lowering during the earthquake), which is analogous to instantaneous local sea-level rise. Stratigraphically, coseismic subsidence is identified as peat-mud couplets where pre-earthquake intertidal peat is suddenly lowered further into the intertidal and subtidal zone, where mud is subsequently deposited, resulting in a distinctive mud-over-peat contact (Atwater 1987). The tsunami generated from the earthquake can also inundate local coastlines, and the resulting overwash sediments can be preserved within salt-marsh stratigraphy as a thin marine sand sheet between the peat (pre-earthquake) and mud (post-earthquake) units (Hemphill-Haley 1995).

XRF as a tool for recognizing paleoearthquakes and tsunamis
Although intertidal microfossils (e.g. foraminifera and diatoms) are among the most widely used proxies for reconstructing paleoearthquakes and tsunamis (Pilarczyk et al. 2014), elemental geochemistry obtained through XRF-core scanning (XRF-CS) is a promising technique for reconstructing long term records of coastal change because of its rapidness and ability to detect even subtle environmental changes preserved within sediment cores (Giang et al. 2023).

XRF-CS offers rapid, continuous and non-destructive analysis of elemental composition for a wide range of geologic materials, including core samples. In XRF analysis, samples are irradiated with X-rays which induce the atoms from the samples to emit characteristic fluorescence photons. Detectors measure the energies of fluorescence photons which, in turn, identify the element and the number of fluorescence photons of that energy, to determine the abundance of a particular element in a given substance.

In theory, XRF analysis identifies all elements based on their characteristic fluorescence emissions, but in practice, XRF is incapable of detecting low atomic number elements (Z <11; e.g. H, C, N, O). Instead, XRF can indirectly measure these elements based on the X-ray scatter measured simultaneously with elemental data. X-ray scatter occurs when an incident X-ray is redirected or changes direction due to an interaction with an electron. Incoherent scattering occurs when the X-ray loses energy to the electron and is more prevalent with lower atomic number elements, while coherent scattering involves no change in X-ray energy and is more common with higher atomic number elements. The incoherent/coherent scattering ratio (ICR) provides insights into the average atomic mass of the total elemental composition.

Along salt-marsh coastlines, the elemental composition of modern marsh sediments shows a consistent relationship with tidal elevation, and is in agreement with marsh zones that are derived from intertidal microfossil assemblages (Giang et al. 2023; Pilarczyk et al. 2014). Generally, tidal flat and low marsh sediments from lower elevations are dominated
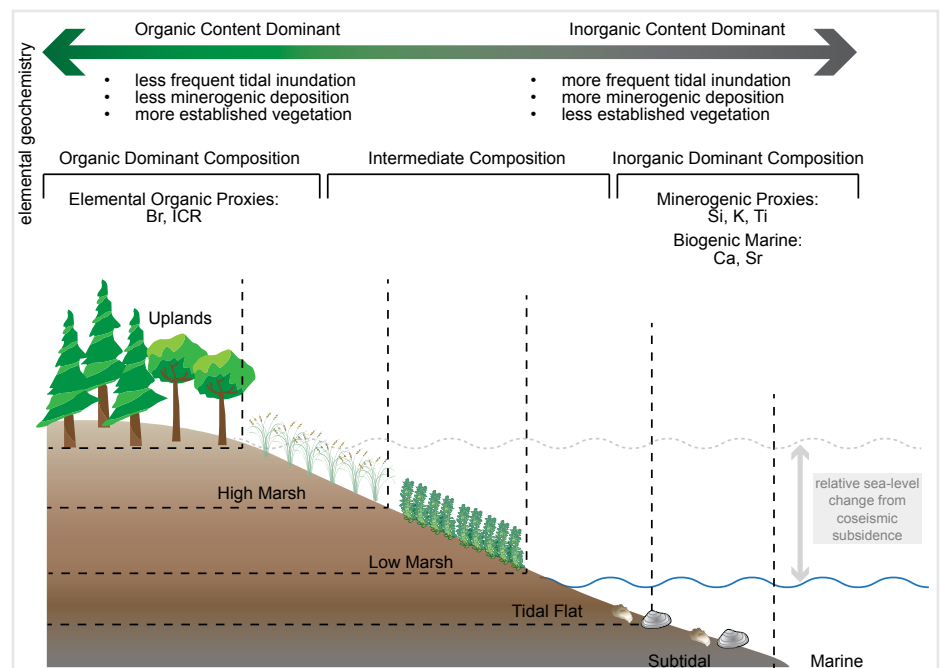
Figure 1: Conceptual model of elemental geochemistry zonation within Cascadia salt marshes. The elemental composition of low elevation (i.e. tidal flat) sediments is dominated by lithogenic (Si, K, Ti, Fe) and biogenic (Ca, Sr) elements, while the composition at high elevations (i.e. high marsh/uplands) is dominated by organic indicators, such as Br and ICR (incoherent/coherent scattering ratio). Relative sea-level change associated with coseismic subsidence is shown in gray, and results in the deposition of tidal flat muds on top of salt-marsh peats.
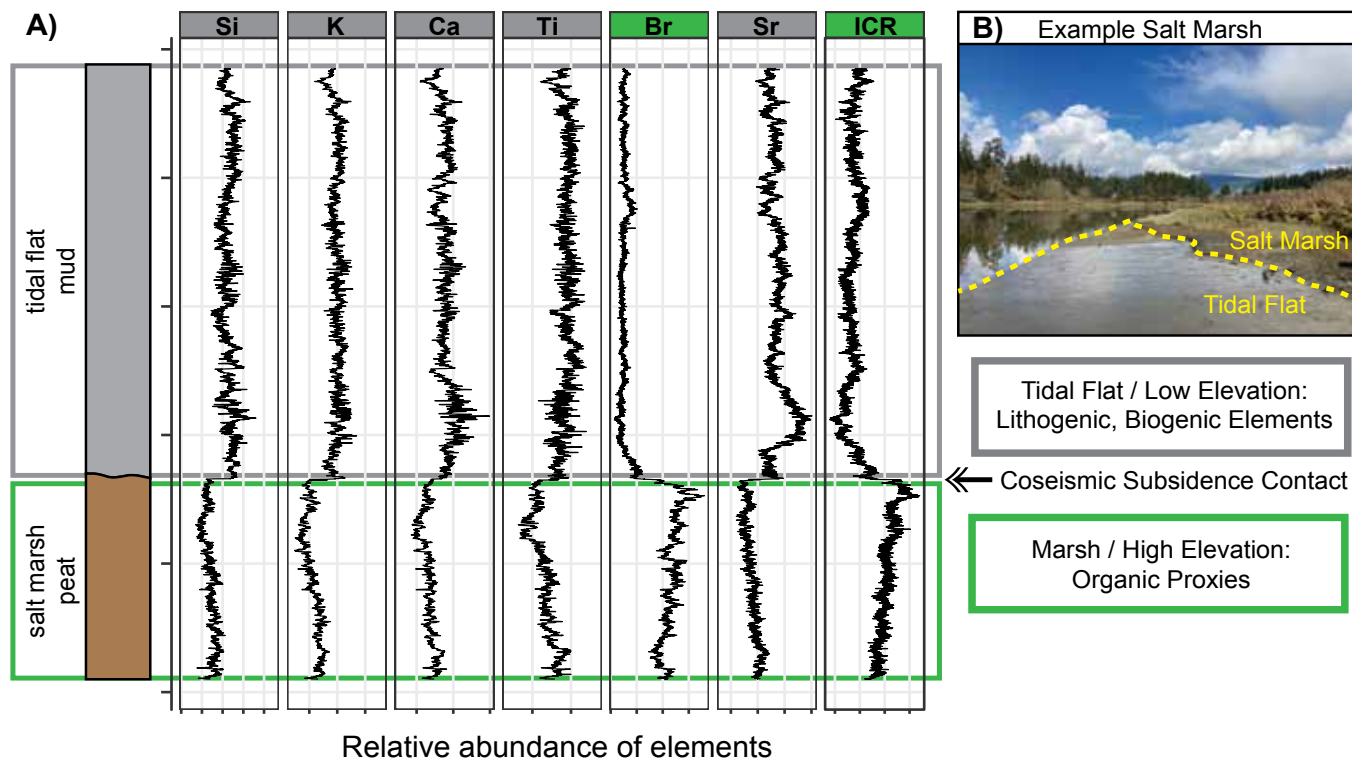
Figure 2: (A) Idealized sediment core collected from a salt marsh and associated conceptual elemental data illustrating stratigraphic evidence for coseismic subsidence. The subsidence contact is recognized by a sharp and abrupt change in lithology and elemental composition. Lithogenic (Si, K, Ti,) and biogenic (Ca, Sr) elements dominant at low elevations are highlighted in gray, while organic elements (Br, ICR), dominant at high elevations, are highlighted in green. **(B)** Typical Cascadia salt marsh where evidence for earthquakes and tsunamis can be found. The tidal flat and salt marsh subenvironments are delineated with the dashed line.

by lithogenic (Si, K, Fe, Ti) and biogenic (Ca, Sr) elements (Fig. 1). At low elevations, frequent tidal inundation remobilizes detrital sediment from the subtidal basin into the intertidal salt marsh. At higher elevations, the elemental composition is dominated by Br (high marsh; Fig. 1); however, despite its high abundance in seawater, Br in marshes is not as dominant at low elevations, but rather at high elevations where tidal inundation is less. This may be the result of Br's involvement in biogeochemical processes that transform mobile Br ions into immobile species within peats and soils (e.g. Keppler et al. 2000).

The ICR is applied as a proxy for organic content because organic forming elements (e.g. H, C, O, N) tend to have lower atomic numbers, while clastic sediments tend to be composed of higher atomic number elements (e.g. Si, Fe) (Woodward and Gadd 2019). The ICR also follows the same trend as Br, where highest values are found at high elevations where vegetation is most established within the intertidal range (Fig. 1). The elemental composition can distinguish subtle differences in the inorganic and organic content of salt-marsh sediments, which is predominantly controlled by tidal inundation.

Elemental geochemistry, obtained through XRF analysis, can resolve continuous, high-resolution elemental variation within sediment cores (Fig. 2). The relationship between modern salt-marsh sediments and elemental geochemistry can be applied downcore to resolve changes in paleoenvironmental conditions, including sudden, high-magnitude changes, such as coseismic subsidence associated with large earthquakes as shown conceptually in figure 2. Coseismic subsidence may be recognized by a dramatic and sharp

change in geochemistry from an organic dominated composition (i.e. Br-rich peats, soils) to a lithogenic and biogenic dominated one (i.e. Si, K, Fe, Ti, Ca, and Sr-rich tidal flat mud; Fig. 2). Elemental geochemistry may be especially useful for recognizing smaller amounts of coseismic subsidence when stratigraphic evidence is not obvious. Data derived from XRF analysis may also be applied as a supplemental proxy in microfossil-based sea- and land-level reconstructions to increase precision (e.g. Cahill et al. 2016). The down-core applications of elemental geochemistry for reconstructing coseismic subsidence still requires ground truthing, but shows promising potential based on the modern relationship between elemental composition and tidal elevation of salt-marsh sediments (Giang et al. 2023).

In addition to delineating the occurrence of coseismic subsidence in marsh stratigraphy, elemental geochemistry can also be used to identify tsunamis. Tsunami sediments preserved in salt marshes are often characterized by high concentrations of seawater ions (e.g. Na^+, Cl^-) and heavy elements from the offshore environment (e.g. Zn, Pb) (Chagué-Goff et al. 2017). In this way, XRF data can identify a marine origin for the anomolous sands, and may provide better estimates of marine inundation limits and lateral extensiveness of these deposits.

Advantages of elemental geochemistry
XRF-CS analysis simultaneously measures a wide suite of elements (Al to U), each with the potential to bolster paleoenvironmental and sea-level reconstructions. The rapid and high resolution (up to 100 µm) capability of the XRF-CS, in particular, enhances our ability to detect subtle changes occurring

over very short timescales. Similarly, XRF-CS offers non-destructive analysis of sediment cores, allowing for flexibility in subsampling strategies where elemental geochemistry can help guide subsequent destructive analyses (e.g. microfossil and grain-size analysis). Elemental geochemistry has many unexplored, but promising, applications that can be applied to the study of paleoearthquakes and tsunamis.

REFERENCES
Atwater BF et al. (2003) In: Developments in Quaternary Sciences. Elsevier, 331-350

Atwater BF (1987) Science 236 (4804): 942-944

Atwater BF, Hemphill-Haley E (1997) US Geol Surv Prof Pap 1576, 108 pp

Cahill N et al. (2016) Clim Past 12: 525-542

Chagué-Goff C et al. (2017) Earth-Sci Rev 165: 203-244

Giang A et al. (2023) MSc Thesis, Simon Fraser University, 63 pp

Hemphill-Haley E (1995) Geol Soc Am Bull 107: 367-378

Keppler F et al. (2000) Nature 403: 298-301

Nelson AR et al. (2021) Quat Sci Rev 261: 106922

Pilarczyk JE et al. (2014) Palaeogeogr Palaeoclimatol Palaeoecol 413: 144-157

Sawai Y et al. (2012) Geophys Res Lett 39: L21309

Woodward CA, Gadd PS (2019) Quat Int 514: 30-43

Comparing recent cyclone and tsunami deposits from southeast India

Chris Gouramanis[1]*, W. Yap[2,3]*, S. Srinivasalu[4], K. Anandasabari[5], D.T. Pham[6] and A.D. Switzer[2,3]

We examined multi-proxy evidence preserved within the 2004 Indian Ocean tsunami and overlying 2011 Cyclone Thane deposits on the southeast coast of India. We found no distinguishing features between the deposits.

Over 35% of the Earth's population lives in coastal zones and is vulnerable to a suite of acute (e.g. storms, cyclones and tsunamis) and chronic (e.g. sea-level rise) coastal hazards (UNEP). Many coastlines and communities are at risk of one or more of these coastal hazards. To properly prepare coastlines that are at risk of these acute coastal hazards, coastal communities and decision makers require detailed knowledge of the occurrence, frequency and magnitude of these events on their coastlines. Fortunately, large storms infrequently impact coastlines, and tsunamis are rare events, but when either event strikes, the outcome can be devastating. Unfortunately, the infrequency of large events makes it challenging for decision makers and communities to prepare.

To overcome this challenge, coastal geological records of both depositional and erosional characteristics have been examined to identify signatures of past coastal hazards (e.g. Switzer et al. 2014). These studies typically focus on areas where a coastal hazard has been encountered (e.g. Jankaew et al. 2008). However, to appropriately identify which coastal hazard has affected a region, modern analogues must be examined to identify characteristics that are unique to each hazard (e.g. Morton et al. 2007). Although much effort has focused on distinguishing between storm and tsunami characteristics in the geological record, these studies have examined deposits of tsunami and storms from different coastlines (e.g. Kortekaas and Dawson 2007; Morton et al. 2007), or have examined deposits that have occurred decades apart and may have undergone alteration (e.g. Nanayama et al. 2000). To date, very few studies have examined the geological signatures of a known tsunami and known storm deposit from the same location (e.g. Pham et al. 2017; Yap et al. 2021). We contribute to this growing body of knowledge by examining the beautifully preserved sedimentary deposits formed by the 26 December 2004 Indian Ocean tsunami (IOT), and the 2011 Cyclone Thane from Devanampattinam on the northern outskirts of Cuddalore, southeast India (Fig. 1a).

The 2004 tsunami and the 2011 cyclone
The 2004 IOT was triggered by a magnitude moment 9.2 earthquake centered off northeastern Sumatra and propagated northwards along 1500 km of the Sumatran–Andaman subduction zone, killing 230,000 people (Fig. 1). The IOT propagated across the Bay of Bengal and struck southeast India at 8:30 a.m. local time, causing approximately 16,000 deaths and US$2 billion

(International Recovery Platform 2004). At Devannampatinam, the tsunami had a maximum run-up height of 7 m and 700 m of inundation; and deposited a 38 cm thick sediment deposit.

Cyclone Thane made landfall near Cuddalore between 6:30 and 7:30 a.m. on 30 December 2011, causing over US$1 billion in damage and killing 48 people (Fig. 1; IMD 2012). At Devannampatinam, the storm surge run up was approximately 2 m, inundated approximately 300 m and deposited 27 cm of sediment.

Comparison of Cyclone Thane and 2004 IOT sedimentary deposits
Using satellite imagery of the region and discussions with local survivors, we identified a site approximately 300 m north of the village of Devannampatinam that preserves the 2004 IOT and 2011 Cyclone Thane deposits (Fig. 1a). The site was a partially vegetated; sandy beach dunes and backshore lagoonal environments formed from the closure of the Pennai River. At this site we excavated the 95 cm deep pit DPM3a and conducted multi-proxy analysis at centimetre-scale resolution that included stratigraphy, sediment grain-size, grain shape, and heavy mineral counts (Fig. 2a). Multivariate statistical analysis of the sedimentary variables demonstrates distinct differences between storm and tsunami deposits (Fig. 2b). We analyzed the microbial communities of 26 samples from the pit (Yap et al. 2021), but present the results of 13 representative samples here (Fig. 2c).

From deepest to shallowest, the sedimentary units observed in Pit DPM3a are an intertidal sand, 38 cm thick 2004 IOT deposit, a 12 cm thick layer of eolian (wind blown) sand, and the 27 cm thick Cyclone Thane deposit

(Fig. 2a). All of the units consist of medium sands (average size from 0.25–0.5 mm). The intertidal unit consists of northward dipping beds and thin horizontal beds, both with distinct heavy mineral layers (10–30%; Fig. 2a). The tsunami deposit consists of two beds separated by thin heavy-mineral laminations. From the bottom to the middle of the beds, the grain size becomes larger, and from the middle of the beds the grain size becomes smaller (Fig. 2a). These two beds represent deposition from two sequential waves, and much of the sediment came from the pre-existing nearshore or onshore environments. The eolian deposit consists of sands that have been partially reworked upper-2004-IOT sediments, some leaves and plastic waste (Fig. 2a). The storm deposit is composed of horizontal layers that consist of different proportions of heavy minerals (15–60%). The layers are thicker at the bottom of the deposit and become thinner towards the top. It is likely that the sediments came from the shoreface or onshore environments (Fig. 2a).

Discriminant function analysis (DFA) of all four deposits indicates that sedimentologically, only the heavy mineral distribution in the storm deposit can distinguish the four units (Fig. 2b). However, at Silver Beach, less than 2 km south of Devanampattinam, Srinivasalu et al. (2007) and Switzer et al. (2012) described 2004 IOT deposits with abundant heavy minerals and dense laminations, in contrast with Pit DPM3a.

Comparison of Cyclone Thane and 2004 IOT microbial communities
Analysis of microbial communities followed standard procedures of extracting deoxyribonucleic acid (DNA) sequences from the sediment (Yap et al. 2021). Microbial

Tsunami height: 7 m
Storm surge height: 2 m
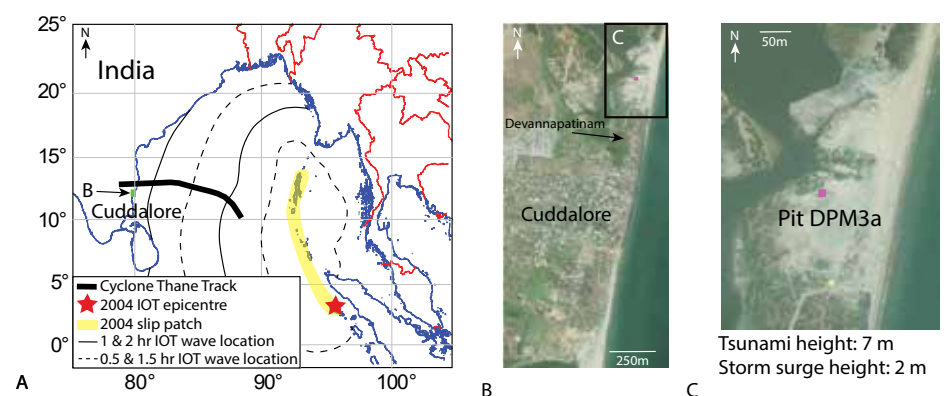
Figure 1: (A) Map of the Bay of Bengal showing the location and travel times of the 2004 IOT and Cyclone Thane storm track. **(B)** Satellite image of the Cuddalore coast showing the location of Devannampatinam and the pit site. **(C)** Satellite image of the beach near Devanampattinam where pit DPM3a was excavated.
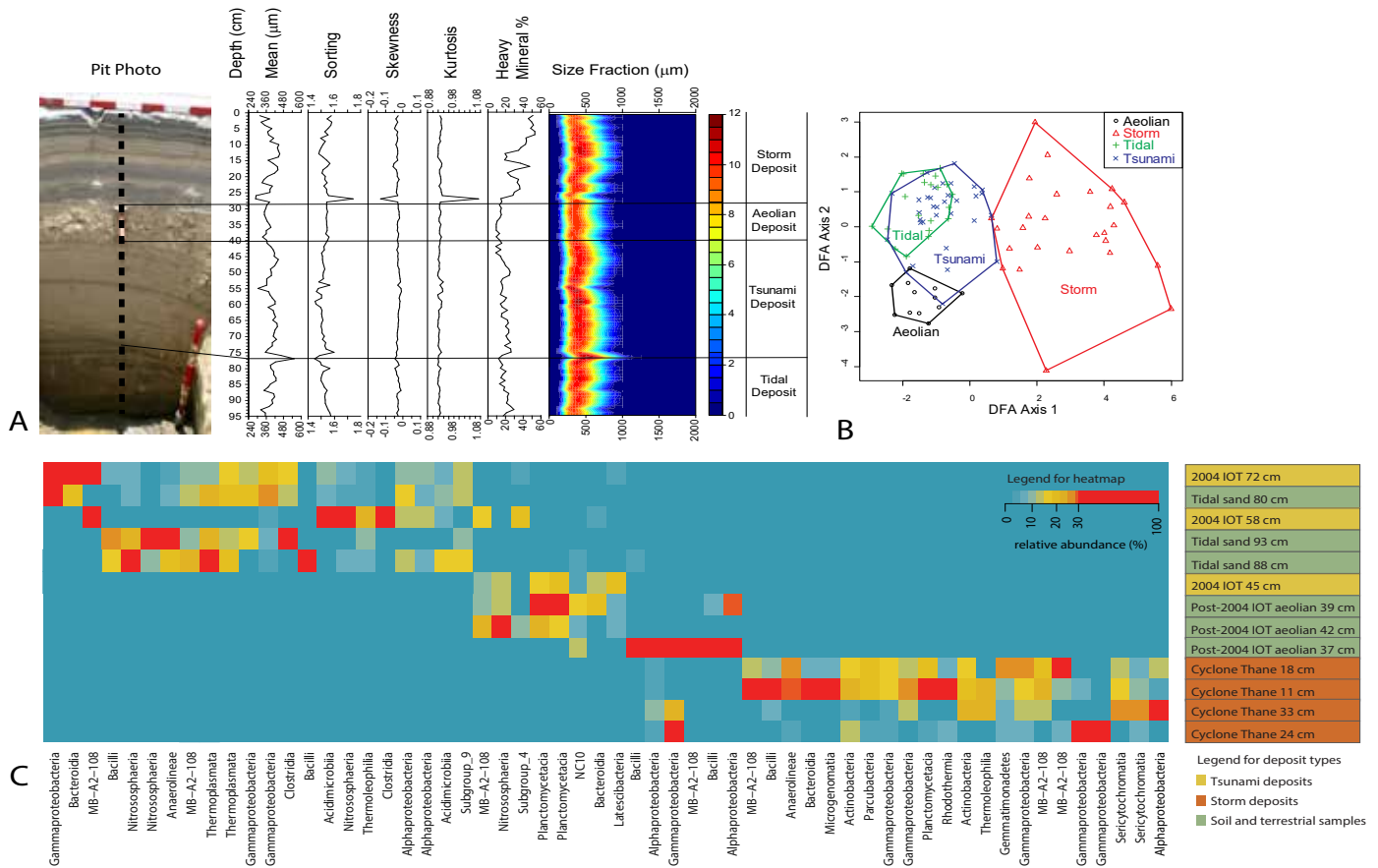
Figure 2: (A) Sedimentological parameters of Pit DPM3a. **(B)** DFA of sediment grain-size characteristics and heavy-mineral content of DPM3a units. **(C)** Microbes heatmap showing the relative abundances of different microbial groups in DPM3a communities. Figure modified from Yap et al. 2021.

metabarcoding analysis performed in this study targets the 16S ribosomal ribonucleic acid (rRNA) gene that identifies archaea, bacteria and eukaryotic taxa, as well as the 18S rRNA gene that is primarily used for identifying eukaryotic taxa. These rRNA markers are functionally similar over evolutionary time within a species, but exhibit variation across different species. The amplified DNA (called an amplicon) is then sequenced through a next-generation sequencer that generates a vast amount of DNA-sequence data. The distinct structure of the DNA sequences are determined (called amplicon sequencing variants – ASVs), and these ASVs are taxonomically distinct, thereby representing different species. Grouping of the average 42,406 DNA sequences resulted in a total of 4971 unique ASVs.

The microbial communities in the Cyclone Thane deposit significantly differed from the microbial communities in the 2004 IOT deposit, whereas the microbial communities within the 2004 IOT deposit were not significantly different from the underlying intertidal and overlying eolian deposits (Yap et al. 2021). The unique taxa preserved in the Cyclone Thane deposit included taxa from the families *Chromobacteriaceae*, *Rubinisphaeraceae*, *Burkholderiaceae*, *Micromonosporaceae*, *Bacillaceae*, *Nocardioidaceae*, *Sporichthyaceae*, *Caulobacteraceae*, and *Chitinophagaceae*, classes Sericytochromatia and Thermoplasmata, and the phylum Parcubacteria (Fig. 2b). No eukaryotic taxa could distinguish between the Cyclone Thane and 2004 IOT deposits.

Although it seems promising that storm and tsunami deposits can be distinguished by their microbial communities, further examination of another modern storm deposits on Phra Thong Island, Thailand, revealed that only taxa from the family *Chitinophagaceae* and class Thermoplasmata were present in both deposits (Yap et al. 2021). Further analysis of modern storm deposits may confirm the global signature of these taxa as unique to storm deposits. As no unique tsunami microbial signatures were present in the 2004 IOT deposits in India or Thailand, it is apparent that no global microbial signature exists for tsunami deposits (Yap et al. 2021).

This analysis focused on developing modern microbial signature analogues from storm and tsunami deposits. However, the microbial communities identified from the stacked 2004 and paleotsunami deposits from Thailand clearly show that the microbial communities become homogenized with non-tsunami sediments with age (Yap et al. 2023). It is likely the same would occur with older storm deposits under similar environmental conditions.

From our analysis of the 2011 Cyclone Thane and 2004 IOT deposits on the southeast coast of India, the sedimentological, stratigraphic and environmental DNA can discriminate recent coastal overwash events. However, modern analogues of both storm and tsunami deposits from the same geographical area are required to accurately discriminate between storm and tsunami deposits preserved in the geological record.

AFFILIATIONS
[1]Research School of Earth Sciences, Australian National University, Canberra, Australia
[2]Earth Observatory of Singapore, Nanyang Technological University, Singapore
[3]Asian School of the Environment, Nanyang Technological University, Singapore
[4]Insitute of Ocean Management, Anna University, Chennai, India
[5]National Institute of Ocean Technology, Chennai, India
[6]VNU University of Science, Vietnam National University, Ha Noi, Vietnam
*These two authors contributed equally to this work

CONTACT
Chris Gouramanis: chris.gouramanis@anu.edu.au

REFERENCES
IMD (2012) Very Severe Cyclonic Storm "THANE" over the Bay of Bengal (25-31 December, 2011): A Report. Cyclone Warning Division, Ministry of Earth Sciences, Government of India, New Delhi, 10 pp

International Recovery Platform (website), accessed 6 April 2011

Jankaew K et al. (2008) Nat 455: 1228-1231

Kortekaas S, Dawson AG (2007) Sed Geol 200: 208-221

Morton RA et al. (2007) Sed Geol 200: 184-207

Nanayama F et al. (2000) Sed Geol 135: 255-264

Pham DT et al. (2017) Mar Geol 385: 274-292

Srinivasalu S et al. (2007) Mar Geol 240: 65-75

Switzer AD et al. (2012) Geol Soc Lond, Spec Pub 361: 61-77

Switzer AD et al. (2014) J Coastal Res 70: 723-729

UNEP (website), Coastal Zone Management, accessed 23 October 2023

Yap W et al. (2021) Comms Earth & Environ 2: 129

Yap W et al. (2023) Mar Geol 457: 106989

Earthquake-related tsunami archives based on sediments from coastal lagoons in the Lesser Antilles

Stefano C. Fabbri[1,2,3,4], P. Sabatier[1], R. Paris[5], M. Biguenet[1,6], S. Falvard[5], N. Feuillet[2], G. St-Onge[3] and E. Chaumillon[6]

Sediment cores from two coastal lagoons in the Caribbean Sea provide evidence of regional and transatlantic paleotsunamis, alongside hurricane-related deposits. We employed sedimentological and geochemical methodologies, complemented by radiocarbon dating, to characterize these events spanning the past 3500 years.

Around 12% of the global population, more than 898 million people in 2020, reside in low-lying coastal areas (≤10 m above sea level; Reimann et al. 2023) that are vulnerable to rising sea level and natural hazards such as hurricanes and tsunamis (MacManus et al. 2021). To prepare for these threats, we must determine the recurrence and intensity of such events beyond instrumental and historical records. Sediment deposits, serving as natural archives, provide vital insights into past tsunamis (e.g. Costa and Andrade 2020) and hurricanes (e.g. Wallace et al. 2021), which are essential for accurate hazard assessment. Coastal lagoon systems are an ideal event archive due to i) their excellent preservation potential as a natural sediment sink, ii) the presence of a sandy barrier separating the ocean from the sink, and acting as a filter for extreme-wave events (EWEs), and iii) their brackish origin, allowing the preservation of inland-mobilized material related to tsunami backwash. Our study investigated sediment cores in coastal lagoons on two Caribbean islands (Saint Martin and Scrub Island) in the Lesser Antilles (Fig. 1).

Earthquake, tsunami and hurricane hazards in the Lesser Antilles

The volcanic arc along the Lesser Antilles was formed by the subduction of the North American Plate under the Caribbean Plate at a rate of 2 cm/yr (Fig. 1a). Although this is one of the most seismically quiet subduction zones worldwide (Cordrie et al. 2022), the area was struck by notable moment magnitudes (M_w) 7 to 8 seismic events, affecting the Caribbean islands over the last 300 years (Feuillet et al. 2011). In addition to intense ground shaking during earthquakes, events in 1843, 1867, 1969, 1985, and 2004 CE generated tsunamis (Cordrie et al. 2022). Historical records and sediment analysis also suggest that the transatlantic Lisbon tsunami of 1755 CE reached the Lesser Antilles, causing tsunami wave heights of more than 2 m, as supported by numerical models (Roger et al. 2011). Apart from earthquakes and tsunamis, the Lesser Antilles islands are also prone to hurricanes, as they are located in the Atlantic hurricane belt. The area of Scrub Island and Saint Martin was struck by 14 hurricanes between 1850 and 2017 CE (NOAA 2020) within a 40 km radius (Fig. 1f). Saint Martin was directly hit by the Category 5 Hurricane "Irma" in September 2017; the strongest hurricane ever formed in the Atlantic zone in historical times (Cangialosi et al. 2018) that broke several meteorological-based records (Fig. 1f). This has spurred

research into historical tsunami and hurricane hazards, nurturing efforts to improve our understanding of EWE recurrence intervals and coastal flooding.

## Methodology for tsunami-and-hurricane deposit analysis

We performed a combination of sedimentological, geochemical, and physical analyses targeting sandy EWE layers for identification and characterization (see Biguenet et al. 2021 and Fabbri et al. 2023 for more details). Furthermore, the cores underwent Loss of Ignition (LOI) and grain-size analyses, which allowed for the identification of variations in grain size, and specific endmembers. Additionally, geochemical analysis using X-ray fluorescence (XRF) was conducted to determine major and trace element contents. X-ray computed microtomography (micro-CT) was used to characterize the sedimentary fabric of EWE deposits (Biguenet et al. 2022; Fabbri et al. 2023). To obtain age constraints on the sediment cores, we developed a chronology based on short-lived radionuclides and radiocarbon ages.

Extreme-wave-event identification and characterization

Sedimentological observations and grain-size analysis enabled the identification and distinction of two sediment facies. Facies 1 (F1) is characterized by fine-grained sediment with a silty matrix rich in organic matter (Fig. 2). It contains ~20% organic matter, one-third silicates and a carbonate content between 35% (Scrub Island) and 48% (Saint Martin), reflecting a setting with very low energy levels, and mirroring the lagoon's background sedimentation. In contrast, Facies 2 (F2) comprises significantly coarser sediments, predominantly consisting of fine to very coarse sands. F2 is dominated by carbonates, constituting ~80% at Saint Martin and 40% at Scrub Island, with minor contributions of organic matter. F2's coarse sandy composition, marked by elevated Ca/Fe and Sr/Br ratios, indicates significant marine-sediment input and suggests high-energy transport processes that can erode and resuspend background sediment. Shells and their fragments, rich in Ca or Sr, denote marine influence, while Br and Fe reflects organic matter from the lagoon or land input, respectively. Both ratios represent marine
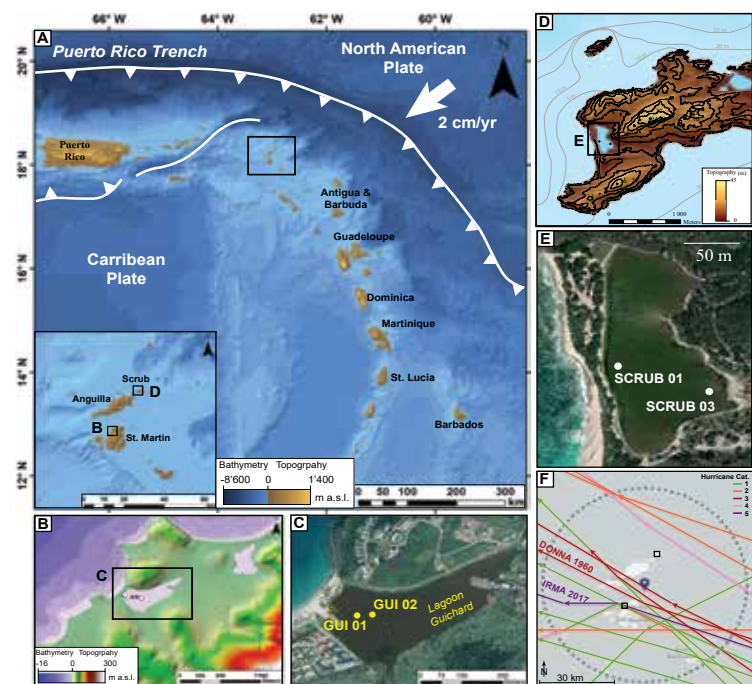
Figure 1: (A) Overview of the Lesser Antilles tectonic setting (modified after Biguenet et al. 2021). Inset: Overview of Saint Martin, Scrub Island and neighboring islands showing the investigated coastal lagoons (black squares). The bathymetry and topographic digital elevation model derived from SHOM (2018) for **(B)** Saint Martin and **(C)** Scrub Island. Satellite images of the coastal lagoon from **(D)** Saint Martin and **(E)** Scrub Island with its sand barriers. **(F)** Historical hurricane tracks (1850–2017) passing within 40 km (blue dashed circle) of the study area (NOAA 2020).
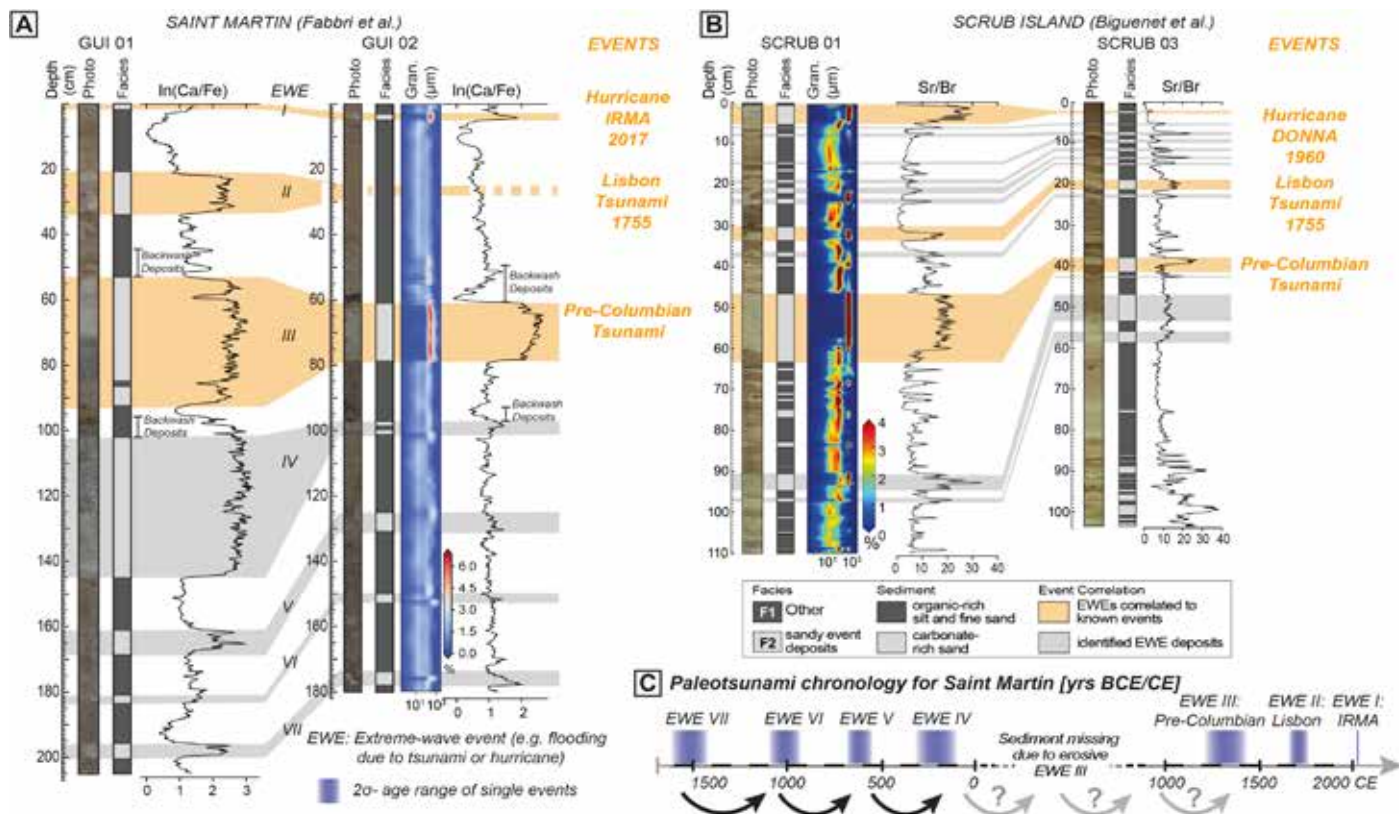
Figure 2: Core-to-core correlation of extreme-wave-event (EWE) deposits on **(A)** Saint Martin and **(B)** Scrub Island. Photograph, log, sediment facies, grain size and Ca/Fe and Sr/Br ratios shown for event identification. **(C)** Paleotsunami chronology for Saint Martin with a 400–500 year recurrence interval over the last 3500 years.

input equally well. Therefore, F2 is interpreted as the facies that likely results from EWEs. Some of the deposits right above the F2 layers (e.g. EWE III) show a geochemical signal rich in fine siliciclastic sediment with organic matter that likely corresponds to backwash deposits (Fig. 2a, b).

The EWE deposits characterized by F2 were of primary interest for cross-core correlation. The thickness of F2 layers decreases landward from GUI 01 to 02 at Saint Martin and SCRUB 01 to 03 at Scrub Island, supporting a marine origin of the deposits. Micro-CT-derived sedimentary fabric of event deposits reveals the spatial and geometrical arrangement of their sand grains, offering insights into flow direction and transport medium strength during deposition. A bimodal low-angle fabric dominated the Pre-Columbian tsunami deposit on both islands, distinguishable from the uni- and multi-modal fabric of other EWEs at these sites (Fig. 2). While there is no unique proxy to distinguish between tsunami and hurricane deposits, our recent results show that paleoflow reconstruction based on micro-CT data may resolve this challenge in the near future.

The recurrence of extreme-wave events
We have identified a total of seven and 25 EWE layers over the last 3500 and 1600 years at Saint Martin and Scrub Island, respectively (Fig. 2). Considering the very small deposit thickness of 1–2 cm of the Category 5 Hurricane Irma at Saint Martin, and the lack of backwash material, older EWEs with thicker deposits must likely be of tsunamigenic origin in this lagoon. This is also supported by CT-derived sedimentary fabric, allowing for a tentative paleotsunami chronology for the island (Fabbri et al. 2023). Moreover, geochemical data (Biguenet et

al. 2021) and sedimentary fabric (Biguenet et al. 2022) enabled the identification of two tsunamis among the 25 EWEs on Scrub Island. Scrub Island appears to respond more sensitively to EWEs (including some historic events), compared to the more sheltered Saint Martin lagoon, which is less exposed to the open ocean.

Between 1500 and 0 yr cal BCE, paleotsunamis occurred every 400 to 500 years on Saint Martin (Fig. 2c). The absence of events between 0 and 1350 yr cal CE is likely due to the extensive erosion caused by the Pre-Columbian tsunami, also identified on Scrub Island, and at the regional scale (Cordrie et al. 2022), emphasizing its destructive force. Engel et al. (2016) reported a possible minor event at ~450 yr cal CE, and a major paleotsunami at ~950 yr cal CE, the former observed on Barbados, Yucatan (Mexico), Anguilla and Scrub Island, potentially filling the chronological void. This allows for two potential hypotheses: 1) A regular seismic cycle of strong tsunamigenic earthquakes every 400 to 500 years with a hiatus due to erosion; or 2) Clusters of megathrust earthquakes, referred to as "super seismic cycles", known from many subduction zones and strike-slip faults worldwide (Philibosian and Meltzner 2020), assuming a phase of seismic quiescence instead of a hiatus.

AFFILIATIONS
[1]EDYTEM, Université Savoie Mont-Blanc, CNRS, Le Bourget du Lac, France
[2]Université de Paris, Institut de physique du globe de Paris, CNRS, France
[3]Institut des sciences de la mer de Rimouski (ISMER), Canada Research Chair in Marine Geology, Université du Québec à Rimouski and GEOTOP, Rimouski, Canada
[4]Institute of Geological Sciences & OCCR, University of Bern, Switzerland
[5]LMV, Université Clermont Auvergne, CNRS, IRD, OPGC, Clermont-Ferrand, France
[6]La Rochelle Université, CNRS, LIENSs, La Rochelle, France

CONTACT
Stefano C. Fabbri: stefano.fabbri@unibe.ch

REFERENCES
Biguenet M et al. (2021) Sediment Geol 412: 105806

Biguenet M et al. (2022) Mar Geol 450: 106864

Cangialosi JP et al. (2018) Hurricane Irma, NOAA and National Hurricane Center, 111 pp

Cordrie L et al. (2022) Earth-Sci Rev 228: 104018

Costa PJM, Andrade C (2020) Sedimentology 67: 1189-1206

Engel M et al. (2016) Earth-Sci Rev 163: 260-296

Fabbri S et al. (2023) 21st Swiss Geoscience Meeting, Mendrisio, Switzerland

Feuillet N et al. (2011) J Geophys Res Solid Earth 116: B10308

MacManus K et al. (2021) Earth Syst Sci Data 13: 5747-5801

NOAA, (2020) Historical Hurricane Tracks (website), accesed 4 April 2023

Philibosian B, Meltzner AJ (2020) Quat Sci Rev 241(1): 106390

Reimann L et al. (2023) Cambridge Prisms: Coastal Futures 1 (e14): 1-12

Roger J et al. (2011) Pure Appl Geophys 168: 1015-1031

SHOM (2018) MNT bathymétrique de façade de Saint-Martin et Saint-Barthélemy (Projet Homonim)

Wallace EJ et al. (2021) J Geophys Res Letter 48(1): e2020GL091145

Characterization of paleotsunami deposits along the western coast of India

Siddharth P. Prizomwala, U. Pandey, A. Tandon, N. Makwana and A. Das

Sedimentary deposits bearing potential paleotsunamis and/or cyclonic-storm records were studied along the western shoreline of India using a multi-proxy approach, as this helps to better assess the source of the wave(s).

The northern Arabian Sea hosts a major tsunamigenic source, i.e. the Makran Subduction Zone (MSZ), which has produced instrumental, historical and paleo-period tsunami waves that have caused damage on the shorelines of western India, Pakistan, Iran, and Oman (Fig. 1a). However, the shoreline of western India in this context has remained unexplored. The western coast of India, owing to its varied geomorphology (rocky coastline to sandy beaches/mudflats) has been impacted by past tsunamis; those footprints are preserved in the form of boulder blocks to sand sheets deposited far inland from the present-day shoreline (Bhatt et al. 2016; Prizomwala et al. 2015, 2018, 2021, 2022). Although the recurrence and larger catalog for the Holocene period are yet to be completed, the evidence of several major tsunamis generated by MSZ has been discussed briefly in recent literature (Prizomwala et al. 2021).

One problem in the study of sandy onshore deposits is that tsunamis are difficult to distinguish from storm deposits (Gouramanis et al. 2024; Yap et al. 2021). However, a combination of multi-proxy techniques can help to better assess the origin of the wave(s) that lead to the sedimentary deposit in question. This paper highlights the use of multi-proxy records in sand deposits to distinguish tsunamigenic sources from other coastal processes, most notably the cyclonic storms, on the western Indian shoreline. The coastlines of Kachchh and southwestern Saurashtra show beach-ridge dune-type assemblages suitable for preserving signatures of such events. Thus, they were used as study sites for the investigation of past extreme events (Fig. 1b).

Tsunami and storm deposits: Process, source, and character

Tsunamis can erode the seabed due to their high energy, and transport the eroded sediment in suspension onshore (supratidal regime). While receding after the maximum inundation, a significant part of the sediment/debris load is often deposited, while a minor part is transported offshore (Fig. 1b). Apart from tsunami waves, cyclonic storm surges also possess a similar character; however, they are of relatively lower intensity compared to tsunami waves. Storm surges are also often known to erode the seabed, but at relatively shallower depths (<10-20 m). Hence, the sedimentary deposits of a tsunami differ from a storm, or other

coastal process-derived deposits, by 1) their inland extent; 2) the presence of deeper sediment and fauna; and 3) the chaotic nature of the deposits (debris filled, lack of sorting) (Chagué-Goff et al. 2011; Dawson and Stewart 2007; Kortekaas and Dawson 2007; Morton et al. 2007; Prizomwala et al. 2018). However, several storms (e.g. Typhoon Haiyan in 2013) deposited sediments with similar characteristics to those from tsunamis, making them more challenging to distinguish (Soria et al. 2017). Therefore, it is crucial to assess the recorded (instrumental) storm history of a region together with a probable worst-case scenario (most intense storm and its characteristics), while comparing and assessing a probable tsunami-deposit inference.
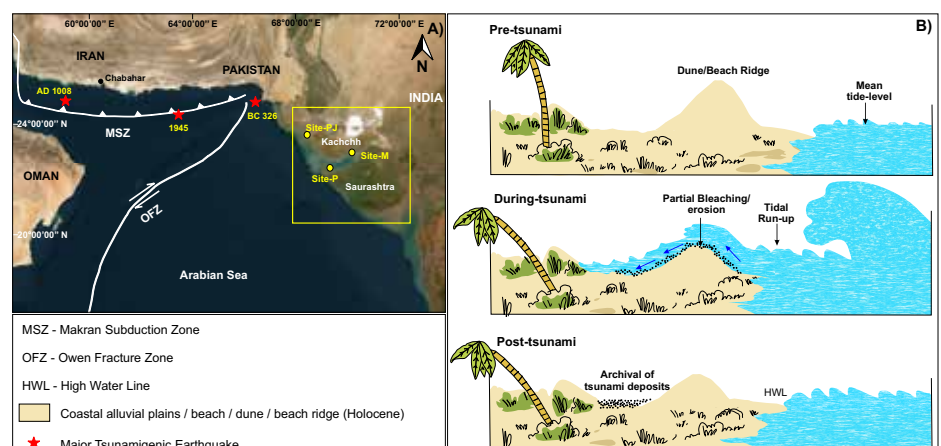
Multi-proxy record of sedimentary deposits from the western coastline of India

Sediment geochemical proxies can be very reliable for discriminating different source signals, particularly when there is a mixing of tsunami-derived sand and local processes (Chagué-Goff 2010; Prizomwala et al. 2018, 2022; Srinivasalu et al. 2008). For example, the sand derived from shallower offshore sand shoals in the Gulf of Kachchh off the Pindara (site-P) and Kachchh (site-M) coastline comes from the Deccan Basalts (Fig. 2a). These sediments are richer in Fe_2O_3, TiO_2, Zr and Sr, owing to their provenance from the Deccan Basalts (see Prizomwala et al. 2018 for details). Their higher concentration in $CaCO_3$ is due to the high content of broken shells and foraminifera in sandy sediments, which are likely derived from

offshore erosion. Previous researchers have inferred that these sands were eroded during historically known tsunami events, such as the 1945 CE tsunami event and the 1008 CE event along the MSZ, and deposited in the form of a sand layer at the Pindara (site-P) and Kachchh (site-PJ & M) coastlines (Prizomwala et al. 2018, 2022). The geochemical signatures are a useful tool for linking offshore geological provenance to the sand layer deposited inland, owing to the extreme event. For the Kachchh coast in particular, the sediments from the Deccan Basalts overwhelms the signature in inferred tsunami sand horizons.

The onshore (landward) extent of sedimentary deposits is one of the most common approaches for distinguishing a tsunami deposit from a probable storm surge deposit (Kortekaas and Dawson 2007; Morton et al. 2007; Prizomwala et al. 2018, 2022). The coastal remnants of the deposits along the Pindara (site-P) coast are observed in the form of sand sheets, reaching up to 580 m inland from the high-water line (HWL) (Fig. 2b). The sand-sheet geometry was probed using multiple shallow pits across the coast. Available records of the most intense storms in the Arabian Sea show a much more limited spatial extent in their inland sediment transport deposit (Prizomwala et al. 2018).

The sedimentological signature of these tsunamis is characterized by the lack of sorted grains, with overall landward fining along with the presence of mud intraclasts, broken shell and foraminifera. These observations demonstrate the high-energy wave

MSZ - Makran Subduction Zone
OFZ - Owen Fracture Zone
HWL - High Water Line
☐ Coastal alluvial plains / beach / dune / beach ridge (Holocene)
★ Major Tsunamigenic Earthquake

Figure 1: (A) Tectonic setup of the northern Arabian Sea with tsunamigenic sources. **(B)** Schematic scenario for a pre-, during- and post-tsunami event, along a with beach-ridge-dune configuration.
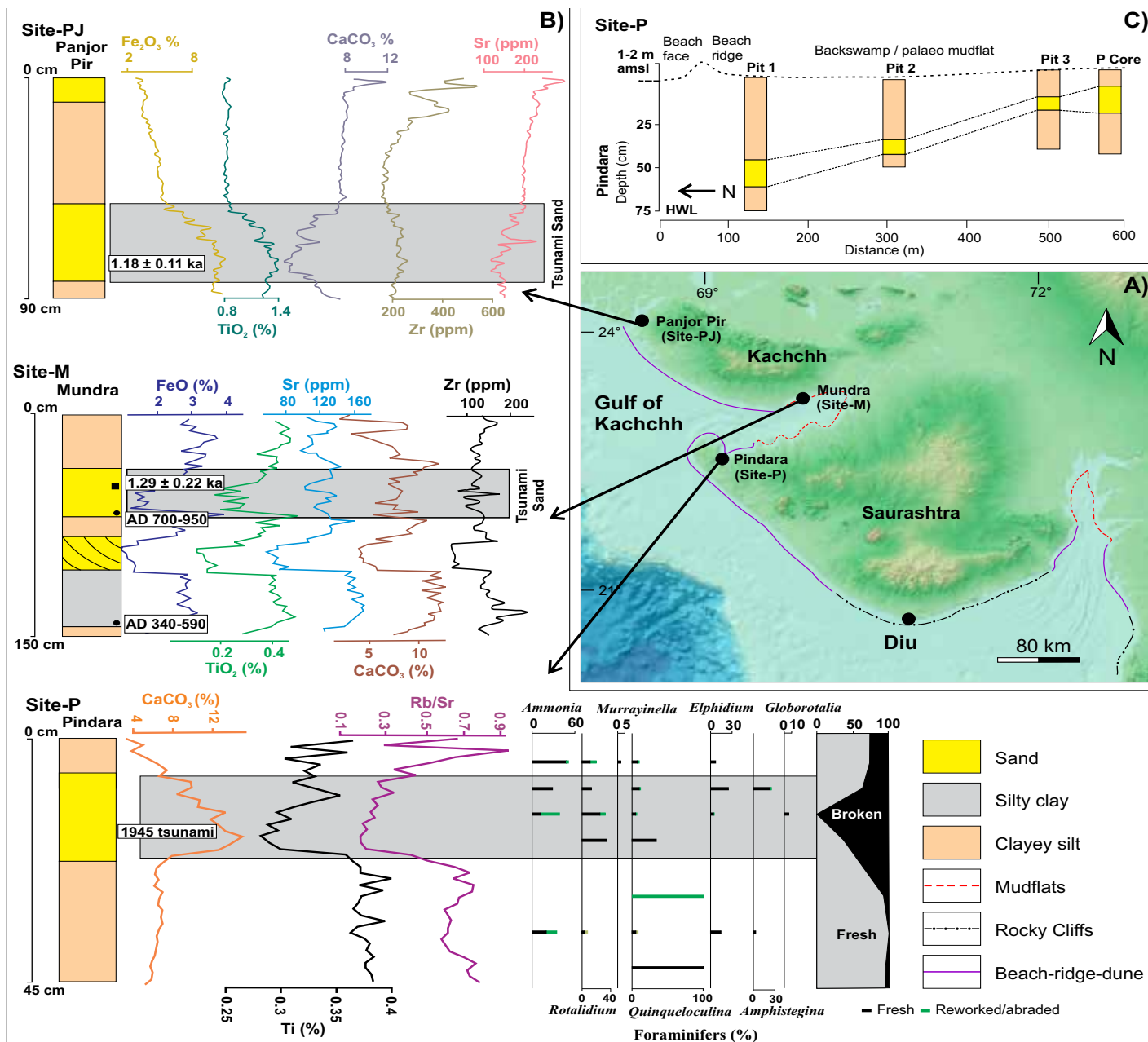
Figure 2: (A) Inset shaded relief map of Gujarat (western India). **(B)** Temporal geochemical and foraminiferal distribution of sedimentary deposits at sites P, PJ and M. **(C)** An onshore extent of tsunami sand layer with across-coast profile of site-P.

character, which essentially eroded the bottom of the offshore seabed (Kortekaas and Dawson 2007; Morton et al. 2007; Shanmugam 2012). Storms, on the other hand, exhibit a comparably better sorting, the absence of mud-intraclasts and the presence of several sedimentary structures. The increase in benthic foraminiferal diversity, and the presence of species occurring offshore, consolidates the assumption of the tsunami origin of these sand layers (Chagué-Goff et al. 2011; Prizomwala et al. 2022).

Outlook
The debate regarding the differentiation of sedimentary deposits from tsunami and cyclonic storm surges from the Arabian Sea requires an investigation of more modern analogues (e.g. Gonu, the only super cyclone in the instrumental history of the Arabian Sea, which occurred in 2007). There is a need to study more of these past tsunamigenic events from the Arabian Sea in order to build a catalog spanning at least the Holocene period. Similarly, compared to tsunamis, the

available data of storms is extremely limited and needs to be augmented using geological records. More robust and complete information regarding the extent, type and nature of super cyclonic storm-surge deposits would help to assess the threshold for differentiating both wave types. Such information is a prerequisite for a better coastal hazard assessment, which is crucial for the safety of the fast-developing coastal infrastructure. A multi-proxy approach involving sedimentology, geochemistry, micropaleontology, and the landward extent of the deposits plays a vital role in determining the source of the wave(s).

CONTACT
Siddharth P. Prizomwala: prizomwala@isr.res.in

REFERENCES
Bhatt N et al. (2016) Nat Hazards 84: 1685-1704

Chagué-Goff C (2010) Mar Geol 271(1-2): 67-71

Chagué-Goff C et al. (2011) Earth-Sci Rev 107(1-2): 107-122

Dawson A, Stewart I (2007) Sediment Geol 200(3-4): 166-183

Gouramanis C et al. (2024) Pages Mag 32(1): 32-34

Kortekaas S, Dawson AG (2007) Sediment Geol 200(3-4): 208-221

Morton RA et al. (2007) Sediment Geol 200(3-4): 184-207

Prizomwala SP et al. (2015) Nat Hazards 75: 1187-1203

Prizomwala SP et al. (2018) Sci Rep 8: 16816

Prizomwala SP et al. (2021) Quat Int 599: 24-31

Prizomwala SP et al. (2022) Mar Geol 446: 106773

Shanmugam G (2012) Nat Hazards 63: 5-30

Soria JLA et al. (2017) Sediment Geol 358: 121-138

Srinivasalu S et al. (2008) Environ Geol 53 : 1711-1721

Yap W et al. (2021) Commun Earth Environ 2 : 129

Tsunami deposits to reconstruct major earthquake chronology in southern Peru

Stéphanie Cuven[1], R. Paris[2], L. Audin[3], S. Mitra[2], L. Gielly[4] and E. Aguirre[5]

A study of tsunami deposits preserved in coastal sedimentary sequences of southern Peru suggests that five very large tsunamigenic earthquakes with moment magnitude (M_w) >8.5 occurred during the last 2500 years, including the 1604 and 1868 CE tsunamis.

Timescales of tsunami and earthquake record

Subduction-zone megathrust faults cause the largest earthquakes on Earth. The recent megathrust earthquakes in 2004 in Sumatra (Indonesia; M_w 9.3) and 2011 in Tōhoku-oki (Japan; M_w 9.1), and their associated tsunamis, highlighted a weakness in the integration of the time factor in hazard evaluation. Indeed, tsunami-hazard evaluation must combine both historical evidence of tsunamis (recorded or observed events) and geological evidence (tsunami deposits). This is particularly critical when the historical catalogs are limited in time, and/or when the largest events have a long period of return, thus being potentially absent from the historical record.

In Peru, the time period covered by the catalogs of earthquakes and associated tsunamis is limited to the last five centuries, with the oldest event dating back to 1582 CE (Comte and Pardo 1991; Dorbath et al. 1990). Time acts as a filter, and very few earthquakes of M_w <7.5 are mentioned in the archives before the 19th century (Kulikov et al. 2005). Paleotsunami studies have the potential to enlarge the timescale of tsunami catalogs up to the early Holocene. This represents a crucial contribution to the assessment of earthquake and tsunami hazards.

Historical tsunamis in southern Peru

In Peru, based on statistics of historical events, the return periods of M_w ~8 and M_w ≥8.7 tsunamigenic earthquakes are estimated at 10 and 100 years, respectively (Kulikov et al. 2005). A total of 10 tsunamigenic earthquakes have occurred in southern Peru (south of Nazca Ridge) since 1530 CE (Comte and Pardo 1991; Dorbath et al. 1990; Okal et al. 2002), including five major events in 1604 (M_w 8.7, with a tsunami up to 16 m high when arriving on shore), 1687 (M_w 8.4, 10 m), 1784 (M_w 8.4, 4 m), 1868 (M_w 8.8, 18 m), and 2001 CE (M_w 8.4, 8.8 m). Regional earthquakes in central Peru (1687, 1746 and 2007 CE) and northern Chile (1615, 1877 and 2014 CE) also generated tsunamis that were observed on the coasts of southern Peru. Trans-Pacific tsunamis caused by far-field sources (Japan, Tonga, etc.) typically produce wave heights lower than 3 m on the coast of Peru.

Additionally, Spiske et al. (2013a) found two tsunami deposits dated 615 BCE–119 CE, and 207 BCE–255 CE, which represent the only evidence of paleotsunamis published so far in southern Peru. Abad et al. (2020) described a coastal boulder-field dated between the 13th and 16th centuries.

Paleotsunami sites and methods

In this study we investigated two coastal sites in southern Peru: the Ite lagoon (south of Ilo) and the Quilca floodplain (south of Camana) (Fig. 1). Samples were collected along trenches, using both U-channels and push cores, as well as bulk samples of available sediments. Laboratory analyses consist of combining XRF core-scanner, SEM (Scanning Electron Microscope), X-ray computed tomography (X-CT), and DNA metabarcoding methods to characterize the structure, grain size, fabric, chemical, mineralogical, and biological compositions of the sediments. This workflow was previously applied to storm and tsunami deposits, as explained in Sabatier et al. (2010), Cuven et al. (2013), Paris et al. (2020) and Biguenet et al. (2022).

We also tested a DNA approach: samples of tsunami and terrestrial deposits were directly collected from the field with sterile devices, immediately dessicated for preservation and processed following the methodology by Bremond et al. (2017), specifically targeting 18S rDNA region V7
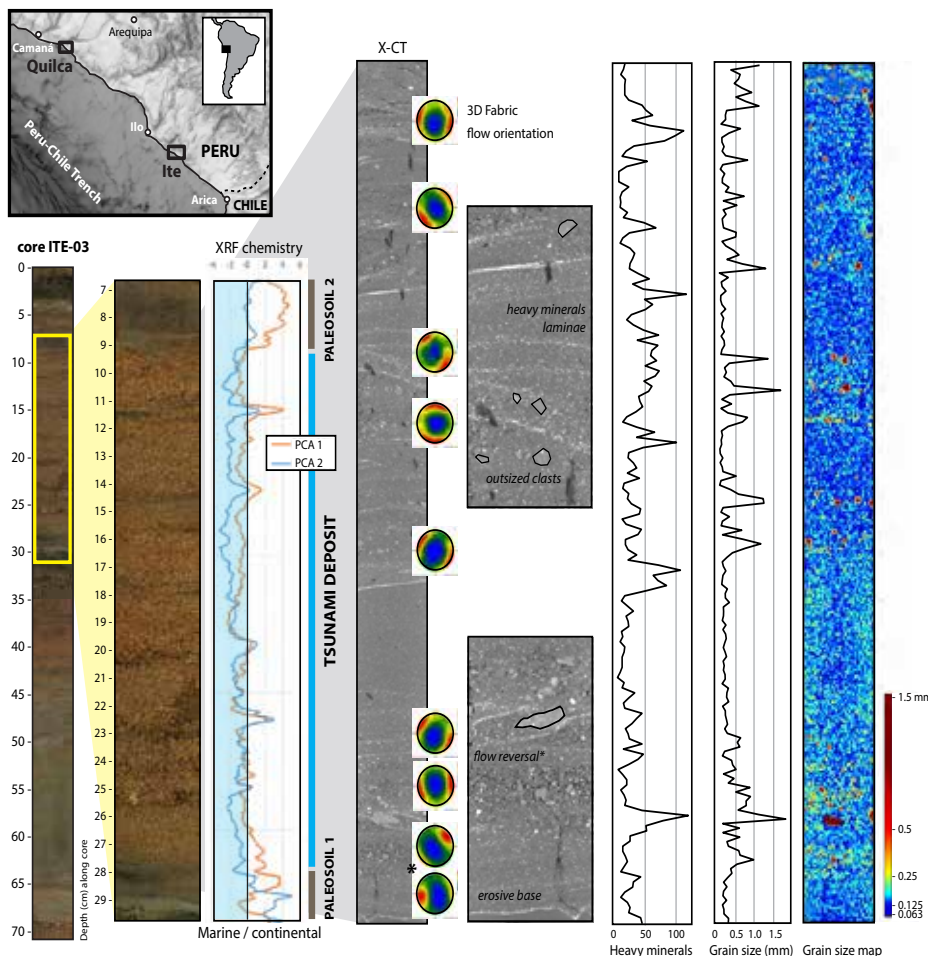
Figure 1: Location of the study sites in southern Peru, and methods used to identify tsunami deposits in the coastal sedimentary record. **(A)** Photography of the core. **(B)** Close-up view of a tsunami deposit. **(C)** Principal Component Analysis (PCA) of XRF core-scanner data. **(D)** X-CT (X-ray computed tomography). **(E)** Stereograms of sedimentary fabric. **(F)** Abundance of heavy minerals. **(G)** Grain-size data inferred from X-CT.

(a region of nuclear DNA encoding 18S nuclear ribosomal RNA, as commonly used for eukaryotes in metabarcoding: Guardiola et al. 2016). Samples of wood fragments and organic sediment were ^{14}C dated at Laboratoire de Mesure du Carbone in France using accelerator mass spectrometry (Dumoulin et al. 2017).
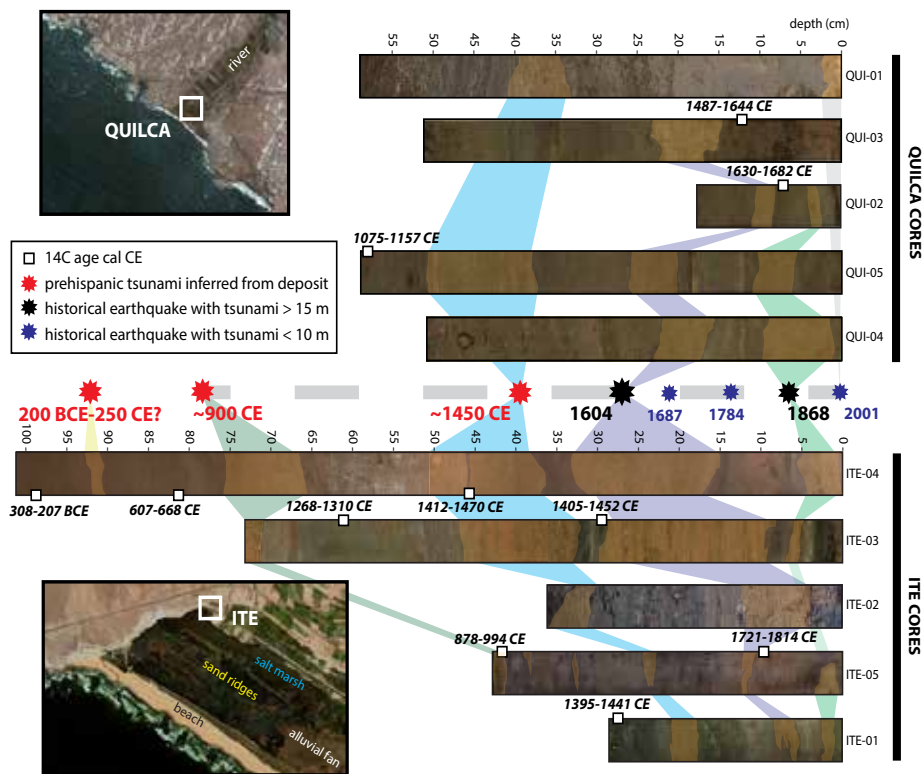
A 2500-year chronology of tsunami deposits

Tsunami deposits identified in the sedimentary sequences appear as fine-to-medium sand units intercalated in dark-brown lagoonal mud at Ite, or brownish overflow silt at Quilca. These sand units are characterized by an increased marine signature compared to background sediments, as evidenced by vertical variations of the chemical composition (Fig. 1). Grain-size distribution shows that the sand units have a variable proportion of silt and clay, which reflects the mixing of different sediment sources. The sand is made of silicate minerals (quartz being dominant), with some oxides, as well as wood, plants, and sparse marine bioclasts (foraminifera, small fragments of shells). DNA analyses record a mixed marine-continental composition, especially in Quilca where DNA show marine algae, ciliates and worms, Pacific coral reef fish, along with brakish diatom species, Andean plants, and terrestrial ciliates and worms.

The base of the sand units is often erosive, thus forming rip-up clasts of mud or soil inside the sand. Their internal structure is emphasized by horizontal to low-angle bedding, heavy-minerals laminae, erosive discontinuities between subunits, and vertical variations of the grain size (including clast-supported lenses of coarse sand, and matrix-supported silt-rich subunits). Different types of sedimentary fabric were inferred from X-CT: flow-parallel fabric oriented landward (wave uprush) or seaward (flow-reversal or backwash), and flow-transverse fabric (Fig. 1).

The sedimentary sequences (and thus the tsunami chronology) are time-constrained by ^{14}C ages that range between 308–207 BCE (100 cm depth) to 1721–1814 CE (10 cm depth) at Ite, and 1075–1157 CE (60 cm depth) to 1630–1682 CE (7 cm depth) at Quilca (Fig. 2). The 1604 and 1868 CE tsunamis are well recorded at both sites. The 1604 CE tsunami deposit is particularly thick (up to 20 cm) at Ite. We also found three prehispanic tsunamis. A major tsunami at ~1450 CE is preserved at both sites. Two older tsunamis are found at Ite: one at ~900 CE, and the oldest one between 200 BCE and 250 CE (which could correspond to the 207 BCE–255 CE event of Spiske et al. 2013a).

Earthquake magnitude versus tsunami-deposit preservation

In southern Peru, the last five major earthquakes ($M_w \geq 8.4$) occurred at quite regular intervals (every 83–133 years), but there is a variability in the rupture extent (Dorbath et al. 1990; Philibosian and Meltzner 2020).

Figure 2: Location of the core samples in Quilca and Ite, and synthetic extended chronology of tsunami events in Southern Peru.

The more extensive ruptures occurred in 1604 and 1868 CE, which is concordant with the tsunami-deposit records. Indeed, historical tsunamis with wave heights >15 m, such as the 1604 and 1868 CE ones, are well recorded in the coastal stratigraphy (tsunami deposits being typically 5–20 cm thick), whereas tsunamis with wave heights <10 m in the study area (e.g. 1687, 1784 and 1877 CE) are apparently not preserved in lagoons that are protected by coastal sand ridges.

As an example, the 2001 CE tsunami had wave heights up to 2.3 m in Quilca (Okal et al. 2002). During our field survey in 2017, traces of the 2001 CE tsunami were still visible in the form of irregular and sparse sand layers (up to 1.5 cm thick at 100 m from the shoreline, but 420 m away from the riverbed), abundant drift wood, and anthropic debris. Spiske et al. (2013b) reported a decrease of the average thickness of the 2001 CE tsunami deposits from 0.5–28 cm to 0.1–6 cm in only six years, and concluded that even in such an arid environment, the sedimentary record of tsunamis may not fully represent a comprehensive tsunami hazard.

Thus, there seems to be a threshold of earthquake magnitude (M_w >8.5 in southern Peru) to generate a tsunami large enough to be preserved in the sedimentary record. Our study reveals that only five very large earthquakes left tsunami deposits in coastal lagoons of southern Peru during the last 2500 years, while 10 tsunamis occurred during the last 500 years.

AFFILIATIONS
[1]Mercator Ocean International, Toulouse, France
[2]Université Clermont Auvergne, CNRS, IRD, OPGC, Laboratoire Magmas et Volcans, Clermont-Ferrand, France
[3]IRD, Université Grenoble Alpes, CNRS, ISTerre, Grenoble, France
[4]Laboratoire d'ÉCologie Alpine, Université Grenoble Alpes, CNRS, LECA, Grenoble, France
[5]INGEMMET, Lima, Peru

CONTACT
Raphaël Paris: raphael.paris@uca.fr

REFERENCES
Abad M et al. (2020) Sediment 67: 1505-1528

Biguenet M et al. (2022) Mar Geol 450: 106864

Bremond L et al. (2017) Quat Sci Rev 170: 203-211

Comte D, Pardo M (1991) Nat Haz 4: 23-44

Cuven S et al. (2013) Mar Geol 337: 98-111

Dorbath L et al. (1990) Bull Seism Soc Am 80: 551-576

Dumoulin J-P et al. (2017) Radiocarbon 59: 713-726

Guardiola M et al. (2016) Plos One 11(4): e0153836

Kulikov EA et al. (2005) Nat Haz 35: 185-209

Okal EA et al. (2002) Seismol Res Lett 73: 904-917

Paris R et al. (2020) Sediment 67: 1207-1229

Philibosian B, Meltzner AJ (2020) Quat Sci Rev 241: 1066390

Sabatier P et al. (2010) Sed Geol 228: 205-217

Spiske M et al. (2013a) Quat Int 305: 31-44

Spiske M et al. (2013b) Earth-Sci Rev 126: 58-73

The camouflaged tsunami record of arid coasts: Looking for sand in the Atacama Desert

Tatiana Izquierdo[1,2] and Manuel Abad[1,2]

The poor preservation potential of tsunami records in arid environments has prevented detailed studies of tsunami-washed sand deposits along these coasts. However, recent studies have shown that evidence of these high-energy marine events is camouflaged within (hyper)arid landscapes.

In general, the study of recent paleotsunamis has been based on the identification and analysis of their onshore deposits, in the absence of historical or archaeological evidence (e.g. Engel et al. 2020; Prizomwala et al. 2024). High-energy waves mix the marine sediments they drag from the seabed with the continental deposits they flood, resulting in a layer of sand containing a melting pot of grains and microfossil remains.

Scientists studying paleotsunamis look for areas where these sediments are trapped and, in most cases, they find them in very similar environmental scenarios: coastal wetlands and lagoons near river mouths, or even continental lakes near the shoreline where waves can reach and deposit the sediment they transport.

The presence of large bodies of freshwater is a common characteristic, as it favors the accumulation of the tsunami deposits. In addition, the subsequent, and continuous sedimentary dynamics buries them, allowing their preservation in the sedimentary record. But, what happens when a tsunami impacts coasts where these freshwater bodies do not exist, such as in the Atacama Desert in Chile, the driest place in the world? Without wetlands, lagoons, estuaries, or deltas, how are the tsunami deposits preserved?

Why study the tsunami record of the southern Atacama Desert?

The Chilean coast is a highly seismic and tsunami-prone hazard zone, owing to the convergent boundary where the Nazca Plate subducts below the South American Plate (Fig. 1). In this setting, tens of earthquakes with focal mechanisms and magnitudes large enough to trigger highly destructive tsunamis must have been generated during the Late Holocene, although no great earthquakes (moment magnitude [M_w] ≥8.6; Klein et al. 2017) have been reported in the historical chronicles of the southern edge of the Atacama Desert (Fig. 1). In fact, only two large-magnitude earthquakes that triggered destructive tsunamis occurred in historic times; in 1819 and 1922 CE (Ruiz and Madariaga 2018).
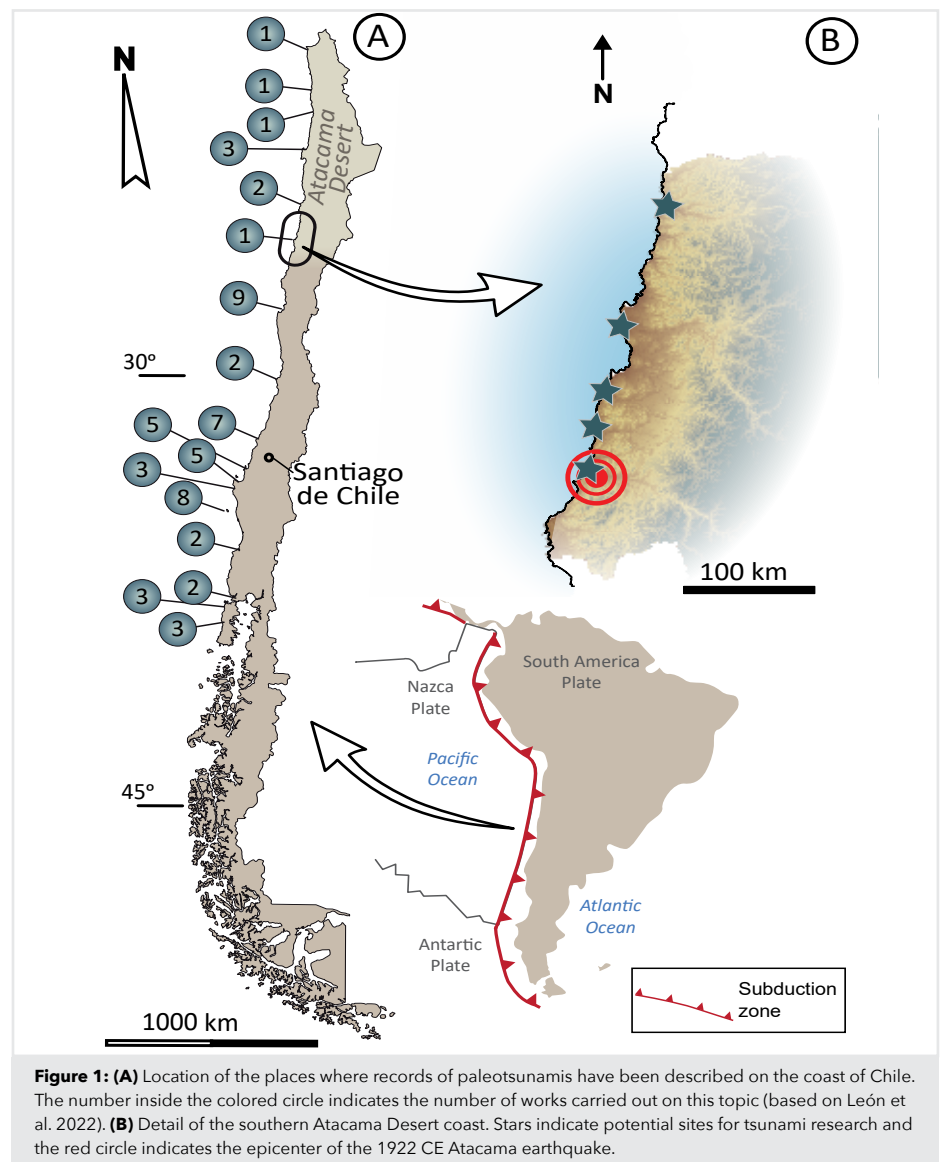
There is still great uncertainty regarding the number and magnitude of large paleotsunami events in this sector of the Atacama

Desert during the Late Quaternary, caused by the challenging accessibility and long distances from major cities that have prevented exploration of these coasts. The less-evident record of tsunami deposits linked to environmental constraints when compared with other zones of Chile contributes to this uncertainty (Fig. 1).

The tsunami record on arid coasts: Boulder deposits

On arid, rocky coasts, such as those of northern Chile, tsunamis are not commonly recorded as sand layers interbedded with finer sediments, but as boulder fields on top of cliffs. Some of these reach weights of hundreds of tons and were moved from areas located up to 10 m above sea level (Abad et al. 2020). These deposits form when the tsunami waves impact the rocky cliff, detach a boulder, creating a boulder niche, and transport it landwards tens to hundreds of meters. The orientation of the boulders can be used to interpret the wave direction, and their size and mass can be used to model the scale of the extreme

Figure 1: (A) Location of the places where records of paleotsunamis have been described on the coast of Chile. The number inside the colored circle indicates the number of works carried out on this topic (based on León et al. 2022). **(B)** Detail of the southern Atacama Desert coast. Stars indicate potential sites for tsunami research and the red circle indicates the epicenter of the 1922 CE Atacama earthquake.

waves and their flow velocities. The advantage of these deposits is that they cannot be reworked by the wind after their deposition; thus, they provide exceptional tsunami evidence on arid coasts that prevail in the landscape without being practically modified over time. Unfortunately, the scenario in which this type of evidence is formed is very specific, and the recording of events through these records is very incomplete. In some cases, a boulder field can even be the result of successive large tsunamis.

The tsunami record on arid coasts: Fine grained deposits

In the absence of cliffs and freshwater bodies that may preserve the large volumes of sand brought from the sea to the coasts of the Atacama Desert, the sediments are deposited on vast coastal plains and become part of the dune fields, which bear little resemblance to the classic description of "tsunamiites" in scientific literature (Shiki and Yamazaki 2008). The apparent absence of this geological evidence should not be interpreted as evidence of its absence. This is perhaps one of the last challenges that remains to be overcome in tsunami science, and it must be addressed from a holistic perspective, in order to determine the tsunamigenic origin of camouflaged morphogenic and sedimentary evidence.

So, where, and how, do we look for "classic" and probably clearer evidence of paleotsunami(s) in the Atacama Desert? Along thousands of kilometers of arid coast there are a few exceptional places in which a combination of geomorphological, climatic and geological factors exist, and small coastal wetlands have been formed, owing to the emergence of groundwater in the permanent absence of surface waters that reach the sea. Nevertheless, the probability of marine high-energy events being recorded and preserved in these environments is low, because several processes may alter them.

Firstly, after the marine flooding occurs and seawater retreats, evaporation of the wet marine sediments begins. This newly deposited material includes sea salts that precipitate, as evaporation continues, forming saline crusts and nodules that will mask the tsunami deposit in the geological record (Fig. 2). In fact, tsunami sand or mud deposits can be misinterpreted as paleosoils in the field. If this salt precipitation process does not occur, the absence of sedimentation in arid environments will not protect them from eolian processes, leading to an incomplete tsunami record.

Finally, ephemeral rivers, where coastal wetlands are formed, are occasionally activated when intense El Niño-Southern Oscillation-related rain occurs in the desert. These continental flows present a strong erosive capacity, even near the river mouth, and can dramatically change the coastal wetland configuration, as occurred after the March 2015 CE rains in Atacama (Abad et al. 2017).
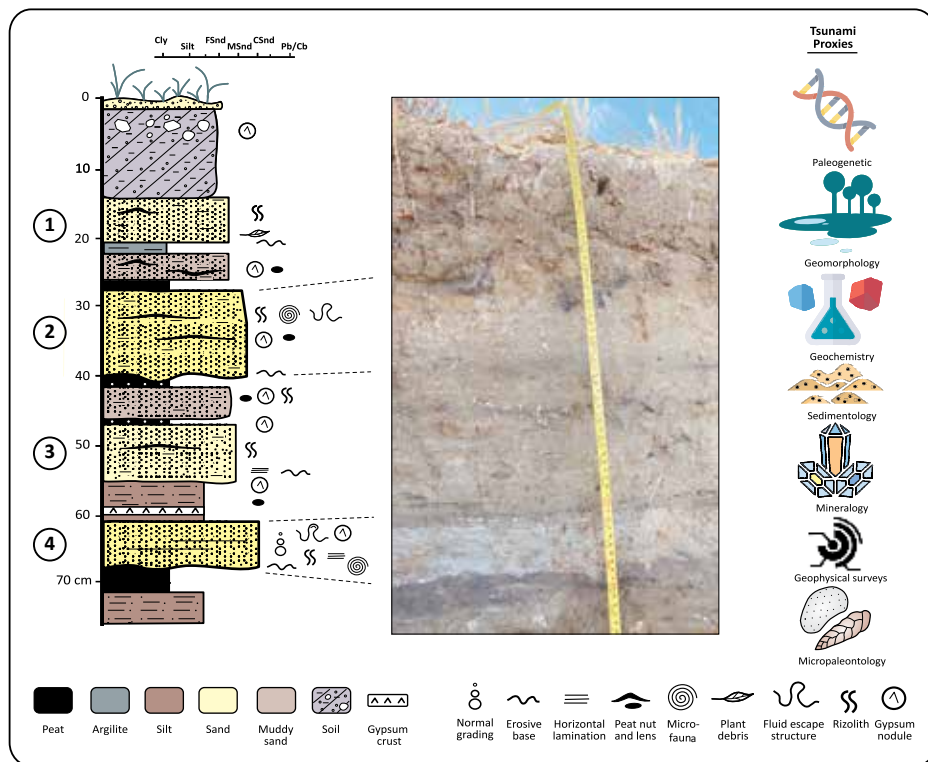
Figure 2: Detailed sedimentological section elaborated in an arid coastal wetland in the southern Atacama Desert. Numbers indicate sand layers of a distinctive lighter color formed by tsunamis. The formation of saline crusts and gypsum nodules, as well as the burrowing of roots, usually mask these records.

A multi-proxy solution

The solution to these issues is neither simple nor straightforward. Only a few sectors of the Atacama Desert coastal segment seem to fulfill the geomorphic requirements, and even at those locations, a multi-proxy detailed study is needed to untangle the paleotsunami record of the last 4000 years. At these locations, each layer, generally less than 10 cm thick, must be sampled and subjected to a variety of analyses looking for the proxy or their combination, which allows us to classify the deposit as sediments formed by a tsunami.

At temperate latitudes, the combination of grain size and micropaleontology or geochemistry is normally sufficient to claim a deposit as a tsunami layer. However, on these arid coasts, grain size may have been modified by eolian rework, microfauna may have been dissolved, and the geochemistry of the sediment may have been altered by later precipitation of gypsum. Thus, we will have an answer only if we consider a more holistic solution. Geomorphological and sedimentological analyses are still key, but they must be combined not only with microfossil and geochemical analyses, but also with mineralogical, geophysical and even environmental DNA analysis to be sure that this sand layer was formed by a paleotsunami (Fig. 2). The effort to unmask this evidence is enormous, and requires the participation of multidisciplinary teams formed by geologists, paleontologists, biologists, and geophysicists, without whom it would be impossible to achieve the ultimate goal of assessing the tsunami hazard to which the southern Atacama coast is exposed.

To date, the low number of tsunami studies on arid coasts has not only led to a misunderstanding of the tsunami events on these coasts compared to temperate and humid areas, but also to underestimating the risk that coastal communities are exposed to by ignoring the recurrence of these high-energy marine events and their magnitude throughout the geological record. Until we understand them, we will continue to search for sand in the desert.

AFFILIATIONS

[1]Department of Biology and Geology, Physics and Inorganic Chemistry, Rey Juan Carlos University, Madrid, Spain
[2]Research Group in Earth Dynamics and Landscape Evolution, Rey Juan Carlos University, Madrid, Spain

CONTACT

Tatiana Izquierdo: tatiana.izquierdo@urjc.es

REFERENCES

Abad M et al. (2017) Geomorphic effects and sedimentological record of flash floods in the Copiapó River salt marsh (Atacama coast, Northern Chile). EGU 2017 General Assembly Conference, Vienna, Austria

Abad M et al. (2020) Sedimentology 67(3): 1505-1528

Engel M et al. (2020) In: Engel M et al. (Eds) Geological Records of Tsunamis and Other Extreme Waves (First Edition). Elsevier, 3-20

Klein E et al. (2017) Earth Planet Sci Lett 469: 123-134

Prizomwala SP et al. (2024) PAGES Mag 32(1): 36-37

Ruiz S, Madariaga R (2018) Tectonophysics 733: 37-56

Shiki T, Yamazaki T (2008) In: Shiki T et al. (Eds) Tsunamiites (Second Edition). Elsevier, 5-7

A palaeo-reanalysis of global monthly 3D climate since 1421 CE

PALAEO-RA Team*

A new reconstruction combines an unprecedented amount of climate observations with 12,000 years of climate model simulations in a data assimilation approach.

Reconstructions using data assimilation

Understanding interannual-to-decadal climate variability and extremes requires long datasets. Climate reconstructions have provided this information for decades. However, to understand the underlying mechanisms and relate climatic changes to atmospheric circulation variability, more comprehensive datasets than hitherto available are essential. One way of achieving this is to assimilate as much high-resolution climate information as possible into climate model simulations that provide physically consistent climate states.

Data assimilation (DA) approaches combining real-world atmospheric information with the physics of a climate model have been extremely successful in atmospheric sciences. In paleoclimatology, they are increasingly used to reconstruct the climate of the last millennium (Franke et al. 2017; Goosse and Paul 2013; Tardif et al. 2019). In DA, a first guess (mostly a modeled climate state) is updated by observations to provide the best estimate of climate consistent with both the model and the observations, as well as consistent with the errors in both. In paleoclimatology, offline DA is often used. In contrast to the online version, in which the updated model state at every assimilation time step is used to initialize a new forecast, offline DA only performs the update. This is possible because for atmospheric models, and over the typically seasonal-to-annual timescale of the assimilation, atmospheric initial conditions hardly matter. Offline DA is simple and versatile and can be used with pre-existing model runs. The latest offline DA product is the Modern Era Reanalysis (ModE-RA) suite of products (Valler et al. 2024). ModE-RA provides monthly output using a seasonal assimilation window, such that monthly mean instrumental or documentary data can be assimilated simultaneously with seasonal proxies (e.g. tree rings, plant or ice phenology).

Comprehensive compilation of observations

Crucially, any climate reconstruction relies on sufficient input data. This is the key strength of ModE-RA, which makes use of many times more observations than previous reconstructions. In addition to a large set of tree ring and other natural proxy records that include, among others, the PAGES 2k Network database (PAGES2k Consortium 2017), ModE-RA uses an extended set of documentary proxies (Burgdorf et al. 2023) and a new set of early instrumental measurements (Lundstad et al. 2023). The latter is a systematic compilation
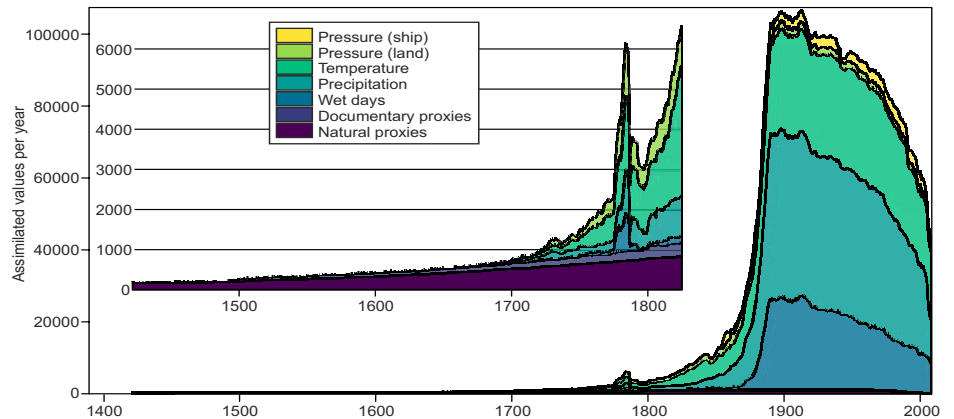
Figure 1: Number of values assimilated per year into ModE-RA, separated into data types.

of most of the available station data (air pressure, surface-air temperature, and precipitation), supplemented by ca. 1500 newly rescued series. Furthermore, air pressure measurements from ships were assimilated (Freeman et al. 2017). An overview of the data sources is given in figure 1. In total, ModE-RA assimilates hundreds (17th century), thousands (18th century) or tens of thousands (19th century) of values per year. Already in the mid-18th century, the number of values from instrumental and documentary data exceeds that of natural proxies. Only series starting before 1890 CE are included. Therefore, the number of series drops off steeply towards the 21st century as series that end are not replaced. This was done to keep the network stable and comparable over a long time period, and to limit the computation time.

The observations are assimilated into an ensemble of 20 atmospheric model simulations (Hand et al. 2023) performed with ECHAM6 and providing data at ca. 2°x2° resolution. These simulations, termed ModE-Sim, were externally forced by greenhouse gas concentrations, solar irradiance and volcanic aerosols, according to the PMIP4 protocol (Jungclaus et al. 2017). Sea-surface temperature (SST) boundary conditions are based on the annual PAGES 2k Network SST reconstructions (Neukom et al. 2019) and augmented by adding intra-annual variability based on ocean-variability modes. After 1780 CE we also assimilated SST and marine-air temperature observations into the ensemble of SST reconstructions using offline DA (Samakinwa et al. 2021).

The offline DA technique is similar to the precursor product EKF400v2, with some

improvements (Valler et al. 2024). We use an Ensemble Kalman Filter approach, with a hybrid background error covariance matrix that blends the ensemble covariance matrix with a climatological covariance matrix. Each of the 20 members of ModE-Sim is updated, hence ModE-RA is an ensemble of 20 members. DA is performed on anomalies from a 71-year moving average, which is added back at the end. This means that on multidecadal to centennial timescales the assimilation does not add much information, and ModE-RA becomes similar to ModE-Sim.

Instrumental data are not homogenized before assimilation, rather, a breakpoint detection is used to segment the data. The assimilation is then performed in three cycles, progressing from long (>50 year) to short (<5 year) series. Intermediate analyses are stored, and the next shorter series are then debiased, relative to this product. This allows for the use of even shorter series, of which there are many.

Example analyses

In addition to the product ModE-RA in which the model simulations for a given year are updated using observations from that year, we also provide ModE-RAclim. In this version, the first guess consists of a random sample of n = 100 from all years and members. The covariance matrix is constructed from the same sample. This means that ModE-RAclim is an ensemble of 100 members and does not see the time-varying boundary conditions of the model. Analyzing all three products together (ModE-RA, ModE-RAclim and ModE-Sim; see Table 1) allows for disentangling where the information in ModE-RA comes from. This is shown in figure 2a–c, which plots ensemble mean temperature anomalies over Europe

in December 1783. The model simulations (Fig. 2c) indicate a 2°C north-south gradient. ModE-RAclim and ModE-RA both show a cooling over Eastern Europe, whereas the Iberian Peninsula is warmer than normal. In this case, most of the information comes from the large number of observations. However, over North Africa, ModE-RA, which sees the boundary conditions, is cooler and more similar to ModE-Sim than ModE-RAclim.

Only the ensemble means are shown in the top row of figure 2, but the 20 (ModE-RA, ModE-Sim) or 100 (ModE-RAclim) members can also be analyzed individually. This is highlighted for 500 hPa geopotential height for the same month in figure 2d. Individual ensemble members provide a more realistic variability over time, whereas the variability of the ensemble mean decreases backward in time, when fewer observations constrain the reanalysis.

Precipitation anomalies in Africa in 1809 CE, after the "unknown" volcanic eruption (Timmreck et al. 2021), indicate a decrease in precipitation due to a decrease of the African monsoon, which can be diagnosed in the 850 hPa wind anomaly field (Fig. 2e). Finally, a 3-year drought period in the 15th century in the USA is studied (Fig. 2f). The 500 hPa geopotential height anomalies indicate a strengthened Great Plains Ridge.

Product	n	prior	obs.
ModE-RA	20	time-varying	Yes
ModE-RAclim	100	invariant	Yes
ModE-Sim	20*	time-varying	No

Table 1: ModE-RA products (n = number of members, obs. = assimilation of observations, *ModE-Sim has additional members not used for ModE-RA).

An important feature of the ModE-RA products is the Observation Feedback Archive, which provides detailed information about each observation that has been considered for assimilation. For instance, it includes station coordinates, 71-year climatology and anomaly, background and analysis departures for all members, forward models, and any relevant quality information.

The new dataset provides the best estimate of monthly climate of the past 600 years, given everything we know; the forcings, the laws of physics and arguably the most comprehensive set of climate information ever used in a reconstruction approach. It builds on efforts from several PAGES groups such as PAGES 2k Network, CRIAS and VICS and will benefit many future analyses. However, it should be noted that on multidecadal-to-centennial scales, the reconstruction mostly follows the model simulations.

AFFILIATIONS
*Stefan Brönnimann, Yuri Brugnara, Angela-Maria Burgdorf, Jörg Franke, Ralf Hand, Laura Lipfert, Elin Lundstad, Eric Samakinwa, Veronika Valler
Institute of Geography and Oeschger Centre for Climate Change Research, University of Bern, Switzerland

CONTACT
Stefan Brönnimann: stefan.broennimann@unibe.ch

REFERENCES
Burgdorf A-M et al. (2023) Sci Data 10: 402

Franke J et al. (2017) Sci Data 4: 170076

Freeman E et al. (2017) Int J Climatol 37: 2211-2232

Goosse H, Paul A (2013) PAGES News 21: 71-79

Hand R et al. (2023) Geosci Model Dev 16: 4853-4866

Jungclaus JH et al. (2017) Geosci Model Dev 10: 4005-4033

Lundstad E et al. (2023) Sci Data 10: 44

Neukom R et al. (2019) Nature 571: 550-554

PAGES2k Consortium (2017) Sci Data 4: 170088

Samakinwa E et al. (2021) Sci Data 8: 261

Tardif R et al. (2019) Clim Past 15: 1251-1273

Timmreck C et al. (2021) Clim Past 17: 1455-1482

Valler V et al. (2024) Sci Data 11: 36
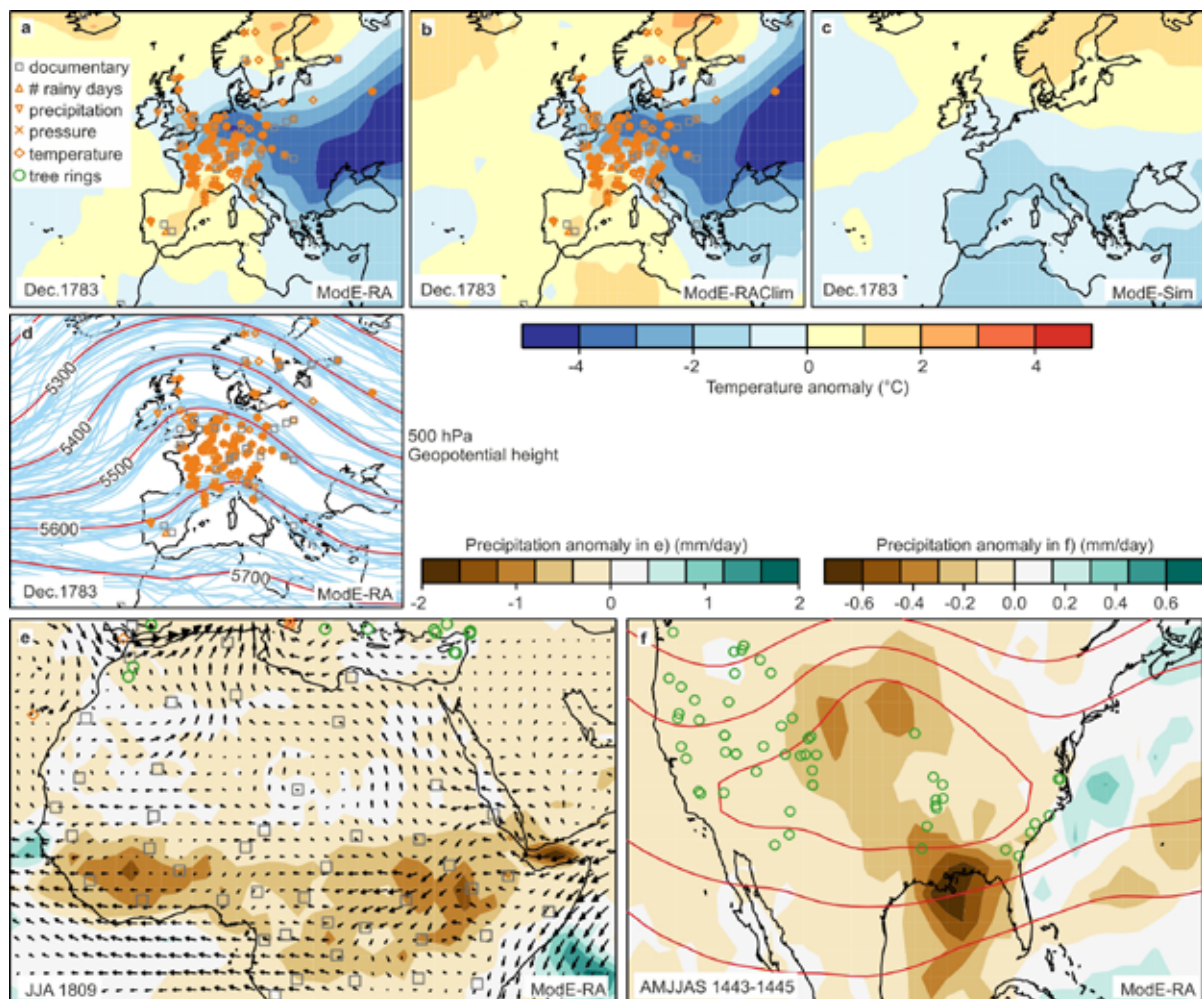
Figure 2: Temperature anomalies (from 1781–1810 CE) in December 1783 CE in **(A)** ModE-RA; **(B)** ModE-RAclim; and **(C)** ModE-Sim. **(D)** 500 hPa geopotential height in December 1783 CE in ModE-RA. **(E)** Anomalies of precipitation and 850 hPa wind in June–August 1809 CE (relative to 1781–1810 CE) in Central and Northern Africa and **(F)** 500 hPa geopotential height over the USA in April–September 1443–1445 CE (relative to 1421–1450 CE). Symbols indicate the assimilated observations. Only the ensemble means are displayed (except in the middle row, where light blue lines show members).

Hidden from plain sight: Sclerosponges as environmental archives of ocean conditions from the surface to the mesophotic zone

Sebastian Flöter[1], G.L. Foster[2,3], A.G. Grottoli[4], P.K. Swart[5], B. Williams[6] and G. Wörheide[7]

Sclerosponges dwell in an underexplored region of reefs. Their massive basal skeleton offers an opportunity as a unique, but underappreciated, paleoenvironmental archive. Here, we give an overview of the paleoclimate potential of sclerosponges and highlight current and future research areas.

Sclerosponges: Dwellers of caves, overhangs and mesophotic zones

Tropical shallow-water coral reefs are colorful, bright environments in which light drives the growth of a plethora of corals and other organisms. Off the well-lit parts of the reef, however, the light gets gradually dimmer and different organisms appear. Caves, overhangs, and the twilight environment of the mesophotic zone represent the refuge for a group that, in evolutionary terms, are the most ancient animals that form a massive calcareous skeleton (Fig. 1a). These organisms are coralline sponges or sclerosponges which were thought to be extinct until their rediscovery in cryptic habitats in the early 20th century.

While their ancient relatives contributed significantly to reef-building during the Paleozoic and Mesozoic, in today's oceans, sclerosponges are important contributors to nutrient cycling, and their massive skeletons cement and stabilize reef structures. The depth distribution of approximately one dozen sclerosponge species spans from surface waters to over 600 m deep, and they are found in the tropical and subtropical regions of the Atlantic, Pacific and Indian oceans (Vacelet et al. 2010). Although leading a life in shaded environments, sclerosponges are important for the movement of elements between living things and the ocean water.

Sclerosponges as paleoclimate archives

Research on sclerosponges dates back to the early 20th century when Joseph Jason Lister (1857–1927) and Randolph Kirkpatrick (1863–1950) investigated "pharetronid sponges" and rediscovered "living fossils" (e.g. *Astrosclera willeyana* Lister, 1900 from the Pacific; Fig. 1b). It was only in 1976 that Veizer and Wendt published the first geochemical analysis of the basal skeleton of *A. willeyana* (Fig. 1b), *Ceratoporella nicholsoni*, and *Petrobiona massiliana*. Together with *Acanthochaetetes wellsi* (Fig. 2), they are currently still the most investigated sclerosponge species.

Since the first geochemical investigations in the 70s, sclerosponges have been successfully used for paleo reconstructions. Their first application as an environmental archive was presented in 1986 by Druffel and Benavides, who used sclerosponges from the Caribbean to fingerprint oceanic anthropogenic CO_2 increases through $\delta^{13}C$ analysis. The observed decrease of ^{13}C, the ^{13}C-Suess effect, results from fossil fuel burning. This effect was later also found in Pacific sclerosponges (Böhm et al. 1996). Radiocarbon analyses revealed the bomb curve; a peak in $\Delta^{14}C$ due to above-ground thermonuclear testing starting in 1955 (Benavides & Druffel 1986). Instrumental advances in geochemistry allowed an increase in the spatial analytical resolution from mm- to µm-scale, which is equivalent to bimonthly resolution in sclerosponge skeletons (Swart et al. 2002). Besides their application to trace atmospheric chemistry, they can be used to reconstruct seawater temperature and $\delta^{18}O$ values by analyzing their trace metal and stable isotope composition. While Wörheide (1998) reconstructed relative temperature changes using $\delta^{18}O$ values, Rosenheim and coworkers (2004) provided the first absolute temperatures through an empirically calibrated Sr/Ca-temperature relationship, with the longest record from a single sponge being ≈ 600 years (Waite et al. 2020).

To achieve any paleoclimate record, a chronology of the skeleton is necessary, and the sclerosponge needs to be dated. Unlike corals or bivalves, sclerosponges lack the presence of an internal annual banding that would allow dating through sclerochronological means, such as with tree-ring chronologies. Dating and growth-rate estimates of sponges have so far been conducted by in situ staining with fluorescent dyes (Fig. 2), $\delta^{13}C$-Suess effect values, the identification of the leaded fuel combustion-Pb peak in 1971, and $\Delta^{14}C$ or U/Th radiometric dating (e.g. Benavides & Druffel 1986; Swart et al. 2002; Wörheide 1998). These methods are currently the only way to determine their age. Compared to tropical corals, coralline sponges are
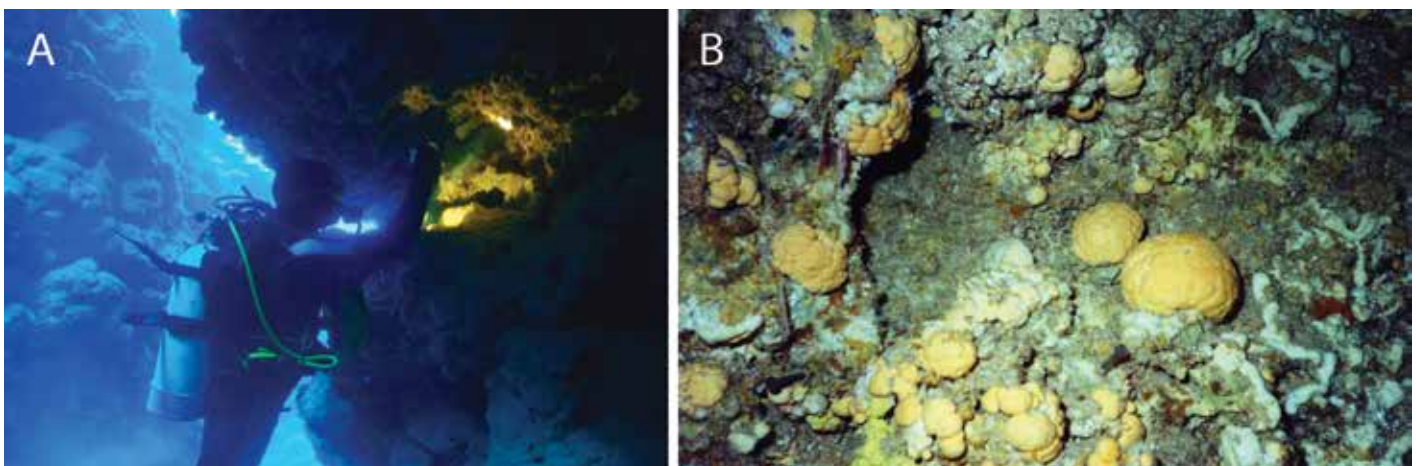
Figure 1: (A) A diver (G. Wörheide) samples sclerosponges in the Coral Sea, Australia. Photo credit: C. Vogler. **(B)** *A. willeyana* (yellow) off Saipan, Northern Mariana Islands. Photo credit: A. Grottoli.

slow-growing at less than 2 mm/year (e.g. Grottoli et al. 2010). Still, they have extraordinary longevity, reaching up to one thousand years (Vacelet et al. 2010). Hence, individuals of *C. nicholsoni* can become larger than 1 m in diameter, emphasizing their potential as a valuable high-resolution environmental archive for extended periods (Lang et al. 1975).

More recent work focused on proxy verification and reconstructing the paleoceanographic history of the Pacific using element ratios, $\delta^{13}C$ and $\delta^{18}O$ values (e.g. Asami et al. 2021; Grottoli et al. 2010, 2020). These studies found little impact of biological activity, the so-called vital effect, on skeletal $\delta^{13}C$ and $\delta^{18}O$ values, or the partitioning of Sr, and they also reported P/Ca ratios as a promising proxy of seawater P concentrations. An improved Sr/Ca temperature calibration for *C. nicholsoni* allowed for water-temperature reconstruction with a precision of <0.5°C (Waite et al. 2018), enabling Waite et al. (2020) to determine how the combination of volcanic activity and anthropogenic forcings drove Atlantic climate variability during the past 600 years.

The anthropogenic change in atmospheric CO_2 has lowered the pH of the ocean. Boron isotopes (skeletal $\delta^{11}B$), a common proxy for seawater-pH reconstruction in corals, showed that *C. nicholsoni* grows close to equilibrium with the seawater borate isotopic composition and links $\delta^{11}B$ variability on the sub-mm scale to seasonal pH changes (e.g. Sadekov et al. 2019). These results emphasize the potential of sclerosponges as a recorder of ocean acidification. Sclerosponges were also applied to trace other anthropogenic pollutions. For example, Pb/Ca ratios are used to trace environmental Pb contamination (e.g. Asami et al. 2021).

In conjunction with their longevity and resistant skeleton, these recent findings concerning the geochemistry of sclerosponges pave the way for establishing them as a valuable archive of climatic, oceanographic and pollution conditions at depths beyond that recorded by scleractinian corals in warmwater reefs.

The future of paleo-sclerosponge science
The importance of the underexplored mesophotic zone makes research on local environmental archives, such as those provided by sclerosponges, urgently required. New sampling and habitat mapping opportunities using affordable underwater drones, or hybrid, remotely-operated vehicles, can increase the accessibility of coralline sponges. Technological advances in the field of omics (genomics, proteomics, metabolomics, etc.), X-ray microtomography and geochemical analytical advances like Laser Ablation Inductively Coupled Plasma Time of Flight Mass Spectrometer (LA-ICP-ToF-MS), or Nanoscale Secondary Ion Mass Spectrometry (NanoSIMS), allow for a wide range of analyses of slow-growing carbonate structures.

Figure 2: A section of *A. wellsi* from Saipan, Northern Mariana Islands. The sample shows an alizarin red stain from a growth-rate experiment. Photo credit: A. Grottoli.

Recent years have seen a huge leap forward in understanding the biomineralization of scleractinian corals to build their $CaCO_3$ skeletons. In sclerosponges, however, very little is known. Arguably, a thorough knowledge of biomineralization is required, to not only form a mechanistic understanding of the impacts of future climate change, but also as a prerequisite for the application of geochemical proxies. Since sclerosponges are among the most ancient multicellular $CaCO_3$ biomineralizers, such insights could also provide unique information about how animal skeletal formation evolved.

So far, diagenesis has only been studied in fossil sponges, but no studies have investigated the fate of the skeletal elemental and isotopic composition and structure after formation. In addition to long-term changes, several other skeletal processes require further studies, such as the extracellular backfill of the skeleton observed in *A. willeyana* (Wörheide 1998) and the chemical heterogeneity in *A. willeyana* and *C. nicholsoni* that could not be linked to environmental variations (e.g. Asami 2021).

Despite these challenges and the limited number of paleo studies, sclerosponges have enormous potential as long archives of past climates in the subsurface of the upper ocean. However, to maximize the potential of these environmental archives, the following issues are pressing areas of sclerosponge investigation: i) dating at sub-seasonal resolution; ii) lab culturing and in situ experiments on the effect of environmental changes on skeletal formation and composition; iii) investigation into possible early diagenesis; and iv) the influence of biomineralization on the geochemistry of the calcareous skeleton.

One exciting aspect of sclerosponges, which was only briefly explored, is the potential to reveal changes in the thermocline structure of the upper ocean. As the ocean warms, the depth at which the thermocline occurs should deepen. Given carefully chosen sampling locations and appropriate geochemical methods, sclerosponges can offer insight into how thermocline depth and heat penetration in the oceans have responded to rising global temperatures.

Addressing these knowledge gaps would be most effective through cross-disciplinary collaboration between paleoclimatologists, (bio)geochemists, microbiologists, geneticists, and physical oceanographers. We hope this article stimulates these collaborations to maximize the study of sclerosponges as a potentially unique climate archive.

AFFILIATIONS
[1]Department of Earth Sciences, University of Geneva, Switzerland
[2]School of Ocean and Earth Science, University of Southampton, UK
[3]National Oceanography Centre Southampton, UK
[4]School of Earth Sciences, The Ohio State University, USA
[5]Division of Marine Geology and Geophysics, Rosenstiel School of Marine, Atmospheric, and Earth Sciences, University of Miami, USA
[6]Kravis Department of Integrated Sciences, Claremont McKenna College, USA
[7]Department of Earth and Environmental Sciences, Ludwig-Maximilians-Universität München, Germany

CONTACT
Sebastian Flöter: sebastian.floeter@unige.ch

REFERENCES

Asami R et al. (2021) Prog in Earth Planet Sci 8: 38

Böhm F et al. (1996) Earth Planet Sci Lett 139: 291-303

Benavides LM, Druffel ERM (1986) Coral Reefs 4(4): 221-224

Druffel ERM, Benavides LM (1986) Nature 321: 58-61

Grottoli AG et al. (2010) J Geophys Res 115: 1-14

Grottoli AG et al. (2020) Geochem Geophys Geosyst 21: 1-14

Lang JC et al. (1975) J Mar Res 33: 223-231

Rosenheim BE et al. (2004) Geology 32: 145-148

Sadekov A et al. (2019) J Anal Atom Spectrom 34: 550-560

Swart PK et al. (2002) Paleoceanography 17: 1-12

Vacelet J et al. (2010) Treatise Invertebr Paleontol 4: 1-16

Veizer J, Wendt J (1976) J Archäol Sci 23: 558-573

Waite AJ et al. (2018) Chem Geol 488: 56-61

Waite AJ et al. (2020) Geophys Res Lett 47: 1-11

Wörheide G (1998) Facies 38: 1-88

Atmospheric dryness recorded in tree rings of *Araucaria araucana* from the northwest of the Patagonian Steppe

Jorge A. Giraldo[1], M. Hadad[2], A. Gonzalez-Reyes[3] and F.A. Roig[4]

Dr. Jorge A. Giraldo, from Colombia, visited the Laboratorio de Dendrocronología de Zonas Áridas, Ladeza-CIGEOBIO (CONICET-UNSJ) in San Juan, Argentina, as a PAGES-IAI International Mobility Research Fellow (1 June–31 July 2023) to explore the dendrochronological potential of tree species from xeric ecosystems in South America to record vapor pressure deficit (VPD). Within this project, Jorge and his collaborators aim to increase knowledge of the long-term variability of VPD and its effects on tree growth over time.

Motivation

The sensitivity of forests to climate change in South America has been of interest to the scientific community over the past decades (Morales et al. 2020; Villalba et al. 2011). However, the scarcity of climatic records from field stations in this region limits our ability to detect the effect of climate change (Garreaud et al. 2009). Dendrochronology can provide valuable climate proxy records over long periods derived from annual tree rings. Therefore, extensive geographic sampling of old trees across an ecosystem can improve current climate databases and refine our inference ability about the role of climate on South American forests (Morales et al. 2020). Under global warming, air dryness (i.e. vapor pressure deficit: VPD) has markedly increased around the globe (Grossiord et al. 2020). VPD is a multidimensional variable combining temperature and relative humidity, enabling measurement of the atmospheric water demand from plants (Yuan et al. 2019). While much attention has been directed towards plant responses to temperature and precipitation independently (i.e. reconstructions of these variables), few studies have isolated the response of plant functioning toward reconstructions of VPD variability using tree-ring width.

Thanks to the support from this mobility research fellowship, it was possible to strengthen a collaborative network between tree-ring research groups from Colombia and Argentina, enabling the investigation of the dendrochronological potential of *Araucaria araucana*, a tree species from the northwest of Patagonia, to reconstruct VPD variation using tree-ring width.

Analysis

Applying standard dendrochronology techniques (i.e statistical and graphical cross dating), we analyzed available samples from three populations of *A. araucana* growing in xeric sites in Argentina (i.e. 131 trees and 244 cores; Fig. 1a), collected by Dr. M. Hadad and colleagues. The similarity between sites (i.e. climate and topography) and the crossdating allowed us to combine them into a single representative chronology for the area (Fig. 1b). Although the oldest tree dates back to 1190 CE, we built a chronology represented by more than five tree series which span from 1377–2019 CE. The measured subsample signal strength (SSS), which is a measure of the variance in common between a subset of samples and master chronology, was higher than 0.85, suggesting the suitability of the dendrochronological chronology for climate reconstructions (1588–2019 CE; Fig. 1b). We compared tree-ring chronology with VPD series estimated from the Climate Research Unit products (CRU). We found significant ($p < 0.05$) correlations between tree-ring chronology and monthly VPD from December ($r = -0.18$), January ($r = -0.38$), February ($r = -0.35$), March ($r = -0.30$), and the mean January–February VPD ($r = -0.46$)

of the previous growing season. We compared the tree-ring width index to the mean January–February VPD record using the split calibration/verification method to test the reconstruction potential of this species. The chronology accounted for 55% of the variance in the calibration period (1982–2016 CE; $r = -0.76$, $p < 0.05$; Fig. 1c), while the full calibration period (1969–2016 CE) explained 44% of the variance (Fig. 1d). In addition, the positive values of reduction of error (RE: 0.64), and the coefficient of efficiency (CE: 0.36) indicate a stability of the relationship, which suggests the suitability of the chronology to be used in reconstructions of VPD back in time.

In conclusion, the results of this mobility research fellowship demonstrate a strong potential of *A. araucana* growing in xeric sites of South America to reconstruct VPD during its growing season. Currently, we are preparing a manuscript to show a reconstruction of the VPD following standard methods. This can improve our understanding of regional/continental VPD variation in Northern Patagonia under the ongoing climate situation.

AFFILIATIONS

[1]Facultad de Ingeniería – Tecnológico de Antioquia Institución Universitaria, Medellín, Colombia
[2]Laboratorio de Dendrocronología de Zonas Áridas. CIGEOBIO (CONICET-UNSJ), Gabinete de Geología Ambiental (INGEO-UNSJ), San Juan, Argentina
[3]Instituto de Ciencias de la Tierra ICT, Facultad de Ciencias, Universidad Austral de Chile, Valdivia, Chile
[4]Instituto Argentino de Nivología, Glaciología y Ciencias Ambientales (IANIGLA), Consejo Nacional de Investigaciones Científicas y Técnicas (CONICET), Mendoza, Argentina

CONTACT

Jorge A. Giraldo: jorge.giraldo76@tdea.edu.co

REFERENCES

Garreaud RD et al. (2009) Palaeogeogr Palaeoclimatol Palaeoecol 281: 180-195

Grossiord C et al. (2020) New Phytol 226: 1550-1566

Morales MS et al. (2020) Proc Natl Acad Sci USA 117: 16816-16823

Villalba R et al. (2011) In: Hughes MK et al. (Eds) Dendroclimatology. Springer: 175-227

Yuan W et al. (2019) Sci Adv 5: 1-13
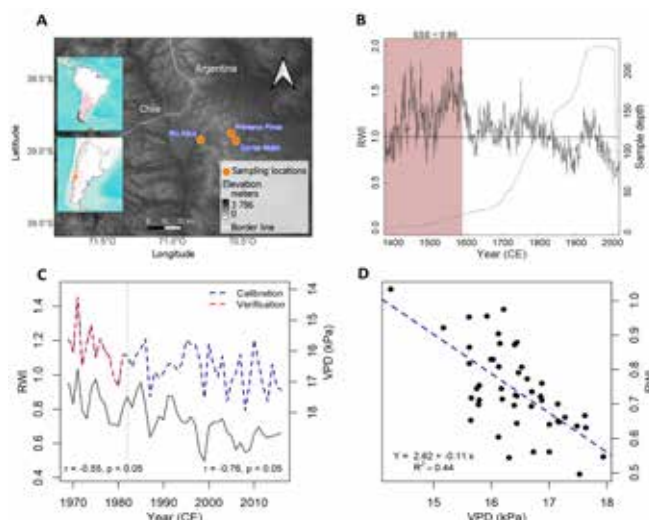
Figure 1: (A) Location of the tree-ring sampling; and **(B)** combined ring width index (RWI) chronology for three sites. SSS: subsample signal strength. **(C)** Graphical relationship between RWI and mean January–February VPD over time and its correlation divided into calibration and verification period. **(D)** Scatter plot of the relationship between RWI and the mean January–February VPD.

Sediment sources and transport pathways to the western South Atlantic since Termination I

Rodrigo S. Martín[1], N. García Chapori[1], C. Laprida[1] and C. M. Chiessi[2]

Lic. Rodrigo Martín, from Argentina, visited the University of São Paulo, Brazil, as a PAGES-IAI International Mobility Research Fellow (23 July – 27 Aug 2023) to perform X-ray fluorescence (XRF) and stable isotope analyses on sediment cores retrieved from the western South Atlantic Ocean. These analyses will help to understand the sediment sources and transport pathways active in the region since Termination I.

The western South Atlantic circulation is dominated by the Brazil-Malvinas Confluence (~38°S) that emerges from the encounter of the southward-flowing Brazil Current and the equatorward-flowing Malvinas Current. The upper slope off Uruguay, however, is strongly influenced by the Brazilian Coastal Current that transports the Plata Plume Water (PPW), derived from the Plata River discharge (Fig. 1a). The northward penetration of the PPW is mainly controlled by the seasonal along-shore wind stress, including the southern westerly winds (SWW), and reaches its northernmost position during the austral winter when the SWW displace to the north (Piola et al. 2008). South of 38°S, the Patagonian margin is controlled by the Malvinas Current, and the low precipitation and strong SWW over the Patagonian Steppe make it a major dust source to the adjacent ocean (Prospero et al. 2002).

The past evolution of the sources and transport pathways of terrigenous sediments deposited at the western South Atlantic since Termination I is poorly understood. To shed light on this issue and provide important insights into the climate and oceanographic variability in this region, we analyzed three radiocarbon-dated marine sediment cores from the Uruguayan and Patagonian margins (Fig. 1a). We used major elemental composition to trace changes in the terrigenous input: Fe/Ca ratio employed as an indicator of terrigenous material of fluvial origin (Arz et al. 1998), and Ti/Al ratio used as an indicator of grain size variation and/or provenance (Govin et al. 2012). Additionally, we analyzed the benthic-foraminifera stable carbon isotopes ($\delta^{13}C$) to gain insight into intermediate water circulation.

Terrigenous input evolution from the western South Atlantic

Our geochemical data indicate that the terrigenous input to the western South Atlantic was higher during Termination I than during the Holocene (Fig. 1b). The lower sea level, together with a northward displacement of the SWW, increased terrigenous material input at the Uruguayan (GeoB22735-2) and Patagonian (AU_Geo02_GC20/21) margins. Nevertheless, the sedimentary pathways at these two regions were different.

At the Patagonian margin, low Ti/Al ratios suggest low eolian input; and high Fe/Ca ratios reflect not only lower sea level, but also enhanced input of fluvial-derived material due to melting of the Patagonian Ice Sheet (Gaiero et al. 2003). At the Uruguayan margin, conversely, high Fe/Ca ratios reflect a major influence of the PPW due to a northern position of the SWW (Piola et al. 2008), whereas the low Ti/Al ratios indicate limited input from the Bermejo River (a major Andean tributary) to the Plata River (Depetris et al. 2003).

During the Holocene, the decrease in Fe/Ca ratios indicates a reduction in the terrigenous input of fluvial origin at both sectors due to sea-level rise and the southward displacement of the SWW. Higher Ti/Al ratios at the Patagonian margin suggest a stronger Patagonian dust plume, whereas at the Uruguayan margin it indicates a major relative contribution of sediments derived from the Bermejo River that carry a signature rich in Ti (Depetris et al. 2003). Preliminary analyses of the Holocene $\delta^{13}C$ indicate that the higher values recorded at the Uruguayan margin since the mid-Holocene indicate a smaller influence of southern-source waters at intermediate depths (García Chapori et al. 2022). Further ongoing analyses will help to evaluate these hypotheses in this key region of the worlds oceans.

AFFILIATIONS

[1]Institute of Andean Studies, University of Buenos Aires-CONICET, Argentina

[2]School of Arts, Sciences and Humanities, University of São Paulo, Brazil

CONTACT

Rodrigo S. Martín: rodrigosmartin88@gmail.com

REFERENCES

Arz HW et al. (1998) Quat Res 50(2) : 157-166

Depetris PJ et al. (2003) Hydr Proc 17(7): 1267-1277

Gaiero DM et al. (2003) Geoch Cosm Acta 67(19): 3603-3623

García Chapori N et al. (2022) J South Amer Earth Sci 117: 103896

Govin A et al. (2012) Geoch, Geoph, Geosy 13(1): Q01013

Piola AR et al. (2008) Cont Shelf Res 28(13): 1639-1648

Prospero JM et al. (2002) Rev Geoph 40(1): 1002
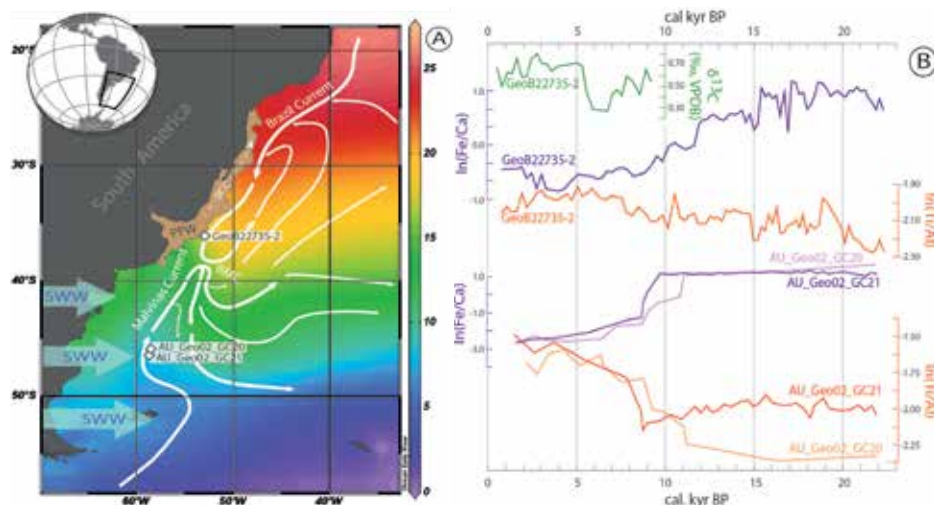
Figure 1: (A) Map showing annual sea-surface temperature of the western South Atlantic. White diamonds represent the analyzed cores. White arrows represent the main oceanic currents (BC: Brazil Current; BCC: Brazilian Coastal Current; PPW: Plata Plume Water). Gray arrows represent the southern westerly winds (SWW). BMC: Brazil-Malvinas Confluence. **(B)** Records of benthic-foraminifera stable carbon isotopes (Cibicidoides-$\delta^{13}C$), ln(Fe/Ca) and ln(Ti/Al) ratios of cores GeoB22735-2 (Uruguayan margin), AU_Geo02_GC20 and AU_Geo02_GC21 (Patagonian margin).

Dust-flux estimates for the last glacial–interglacial cycle in southern South America based on loess deposits

Gabriela Torre[1,2], D. Gaiero[1,2], A.O. Sawakuchi[3] and T.D. Minelli[3]

Dr. Gabriela Torre, from Argentina, visited the Universidade de São Paulo, Brazil, as a PAGES-IAI International Mobility Research Fellow (October–December 2023) to determine the age of eolian records through Optically Stimulated Luminescence (OSL). The new ages enabled determination of the chronological framework of dust deposition in southern South America, together with dust fluxes in the region. This project aims to expand understanding of the dynamics of atmospheric dust, and its influence on past climatic variabilities.

Past climatic fluctuations recorded in ice cores indicate great variability in past fluxes of atmospheric dust, emphasizing their key role in changes in the global climate system. Atmospheric dust is an important component of the climate system, affecting and responding to climate changes through a series of complex feedbacks involving nutrient cycling, albedo, radiative forcing, and cloud formation (Bullard et al. 2016). However, the role of dust in climate forcing remains poorly understood, and represents one of the largest uncertainties in climate-model simulations (Adebiyi and Kok 2020; Heavens et al. 2012). Atmospheric dust generated on the continents is a fairly unknown variable of the climate system, and loess sequences are the main records of continental dust deposition. In this sense, the loess-paleosol sequences from Argentina are the most extensive paleorecord of eolian material in the Southern Hemisphere.

The fellowship investigated the dust cycle recorded in loess-paleosols through the determination of dust accumulation rates for the past glacial–interglacial periods. The comparison between dust fluxes at the continental loess deposits with those recorded at more distal regions (south Atlantic Ocean and Antarctic Plateau) will allow us to improve our knowledge related to the dynamics of dust during the last glacial–interglacial cycle. We applied OSL techniques in two loess-paleosol sequences, located in elevated regions, to increase the spatial resolution of previous studies in dust archives (Torre et al. 2022), and to enhance the spatial resolution of paleoclimatic studies in the continental region of southern South America.

Research activities
1) Sample selection: A total of 20 samples were collected for OSL determinations from two loess-paleosol sections exposed in relatively elevated regions – Las Carreras section at ~2290 m asl and Majada de Santiago section at 1600 m asl (Fig. 1). These sections were sampled vertically every 20 cm for the uppermost 2 m by embedding PVC pipes 1.5" in diameter.

2) Equivalent dose determination: All sample preparation was performed in a lab room with red/orange light conditions. Samples were open and sieved to separate fine sand from silt-size particles. Then, samples were treated with HCl and H_2O_2 hydrogen peroxide to eliminate carbonates and organic matter. Thereafter, quartz grains were isolated through heavy liquid separation methods. The concentrates were subjected to HF attack for 40 minutes. This procedure removes remanent feldspar grains and the outer ring of quartz grains.

3) Dose rate determination: Dose-rate calculation was performed through the determination of ^{238}U, ^{232}Th and K concentrations. For this purpose, samples were dried and stored in plastic containers previously sealed for more than 20 days. Dose rate was determined through high-resolution gamma-ray spectrometry with a high-purity germanium detector and corrected for moisture content (water weight/dry sample weight) of each sample. Also, dose rate was corrected for the cosmic rays dose rate, which is estimated as a function of depth, altitude and latitude of each sample.

Outcomes
Infrared stimulation tests showed a significant contamination of feldspar in the quartz concentrate samples even after several HF attacks. Due to reduced sample size, and difficulty in obtaining pure quartz aliquots, luminescence dating had to be applied in silt-sized polymineral aliquots. Toward the end the fellowship, the 4-11 μm fraction was isolated through settling in distilled water, followed by acid attacks. Equivalent doses of the silt fraction were measured in December 2023 and January 2024.

Once the measurements of dose rate and equivalent doses for each sample are ready, we will be able to calculate the age of deposition of each level (i.e. age(yr)= equivalent dose(Gy)/dose rate (Gy yr^{-1})). These ages will provide a chronological framework of the different geochemical and physical parameters already determined for the loess samples. Also, these ages will allow the correlation of loess sections with other paleoclimatic records of the Southern Hemisphere, improving the spatial resolution of paleoclimatic studies. Moreover, the detailed chronology will allow the

determination of the mass-accumulation rates of eolian sediments. This proxy will be a valuable contribution to the modeling community working on the past glacial cycle, and will also allow us to compare dust fluxes between different dust records, which surely will improve the understanding of past dust variability.

AFFILIATIONS
[1]Facultad de Ciencias Exactas, Físicas y Naturales, Universidad Nacional de Córdoba, Argentina
[2]Nacional de Investigaciones Científicas y Tecnológicas (CONICET), Centro de Investigaciones en Ciencias de la Tierra (CICTERRA), Córdoba, Argentina
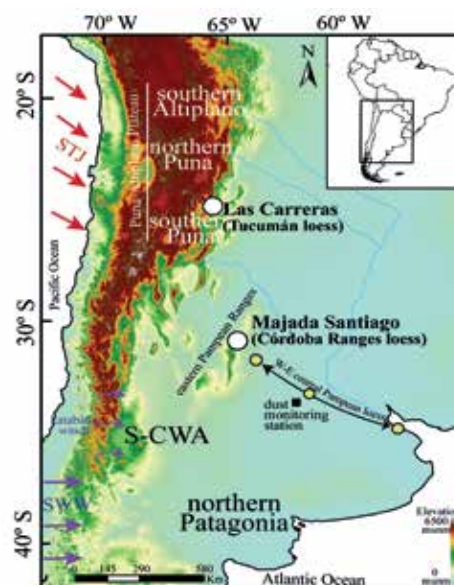[3]Instituto de Geociencias, Universidade de São Paulo, Brazil

CONTACT
Gabriela Torre: gabrielatorre@unc.edu.ar

REFERENCES
Adebiyi AA, Kok JF (2020) Sci Adv 6: eaaz9507

Bullard JE et al. (2016) Rev Geophys 54(2): 447-485

Heavens NG et al. (2012) J Adv Mod Earth Syst 4(4): M11002

Torre G et al. (2022) Earth-Sci Rev 232: 104143

Figure 1: Map showing the location of the two loess sections studied in this work (white circles): Tucumán section and Córdoba section. The yellow circles indicate previously studied loess sections within the Pampean Plain.

What signs of climate variability can be extracted from the quantitative wood anatomy of *Cedrela fissilis* Vell. rings?

D. Ricardo Ortega-Rodriguez[1], J.G. Roquette[2], L.A. Portal-Cahuana[3] and L. Yáñez-Espinosa[4]

Dr. D. Ricardo Ortega-Rodriguez, from Brazil, traveled to the Instituto de Investigación de Zonas Desérticas of Universidad Autónoma de San Luis Potosí, Mexico, as a PAGES-IAI Mobility Research Fellow from 6 August to 6 November 2023. Under the coordination of Dr. Laura Yáñez, he evaluated the potential of interannual variations of the anatomical-elements proportion of *Cedrella fissilis* to study climate variability.

A decrease in precipitation, and an increase in temperature and evapotranspiration, has been observed in the southern region of the Amazon basin since 1970 CE, as well as an increase in the length and severity of the dry season since 1990 CE (Fig. 1a). These extreme conditions suggest an alarming future, with possible forest dieback (Lovejoy and Nobre 2018). In this context, timeseries studies of growth-ring parameters (dendrochronology) are an essential tool to understanding the climate variability and periodicity of extreme events on an annual scale, and possible adaptive processes of species.

Background of the dendroclimatic analysis of *Cedrela fissilis*
The *C. fissilis* population analyzed during this fellowship was collected in Rondonia, Brazil, in the southern region of the Amazon basin. Previous studies of this population show that the increase in the frequency of droughts after 1990 CE led to a long-term trend of decreased growth, and an increase in wood density (Ortega Rodriguez et al. 2023a). Furthermore, during dry years, *C. fissilis* showed narrower, less-dense rings, lower concentrations of S and Ca, and higher δ^{18}O (the opposite was found in wet years; Ortega Rodriguez et al. 2023b). The observed long- and short-term adaptation by this species requires a better understanding of the trade-off processes between structural, transport and storage tissues. This can be achieved by using quantitative wood-anatomy methods.

Quantitative wood anatomy as a climate proxy
We obtained gray-tone images of 11 *C. fissilis* individuals (14 radial samples) through X-ray densitometry (Quintilhan et al. 2021), and classified and measured the proportion (%) of vessel (VA, a transport tissue), fiber (a structural tissue, FA) and parenchyma (a storage tissue, PA) areas in ImageJ software. Then, we obtained a timeseries (1970–2018 CE) of these anatomical parameters. We also evaluated the cross-dating among series using the COFECHA program and removed the age-size-related and non-climatic trends using the ARSTAN program.

Raw series trend showed a significant (p < 0.05) increase in VA% (r = 0.38) and FA% (r = 0.54) similar to the increase observed in RD; while PA (r = -0.70) showed a decrease, mainly since 2000 CE, similar to the trend observed in RW (Fig. 1b) (Ortega Rodriguez et al. 2023a). Furthermore, during dry years there was a higher and lower VA% and FA% in tree rings, respectively, without significant alterations in the PA%.

Contrary to expectations, there were no significant correlations between anatomical

variables and precipitation, temperature, or the difference between precipitation and potential evapotranspiration (P-PET). Positive and significant correlations between the PA% and the standardized precipitation-evapotranspiration index (SPEI) values at the beginning of the rainy season (September–November) of a previous year were identified. In contrast, the FA% showed positive, and significant, correlations with the SPEI values of the end of the rainy season (March–May) of a previous year and the beginning of the rainy season (September–November) of the current year.

Final comments
The SPEI signal recorded in the PA% and fibers may suggest the importance of these variables for compensation strategies between storage tissues and structural support formed by *C. fissilis* in response to dry conditions. Furthermore, the opposite trend of both parameters suggests a vulnerability of the normal growth and wood density conditions of the species, in response to climate change, mainly since 2000 CE, when extreme droughts became more frequent in the region.

AFFILIATIONS
[1]Departamento Ciencias Florestais, Universidade de São Paulo, Piracicaba, Brazil
[2]Departamento de Fisica Ambietal, Universidade Federal de Mato Grosso, Brazil
[3]Escuela Profesional de Ingeniería Forestal, Universidad Nacional Toribio Rodríguez de Mendoza de Amazonas, Chachapoyas, Peru
[4]Instituto de Investigación de Zonas Desérticas, Universidad Autónoma de San Luis Potosí, Mexico

CONTACT
D. Ricardo Ortega-Rodriguez: dai.ricardo.or@gmail.com

REFERENCES
Lovejoy TE, Nobre C (2018) Sci Adv: eaat2340

Ortega Rodriguez DR et al. (2023a) Agri For Meteorol: 333

Ortega Rodriguez DR et al. (2023b) Sci Total Environ 871: 162064

Quintilhan MT et al. (2021) Dendrochronologia: 125878
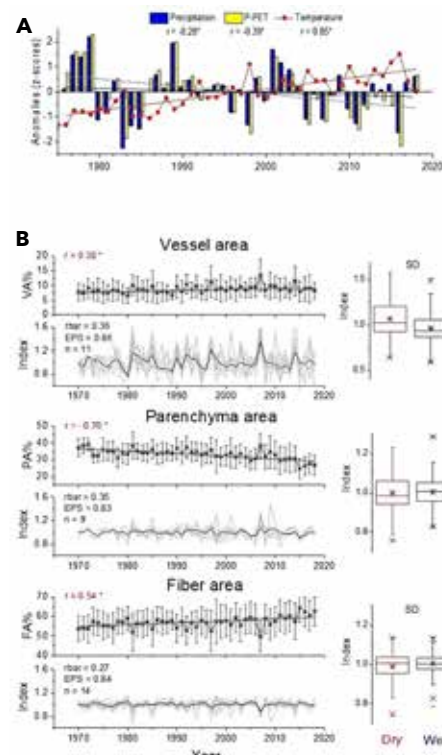
Figure 1: (A) Bar plots show anomalies (standardized values) of total annual precipitation (P), total annual difference between precipitation and potential evapotranspiration (P-PET), and mean annual temperature (T). **(B)** Mean raw series with ± standard error, mean index residual chronologies (black lines) and number of trees and radii (bottom gray shading) of the proportion of vessel (VA%), parenchyma (PA%) and fiber area (FA%) in tree rings, and boxplot of normalized parameters in dry (red) and wet (blue) years (significant difference between means, SD, p < 0.05).

The 5th Summer School on Speleothem Science

Petronela Ševčíková[1], M. E. Della Libera[2], J. Cauhy Rodrigues[2], E. Patterson[3], G. Utida[4], M. Holten Løland[5], B. Tiger[6] and C. Gould[7]

The 5th Summer School on Speleothem Science (S4), São Paulo, Brazil, 6–13 August 2023

About S4

Speleothem science is integral to reconstructing past climates and environmental and archaeological change. S4 is a student-organized training school taught by leading experts, that provides an informal space to share knowledge on traditional and state-of-the-art research and methods applied in the field. Participants share and discuss their own research with peers and get valuable feedback from experts. The event is particularly suited for MSc and PhD candidates whose research interests are closely related to speleothem science. After four successful summer schools held in European cities (Heidelberg 2013, Oxford 2015, Burgos 2017, and Cluj-Napoca 2019) the current organizing committee made it a priority to significantly increase S4's diversity and accessibility with a major geographical relocation of S4 2023 to Brazil.

The current school

The 5th S4 was hosted at the Institute of Geosciences, University of São Paulo (USP). This year's summer school program was full-size again, after a long COVID break of four years, during which we organized two small S4 events – S4 Online, and MiniS4 2022, Innsbruck, Austria. The organizing committee that was formed in 2019 after the summer school in Cluj-Napoca was strengthened by new members recruited during MiniS4.

A total of 59 students, including bachelor, masters, PhD and postdoctoral researchers, from 25 countries participated: 28% of the students came from South America, 24% from North America, 23% from Europe, 18% from Asia and 7% from Africa (Fig. 1). We are happy to share that the proportion of male and female participants was exactly 50%. The accessibility was greatly enhanced by support from several funding sources, including PAGES, that helped to lower the registration costs by 50%. Additionally, 19 partial or full travel grants and 17 registration fee waivers were awarded.

The scientific program consisted of two main parts. The first three days were dedicated to lectures and workshops at the Institute of Geosciences at USP. We started with an overview of speleothem-paleoclimate research in South America, followed by lectures on speleothem growth, radiogenic dating methods, and the use of proxies as stable isotopes and trace elements. The paleothermometry lecture discussed the use of fluid inclusions and clumped isotopes, as well as useful tips for their application. Substantial time was dedicated to speleothem petrography, with a lecture and workshop where participants

learned novel and time-efficient approaches for using petrography as a paleoclimate proxy. Among the less traditional methods, attendees enjoyed the speleothem paleomagnetism lecture, followed by a tour of the paleomag laboratory. Further, participants learned about speleothems and climate models, attended an interesting workshop on time-series analysis, and reviewed the multi-proxy approach in paleoclimatology. The summer school concluded with a lecture on the SISAL database, its history and use, and an invitation to join this great effort of the speleothem community! We sincerely thank all the experts who participated and gave fascinating lectures for the new generation of speleothem scientists.

Fieldtrip

Following the three-day lecture portion, we traveled to the Alto Ribeira Touristic State Park for a field trip to the beautiful and large caves of the Mata Atlântica rainforest. The participants visited six Precambrian limestones caves, and discussed their genesis, the formation of speleothems, and deposition of cave sediments and emphasized ethical and environmentally friendly sampling methods. In the evenings, we organized lectures on cave monitoring with practical examples, a lecture on diversity, equity and inclusion in speleothem science, a lecture on the geomorphology and genesis of caves, and a discussion on ethics in field research, focusing on the topic of scientific neocolonialism.

To provide participants with resources for later reference, we recorded all lectures; the recordings are available on our YouTube channel (youtube.com/@speleothemscience-summersch5335). Traditionally, after each S4 summer school, a new organizing committee is formed by the participants. News and information about the upcoming 6th Summer School on Speleothem Science can be found on the event webpage: speleothemschool.com.

AFFILIATIONS

[1]Department of Air Quality, Slovak Hydrometeorological Institute, Bratislava, Slovakia
[2]Institute for Geosciences, Johannes-Gutenberg-Universität, Mainz, Germany
[3]Department of Earth System Science, University of California, Irvine, USA
[4]Institute of Geosciences, University of São Paulo, Brazil
[5]Department of Earth Science, University of Bergen, Norway
[6]Department of Earth, Atmospheric, and Planetary Sciences, Massachusetts Institute of Technology, Cambridge, USA
[7]School of Geography, University of Melbourne, Australia

CONTACT

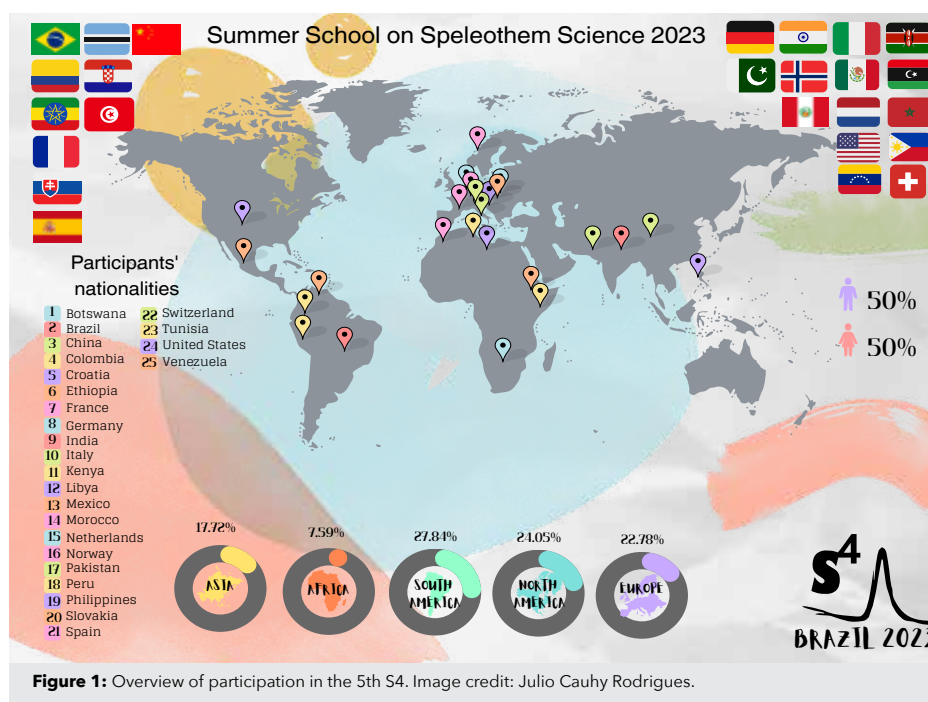Petronela Ševčíková: nela.filipcikova@gmail.com

Figure 1: Overview of participation in the 5th S4. Image credit: Julio Cauhy Rodrigues.

Dendrochronological potential of the tropical wet miombo trees unveiled through African Fieldschools

Participants of the 3rd African Dendrochronological Fieldschool, 2023*

3rd African Dendrochronological Fieldschool, Kitwe, Zambia, 24 July–2 August 2023

Environmental challenges have had a negative impact on African forest resources, which has subsequently adversely affected some ecosystem services that are required for the survival of people. Dendrochronology is a science that helps solve these problems. However, the use of dendrochronology in Africa has been limited due to a lack of experts to support research and training. The African Dendrochronological Fieldschool program was established to develop human capacities in the field of tree-ring science and research. The program was initiated by the Copperbelt University (CBU); through the Copperbelt University Africa Centre of Excellence for Sustainable Mining (CBU-ACESM) in Zambia, to provide basic scientific knowledge and skills to participants in sample collection, preparation, tree-ring measurement, cross-dating, chronology building, and interpretation of results. After completing the training, participants are expected to have gained basic knowledge to help solve various environmental problems.

Training format
The training adopts the North American Dendroecological Fieldweek format. Participants are introduced to various projects on the first day after touring the potential sampling sites. Each participant then chooses the project of their interest. The assigned facilitator takes participants through the project, from the beginning to the end of the training (Speer et al. 2006).

Study focus
During the training, participants were divided into four groups to focus on four different topics in the wet miombo woodlands of Zambia:

i) Dendroecology: Establishment of the arboreal diversity and dynamics of wet miombo woodlands.

ii) Dendroclimate: Determining the effects of precipitation on the growth of *Brachystegia longifolia* and *Julbernardia paniculata*.

iii) Dendrochemistry: Evaluation of the metal concentration in *Brachystegia longifolia* induced by copper mining pollution.

iv) Wood Anatomy: Determining the anatomy of selected tree species from the wet miombo woodlands.

Field sample collection
All samples were collected from the African Explosive Limited (AEL) site in Mufulira

District on the Copperbelt Province of Zambia (Fig. 1).

Laboratory sample preparation and analysis
After sample collection, tree-ring cores were mounted, sanded and scanned. We measured tree-ring widths in the software application CooRecorder and cross-dated using CDendro (Maxwell and Larsson 2021). We also used COFECHA program (Holmes 1983) to check the dating quality of samples.

Workshop outcome
Organizers and six facilitators from three different countries (USA, UK and Zambia) trained 25 people from 10 countries (Democratic Republic of Congo, Egypt, Ghana, Kenya, Mexico, Mozambique, Namibia, USA, Zambia, and Zimbabwe). Each of the four groups (Dendroecology, Dendroclimate, Dendrochemistry, and Wood Anatomy) that we formed during the training reported interesting results. The Dendroecology group worked on 49 tree species that were sampled in a half hectare plot, and found that the Fabaceae family plants had the highest species richness with 28.5%. This group further found that wet miombo tree species produce annual growth rings responsive to seasonal climate, and are useful for dendrochronology. They determined a series intercorrelation of 0.45 and average mean sensitivity of 0.465 from a master chronology of 14 tree species. The

dendroclimate group recorded a significant positive relationship (r-value = 0.589, p-value = 0.0005) between ring width of a mixed species chronology of *B. longifolia* and *J. paniculata*, and precipitation totals for Zambia's wet season (October–April). The group that worked on dendrochemistry found that arsenic, barium, calcium, lead, zinc, manganese, and strontium bio-accumulate in *B. longifolia*. Workshop participants also worked on a number of trees from the wet miombo woodlands, which included the common species of *Brachystegia, Julbernardia* and *Isoberlinia* to understand their anatomical properties. The species were found to be diffuse porous.

AFFILIATIONS
*See the online version for the complete author list

CONTACT
Justine Ngoma: justinangoma@yahoo.com

REFERENCES

Holmes RL (1983) Tree-Ring Bull 43: 69-78

Maxwell RS, Larsson LA (2021) Dendrochronologia 67: 125841

Speer JH et al. (2006) Professional Paper of the Indiana State University, Department of Geography, Geology and Anthropology 23: 3-14
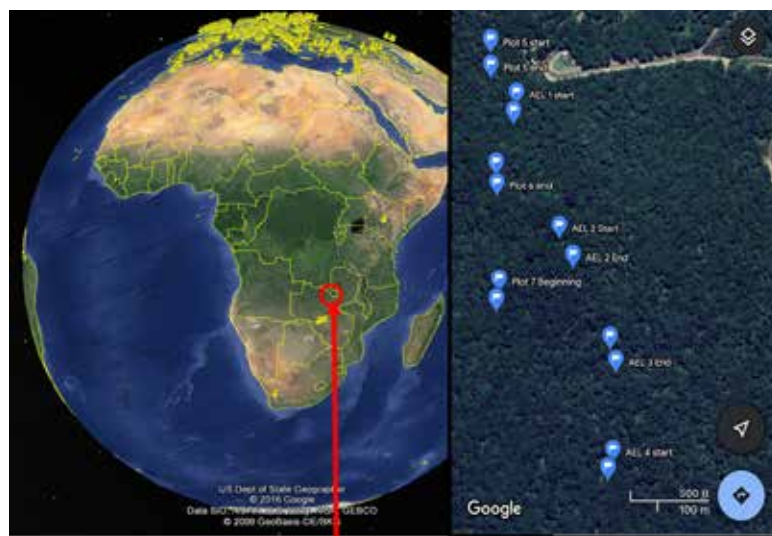
Figure 1: Distribution of sample sites at the AEL site in ßMufulira District, Zambia. The yellow pinpoint icons show the locations with chronologies as reported in the International Tree-Ring Data Bank (ITRDB - notice the lack of chronologies in sub-Saharan Africa). The blue pinpoint icons show the beginning and end of the 40 m transect for the dendroecology study.

An initiative to better understand the future ice-ocean-atmosphere interactions between the Southern Ocean and Antarctica from the past critical periods

Abhijith U. Venugopal[1], M.E. Weber[2], M.O. Patterson[3], F. Lamy[4] and E.D. Keller[5]

INSTANT-SOAS workshop, Trieste, Italy, 11 September 2023

Context

Understanding the exchange of heat and mass between the Southern Ocean (SO) and Antarctica facilitated by dynamicallydriven currents, such as Antarctic Circumpolar Current (ACC), is critical for constraining the stability of Antarctic Ice Sheet (AIS) (Martinson 2012) (Fig. 1). As the instrumental records that would inform ice-ocean-atmosphere interactions are minimal, the Southern Ocean-Antarctic Interactions (SOAS) subcommittee, formed in the framework of the SCAR Instabilities and Thresholds in Antarctica (INSTANT) Programme, aims to circumvent this limitation by examining past critical periods, and facilitate the dialogue and collaboration between the proxy and modeling communities. To lay out the objectives and identify the priorities for the subcommittee, the first in-person workshop was held during the SCAR-INSTANT conference on 11 September 2023 in Trieste, Italy. The following sections highlight the objectives of the program, and existing knowledge gaps.

Objectives of the SOAS program

The main science questions that the subcommittee aim to address are as follows: a) What can we learn from new and emerging records of past AIS, ACC and Southern Hemisphere Westerly Wind dynamics?; b) What is the role of changing winds, and surface-, intermediate- and deep-water circulation of the ACC on the growth and decay of the AIS?; c) How do we integrate SO records with those from the Antarctic continent (e.g. from ice cores), and the Southern Hemisphere mid-latitudes (e.g. lakes, moraines)?; d) How do recent findings for the geologic past inform numerical modeling of AIS mass loss, global sea-level rise and thermohaline circulation, and help assess their impacts on global climate?

A major goal is to bring the paleoclimate communities together to decipher past tipping points of climate as the most critical periods where model calibration, and general understanding of involved processes, is required. Such periods of interest include millennial-scale variability, the last glacial termination, the last interglacial, the Mid-Brunhes, Mid-Pleistocene Transition, the Mid-Pliocene warm period, and the Mid-Miocene. Those were periods when the changes in CO_2, temperature and sea level were significant – all possible scenarios to constrain the sensitivity of future AIS.

Research and collaboration gaps: Paleo-proxy and modeling perspectives

Accurately modeling ice-atmosphere-ocean interactions in different past climatic states is challenging due to technical and computational limitations, as well as gaps in our process understanding (Colleoni et al. 2018). Experiments from Paleoclimate Modelling Intercomparison Project (PMIP) Phase 4 have highlighted paleo-bathymetry, sub-surface melt rates, sea ice, polynya and bottom-water formation, and the timing and amount of meltwater entering the polar ocean, as some of the major factors that contribute to uncertainty in paleoclimate model simulations (Kageyama et al. 2018).

While the models remain notably sensitive to the choice of meltwater scenario (e.g. Chadwick et al. 2023), sea-ice conditions and paleo-bathymetry, there are only limited constraints on these parameters (e.g. Weber et al. 2014). New proxies, as well as more spatial coverage in the SO for traditional proxies, are essential.

A major challenge for the proxy community is to fill gaps in observational data by increasing the spatial coverage from what currently exists in the International Ocean Discovery Program, and its predecessor programs, as regional variability in the ice-ocean-atmosphere processes can be significant. Furthermore, while marine records provide proxy-based information on processes happening at the ice margin, they do not provide direct observations of inland ice retreat. This knowledge on inland ice retreat ultimately helps quantify sea-level contributions from the various Antarctic catchments that modeling experiments aim to assess for future projections (Patterson et al. 2022). Land-based geological and ice-core drilling efforts are the only means to ground truth-modeling experiments that examine such contributions, and reduce uncertainty surrounding the extent of ice retreat under future warming scenarios.

Improved modeling of the evolution of the Antarctic-SO system would require identifying regions of highest priority to target for traditional and/or new proxy data, which may be better facilitated through the accessibility of paleoclimate model data by the proxy community. The paleoclimate community has identified that accessing model outputs acts as a major limitation to performing data-model intercomparison studies that may facilitate site selection, and proxy development.

Through this seven-year-long program, we plan to provide a timely synthesis of progressive knowledge of SO-Antarctic interactions, and provide a platform to foster collaborations that would minimize the knowledge gaps identified here.

AFFILIATIONS
[1]School of Physical and Chemical Sciences, University of Canterbury, Christchurch, New Zealand
[2]Institute for Geosciences, University of Bonn, Germany
[3]Department of Earth Sciences, Binghamton University, USA
[4]Alfred Wegener Institute, Helmholtz-Centre for Polar and Marine Research, Bremerhaven, Germany
[5]GNS Science, Lower Hutt, New Zealand and Antarctic Research Centre, Victoria University of Wellington, New Zealand

CONTACT
Abhijith U. Venugopal: abhijtih.ulayottilvenugopal@canterbury.ac.nz

REFERENCES
Chadwick M et al. (2023) Paleoceanogr Paleoclimatol 38: e2022PA004600

Colleoni F et al. (2018) Nat Commun 9: 2289

Kageyama M et al. (2018) Geosci Model Dev 11: 1033-1057

Martinson DG (2012) Palaeogeogr Palaeoclimatol Palaeoecol 335: 71-74

Patterson MO et al. (2022) Sci Drill 30: 101-112

Weber ME et al. (2014) Nature 510: 134-138
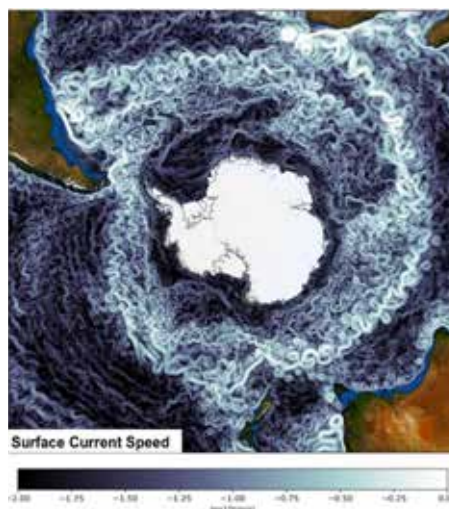
Figure 1: Visualization of the ACC showing modeled modern-surface current velocities with prominent eddies shaping ocean transport ,and exchange among SO and Antarctica.
Model: FESOM2 (Finite-volumE Sea ice-Ocean Model, formulated on unstructured mesh, fesom.de) Setup: ROSSBY4.2; Simulations: Dmitry Sein (AWI); Visualization: Nikolay Koldunov (AWI). Image credit: Nikolay Koldunov.

Instabilities and thresholds in Antarctica

SCAR INSTANT Conference Organizing Committee*

SCAR INSTANT International Conference, Trieste, Italy 11–14, September 2023

Current deep uncertainties in the projected global mean sea-level rise result from knowledge gaps in the physical processes involved in the response of the Antarctic Ice Sheet (AIS) to global warming in the coming decades to centuries (Fox-Kemper et al. 2021). Many of the ice shelves fringing Antarctica are at risk of rapid thinning, or collapse, due to oceanic and atmospheric warming, with likely impacts on the position of the ice-sheet grounding line. It is critical for the ice-sheet community to determine whether Antarctica's margins have already crossed a tipping point, and if so, when and how much mass loss will take place. A multi-disciplinary approach is required to advance the state of knowledge on tipping points spanning a large range of spatio-temporal scales and components of the polar-climate system. This is the overarching objective of the SCAR Instabilities and Thresholds in Antarctica (INSTANT) Scientific Research Programme (Colleoni et al. 2022).

Launched in February 2021, INSTANT held its first in-person conference in Trieste, Italy, in September 2023. The conference had two main objectives: foster multidisciplinary science, and promote and support early-career scientists' (ECS) engagement in networks. The first objective was achieved via morning plenaries dedicated to each INSTANT theme (Fig. 1): Atmosphere-ocean-AIS interactions from past to future; Earth-AIS interactions; AIS contribution to sea-level projections. Participants were therefore exposed to cutting-edge research across themes, disciplines and techniques, and this continued with open poster sessions. Afternoon community-driven workshops were organized by INSTANT subcommittees and INSTANT partner initiatives (Fig. 1). A mini-symposium on the last day of the conference – Melting Ice and Rising Seas, telling stories and engaging people – enabled interaction with policy-makers, stakeholders and practitioners, as well as indigenous advocates, writers and journalists. The conference demonstrated the need to discuss these important societal matters. Addressing the second objective, ECS led two workshops: one on how to handle a multidisciplinary science career, the second on translating science to policy. The INSTANT Programme thanks its sponsors who funded the attendance of 43 ECS. Many pre-conference and post-conference workshops also took place.

This was the first in-person conference dedicated to Antarctic research since the pandemic (the last SCAR Open Science Conference was online in 2022). Nearly 300 scientists from 25 countries participated; one third of whom were ECS (shorturl.at/izBCZ). The outcomes from the conference emphasize the urgent need to close the knowledge gap on:

(1) The physics driving ice-sheet grounding line dynamics, subglacial hydrology (and role of geothermal heat flux), and ice-shelf calving. These are all important mechanisms for understanding and computing ice-sheet instabilities and mass loss from Antarctica, but are currently heavily parameterized in models;

2) The physical processes at the interface between the ice sheet and the ocean, which are still poorly known due to the paucity of observations;

(3) Surface-mass balance over the Antarctic Ice Sheet and surface melting, which remain poorly constrained because observations are very localized in space and time;

(4) The impact of glacial-isostatic adjustment on ice-sheet instabilities, which is still poorly understood because our knowledge of the lithosphere and mantle rheology underneath the ice remains limited, and these processes are not always captured in dynamic models;

(5) Ice-sheet instabilities over multi-centennial timescales, to determine whether some Antarctic ice shelves have crossed their tipping point. The timespan of satellite observations indicating a rapid thinning of West Antarctic ice shelves is too short, so paleoclimatic evidence is needed to provide constraints on a longer timescale.
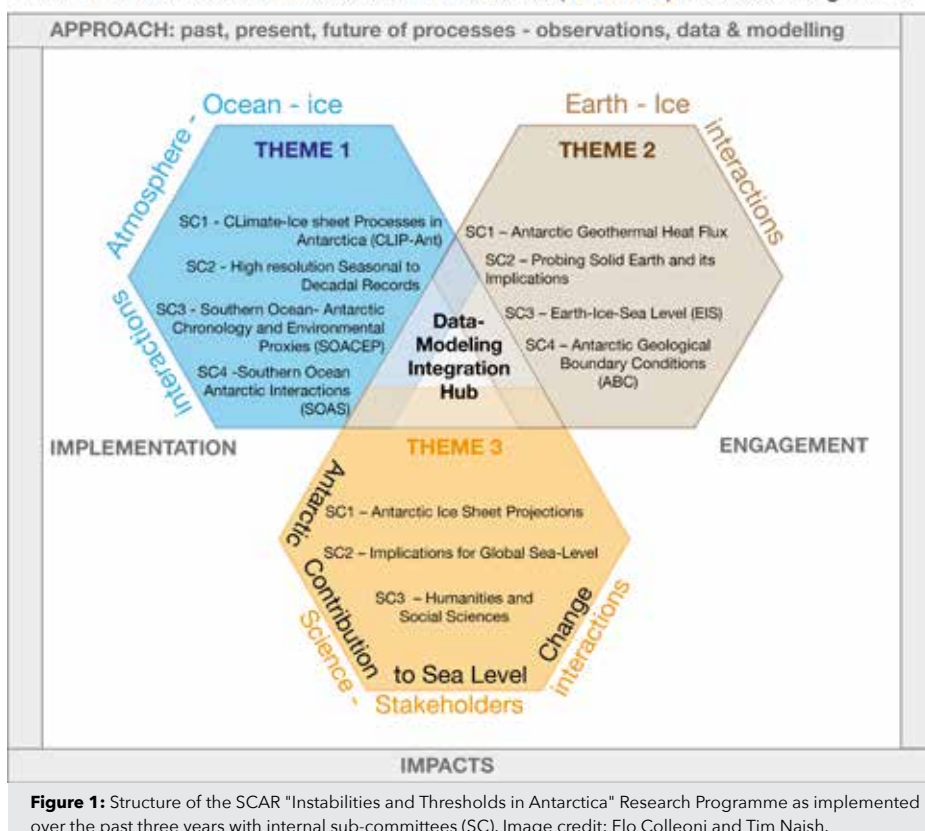
The key themes emerging from this conference are the need to advance science collectively by sharing data and models with the community, and the need to maintain global and regional observational networks (for example to avoid gaps in satellite programs, or the dismantling of geodetic networks). Both require international coordination and sharing of research infrastructures and strengthening of cooperation between the member states of the Antarctic Treaty. The conference was endorsed by the UN Ocean Decade. Recording from the INSTANT Conference is available on the YouTube channel of the SCAR INSTANT Programme.

AFFILIATIONS
*See the online version for the complete author list

CONTACT
Florence Colleoni: fcolleoni@ogs.it

REFERENCES

Colleoni F et al. (2022) Eos: 103

Fox-Kemper B et al. (2021) In: Masson-Delmotte V et al. (Eds) Climate Change 2021: The Physical Science Basis. Cambridge University Press, 1211-1362

Figure 1: Structure of the SCAR "Instabilities and Thresholds in Antarctica" Research Programme as implemented over the past three years with internal sub-committees (SC). Image credit: Flo Colleoni and Tim Naish.

Young researchers explore climate histories

Alexander Hibberts[1] and Heli Huhtamaa[2,3]

Climate in History: Summer school for early-career researchers, Aeschi bei Spiez, Switzerland, 16–20 August 2023

Historians have much to contribute to paleosciences, especially to the study of past climatic changes. Written records, for example, offer invaluable climate data, allowing high-resolution reconstructions. Similarly, the interaction between humans and past environments can help us better understand the complexity of climate-society entanglements on various temporal scales – ranging from rapid environmental degradation to multi-centennial dynamics of societal adaptation and resilience.

However, few historians conduct research on, or teach about, past climatic changes. At the same time, the next generation of historians have expressed a growing interest in incorporating the study of climate into their examination of the past.

The Climate in History summer school, held in Aeschi bei Spiez near the Lake of Thun, Switzerland, provided a vital opportunity to redress this imbalance. The summer school gathered a cohort of PhD and early-postdoctoral researchers for four days of talks, seminar discussions, activities and group work. The keynote talks and related exercises were led by international experts, including members the PAGES 2k Network, VICS, and CRIAS working groups. In addition, Patrick Cho welcomed the next generation of climate historians to join the PAGES Early-Career Network (ECN).

Building the basics
Stefan Brönnimann opened the summer school with a crash course on climatology. His keynote took us on a whistle-stop tour of the fundamentals of weather, climate and global patterns of change over time. Further talks explored different climate proxy data types. Andrea Seim introduced the use of tree rings to detect past temperature and precipitation variability, while Michael Sigl demonstrated how scientists detect volcanic signals from ice-core evidence.

The second day brought additional methodological discussions. Elena Xoplaki introduced further climatological basics and demonstrated how paleomodeling can help historical research. Sam White explained the utility of indexing historical documentary data – from the archives of societies – for past climate reconstructions (Camenisch et al. 2022). Elaine Lin's REACHES database, a collection of written weather records from China for the last 3000 years, was introduced as an exemplar (Wang et al. 2018). Christian Rohr, who discussed what climatic information pictorial sources might contain, delivered the last keynote talk.

Each keynote talk was followed by exercises making use of the methodology or source base discussed, suggesting a pedagogical approach attendees could transfer back to their own institutions. All speakers compellingly communicated how accessing climate data can generate new narratives of the past.

The Skippon diary
The main segment of the summer school centered around applying newly learned techniques to an exciting primary source: a weather diary produced by Sir Philip Skippon, a Suffolk gentleman, between 1673 and 1674 CE.

Attendees were divided into groups to transcribe and interpret different chronological sections. The data was subsequently compared to other material, including state-of-the-art reanalyses, weather diaries from northern England and instrumental observations recorded in Paris. These suggested the Skippon diary was a relatively reliable indicator of weather patterns.

Final reflections
The summer school provided a rare, but essential, opportunity for humanities-based historians to acquire training in methods drawn from the climate sciences. Crossing firmly fixed disciplinary boundaries was not easy and demanded patience and perseverance from all participants, many of whom had never been trained in quantitative data analysis.

However, the value of interdisciplinary collaboration was made clear when historians brought their skills in source criticism to bear on the use of historical documents in past climate reconstruction. Not all sources are reliable and must be judged in a cultural context to extract meaning. Acknowledging this enables historical data to be used more sensitively, and with better results, when reconstructing past climatic change and its impacts on human society.

Teaching and learning across disciplines may be what is needed to drive "positive change" in higher education, and foster a deeper constructive critique of our current climate crisis and necessary responses (McCowan 2023). Historians can, and should, be an important part of this conversation. As Andrea Seim succinctly argued at the summer school: "The past is the key to the future."

AFFILIATIONS
[1]Department of History, University of Durham, UK
[2]Institute of History, University of Bern, Switzerland
[3]Oeschger Centre for Climate Change Research, University of Bern, Switzerland

CONTACT
Heli Huhtamaa: heli.huhtamaa@unibe.ch

REFERENCES
Camenisch C et al. (2022) Clim Past 18 (1): 2449-2462

McCowan T (2023) Teach High 28 (5): 933-952

Wang PK et al. (2018) Sci Data 5 (1): 1-14

Figure 1: Extract from Philip Skippon's diary from 9–13 August 1673 CE (19–23 August 1673 in Gregorian calendar). Skippon recorded in his calendar personal and societal events as well as detailed weather observations. On the left, Skippon documented hearing gunfire associated with the Third Anglo-Dutch War from his home at Wrentham on 11 August 1673 CE. He also noted Cambridge scholars visiting a boy in his village on 13 August 1673 CE who could read Latin, Hebrew, Arabic, and Greek. On the right, he recorded daily lunar phase, wind direction, thermos- and barometer readings, and descriptive weather observations (from left to right).

The atypical interglacial of MIS 11c and the long-term change in interglacial intensity over the past 800 kyr

Marie Bouchet[1], A. Donner[2], M. Grimmer[3], C. Jasper[4], F. Krauss[3], E. Legrain[5] and P. Vera Polo[6,7]

Final QUIGS workshop, Grenoble, France, and online, 19–22 September 2023

Eleven interglacials have been identified in the past 800 kyr (Past Interglacials Working Group of PAGES 2016). Around 430 kyr BP, a change in interglacial strength, known as the Mid-Brunhes Event (MBE), was observed in atmospheric CO_2 levels, and in proxy records of Antarctic and global surface temperatures, marking a transition to stronger interglacials, such as Marine Isotope Stages (MISs) 5e and 11c (Fig. 1). While the onset of interglacials seems linked to an increased Northern Hemisphere summer insolation, uncertainties persist due to complex interactions involving astronomical forcing, ice volume, CO_2 levels, and temperature.

Active research areas in Late Pleistocene interglacials focus on those not aligning with the astronomical theory of ice ages, and on long-term changes in interglacial intensity over the past 800 kyr. To address these topics, the PAGES working group on Quaternary Interglacials (QUIGS) convened in Grenoble, France. Here we highlight some of the topics covered, and a few of the presentations that led to particular areas of discussion.

The unusual MIS 11c interglacial is known for its prolonged high sea-level and atmospheric CO_2 concentrations, despite weak summer-insolation forcing (Tzedakis et al. 2022). The prolonged Termination V was suggested to be associated with the largest sea-level contribution from the Greenland Ice Sheet over the last 800 kyr. Alessio Rovere showed how large ice sheets may drive high sea-level stands, with MIS 12 believed to have featured one of the most extensive glaciations (Batchelor et al. 2019). Claire Jasper's study of iceberg rafted debris (IRD) in the Southern Ocean's Atlantic sector, during Termination V and MIS 11c, indicated a protracted period of Antarctic Ice Sheet iceberg discharge and melt. Steve Barker suggested that the asynchronous phasing of obliquity and precession during Termination V (Fig. 1) may explain the prolonged nature of this deglaciation.

The necessity to develop a coordinated modeling protocol over the Termination V-MIS 11c time period was discussed. In this framework, the group agreed on the importance of constraining the volume and extent of the MIS 12 ice sheet, and developing a coherent temporal framework for the rate of sea-level rise, and for various paleoclimate proxies representative of different parts of the Earth System across the deglaciation.

The second part of the discussions delved into the MBE, addressing challenges related to the metrics of interglacial intensity. Mean Ocean Temperature reconstructed by Markus Grimmer emerged as a potential metric for distinguishing between strong and weak interglacials. A debate arose regarding the classification of early interglacial peaks in CO_2, known as overshoots, and whether they are part of the interglacial or termination. Takahito Mitsui presented a model predicting interglacial intensity based on the previous glacial strength and summer insolation, received at both northern and southern high latitudes during deglaciation. According to Mitsui et al. (2022), the increase in interglacial intensities after the MBE is related to the amplitude increase in obliquity cycles. Finally, Quizhen Yin pointed out that in some records, such as Chinese loess, there is no discernable increase in interglacial strength across MBE. This observation gave rise to the alternative suggestion: can we use records where MBE is not detectable to understand what causes the observation of MBE in other records? In conclusion, an outline for a short position paper effort was defined on our current knowledge of interglacial intensity, incorporating both paleoclimate records and modeling.

The QUIGS leadership team thanks all the participants who engaged in this final workshop, and throughout the QUIGS adventure, extending thanks to PAGES for their continuous support.

REFERENCES

Batchelor CL et al. (2019) Nat Commun 10: 3713

Bouchet M et al. (2023) Clim Past 19: 2257-2286

Donders T et al. (2021) Proc Natl Acad Sci 118: e2026111118

Mitsui T et al. (2022) Clim Past 18: 1983-1996

Past Interglacials Working Group of PAGES (2016) Rev Geophys 54: 162-219

Tzedakis PC et al. (2022) Quat Sci Rev 284: 107493
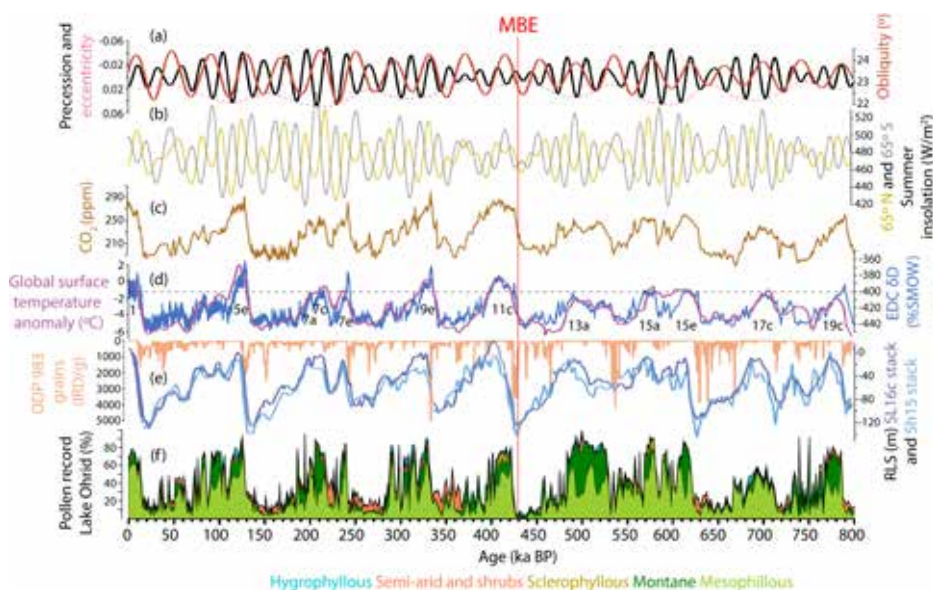
Figure 1: Paleoclimate reconstructions over the last 800 kyr (modified from Tzedakis et al. 2022). **(A)** Eccentricity (red dashed), precession (black), obliquity (red solid), and **(B)** summer solstice insolation at 65°N (orange) and 65°S (gray). Antarctic EDC ice-core records of **(C)** atmospheric CO_2 and **(D)** δD of ice (blue) on AICC2023 timescale (Bouchet et al. 2023). A 400‰-threshold (dashed line) separates pre- and post-MBE interglacials. Global average surface temperature (anomaly vs. present) (purple). **(E)** IRD in North Atlantic ODP Site 983 (salmon); two reconstructions of relative sea level (dark and light blue). **(F)** Pollen from Lake Ohrid (Donders et al. 2021).

Fire science Learning AcRoss the Earth System (FLARE) workshop

Douglas S. Hamilton[1], M.M.G. Perron[2], J. Llort[3], S. Hebden[4] and M.H. Morrill[5]

FLARE workshop, Bermuda, and online, 18–21 September 2023

Fire is a key component of the Earth System, modified by, and impacting on, human activities. It shapes and regulates terrestrial ecosystems (Pausas and Bond 2020), but also drives changes in weather, climate (Hamilton et al. 2018), carbon (Lasslop et al. 2019), and nutrient cycling (Perron et al. 2022) through the many complex interactions of fire and its emissions in the Earth System. From land to ocean, from vegetation to human society, and from the past to the future; fire is a truly transdisciplinary research topic.

Although fire is an integrated component of the Earth System, integrated research across disciplines, institutions and fire practitioners is currently lacking. As a result, it is difficult to obtain the much-needed holistic understanding of how rapid changes in wildfire activity will impact ecosystems and society in the coming decades.

Diverse expertise from across the geosciences and social sciences is needed to fully appreciate and identify the main challenges in fire science. The changing trends in fire intensity and its spatial reorganization, in response to climate change, are altering the interactions between fire and other components of the Earth System, including society (Kala 2023). This clearly signals an urge for better communication between scientific, societal, stakeholder, and government representatives.

To address this need, the ambition of the FLARE (Fire science Learning AcRoss the Earth system) workshop was to gather a transdisciplinary international panel of researchers and fire practitioners.

Participants discussed the challenges in understanding fire behavior and its impacts across the world and over varied timeframes, the tools that we have, and the need to address these challenges, as well as how to better communicate across disciplines. The goal is to synthesize this knowledge and formulate a roadmap for more integrated wildfire research over the next five to 10 years.

Held from 18–21 September 2023, FLARE gathered experts from disciplines across the Future Earth global research network. Expertise in physical and social science, remote sensing, fire communicators and artists, operational fire scientists, and fire managers were all present. Participants represented 14 countries, and both early-career and gender equity were achieved overall. The workshop was held in a hybrid format, with 15 onsite participants invited to meet at the Bermuda Institute of Ocean Sciences (BIOS, bios.asu.edu) and 22 participants online. The four-day workshop included lightning presentations from each participant, 20 keynote talks, lively discussions, and four in-depth breakout sessions.

The workshop highlighted a poor constraint on "impacts of fires on the Earth System" which stem from a lack of communication between relevant fields of expertise. In particular, a disconnection was identified between the scientific aspect of fire and the societal implications of fire events. Workshop participants identified three main challenges that need to be addressed by the global fire community:

(Challenge 1) Unifying transdisciplinary research around common boundary objects, starting with "Fire's role in the carbon cycle";

(Challenge 2) Better characterizing "Fire and extreme events";

(Challenge 3) Taking a holistic approach to understanding "Fire interactions with humans".

The FLARE workshop also included an onsite public engagement event organized by the US Consul General Office of Bermuda. Dr Ben Poulter (NASA) visited students at the Warwick Academy to discuss NASA's role in Earth science, climate change and blue carbon ecosystems. Additionally, fire-science illustrators Miriam Morrill and Jessie Thoreson captured the transdisciplinary collaboration process during the workshop, characterizing the carbon cycle as a potential boundary object for collaborative global fire science connectivity (Fig. 1).

Ongoing work now addresses the identified challenges, and during 2024 a roadmap for coordinated wildfire research, in the form of a white paper, will be produced. As part of the white paper, FLARE plans to include a dedicated early-career researcher perspective on the workshop and its outcomes, as well as recommendations for inclusive fire science across different communities.

AFFILIATIONS
[1]Carrera de Biología Marina, Universidad Científica del Sur, Lima, Perú
[2]Programa Doctoral en Recursos Hídricos, Universidad Nacional Agraria la Molina, Lima, Perú
[3]Dirección de Asuntos Antárticos, Ministerio de Relaciones Exteriores, Lima, Perú
[4]Centro Universitario Regional Este, Universidad de la República, Rocha, Uruguay
[5]Instituto de Oceanografia, Universidade Federal do Rio Grande, Brazil

CONTACT
Douglas S. Hamilton: dshamil3@ncsu.edu

REFERENCES
Hamilton DS et al. (2018) Nat Comms 9: 3182

Kala CP (2023) Nat Hazards Res 3: 286-294

Lasslop G et al. (2019) Curr Clim Change Rep 5: 112-123

Pausas JG, Bond WJ (2020) Trends Ecolo Evol 35: 767-775

Perron MMG et al. (2022) Atmos Res 270: 106084

WILDFIRE BURNING	PRESCRIBED FIRE	DETRITUS & SOILS	SNOW & ICE	LAND BIOTA	FRESH WATER & WETLANDS	MARINE BIOTA	CAPTURE /REMOVAL
BLACK	GREY	BROWN	RED/PINK	GREEN	TEAL	BLUE	PURPLE
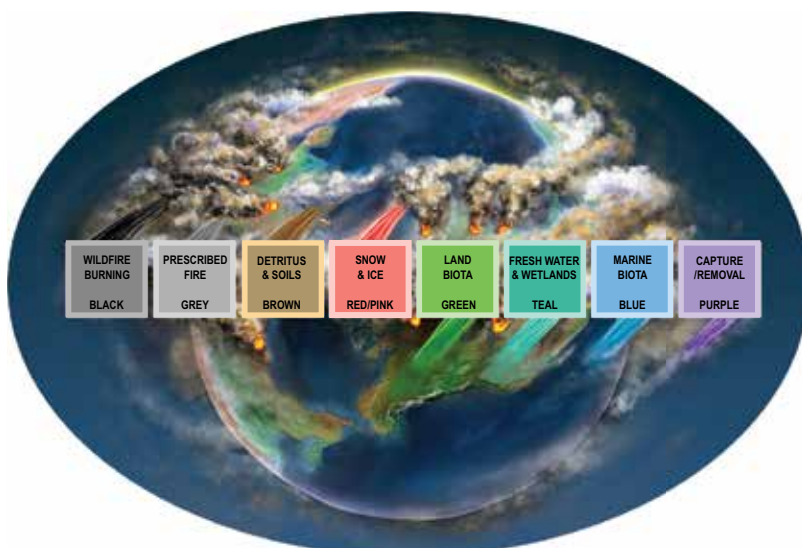
Figure 1: An eye on fire's role in the carbon color spectrum. Upward pointing box "tails" indicate carbon sources, and downward pointing box "tails" indicate carbon sinks.

Holocene-scale lake sediment Pb records, a database and review

John F. Boyle[1], M. Moyle[1] and N. Dubois[2]

3rd Human Traces Pb records project workshop, Liverpool, UK, and online, 20–21 September 2023

The Human Traces (pastglobalchanges.org/human-traces) working group (WG) focuses on the long legacy of pre-Anthropocene human impacts, and how they manifest themselves in different parts of the world and in different types of stratigraphic records. The activities of the WG aim to address the knowledge gap concerning spatial and temporal variations in early human impacts on ecosystems, with the overarching goal to create a global synthesis of human traces in geologic archives. Following a presentation on Greenland ice-core Pb records by Professor Joe McConnell at an earlier Human Traces workshop (see McConnell et al. 2018), a discussion identified the need to link environmental archives more fully to address some specific questions about regionality of long-transported atmospheric Pb pollution. A Pb records sub-group was established with the aims of: 1) assembling long (Holocene) lake and peat sediment Pb records from around the world, for comparison with these high-resolution ice-core records, and to produce a database that will be of wider use to the paleocommunity, and 2) reviewing methodological approaches to collecting Pb sediment records.

A hybrid workshop was held on 20–21 September 2023 at the Department of Geography & Planning, University of Liverpool. Twelve individuals attended in person, with a further seven online. The primary aims of the workshop were to: 1) review records assembled by the participants, and choose regions for a global synthesis paper; 2) identify: data gaps, common narratives, significant periods and their spatial footprints, and factors influencing Pb distribution, and 3) develop papers on methodologies and grand challenges.

Global synthesis paper
Having identified a number of existing and potential long Pb records in peat and lake sediment archives across the globe (Fig. 1a), we discussed approaches to identifying regions for a global synthesis paper. We concluded that the two ideal approaches of identifying regions based on 1) statistical analysis of pattern, or 2) analysis of metallurgical historical/archaeology, were impractical. The former lacks sufficient data points, and the latter is of a complexity beyond the scope of a single paper. Instead, we agreed on regions based on the collective experience of the workshop participants (Fig. 1b). These regions were not given strict definitions, and we have subsequently decided

to use the IPCC region polygons, slightly modified to meet our needs by some splitting and merging.

The records identified at the meeting (N=192) clearly do not include all existing datasets. We continue to add sites as we find them and welcome suggestions. We have deliberately included regions that contain no sites. For these we can predict what patterns are expected, and can predict areas where suitable sites may occur. Each region in the global synthesis will receive just one page of figures and text. The figures will show a small number of sites, selected to be representative of the regions, and the text will offer a chronological account of the major features of the records, with reference to known historical and archaeological narratives. A short global summary will compare and contrast the regions, identifying major trends, information gaps and new research questions.

Methodological issues
A productive discussion was held about methodological issues such as appropriate analytical techniques (is scanning XRF sufficiently precise?), source identification by isotopes or by enrichment factors, whether fluxes or concertation data should be preferred, and approaches to variable chronological confidence. We concluded that the body of published records could have been more usefully combined had there been some agreed community standards in methodology and reporting. In response, we have decided to write a methods paper aimed at research students and early-career

researchers (ECRs), and cover the full process from site selection, choice of methods, data processing, and reporting standards, and have sketched out a plan for this paper.

Other outputs
The initial objective of the WG was to generate a community database of long Pb records (to be hosted by Neotoma), with an associated published description and analysis of the records found. This remains the primary planned output. The "Global Synthesis" and the "Methods" papers described above will supplement this work and provide a contribution to the wider research community of exceptional value. In addition to this, we recognize that a number of research pathways may arise from the new dataset. To reflect this, we decided to write a "Grand Challenges" paper, covering topics such as: distinguishing the impacts of historical empires on the ancient global Pb pollution signal; distinguishing mining from metallurgical signals; and separating the signal of Pb due to silver mining from later direct Pb mining.

REFERENCES
McConnell JR et al. (2018) Proc Natl Acad Sci USA 115: 5726-5731

Figure 1: (A) Long Pb records in peat and lake sediment identified at the workshop. **(B)** Provisional regions for global synthesis.

1 Britain & Ireland
2 Scandinavia
3 Central Europe
4 Southeast Europe
5 Southwest Europe
6 Russia
7 Mediterranean Africa
8 Sub Saharan Africa
9 South Asia
10 East Asia
11 Southeast Asia
12 Southwest Asia
13 Oceania & Australia
14 Arctic North America
15 Eastern North America
16 Western North America
17 Caribbean
18 Central America
19 Amazonia
20 Northern Andes
21 Southern Andes
22 Eastern South America
23 Antarctica

Generating high-resolution chronological databases with varves and tephra

Adrian P. Palmer[1], A. Beckett[1], A. Brauser[2], C. Blanchet[2], C. Martin-Puertas[1], A. Ramisch[3] and A. Brauer[2]

The PAGES Data Stewardship Scholarship has added new tephra datasets to VARDA, an online global database of varve records, to enhance high-resolution chronology construction.

Annually laminated (varved) sediments are recovered from lakes and ocean basins in different climatic settings and provide the opportunity to examine past environmental and climatic changes at the highest possible temporal resolution, comparable to tree-ring and ice-core chronologies. The Varved Sediments Database (VARDA) was built to explore the spatial and temporal distribution of terrestrial varved archives (Ramisch et al. 2020). VARDA includes information on the location of varved sites, the duration of the varve record and available proxy datasets, and is openly accessible at varve.gfz-potsdam.de. In addition to varve counting, the database contains radiometric dating measurements (e.g. ^{14}C) that enable varve chronologies to be anchored to an absolute timescale.

An important milestone in the development of VARDA is the inclusion of tie-points that can help link spatially distant archives to understand the spatio-temporal complexity of abrupt climate change. Indeed, the combination of accurate dating, solid tie-points and annually resolved archives would be a step-change to detemine the regional environmental variability during climatic transitions, and leads or lags between forcing and responses.

The purpose of the PAGES Data Stewardship Scholarship (DSS) was, therefore, to review and incorporate volcanic-ash (tephra) layers identified in varved-lake sequences in VARDA. Tephras are airborne, near-instantaneous deposits that spread over large regions, and can be distinguished by their specific mineralogical and chemical composition. In the last two decades, there has been an increase in the use of non-visible (crypto-)tephra layers within lake-sediment sequences that greatly densified the tephra framework. Also, the correct attribution of a tephra layer to a volcanic-source area, and a specific eruption of a known age, requires measurement of the geochemical composition of individual tephra shards, generating a wealth of new data. We therefore aimed to collect and incorporate recent tephra findings in varved sediments to VARDA, including their geochemical datasets. We first focused on the last deglaciation time period, i.e. between 25–8 kyr BP.

The scholarship initially had a European focus and explored the varve-lake records with tephra horizons from both VARDA and new published datasets. This information was used to decide how the metadata would be presented and accessed within the database, and to identify the mandatory/optional datasets. From 33 lakes in Europe, 22 contained tephra layers and 19 have associated geochemical datasets updated into VARDA. In total, there are 49 discrete, known tephra layers within the time period with volcanic sources from Iceland, Eifel, Massif Central, Hellenic Arc and Italy across these sites. There are 19 tephra horizons represented at more than one site that will

enable more precise synchronization and comparisons between the varve records. On the VARDA landing page, it is now possible to search with different filters for 'varves', 'tephra' and 'tephra chemistry', examining the map for those sites with tephra, and accessing the geochemistry datasets. The geochemical data also includes metadata related to the analytical procedure followed, such as the instrument and secondary standards used. Further information on the European datasets are provided in Beckett et al. (2024), who identify key outcomes from this work as: i) a single repository for tephra geochemical data within varve records, ii) better understanding of the time periods with multiple eruptions, iii) the spatial distribution of the key eruptions, and iv) the potential for new varved sites to contain speciflc tephra horizons.

This work is moving toward the final completion of the DSS by extending the tephra geochemistry information in a spatial and temporal context. Identification of an additional 32 lake records beyond Europe, and extending the time window to between 125 kyr and the present day, will expand the scope of the database and explore the potential regional and hemispheric interconnectivity of the varve records when linked using tephra horizons. The Varve Database will not only benefit the paleolimnological and lake research communities, but also aid other disciplines when trying to establish links between marine and terrestrial systems.

AFFILIATIONS
[1]Department of Geography, Royal Holloway, University of London, UK
[2]GFZ German Research Centre for Geosciences, Helmholtz Centre Potsdam, Germany
[3]Department of Geology, University of Innsbruck, Austria

CONTACT
Adrian P. Palmer: a.palmer@rhul.ac.uk

REFERENCES
Beckett A et al. (2024) Earth Syst Sci Data 16: 595-604
Ramisch A et al. (2020) Earth Syst Sci Data 12: 2311-2332

Figure 1: The VARDA interface with an example of four tephra horizons selected in the filter function, with lake sites in Western Europe that contain those records.

The CoralHydro2k Seawater δ18O Database

Alyssa R. Atwood[1], A.L. Moore[1], S. Long[1], R. Pauly[1], K.L. DeLong[2], A. Wagner[3] and J.A. Hargreaves[4]

The PAGES Data Stewardship Scholarship contributed to the development of an updated metadata-rich database of seawater δ18O data by the CoralHydro2k Network.

The oxygen isotopic composition (δ18O) of seawater is a powerful tracer of the global water cycle, providing valuable information on the exchange of water between the ocean, atmosphere and cryosphere, as well as on ocean-mixing processes (LeGrande and Schmidt 2006). As such, these data provide an additional degree of freedom for understanding the complex hydroclimate system, beyond what standard oceano-graphic variables like temperature and salinity can offer. The integration of water isotopes into climate models has also made them an important diagnostic for assessing model performance and skill. Furthermore, because seawater isotopes form the basis of paleoclimate proxies based on the δ18O of marine carbonates, they provide a "common currency" that links paleoclimate recon-structions, modern climate observations and isotope-enabled model simulations, allowing hydrological processes to be evaluated on a wide range of time and spatial scales (Dee et al. 2023).

In recognition of the broad value of seawater δ18O data, and the growing number of seawater δ18O datasets that have been generated over the last decade, the CoralHydro2k Seawater δ18O Database project (pastglobalchanges.org/science/wg/2k-network/projects/coral-hydro/intro) was launched in 2020 to recover "hidden" seawater oxygen-isotope data that were not easily findable. Over the past three years, we have integrated these records with data from public databases and repositories to create a new, centralized, machine-read-able, and metadata-rich database that aligns with findability, accessibility, interoperabil-ity, and reusability (FAIR) standards.

Database overview
The new database consists of 18,615 seawater δ18O observations from 107 datasets. O these data, 53% were not previously available in public databases or data repositories. These "hidden" data were recovered via direct author submission (39%), scientific papers (12%) and theses/dissertations (2%). The other 47% of the data were gathered from public databases and repositories, with the largest contributions from the GEOTRACES 2021 Intermediate Data Product (13%; Schlitzer et al. 2021), the NASA GISS Global Seawater Oxygen-18 Database (10%; Schmidt et al. 1999), PANGAEA (7%), CISE-LOCEAN Seawater Isotopic Database (7%; Reverdin et al. 2022), and GLODAPv2 (3%; Key et al. 2015; Olsen

et al. 2016). When recovering "hidden" data, we collected data from all regions and all depths of the global ocean. Our public data curation efforts were focused on the upper 50 m from 35°N to 35°S to align with the goals of CoralHydro2k (Fig. 1).

The extensive metadata is a unique aspect of the database. Only eight metadata fields are required, but an additional 44 optional metadata fields provide important support-ing information, including isotope-analysis technique, sample collection and storage notes, site information, paired salinity, temperature, and seawater δ2H values. This template provides a set of best practices for reporting seawater isotope data.

EarthChem community for dataset DOIs
A second achievement of the project was the development of a Seawater Oxygen Isotopes Community within the EarthChem Library, an open-access repository for geochemical datasets (earthchem.org/communities/seawater-oxygen-isotopes), where researchers can submit their seawater isotope data and obtain a dataset DOI. We hope that the creation of this site helps researchers publish their seawater isotope datasets, minimizing the number of "hidden" datasets. The template provided on the EarthChem Seawater Oxygen Isotopes community webpage is aligned with the CoralHydro2k Seawater δ18O Database to facilitate future updates to the database.

Current and future plans
We are currently preparing a database description paper. Once published

Figure 1: Seawater δ18O measurements from **(A)** the surface ocean (upper 5 meters of the water column) and **(B)** the subsurface ocean (below 5 meters of the water column).

(expected in 2024), the CoralHydro2k Seawater δ18O Database will be available in the NOAA/World Data Service for Paleoclimatology archives: ncei.noaa.gov/access/paleo-search/study/35453, with additional data visualization features provided through waterisotopes.org.

This database represents an important step towards increasing the availability and usability of seawater isotope data. As future investments in water isotope observation networks become available, this data will be well-suited to tackle 21st-century research questions related to ocean changes in the past, present and future.

AFFILIATIONS
[1]Earth, Ocean and Atmospheric Science Department, Florida State University, Tallahassee, USA
[2]Department of Geography and Anthropology and Coastal Studies Institute, Louisiana State University, Baton Rouge, USA
[3]Department of Geology, California State University, Sacramento, USA
[4]MARUM – Centre for Marine Environmental Sciences, University of Bremen, Germany

CONTACT
Alyssa R. Atwood: aatwood@fsu.edu

REFERENCES
Dee S et al. (2023) Environ Res: Climate 2: 022002

Key RM et al. (2015) Global Ocean Data Analysis Project, Version 2 (GLODAPv2), ORNL/CDIAC-162, NDP-093. Carbon Dioxide Information Analysis Center, Oak Ridge National Laboratory, US Department of Energy

LeGrande AN, Schmidt GA (2006) Geophys Res Lett 33: L12604

Olsen A et al. (2016) Earth Syst Sci Data 8: 297-323

Reverdin G et al. (2022) Earth Syst Sci Data 14: 2721-2735

Schlitzer R et al. (2021) The GEOTRACES Intermediate Data Product 2021.

Schmidt GA et al. (1999) Global Seawater Oxygen-18 Database - v1.22
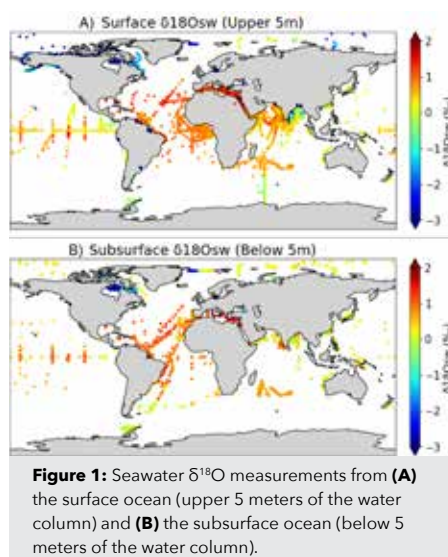
A Southern Ocean sea-surface temperature compilation for the Last Glacial Cycle

Lena M. Thöle[1], Z. Chase[2,3], N. McKay[4], X. Crosta[5] and K. Kohfeld[6]

The PAGES Data Stewardship Scholarship program allowed us to compile and transform Southern Ocean sea-surface temperature data into the LiPD format, increasing the interoperability and, thus, facilitating analyses and comparisons.

Motivation

The C-SIDE working group (pastglobal-changes.org/c-side) has been diligently working towards unraveling the complexity of past Southern Ocean dynamics, with a specific focus on the role of Antarctic sea ice. Previous efforts, spearheaded by Chadwick et al. (2022), aimed to investigate the different patterns in sea-ice dynamics over the Last Glacial Cycle (130–12 ka). One of the primary objectives was the compilation of a comprehensive dataset on Antarctic sea ice, laying the groundwork for a deeper understanding of its dynamics in different regions on a glacial-interglacial timescale.

However, Antarctic sea ice, while a crucial component of Southern Ocean dynamics, is just one of many processes governing the region's past oceanographic – and thus global climate – changes. Furthermore, the interplay of different processes remains unclear. Amongst these processes, sea-surface temperature (SST) dynamics seem to be the obvious first candidate to strongly influence sea ice, and vice versa.

Recognizing the need for a holistic approach, we sought to provide insights into circumpolar Southern Ocean SST changes. To achieve this, we meticulously compiled previously published SST data, positioning our project within a broader context of Southern Ocean dynamics. By undertaking this comprehensive analysis, we aimed to uncover not only the isolated impacts of SST, but also its potential co-dependencies with other factors, foremost sea-ice dynamics.

Southern Ocean SST data compilation and LiPD format standardization

The initial phase of our project involved the compilation of previously published SST data. Here, our focus lay on expanding on efforts by Kohfeld and Chase (2017), mostly adding later datasets. We considered datasets of all resolutions and proxies that cover the Last Glacial Cycle. In the future, the inclusion of certain proxies might be under debate if results point to a misuse of that proxy as an SST proxy.

A first main outcome from the compilation is the distribution of cores, and the scarcity of cores and data for certain regions and zones (Fig. 1). The low number of records from the Antarctic Zone limits the possibilities of investigating connections to sea ice, as well as calculating basin-spanning SST gradients. Furthermore, the Pacific basin is strongly underrepresented, limiting the significance of general findings.

To enhance interoperability and facilitate the seamless reuse of our data compilation, we adopted the LiPD format (McKay and Emile-Geay 2016). This decision was underpinned by the LiPD format's provision of standardized metadata and vocabulary, streamlining the process of data interoperability and reusability for fellow researchers. The LiPD format not only aligns with best practices in data management, but also reflects our commitment to contributing to a collaborative and interconnected (paleo)research environment.

One of the most challenging aspects we encountered was reconciling variations in age models and proxy calibrations across and within different datasets. Addressing these discrepancies proved very challenging due to limited documentation on changes, reasoning and references to previous data. Similarly, retracing these steps and recalibrating both age-model constructions and proxy calibration was hindered by the sparse documentation and availability of raw data. With the compiled and standardized dataset at our disposal, we could start analyzing the patterns and dynamics of past SST in different basins and zones of the Southern Ocean for the Last Glacial Cycle.

Current and future plans

The C-SIDE Southern Ocean SST data compilation, together with our analyses scripts (in R), will be made available on PANGAEA and the LiPDverse website (lipdverse.org). A future project, granted by the Dutch Research Council (NWO), will aim to expand this database and include other proxy data for the Southern Ocean. This will further enhance the interoperability of past Southern Ocean data, and facilitate disentangling different processes driving CO_2 storage and release, and comparison to models. Our team is preparing a manuscript describing the data compilation, analyses and new results emerging from this SST overview for the Southern Ocean.

DISCLAIMER

AFFILIATIONS

[1]Department of Earth Sciences, Utrecht University, Netherlands
[2]Institute for Marine and Antarctic Studies, University of Tasmania, Hobart, Australia
[3]The Australian Centre for Excellence in Antarctic Science (ACEAS), University of Tasmania, Hobart, Australia
[4]School of Earth and Sustainability, Northern Arizona University, Flagstaff, USA
[5]University of Bordeaux, CNRS, Bordeaux INP, EPOC, UMR 5805, Pessac, France
[6]School of Resource and Environmental Management and School of Environmental Science, Simon Fraser University, Burnaby, Canada

CONTACT

Lena Thöle: l.m.thole@uu.nl

REFERENCES

Chadwick M et al. (2022) Clim Past 8(18): 1815-1829

Kohfeld KE, Chase Z (2017) Earth Planet Sci Lett 472: 206-215

McKay NP, Emile-Geay J (2016) Clim Past 4(12): 1093-1100.
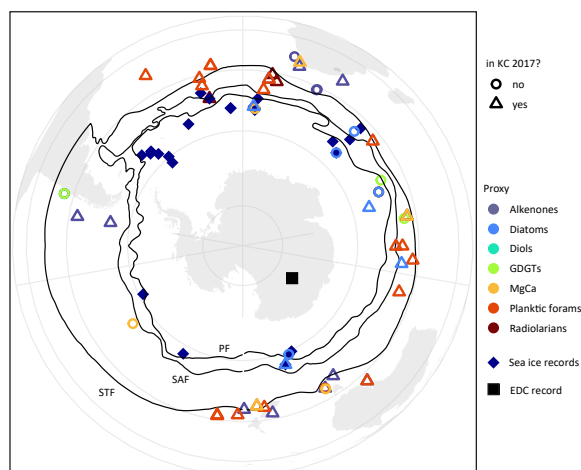
Figure 1: Overview map of compiled SST proxy data for the Last Glacial Cycle. KC 2017: Kohfeld and Chase (2017).

A global database of carbon and oxygen isotopes for the last deglaciation

Juan Muglia[1], S. Mulitza[2], J. Repschläger[3] and A. Schmittner[4]

The PAGES Data Stewardship Scholarship (DSS) contributed towards the completion of the first version of a database of carbon and oxygen isotopes from benthic foraminifera in deep-ocean sediment cores.

The Ocean Circulation and Carbon Cycling (OC3) working group (pastglobalchanges.org/science/wg/former/oc3) started in 2014. OC3 brought together researchers with a scientific question: What global changes can explain variations in ocean carbon and oxygen isotope ratios ($\delta^{13}C$ and $\delta^{18}O$) in benthic foraminiferal samples from deep-sediment cores? Of particular interest was the transition between the Last Glacial Maximum (LGM, 23–19 kyr BP) and early last deglaciation (19–15 kyr BP), where a first increase in atmospheric CO_2 from glacial values (~180 ppm) is observed in ice-core data (Petit et al. 1999). $\delta^{13}C$ from tests of benthic foraminifera in deep-ocean sediment cores is used in paleoceanography as a tracer for past deep-water mass structure (Curry and Oppo 2005). $\delta^{18}O$ from the same samples is used as a tracer for deep-water temperatures and $\delta^{18}O$ of sea water (Lynch-Stieglitz et al. 1999). Despite relatively large amounts of existing data, the use of stable isotopes in paleoclimate research is hindered by several issues, such as:

1) formatting differences among sites;

2) differences in the methodologies used to calculate age models and/or;

3) offsets due to different species used to measure stable isotopes, and species-specific corrections included in some data.

The OC3 community established standards to homogenize benthic foraminifera isotope data and age models from different sources. In 2021, OC3 was granted a DSS from PAGES, which enabled us to finish the database product in early 2023. The database is available at zenodo.org/records/10391267, and a description paper was published (Muglia et al. 2023). It includes 287 globally distributed coring sites (Fig. 1). A *csv* file format was chosen, which makes the files both machine- and human-readable. A quality check on the data and age models was performed before their inclusion in the database. To be able to resolve the rapid changes associated with the last deglaciation, we only include data with temporal resolution of 1 kyr or better (Fig. 1). Stable isotope data from the genus *Cibicidoides* were preferred. The choice minimizes offsets from contemporaneous $\delta^{13}C$ of dissolved inorganic carbon in the overlaying bottom water. A toolbox written in Python calculates time slices, selects data by its time resolution, and plots data in time series, map, or vertical section formats. It is available in the database repository.

One important goal of OC3 is to quantify age-model uncertainties. For this purpose, we included different age models for sediment cores, if multiple age-model approaches were available. This enables an evaluation of the sensitivity of the reconstructed time evolution of benthic foraminiferal $\delta^{13}C$ and $\delta^{18}O$, with respect to different age models. We found that offsets in time series of isotope ratios obtained from using different age models are typically smaller than the uncertainties in those age models. This suggests that the direction of changes in stable isotope ratios may be captured, irrespective of the age-model approach used. Due to its global coverage and high temporal resolution, the OC3 database allows scientists to reconstruct a four-dimensional picture of changes in $\delta^{13}C$ and $\delta^{18}O$ through the last deglaciation. The database is useful for modelers to compare with computer simulations of the deglacial state, and for paleoclimatologists to study past deep-ocean and carbon-cycle changes. The database structure can also be used as a template for compilations of other paleoceanographic data in the future.

Future plans

The OC3 database is an ongoing project, with updates and additions performed as new coring sites and age models are published in the literature, or provided by our collaborators. The database will be combined with visualization tools of PaleoDataView (marum.de/Dr.-stefan-mulitza/PaleoDataView.html). In addition, we plan to translate the database into formats compatible with the LinkedEarth initiative.

Benthic foraminifera $\delta^{13}C$ and $\delta^{18}O$ are useful, but limited, tracers for deep-ocean characteristics. Expanding the database with other paleo-tracers, such as radiocarbon ages, Pa/Th or Neodymium, will provide a more complete picture of the ocean in past-climate scenarios. For this reason, in a future project, the database will be expanded to include these tracers.

AFFILIATIONS
[1]Centro para el Estudio de los Sistemas Marinos, CONICET, Puerto Madryn, Argentina
[2]MARUM – Center for Marine Environmental Sciences, University of Bremen, Germany
[3]Department of Climate Geochemistry, Max Planck Institute for Chemistry, Mainz, Germany
[4]College of Earth, Ocean, and Atmospheric Sciences, Oregon State University, Corvallis, USA

CONTACT
Juan Muglia: jmuglia@cenpat-conicet.gob.ar

REFERENCES

Curry WB, Oppo DW (2005) Paleoceanography 20(1): PA101

Lynch-Stieglitz J et al (1999) Nature 402(6762): 644-648

Muglia J et al. (2023) Sci Data 10: 1-131

Petit JR et al. (1999) Nature 399(6735): 429-436
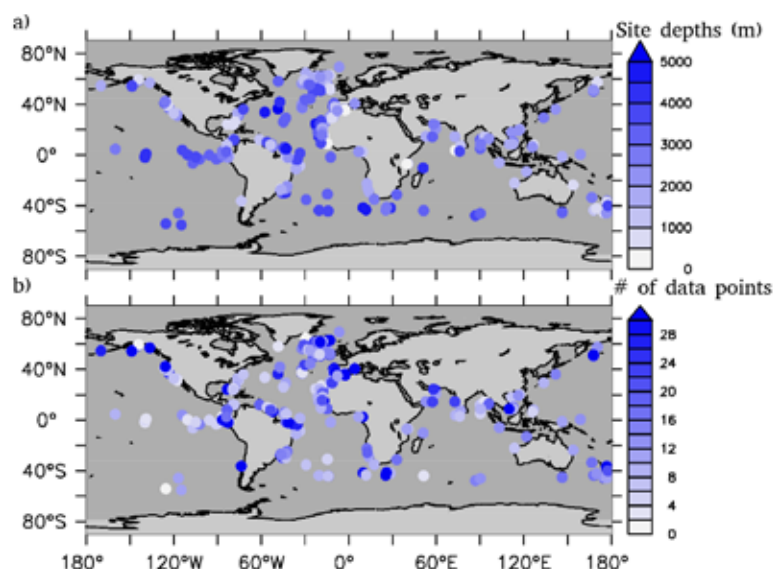
Figure 1: (A) Positions and depths (in m) of all sites included in our database. **(B)** Number of data points at each site in the 21–15 kyr BP time interval. Figure modified from Muglia et al. 2023.

Spatial distribution of paleorecords across Brazil: Clues for the changing climate and past civilizations

Lola Varga[1], A. Filippova[2], N. Kaushal[3] and G. Koren[1]

The availability of paleorecords is fundamental for studying past climate and human activities. Here we report on the availability of paleo data in Brazil, a country with diverse landscapes including rainforests, savannas and wetlands. Within Brazil, our main focus is on the Amazon region, a key region for carbon sequestration, regional water supply, a hotspot for biodiversity, and home to current and past Indigenous cultures.

We have evaluated the availability of paleorecords in Brazil from four widely used repositories: (1) NOAA's World Data Service for Paleoclimatology; (2) Neotoma Paleoecology Database; (3) PANGAEA Data Publisher for Earth & Environmental Science; and (4) various datasets collected by PAGES working groups. This approach largely follows the analysis performed for India (Kaushal et al. 2021) that appeared in an earlier issue of *Past Global Changes Magazine*.

For each data record retrieved from the databases, we first checked for duplication: we did not add another entry if the record already existed in our overview. Further, we noted the name, coordinates (latitude, longitude) and the archive type. In total, we found 366 paleorecords for 21 different archive types. The most abundant archive types are charcoal (161), shells (67) and pollen (32). A full list is available via Zenodo (doi. org/10.5281/zenodo.10466814).

We also plotted the data on a map (Fig. 1). Initially, this resulted in cluttering and overlapping markers. To increase visibility, we included a larger marker representing five records of the same type, and avoided overlapping of other types by introducing an aggregate representation. We note that most of the records are located in a relatively narrow zone around the coast and along rivers, whereas the further inland regions are less densely covered. In particular, the Amazon forest region in northwestern Brazil has poor paleodata coverage in the four examined databases.

The Amazon region is particularly sensitive to changes in hydroclimatic conditions, and to better understand this sensitivity we need hydroclimate proxies. Tree rings can provide information on rainfall over the Amazon and its variability on the El Niño-Southern Oscillation (Brienen et al. 2012). In the Amazon, the El Niño phase leads to drought conditions which impacts the hydrological cycle across the basin (van Schaik et al. 2018). This can result in increased mortality, fires and reduction in photosynthetic capacity in the affected parts of the forest (Koren et al. 2018). Besides tree rings, speleothems can also provide constraints on hydroclimate and

biodiversity in the Amazon basin (Cheng et al. 2013).

Remote sensing provides opportunities to study regions that are poorly covered by local measurements, and that are not easily accessible. Usually, remote sensing informs on current activities, but a notable exception is LiDAR technology, which has uncovered the location and extent of pre-Columbian settlements across the Amazon region. A recent study by Peripato et al. (2023) suggested that there are still many pre-Columbian earthworks to be found. Although one could argue that these measurements should also be considered paleorecords, we have not included them in our overview here.

We hope that this overview will be useful for researchers studying past climate in Brazil. Our analysis could inspire researchers to target locations for future research where there are currently gaps in data. We also encourage researchers who have already collected paleorecords in Brazil, but have not yet made their data available in one of

the four major paleo data platforms, to do so. Further, we hope that this will support other initiatives such as the INQUA-funded pSESYNTH project that aims to increase data availability and discovery from the Global South, as reported by Kulkarni et al. (2023).

AFFILIATIONS
[1]Copernicus Institute of Sustainable Development, Utrecht University, Netherlands
[2]GEOMAR Helmholtz Centre for Ocean Research Kiel, Germany
[3]American Museum of Natural History, New York, USA

CONTACT
Gerbrand Koren: g.b.koren@uu.nl

REFERENCES

Brienen RJW et al. (2012) Proc Natl Acad Sci USA 109: 16957-16962

Cheng H et al. (2013) Nat Commun 4: 1411

Kaushal N et al. (2021) PAGES Mag 29: 50-51

Koren G et al. (2018) Phil Trans R Soc B 373: 20170408

Kulkarni C et al. (2023) PAGES Mag 31: 30-31

Peripato V et al. (2023) Science 382: 103-109

van Schaik E et al. (2018) Phil Trans R Soc B 373: 20180084
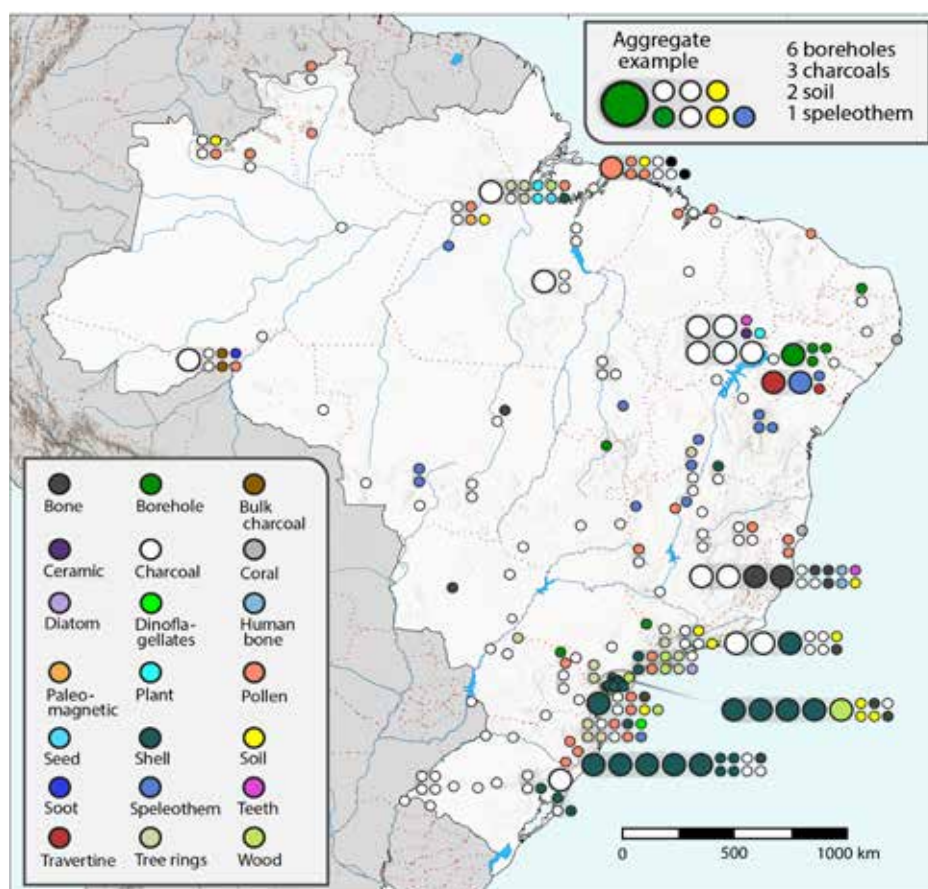
Figure 1: Spatial distribution of paleorecords across Brazil. The color of the markers indicates the type of paleo archive (bottom left legend) and the size of the marker indicates a single (small circle) or five (large circle) records. Records that are in close proximity, and that would overlap, are visualized as an aggregate (top right legend, 100% enlarged for visibility). In such cases, the lower left of the aggregate corresponds to the location of the records.

What defines an "early-career researcher" in the paleosciences?

Georgina M. Falster[1,2] and PAGES Early-Career Network Steering Committee Members*

Early-career researchers (ECRs) are important contributors to global change research (e.g. Andersen 2023). To support the development of ECRs, there are funding and opportunities available only to ECRs. Additionally, "early-career" status allows researchers the freedom to gain experience across various aspects of their careers and provides a foundation for a global community of developing paleoscience researchers.

However, the definition of "early-career researcher" varies between relevant scientific organizations. For example, PAGES defines an ECR as an undergraduate or postgraduate student, or a scientist within five years of completing their PhD. The European Geosciences Union defines an ECR as a student, PhD candidate or practicing scientist who received their highest degree within the past seven years. The American Geophysical Union defines an ECR as a scientist who received their highest degree within the past 10 years. Each institution allows flexibility for career breaks.

In 2023, the PAGES Early-Career Network (ECN) ran a survey seeking input from self-identified paleoscience ECRs on what they consider to be the meaning of the term "early-career researcher" (Fig. 1). The 66 responses were highly varied, falling into three broad groups. Approximately one quarter of respondents defined ECR based on employment status. Another quarter suggested a more nuanced definition. Most of the remainder based their definition on a certain number of years since award of a researcher's highest degree (ranging from three to 15 years). Among those defining ECR by "years post degree", only two explicitly mentioned career interruptions (e.g. parental or carer leave, or COVID-19).

Of the respondents defining ECR by employment status, most suggested that ECRs are researchers who have not secured permanent jobs. By contrast, respondents suggesting more nuanced definitions generally felt that ECR status can result from more qualitative indicators, including a limited publication record, working under more senior academics, having limited experience, still developing skills and collaborations, and still establishing their research direction and identity.

Several respondents stated the importance of self-identification, implying there is a strong mentality component to being an ECR. A further 10 respondents indicated that part of being an ECR is the requirement of support from ECR groups and/or more experienced academics – and that ECRs are researchers who are still learning, and who have the right to make mistakes.

An important question, then, is: What distinguishes early- from mid-career researchers? One key aspect is eligibility for opportunities only available to ECRs. But evidently, there are more nebulous aspects to this transition, such as a feeling of readiness and independence, or acquiring a certain level of knowledge and experience. In any case, we would argue that: 1) the need for support; and 2) continued learning are constants throughout an academic's career. In the words of the lead author: "As someone who is approaching five years post-PhD, I am still learning as much as I did as a student, and I certainly still make mistakes."

Finally, there is also variability as to when members of the ECR community believe one becomes an ECR. Survey responses ranged from "when you start doing research" to "recently finished a PhD". The prevailing opinion was that any student undertaking research – including undergraduate researchers, Masters students, and PhD candidates – should be considered an ECR until they stop active research, or transition to mid-career researcher.

In summary, results of our survey demonstrate that paleoscience ECRs lack a coherent global identity. It is possible that this reflects variability in institutional definitions of an ECR, which may in turn be because the definition needs to be somewhat fluid. "Hard" definitions (accounting for career breaks) are required to ensure funding reserved for ECRs is awarded to ECRs, but on the other hand, guidance, mentoring and peer support should be available to anyone who feels they need it. Understanding that there is variability within the way the global paleoscience ECR community views itself may help ECRs better understand their "place" in the academic community, and to modulate their expectations of themselves, and of their peers.

REFERENCES
Andersen JP (2023) Quant Sci Stud 4(2): 394-422
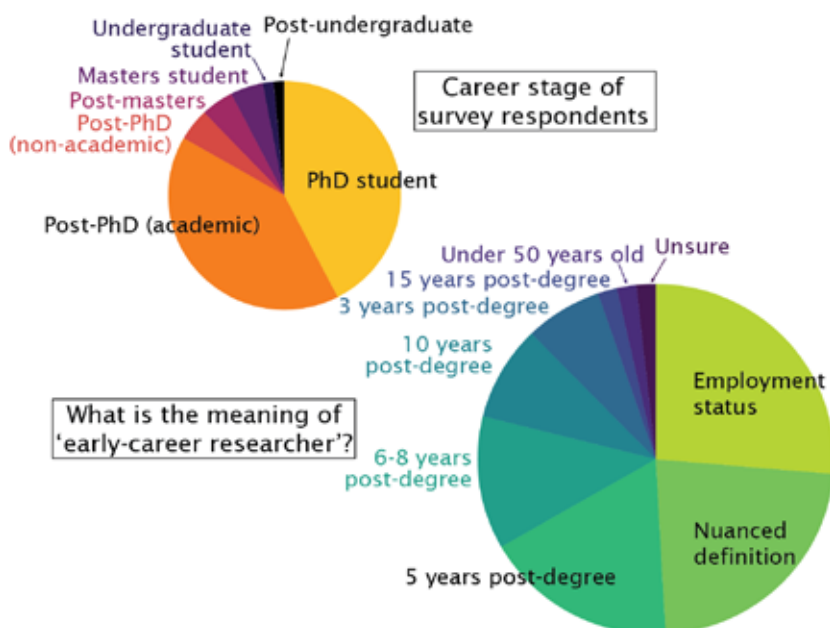
Figure 1: Career stage of the 66 survey respondents, and summary of responses to the question: In your own words, what would you consider to be the meaning of "early-career researcher"?

CONTENTS